AN ABSTRACT OF THE THESIS OF

Alexander John Nyers for the degree of Master of Arts in Applied Anthropology presented on June 11, 2013.

Title: A Provenance Study of Crypto-Crystalline Silicates at the Cooper's Ferry Site: A Geochemical Approach.

Abstract approved:

Loren G. Davis

A provenance study of crypto-crystalline silicates was performed at the Cooper's Ferry archaeological site in west-central Idaho on the Columbia Plateau. In this research, the author used instrumental neutron activation analysis as well as portable x-ray fluorescence to examine and characterize the geochemistry of 300 geologic samples of crypto-crystalline silicates from six different sources in the region surrounding Cooper's Ferry. The author then examined approximately 600 archaeological artifacts from Cooper's Ferry using portable x-ray fluorescence and attempted to correlate archaeological artifacts to examined geologic sources using a multivariate statistical approach. This research finds that the tool stone of approximately 24 percent of artifacts examined originated from a sampled local chert source.

This research also examined the ratio of possible chert sources scene in the archaeological record by using multiple cluster analysis techniques and finds that no

observable founder effect is seen at Cooper's Ferry. Furthermore, there seems to be a long standing transfer of crypto-crystalline silicate source knowledge at Cooper’s Ferry, indicating an extended period of cultural stability at the site. This stability can be extrapolated as a single cultural group residing at the site throughout its occupation history - approximately 11,000 to 8,000 RCYBP.

A Provenance Study of Crypto-Crystalline Silicates at the Cooper's Ferry Site: A Geochemical Approach

by
Alexander John Nyers

A THESIS

Submitted to

Oregon State University

in partial fulfillment of
the requirements for the
degree of

Master of Arts

Presented June 11, 2013
Commencement June 2014

Master of Arts Thesis of Alex Nyers presented on June 11, 2013

APPROVED:

Major Professor, representing Applied Anthropology

Director of the School of Language, Culture, and Society

Dean of the Graduate School

I understand that my thesis will become part of the permanent collection of Oregon State University libraries. My signature below authorizes release of my thesis to any reader upon request.

Alexander John Nyers, Author

ACKNOWLEDGEMENTS

Thanks to all the folks in Oregon State University's Department of Anthropology as well as the Idaho BLM for helping me make this happen. Thanks to Dr. Loren Davis and Dr. Leah Minc. Without their continued support and guidance, this project would have ended before it began. Finally, a special thank you to my wife Kirsten and daughters Alexandra and Penelope. You have put up with so much and have always supported me in this crazy endeavor. This work is dedicated to you. Thank you! ☺

TABLE OF CONTENTS

TABLE OF CONTENTS (Continued)

TABLE OF CONTENTS (Continued)

TABLE OF CONTENTS (Continued)

TABLE OF APPENDICIES

TABLE OF APPENDICIES (Continued)

LIST OF FIGURES

LIST OF FIGURES

LIST OF FIGURES (Continued)

LIST OF FIGURES (Continued)

LIST OF FIGURES (Continued)

LIST OF APPENDIX FIGURES

LIST OF APPENDIX FIGURES (Continued)

Page

LIST OF TABLES

Page

LIST OF TABLES (Continued)

Page

LIST OF APPENDIX TABLES

Page

Chapter 1: Introduction

The idea of linking geochemical signatures of artifacts to their source locations within a landscape, a concept known as *provenance*, has become common practice in archaeological research over the past 50 years (Glascock & Neff, 2003; Shackley S, 2012). Provenance studies examining ceramics and obsidians help archaeologists reconstruct trade patterns, socioeconomic interactions (Nadooshan et al., 2013; Minc, 2009), as well as mobility patterns (Sheppard et al., 2010) across the globe. For example, in his work "Stone Artefact Production and Exchange Among the Northern Lesser Antilles", Knippenberg performed a survey of geologic cherts across several Caribbean islands (Knippenberg, 2006). Using a combination of Inductively Coupled Atomic Emission Spectroscopy as well as geologic thin sections, Kippenberg was able to characterize as well as discriminant between cherts from several different islands in the area. Kippenberg then examined archaeological artifacts from several different islands using the same methods, and examined the results using a combination of exploratory data analysis techniques as well as discriminant function analysis. Using these methods Kippenberg statistically linked many of the archaeological artifacts tested to their geologic source locations. This linking allowed him to examine inter-island trade patterns, finding that some chert sources were used hundreds of km from their source locations, as well as how patterns of exchange changed over time (Knippenberg, 2006).

In another provenance study, “Lithic Source Use and Paleo-archaic Foraging Territories in the Great Basin”, Jones et al. examined over 840 obsidian artifacts from various terminal Pleistocene to early Holocene (TP-EH) archaeological sites across the Great Basin using energy dispersive x-ray fluorescence (Jones et al., 2003). Jones et al. (2003) then compared the resulting data to established sources across the region. Using these data, they postulated that there were five distinct conveyance zones within the great basin during the TP-EH period, with obsidians moving within but not across zones (Jones et al., 2003 : 31-32). This research helped further our understanding of early foragers across the region.

A third example of a successful provenance study, “Source Determination of White River Group Silicates from Two Archaeological Sites in the Great Plains”, examined the geochemistry of five chert sources via Instrumental Neutron Activation Analysis (Hoard, et al., 1993). While a small amount of overlap was present between two geologic sources (Hoard, et al., 1993, p. 702), for the most part sources were successfully discriminated. Hoard et al. then compared these data with artifacts examined from two archaeological sites, one a Clovis site and the second a Middle archaic to late prehistoric period site in the Central Plains. Using this technique, archaeological artifacts were able to be statistically grouped into three categories, two that were internally consistent but did not match tested sources, and a third which was able to be assigned to an examined geologic source (Hoard, et al., 1993 :

706). This study showcased that differentiation of chert sources, and that assignment of chert artifacts to geologic sources is possible on the Great Plains.

In contrast to the Great Basin, obsidian appears in archaeological sites in low numbers throughout the Pacific Northwest's Columbia River Plateau. Instead, crypto-crystalline silicates, are the dominant toolstone of choice (Hess, 1996; Figure 2; Tables 1:2). In the 1997 excavation of Cooper's Ferry (10IH73), 41,797 of the 47,578 recovered artifacts - roughly 88 percent - were chert[1]. While cherts dominate many prehistoric archaeological assemblages, only limited quantitative archaeometric work has been done to establish their provenance based on chemical analysis, and with varying levels of success. For example, at the time of this writing, there were 180 articles dealing with obsidian sourcing and 366 articles dealing with the sourcing of ceramics in the *Journal of Archaeological Science*, yet only eight articles on chert provenance studies[2]. On the Columbia River Plateau, only a single published study is available, the Mack Canyon site in north-central Oregon (Hess, 1996). Hess addresses the lack of studies on the Plateau as possibly being because of the high number of regional chert sources (Hess, 1996):

> *Second, the large number of chert sources in the Columbia Plateau will make regional provenance analysis difficult. The total number of chert sources in the Columbia Plateau is unknown, but amateur collectors have found dozens (Edmondson, 1991; Pattie, 1991). Kititttas County,*

---

[1] Quantities calculated from original artifact catalog.
[2] Searched on 5/7/2012 using http://www.sciencedirect.com. Search terms were "ceramic provenance", "obsidian provenance", and "chert provenance".

> *Washington, which covers about 5980 sq km and is one of the best surveyed counties in the Columbia Plateau, contains over 40 chert quarries (R. Whitlam, personal communication, 1992), resulting in a density of about one quarry for every 150 sq km. Although natural processes may have created many of the artifacts at these "quarries" (Bicchieri et al., 1995), it does point out the large number of chert sources available to prehistoric flintknappers. Many sources are liable to remain un-known simply because of their vast number and the lack of comprehensive surveys.*

Although the task of finding and studying large numbers of chert sources may seem initially daunting, large scale survey and chemical characterization of chert sources is becoming more feasible as technologies such as portable xrf (PXRF) become more commonplace. Additionally, building a chert provenance database of many closely spaced geologic sources has a clear advantage of being able to examine prehistoric mobility and exchange patterns on a granular level. Finally, because obsidians make up about 2.5% of Plateau artifact assemblages by volume, and cherts 75% (Figure 2; Table 1), the value of building a Plateau chert provenance database seems a worthy endeavor.

Studies that focus on the sourcing of cherts through quantitative methods often suffer from the use of sample sizes that are inadequate for successful characterization of chert sources (Luedtke, 1992); (Table 2). Traditional methods of establishing provenance of cherts based on macroscopic observations, such as color or texture (see Cottrell (1985) for an example of this technique) can be unreliable due to variations both within single nodules of chert as well as within single outcrops

and sources (Luedtke, 1992, pp. 70-71); (Shackley S. , 1987). This is due to a commonly held belief that cherts cannot be chemically sourced due to inter-source homogeneity being larger than intra-source heterogeneity (Skinner, C., 2008, personal communication); (Luedtke, 1978); (Luedtke, 1979); (Hess, 1996). This lack of provenance studies of cherts on the Columbia River Plateau combined with the amount of chert artifacts found in the archaeological record outlines the immediate need for quantitative analyses of cherts in the region. In an effort to make initial progress on meeting this need, this thesis will attempt to determine the provenance of chert artifacts from the formed tools and debitage recovered in the 1997 excavation of the Cooper's Ferry site. Excavation at this site recovered more than 40,000 chert artifacts from buried cultural components that may date from the late Pleistocene to early Holocene, and represents a suitable case study for examining whether chert sourcing is possible within the Columbia River Plateau.

Research Objectives

The primary focus of this research is to determine the feasibility of sourcing chert artifacts from the Columbia River Plateau through a case study at the Cooper's Ferry archaeological site. This research will be guided by seeking to answer the following questions:

1. Are geologic chert sources located in the area surrounding the Cooper's Ferry site?
2. Can these chert sources be defined and differentiated on the basis of their inherent geochemistry?
3. Can chert artifacts from the Cooper's Ferry site be statistically correlated to geologic chert sources in the Lower Salmon River Canyon?
4. How does studying chert artifact provenance at Cooper's Ferry inform our understanding of early human use of chert toolstone, and what are the larger implications of this study?

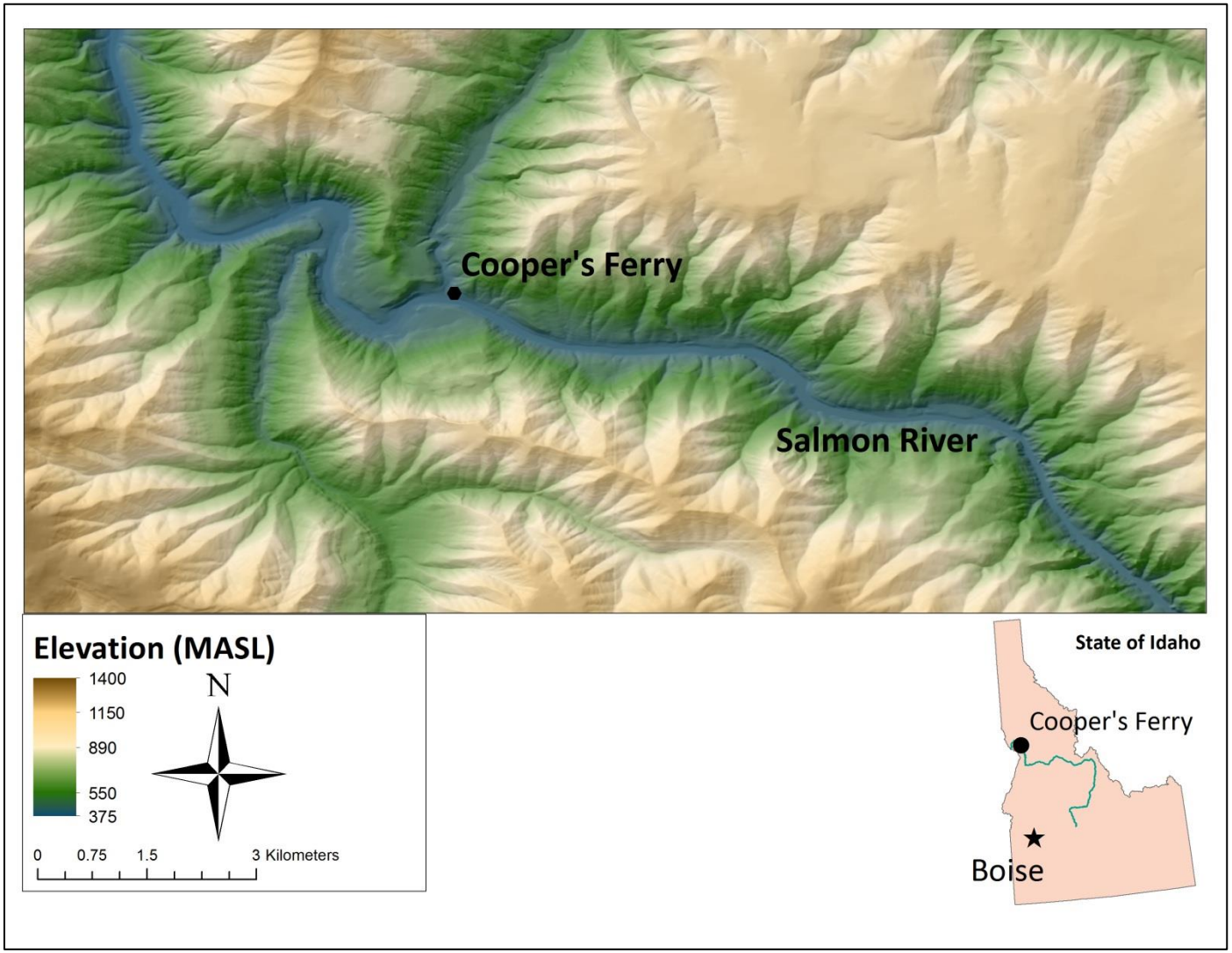

Figure 1 - Cooper's Ferry site location.

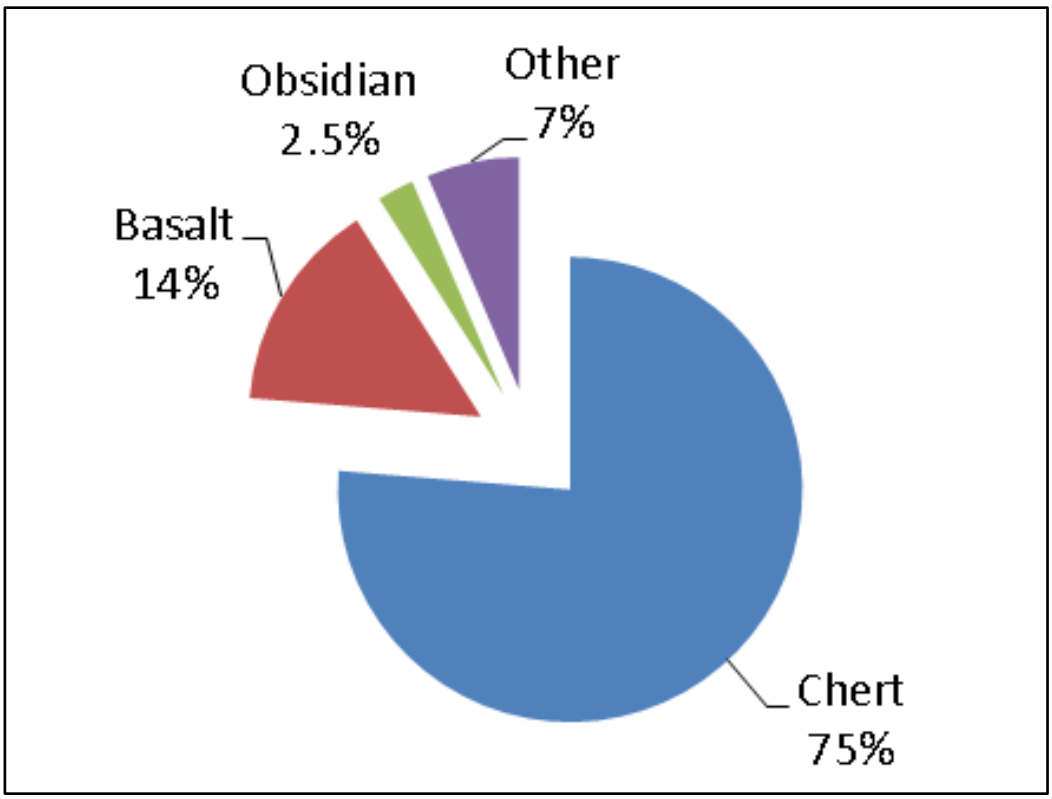

Figure 2 - Distribution of material types found in archaeological sites on the Columbia River Plateau.

Site Name	Chert	Basalt	Obsidian	Other	Source
10ih73 (1997)	87.9%	2.6	.2%	9.4%	Original Field Catalog
10np313	90.6%	6.5%	1.4%	1.5%	Lyon, J., 1995
10np314	78.8%	5.7%	15.5%	0.1%	Lutterell et al., 1997
10np315	78.1%	17.7%	4.1%	0.1%	Lutterell, 1996
35gm9	88.7%	7.5%	2.9%	0.3%	Dunmond and Minor, 1983
45ch254	88.0%	8.0%	0.0%	4.0%	Schalk et al., 1983
45ch309	70.6%	28.6%	0.2%	0.6%	Stephens et al., 1991
45ch409	76.0%	8.0%	2.0%	14.0%	Schalk et al., 1983
45ch57	56.0%	20.0%	2.0%	22.0%	Schalk et al., 1983
45ch58	34.0%	15.0%	1.0%	41.0%	Schalk et al., 1983
45do407	91.5%	5.0%	2.5%	1.0%	Schalk et al., 1983
45do408	91.0%	1.5%	0.0%	1.0%	Schalk et al., 1983
45do417	69.0%	19.0%	1.0%	11.0%	Schalk et al., 1983
45fr50	64.0%	30.0%	5.0%	1.0%	Hicks, 2004

Table 1 - Distribution of material types found in archaeological sites on the Columbia River Plateau.

45wt39	74.1%	21.8%	0.5%	3.7%	Yent, M. 1976
Wells Reservoir Arch Project *	66.6%	32.3%	1.1%	0.0%	Chatters et al., 1986
Average:	**75.3**	**14.3%**	**2.5%**	**6.9%**	
* Includes sites:					
45do372					
45do387					
45ok382					
45ok383					
45ok419					
45ok422					
45ok424					
45ok426					
45ok69					
45ok74					

Table 1 - Distribution of material types found in archaeological sites on the Columbia River Plateau (cont.).

Methods Used	Number of Sources	Number of Samples Per Source	Number of Artifacts	Statistical Methods Used	Location of Study	Author
INAA	11	5 - 10	23 to 45	Unspecified	Interior Plateau of British Columbia	Kendall, 2010
INAA	5	10 - 20	37	D^2 of first four principal components	Great Basin	Lyons et al., 2003
INAA	3	5 - 10	6	D^2 of first four principal components	Ohio River Valley	Glascock, 2004
ICP-MS & INAA	2	3, 18	4	D^2 of discriminant canons	Columbia River Plateau	Hess, 1996
INAA	8	10 - 30	43	D^2 of discriminant canons	Great Basin	Hoard et al., 1993
INAA	6	9 - 49	30	bivariate plots	New York	Jarvis, 1988
INAA, EMPA, XRD	12	15	289	bivariate plots of ratio data	Alaska	Malyk-Selivanova et al., 1998
EDXRF	1	20	24	cluster analysis and bivariate plot of principal components	New York	Rafferty et al., 2007
EDXRF	2	9 - 29	42	bivariate plot of principal components and spider diagram	Quebec	Gauthier et al., 2012
INAA	6	10 - 49	3	D^2 of first 8 principal components, discriminant analysis	North Dakota	Huckell et al., 2011
ICP-AES, ICP-MS, LA-ICP-MS	4	50	5	Bivariate plots of principal components, ANOVA	Northern England	Evans, et al., 2007
ICP-AES	14	6-21	50	D^2 of discriminant canons	Lesser Antilles	Knippenberg, 2006

Table 2 - Sample of geochemical chert studies over the last 25 years. Acronyms are defined as follows: INAA - Instrumental Neutron Activation Analysis, ICP-MS - Inductively Coupled Plasma Mass Spectrometry, EMPA - Electron Microprobe Analysis, XRD – X-ray Diffraction, ED-XRF – Energy Dispersive X-ray Fluorescence, ICP-AES – Inductively Coupled Plasma Atomic Emission Spectroscopy, ICP-MS – Inductivly Coupled Plasma Mass Spectroscopy, LA-ICP-MS – Laser Ablative Inductively Coupled Plasma Mass Spectroscopy,

Chapter 2: Background

Chert Formation Processes

Cherts are formed when silica settles out of a liquid suspension, or when silica atoms replace some other type of atom (carbon or sodium for example) in a rock matrix (Luedtke, 1992). Silica from cherts can be either biogenic or non-biogenic in origin, and can form in many different depositional environments. For example, in silica-rich rhyolitic lava flows, cherts can form in voids and vesicles within the flow. Cherts also form in less vesicular lavas, typically within joints and cracks within the flow as well as in features such as tree casts (Cummings et al., 1989). Cherts can form in contact regions between lava flows and fine grained sediments or sedimentary rocks, or around hot spring margins (Hesse, 1989). Finally, cherts can form in marine or lacustrine environments from the remains of silica rich diatoms or radiolarian sponges (Knauth, 1979).

By definition, all cherts are chemical precipitates. Cherts can form through either direct precipitation of colloidal silica, or through diagenesis of preexisting Opal A or Opal CT[3] (Knauth, 1994); (Knauth, 1979); (Cummings et al., 1989); (Williams & Crerar, 1985). These diagenetic pathways take the form of Opal A → Opal CT → microcrystalline quartz, Opal CT→ microcrystalline quartz, or can phase shift multiple

[3] Opal A and Opal CT refer to the differing crystalline lattices of the opal matrix. Opal A has an amorphous, non-crystalline-structure, whereas Opal CT is paracrystalline in structure.

times between Opal-CT and microcrystalline quartz. Changes can happen repeatedly depending on the conditions of the local environment. Each phase change in this pathway is accompanied by a dissolving of silica back into solution followed by subsequent re-precipitation. Chert formation times are dependent on the concentration of silica in suspension, the type and amount of particulate matter within the water body containing the colloidal silica, water acidity, and ambient temperature and pressure (Knauth, 1979).

Cherts can be split into two main categories: those that form via biogenic silica and those that form from non-biogenic silica. Biogenic cherts tend to form in carbonates, fossil woods, and some evaporates, while non-biogenic based cherts form in lacustrian, pedogenic, hydrothermal, and volcanic environments (Hesse, 1989). It should be stressed however that these tendencies, while being typical, are not absolute and that petrological as well as geochemical analyses are required to ascertain silica origin in cherts. In the LSRC, marine, volcanic, and pedogenic cherts are seen and will be discussed below. Magadi type cherts, while not present in the direct study area, are found fairly close by in eastern Oregon (both *in situ* as well as in archaeological contexts) and as such will also be discussed.

Marine Chert Formation

Cherts form some of the oldest sedimentary rocks on earth, with some marine cherts being dated to over 3.5 billion years old (Gregorio & Sharp, 2006). As previously stated, the silica that forms cherts can be either biogenic in nature, originating from

organisms such as diatoms and sponges, or inorganic, with silica coming from various fluid-rock interchanges (Knauth, 1979)**;** (Williams & Crerar, 1985)**;** (Murray, et al., 1992). Possible vectors for silica enrichment include tephra deposition or undersea hydrothermal venting (Grenne & Slack, 2003); (Van den Boorn et al., 2010)**.**

Once radiolarians and sponges evolved (and more so with the evolution of diatoms), global marine chert formation drastically increased (Knauth, 1994). During their lifespan, these organisms extract silica out of sea water for both cell wall buttressing (known as frustules or tests) as well as other biologic processes, such as DNA synthesis (Racki, 2000). Upon death, their silica-rich bodies slowly drop through the water column towards the sea floor. The rate of eventual deposition and accumulation on the sea bed is determined by a number of factors, including, but not limited to, water PH, temperature, pressure, and depth (Knauth, 1979); (Figure 4). Many, if not most of these organisms do not reach the sea floor, dissolving instead back into the water column. Those that do reach the bottom accumulate into siliceous oozes and opal-A rich limestone deposits (Knauth, 1994). Because most of these limestone deposits tend to form in relatively shallow marine environments near coastlines, they often become saturated with both marine and meteoric water. This water has the effect of dissolving the opal-A within the limestone matrix and then re-depositing it as opal-CT or chert either in vesicles or on impermeable layers within the limestone (Knauth, 1979); (Figure 5). Deep sea siliceous oozes, given that they do not dissolve back into the water column, also follow the opal → chert

pathway previously described once a sufficient burial depth has occurred (DeMaster, 2005).

Cherts in Volcanic Contexts

Chert formation is by no means restricted to marine environments. Cherts can form in basaltic, andesitic, and rhyolitic lava flows. After the initial flow cools, meteoric waters begin to percolate through the rock matrix. As in limestone chert formation, these waters dissolve silica embedded within the rock matrix, and then redeposit it into vesicles, cracks, and other voids within the flow. Different types of voids tend to form different types of cherts, depending on the size and shape of the void and the length of time of silica rich water inundation, with longer inundation times leading to increased quartz crystal size (Hesse, 1989); (Knauth, 1994). For example, when silica rich waters deposit their silica in the gas bubbles in vesicular lava flows, amygdaloidal agates are formed. Typical macroscopic traits of these agates include crypto-crystalline rinds, various concentric banding patterns, and sometimes macrocrystalline quartz interiors due to the agate interior having increasingly long amounts of silica inundation time (Figure 4 and 6). Cracks that form in the body of lava flows allow for increased penetration of water into the body of the flow, speed the weathering of parent flow, and act as a route for chert formation. Typically, crack infilling cherts are found in the basaltic lava flows surrounding the study area, as opposed to amygdaloidal cherts, which are found in more gas rich lavas such as rhyolites or andesites. Nodules of cherts that were originally formed via crack infilling

can sometimes appear to be amygdaloidal in nature when not found *in situ* because they can share some of the features of amygdaloidal agates. For example, crack infilling cherts can contain banding patterns or have crypto-crystalline rinds with macrocrystalline interior, and can adopt an amygdaloidal shape when weathered.

Silicified Sediments

In certain circumstances, fine grained sediments such as silts, clays, and volcanic tuffs can also form crypto-crystalline silicates. In these situations, sediments become silicified during burial and subsequent diagenesis, providing that some form of parent silica is available for dissolution and subsequent precipitation. Parent silica can be contributed from silica locked within the sediments themselves as well as nearby silica rich materials, such as volcanic tuffs, limestone formations, or overlaying lava flows. Increasing groundwater PHand temperature will hasten the silicification process (Williams & Crerar, 1985; Figure 4). Minerals that are easily weathered (e.g. carbonates) are replaced by colloidal silica, which then transitions into various phases of quartz. Pore spaces between minerals can also become infilled with quartz, leading to the chertification of the sediment.

Magadi Cherts

Magadi cherts, or cherts that replace sodium silicates such as magadiite and kenyaite, have a different formation process than those preciously discussed. These cherts form in alkali lake basins such as their namesake, Magadi Lake in Kenya. In these evaporitic environments, sodium and silica are raised to very high levels by

continued evaporation of waters that have leached sodium and silica from parent bedrock. As the concentration of sodium and silica rise, they are deposited on the lake basin floors and form microcrystalline sodium silica hydrates, such as magadiite ($NaSi_7O_{13}(OH)_3 \bullet 4(H_2O)$). These deposits are then weathered by more acidic waters and the sodium becomes preferentially removed from the matrix, leaving the silica behind (Eugster, 1967). While these cherts are not found directly in the study area, they have been found a few hundred km to the south near Burns, Oregon (Lyons et al., 2003: 1141).

While all cherts form primarily from precipitated silica, other elements are also deposited with the silica that can serve to indicate the origin of the chert (Allwood, et al., 2010); (Murray, et al.., 1991)**.** Some elements, such as rare earth elements, Ti, or Fe become locked into the SiO_2 matrix during the initial formation of the cherts and are extremely resistant to post formation changes (Owen et al., 1999); (Murray R., 1993). Other elements, such as Ca, Mn, or Mg are more mobile in the silica matrix, and change through weathering and diagenesis of the chert (Gauthier et al., 2012); (Murray R. , 1993; Figure 7). The initial concentrations and ratios of these elements are dependent on a number of conditions, such as, but not limited to, the formation pathway of the chert, the surrounding lithology, the concentrations of trace elements in the waters depositing the chert, atmospheric conditions, and water PHand salinity (Pufahl & Hiatt, 2012). Because of this, different formation processes, subsequent diagenetic pathways, and varied microclimatic weathering environments

all cause different ratios of these elements to be present within different formations of host rock. These inherent differences make provenance sourcing of cherts possible.

Local Geology

In order to attempt a provenance study of lithic raw materials, an understanding of the local geologic history as well as the formation processes of the raw material in question is necessary. The study area of this research centers on the lower Salmon River canyon (LSRC) of western Idaho. The LSRC is a geographically diverse region, with four prominent geologic features all meeting in the immediate vicinity (Figure 8). To the north and northwest, Miocene aged flood basalts that are hundreds to thousands of meters thick dominate the landscape and to the southeast plutonic rocks are commonplace. To the northeast, an arc of Proterozoic metamorphic rocks dominate, while to the south and southwest Triassic rocks of accreted island-arc terrain covers the area (Figure 8). Cherts are known to be present in three of these four geologic formations. The Idaho Batholith to the southeast is not known to form cherts, and will not be discussed here.

Cherts are classified as sedimentary chemical precipitates (Luedtke, 1992, pp. 5-15). Cherts can be crypto-crystalline or have a fibrous crystalline structure with bonds between crystals stronger than the individual crystals of which they are composed of.

This strength causes cherts to shear through their individual crystals instead of around each crystal face when struck, making the precisely controlled removal of flakes possible during flint knapping.

Belt Supergroup

The oldest rocks in the LSRC region are a Proterozoic-aged geologic formation northeast of the study area that separates the Bitterroot and Atlanta lobes of the Idaho Batholith (Figure 8). Known as the "Belt Supergroup", this formation extends from southern Canada down through the panhandle of Idaho and has been dated to roughly 1.4 billion years old (Evans et al., 2000). Rocks in this formation were originally formed through sedimentary processes in environments, "ranging from alluvial fans to mudflats to moderately deep water (below wave base)" (Maliva, 2001:888). Most Belt Supergroup rocks have been subjected to extensive diagenesis and metamorphism, and are now composed chiefly of argillites, quartzites, and siltites (Link et al., 2007).

Cherts make up less than 1% of the rocks in the Belt Supergroup (Maliva, 2001). They are typically found as nodules within metamorphosed sedimentary deposits throughout the supergroup, and tend to be oolitic or stromatolitic in structure and devoid of fossils (Maliva, 2001). These cherts are thought to be replacement based instead of direct precipitates. Forming through silica enriched sea water from fluid-rock interchanges with silica rich minerals such as clays and volcanic tuffs. While

chert formation has been documented in this geologic region, no cherts associated with the Belt Supergroup were found during this research.

Wallowa Arc Terrain

The LSRC region also contains an allochthonous landform known as the Wallowa Arc accreted terrain. This landform is the result of a volcanic island arc being scraped on to the western edge of the North American plate due to tectonic forces during the Mesozoic era. Though large swaths of this landform were buried in the Miocene by the Columbia River Basalts, it is exposed in the Seven Devils mountain range as well as in portions of the Snake and Salmon River canyons (Figure 8). The Wallowa Arc terrain contains plutonic as well as extrusive volcanic rocks formed from the Permian to the Triassic, and is capped by sedimentary strata including shales, sandstones, and limestones that date from the Pennsylvanian to Jurassic (Figure 9); (Vallier, 1998); (White, et al., 1992). Cherts are found as isolated nodules and in thin beds in the sedimentary stratum from the Coon Hollow Formation that caps the Wallowa Arc terrain. One chert source, dubbed the “Seven Devils Chert Source” was found during this research in the Wallowa Arc Terrain (Appendix G – Seven Devils Geologic Samples).

Columbia River Basalt Group

The Columbia River Basalt Group (CRBG) is comprised of a series of Miocene aged flood basalts originating from eastern Washington State. These flows did not erupt from a traditional volcano but instead were formed by large rifts, some over 150km

in length, pouring out basaltic lava across the region (Straub & Link, 2013). This outpouring created a “layer cake” topography across the Columbia River Plateau (Straub & Link, 2013). Individual basalt flows vary in thickness but typically range from a few meters to a few tens of meters thick, depending on location. Major flood events range from tens to hundreds of meters and in some places over a kilometer thick. In total, four major eruptive flood events took place. From oldest to youngest, they are the Imnaha, Grande Rhonde, Wanapum, and Saddle Mountain Basalt flows (Reidel et al., 2003). These flows are differentiated by magnetic polarity, radiometric dating, petrographic analysis, and geochemical analysis. Most of the study area of this research is covered by the Grande Rhonde subgroup (Figure 8). In between individual flow events, rivers, which were dammed by CRBG flows, formed large, shallow lakes across the region in which rich ecosystems formed. Sediment deposition, mainly in the form of silts and clays as well as some tuffs from surrounding volcanos, occurs in low energy lacustrian environments. These sediments, known in the area as the “Latah Formation” were buried by subsequent lava flows and due to post burial diagenesis, became lithified into fossil rich mudstones, shales, and tuffs (Hostermann, 1960; Kirkham & Melville, 1929). In some areas, increasing heat and pressure from continued burial due to subsequent flow events caused these rocks to become partially silicified, sometimes to the point at which they became knappable and could be used as a viable toolstone for native peoples.

Cherts from the Cooper's Ferry Site

Cooper's Ferry is located on an alluvial terrace approximately 61 km from the confluence of the Salmon and Snake Rivers in the lower Salmon River canyon of western Idaho (Figure 1); (Figure 12). This research focuses on artifacts recovered from the 1997 excavation of the site conducted by Dr. Loren Davis (Davis L. G., 2001). In this excavation, a 2x2 m test pit was excavated on an alluvial terrace at the confluence of Rock Creek and the Salmon River. Eight separate lithostratigraphic sedimentary units were excavated, as well as a critical pit feature at the bottom of the excavation which was buried by glacial loess (Figure 11). This pit feature was produced four western stemmed projectile points (Davis L. G., 2001). Dates from mammalian bone and wood recovered at the site date from 12000 to 7300 RYBP, though are mixed in vertical sequence, probably due to bioturbation (Davis & Schweger, 2004). This research project examined the geochemistry of all formed tools from the 1997 excavation (n=215) as well as 391 pieces of debitage randomly sampled from the artifact population.

Figure 3 - Chert in limestone formation. Trowel is pointing towards chert. Photo from Biagi & Nisbet, 2010.

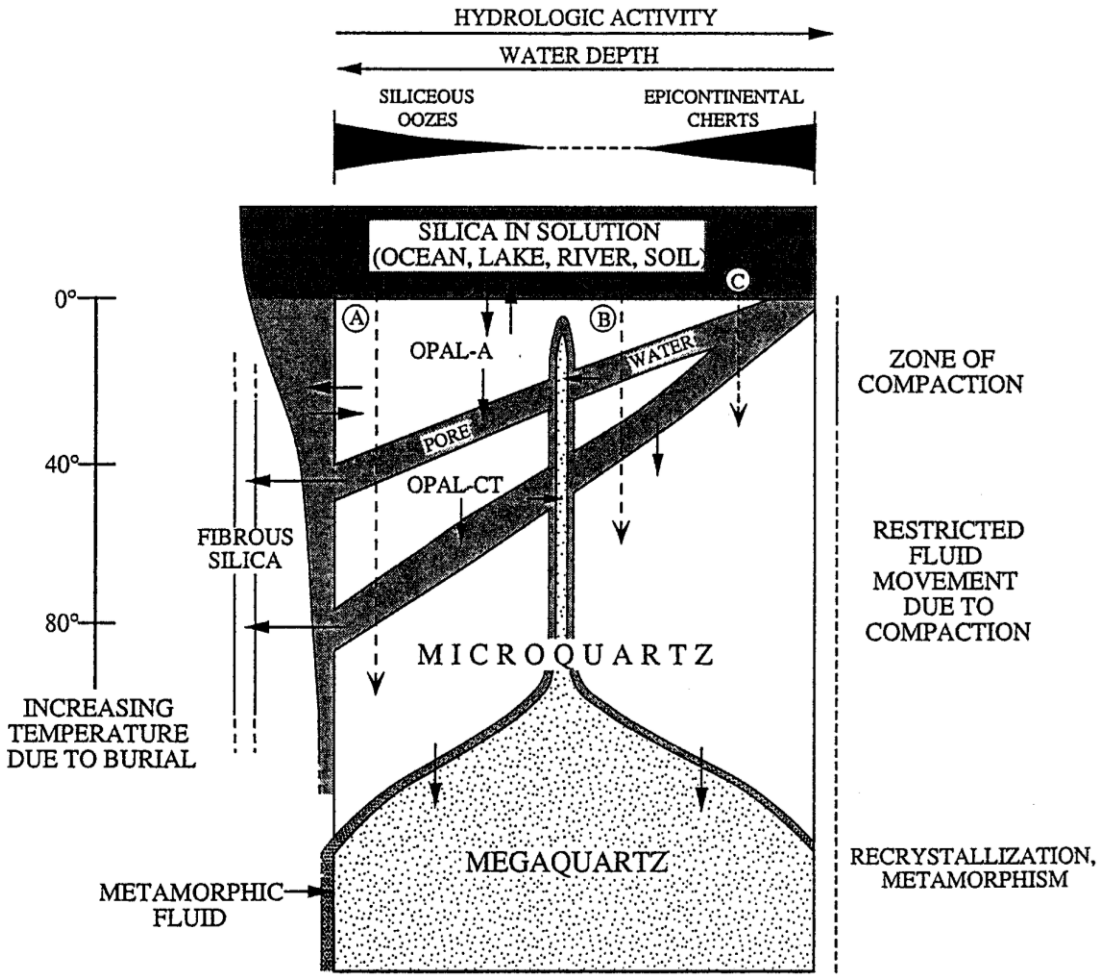

Figure 4 - Silicification formation pathways, from Knauth, 1994. Original caption is as follows: "*Schematic diagram of major authigenic silica phases and their possible diagenetic transformations. Vertical dimension represents qualitative burial depth with associated increase in temperature and loss of permeability. Horizontal scale represents qualitative depth of initial depositional environment. In general, deep sea oozes lie to the left of the diagram, while epicontinental deposits lie toward the right. Diagenetic path 'A' represents silica initially deposited as opal-A (diatoms, radiolarians) which then transforms to opal-CT and then microquartz via solution-reprecipitation steps. Path 'C' represents early diagenetic cherts in which microquartz forms during shallow burial. Megaquartz forms by metamorphic recrystallization of microquartz or by direct growth into voids at any stage of burial. Fibrous silica can grow in vugs and fractures at all burial depths.*". Figure caption from Knauth, 1994. pg 239, Figure 4.

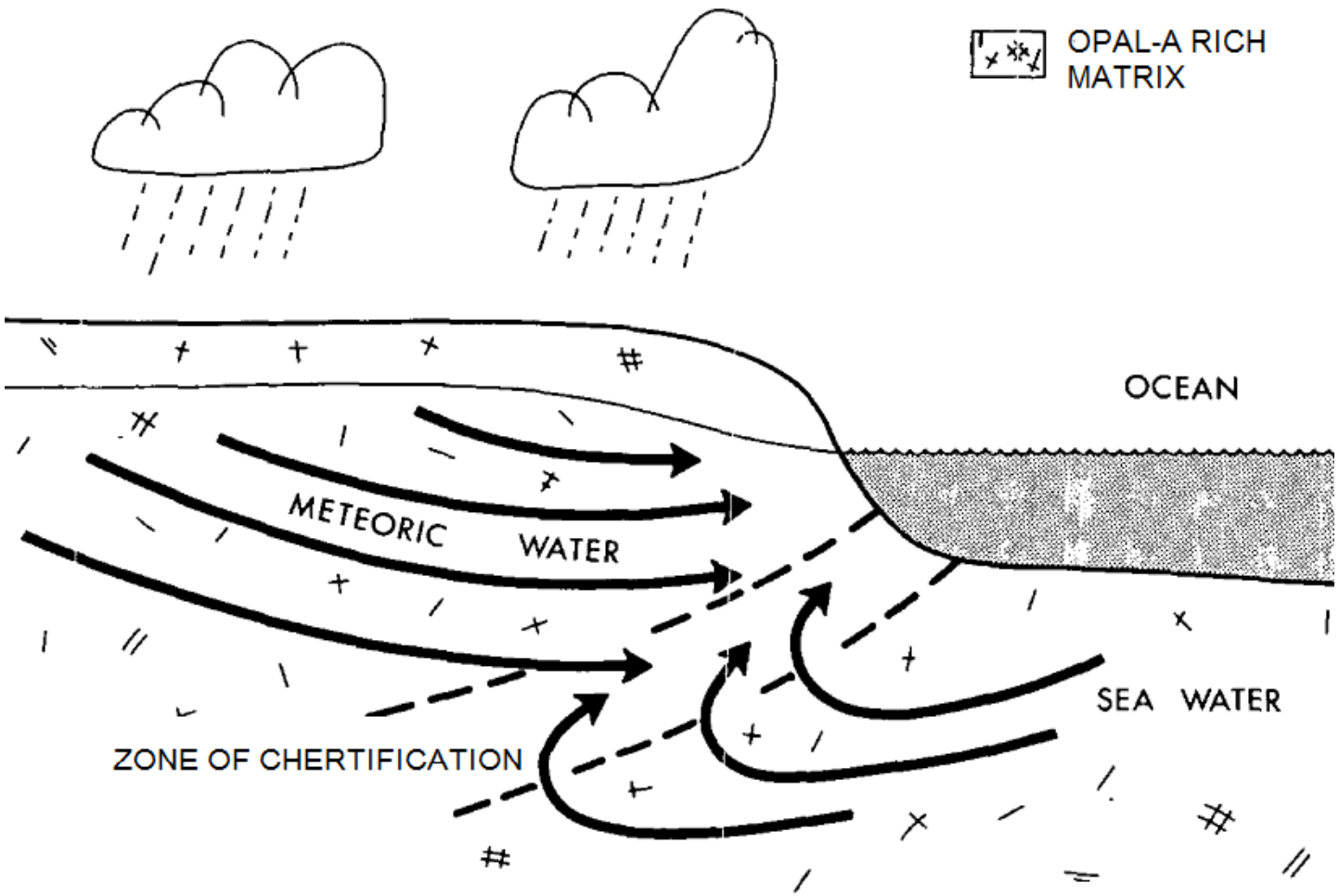

Figure 5 - Chert formation in coastal environments. Modified from Knauth, 1979.

Figure 6 -Typical agate. Note the banding and macrocrystalline interior.

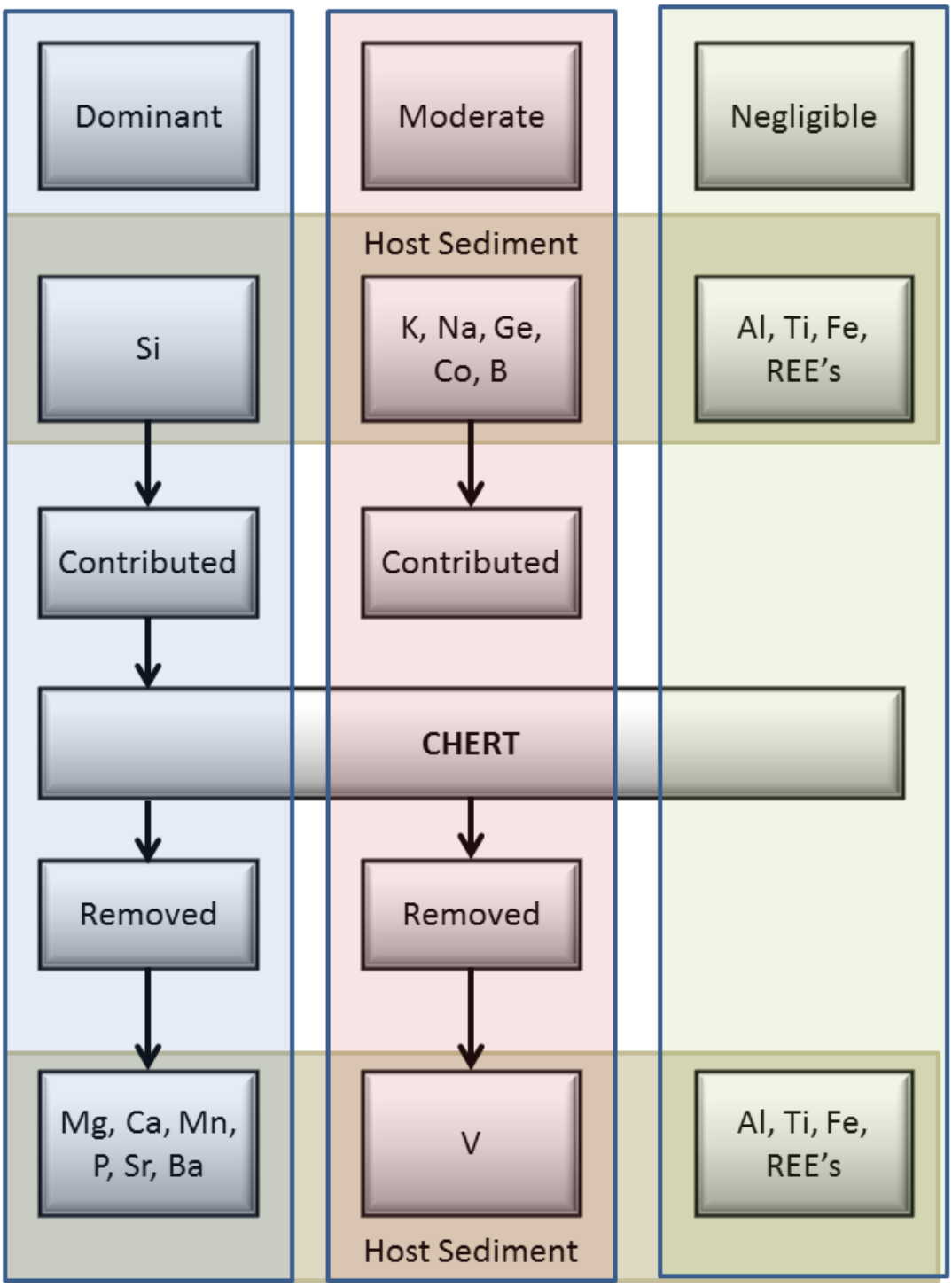

Figure 7 - Diagenesis effects on chert chemistry. Modified from Murray 1993:215.

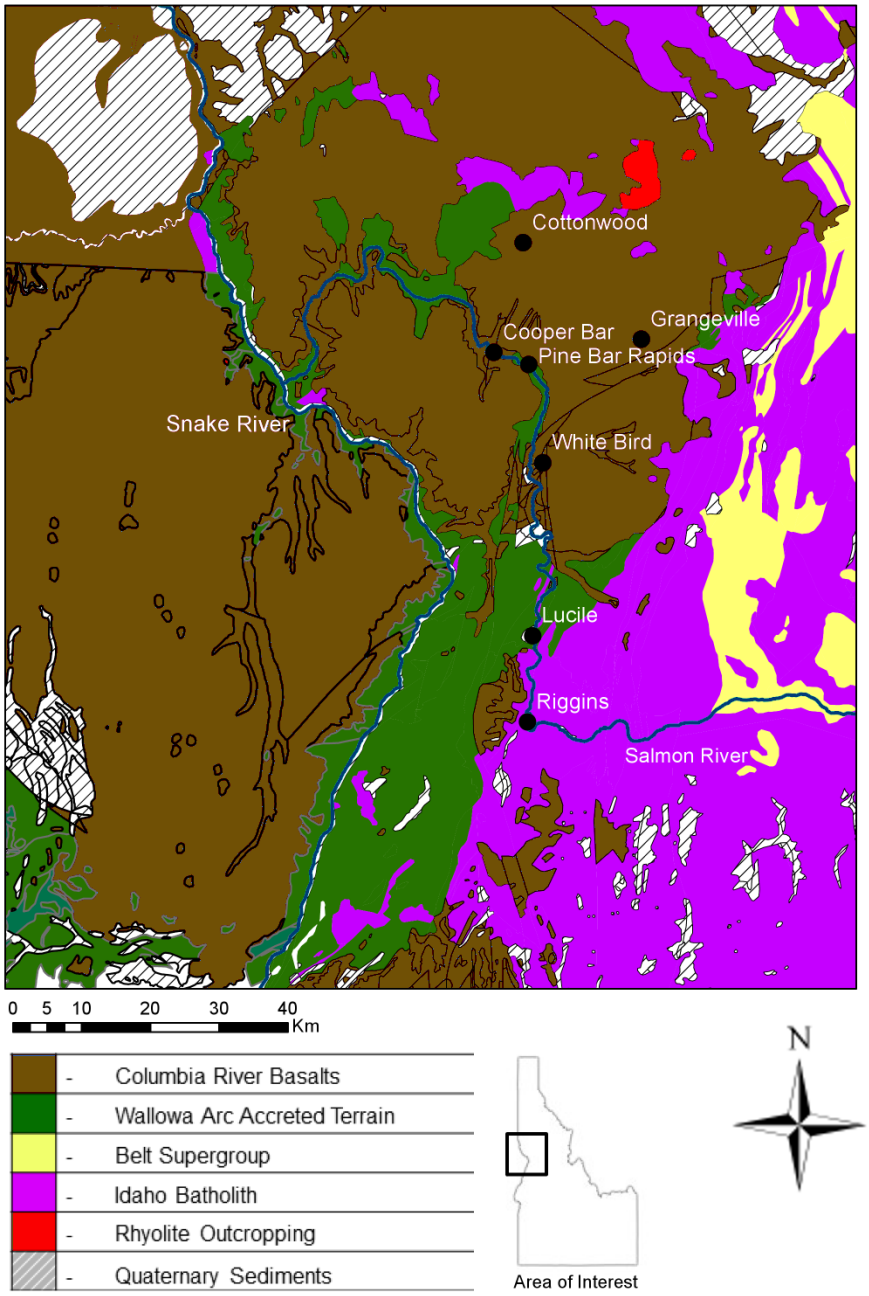

Figure 8 - Regional Geology of Study Area. Redrawn from Geologic Map Geodatabase of Idaho, version 1.2009.2

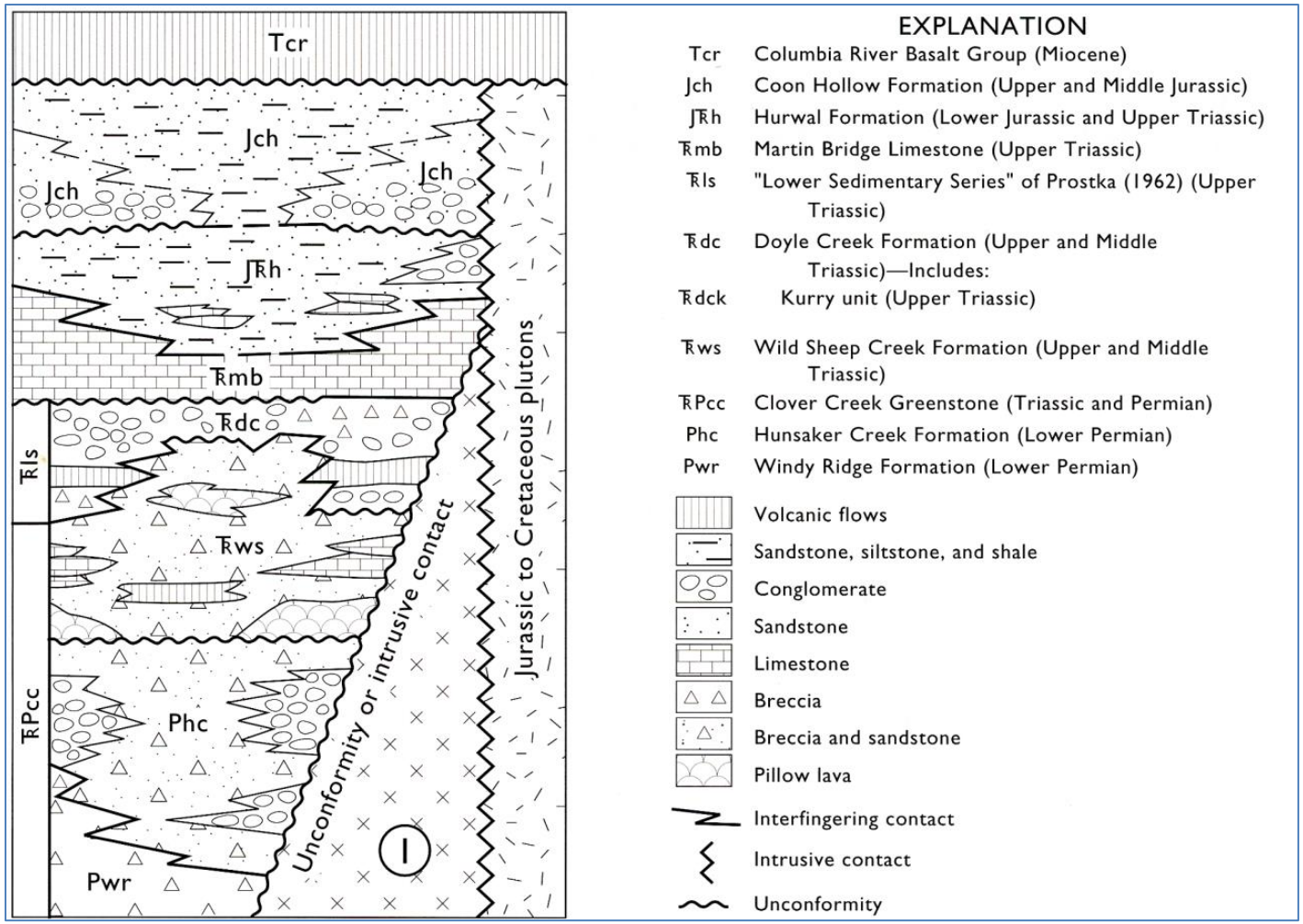

Figure 9 - Wallowa Arc Terrain. From Vallier, 1998.

Figure 10 - Grande Ronde Basalts of the Columbia River Basalt Group. Photo taken along Grande Ronde River, courtesy of Skål Williamborg.

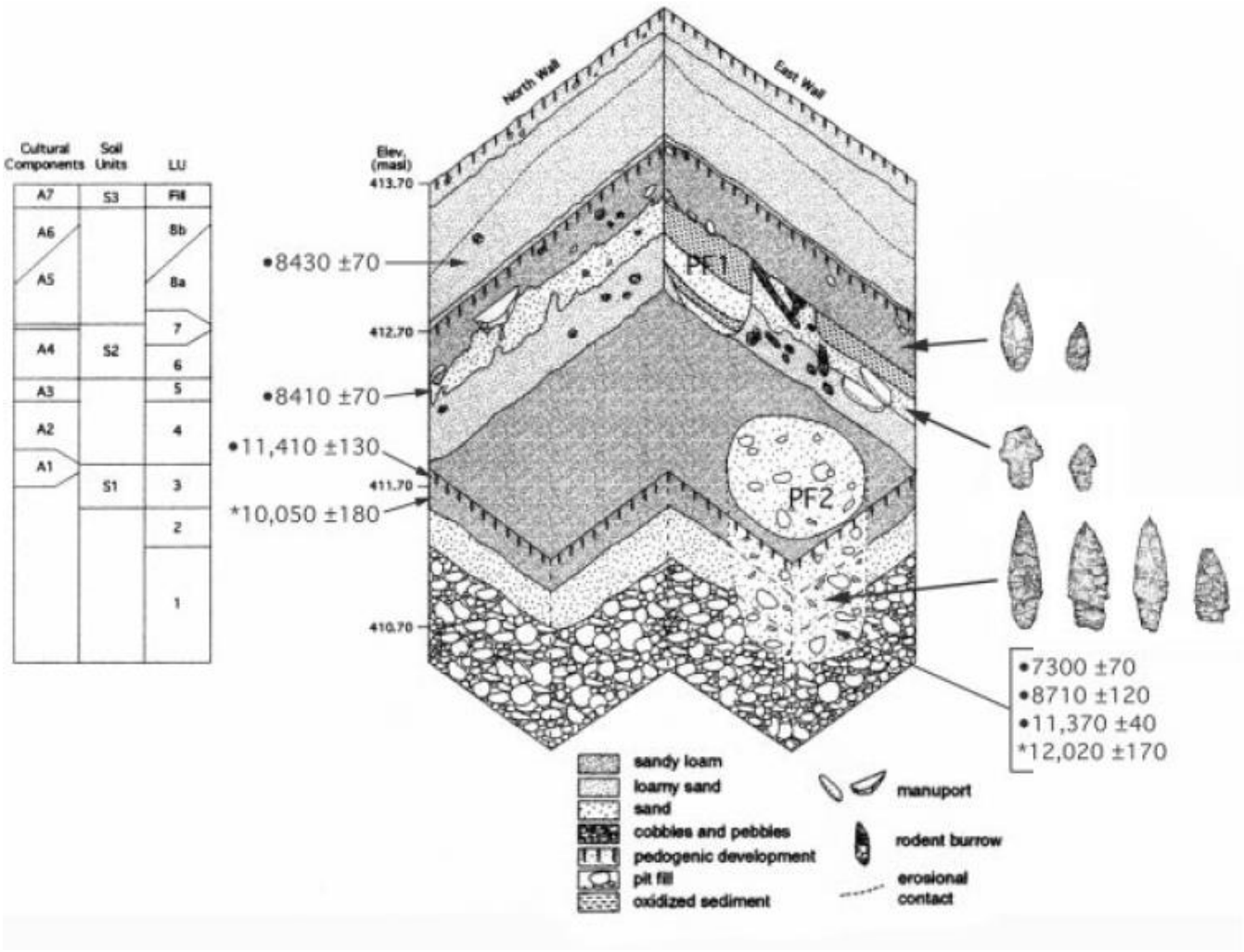

Figure 11 - Stratigraphic sequence of Unit A from 1997 excavation of Cooper's Ferry (Davis, 2001: Figure 100).

Figure 12 – Overview of the Cooper's Ferry site location.

Chapter 3: Materials and Methods

Methods

In order to address questions related to how foraging peoples used chert toolstones through time at the Cooper's Ferry site, a geochemical provenance system must be established and used to evaluate artifactual cherts. The following steps and their associated methodologies will be discussed in this chapter:

1. Locate chert sources in the study area.
2. Process chert samples from each source located using INAA.
3. Compare and differentiate sources using INAA data.
4. Calibrate PXRF device using NIST, USGS standards as well as INAA readings from step 3.
5. Collect additional samples from local chert sources for PXRF analysis.
6. Examine geologic sources using PXRF.
7. Compare and differentiate sources using PXRF data.
8. Examine artifacts from Cooper's Ferry excavation using PXRF.
9. Compare data from Cooper's Ferry artifacts to geologic sources tested.

An initial survey of the LSRC conducted by this author in 2005 resulted in the discovery of nine separate chert sources, four of which were previously described. The remaining samples tested were silicified sediments associated with Latah

formation deposits as well as agates from a Columbia River Basalt outcrop directly above Pine Bar campground[4]. To gain an understanding of what the relative intra-source homogeneity and inter-source heterogeneity of these cherts were, 76 chert samples were selected for INAA analysis. While this sample size was inadequate for a complete quantitative chemical characterization of these sources (see Luedtke, 1992 for a discussion of adequate sample sizes of cherts), the resulting data was able to show concentration trends as well as to provide a proof of concept for later XRF analysis. INAA results also allowed for later cross checking and calibration of the XRF device used in this analysis. During subsequent surveys, two more sources were found.

In total, 600 artifacts from the Cooper's Ferry archaeological site were compared to 300 samples from six different crypto-crystalline silicate sources using a combination of Instrumental Neutron Activation Analysis, energy dispersive x-ray fluorescence, and multivariate statistical techniques. With these techniques, geologic sources of chert were differentiated with a high degree of success. Furthermore, over 20 percent of artifacts tested fell within a single standard deviation of an examined chert source.

[4] Four of the sources tested initially were not extensive enough for adequate sample sizes during PXRF sample collection and therefore were not included in later analyses.

Instrumental Neutron Activation Analysis

Instrumental Neutron Activation Analysis (INAA) is a bulk elemental analysis technique that has become commonplace in elemental research. Highly sensitive, INAA can measure a host of different elements at the percent level down to parts per billion concentrations, and in some cases parts per trillion (Glascock & Neff, 2003). In INAA, prepared samples are placed within the neutron flux of a nuclear reactor. Atoms within the sample being exposed to the flux are bombarded with neutrons. When neutrons collide with nuclei of the atoms in a sample, they form what is known as compound nuclei, and become excited into unstable states. Once removed from the neutron flux, these unstable isotopes decay at specific known rates and energies, giving off both prompt as well as delayed gamma rays (Figure 13) (Glascock & Neff, 2003). After samples are removed from the reactor, they are placed next to a gamma ray detector (in this case a germanium based crystal detector). When a gamma ray is released from the sample, it impacts the detector, and is converted to an electrical charge. This charge is converted by a digital signal processor and is then sent to a counting application on a dedicated computer (Glascock & Neff, 2003). The computer records the energy level of the charge in KeV and the number of impacts of gamma rays on the detector per second at its particular energy level. The number of impacts is converted to counts per second (cps) at specific energy levels, which is then converted to elemental concentrations. Concentrations are quantified by using a number of reference standards that are selected based on the type of material

being used in order to bracket expected concentrations. Because this technique allows for measurement of such minute trace element concentrations and because it involves working with a potentially dangerous suite of chemicals and radioactive isotopes (as well as being a relatively expensive technique) INAA demands exacting controls on research design, sample preparation, handling, and analytical methods to get accurate results.

To activate samples, 500 mg of powdered chert was encapsulated in ultrapure quartz tubing and irradiated at 1MW for 30 hours. After irradiation, two separate counts were performed, the first at one week after irradiation to measure medium half-life isotopes, and the second one month after irradiation to measure longer half-life isotopes. A separate 60 second run at 1MW was also performed on 100 mg samples of powdered chert to analyze short half-life element concentrations. INAA requires the use of documented reference standards to calibrate the analysis to known values and a check standard that is used to check for errors across analyses. Standards SRM 278, NIST 688, and NIST 1633a were used for the creation of calibration curves in this analysis for both short and long irradiation testing.

Sample Preparation

Special care must be taken to avoid any contamination of INAA samples. Common sources of contamination when performing INAA include oils and sweat from the skin, cross contamination from previously processed samples, ambient dust, inadequate cleaning of samples, and contamination of samples from equipment used

for sample processing. To prepare samples for INAA, the following procedure was used:

1. Select a chert nodule to be sampled. Wash thoroughly with tap water and dry in drying oven.
2. Wrap chert nodule in several layers of paper towels and place in a 20 ton hydraulic press equipped with Teflon pressure plate covers.
3. Apply enough pressure to shatter nodule (typically 8-10 tons of force per square inch).
4. Select a few flakes from the shattered nodule that had minimal amounts of cortex or other contaminants (metal from rock hammer during initial removal of chert from geologic source, for example).
5. Remove smaller flakes from resultant shatter using dear antler hammer, making sure to remove any cortex. Select three to five grams of chert flakes were for further processing.
6. Scrub flakes with DI water, let sit in 10% nitric acid bath for 24 hours.[5]
7. Rinse flakes with DI water, then allow samples to soak in 10% RBS 35 bath for 24 hours.[6]

---

[5] Nitric acid is an oxidizer that was used to remove any possible metal contamination from the surface of the cherts being analyzed.
[6] RBS 35 Detergent Concentrate is a product manufactured by Thermo Scientific designed to clean glassware through a "…mixture of anionic and nonionic surfactants".

8. Scrubbed flakes with DI water, then covered them and placed in a drying oven for 48 hours.
9. Examined each flake for any contamination or large inclusions/cracks. If any were present, the material in question was removed.
10. Crushed the flakes in an artificial sapphire mortar and pestle to coarse sand size particles.
11. 500 Mg of chert was encapsulated into ultrapure quartz tubing using a natural gas torch and submitted for irradiation.

As previously discussed, two different types of analyses were done via INAA on each sample, a long irradiation on a rotating “lazy susan rack”, and a short irradiation on a pneumatic tube system known as a “rabbit” system to examine short half-life element concentrations. Sample preparation was slightly different for rabbit analysis. Instead of 500 mg of chert being encapsulated in ultrapure quartz tubing, 100 mg of chert was encapsulated in polyethylene tubes which were sealed using a wide tip soldering iron.

Energy Dispersive X-ray Fluorescence

XRF analysis is an attractive method of examining artifact chemistry due to its minimal laboratory preparation time, low cost of analysis, non-destructive nature, and general availability (Shackley S. , 2012). XRF has also been miniaturized to the point that field use is feasible through the use of a variety of commercially available portable devices. For these reasons, portable XRF (PXRF) was selected for use as a

second quantitative elemental analysis technique for this chert provenance sourcing study.

PXRF works by bombarding atoms in a sample being tested with x-rays generated either by radioactive isotopes or by an x-ray tube. When x-rays interact with electrons in the target atom, sometimes an inner shell electron is kicked out and subsequently replaced by an outer shell electron (Shackley S. , 2012). When this occurs, excess energy is released in x-ray form, some of which can be captured by a detector chip. The emitted x-rays are recorded by the detector and converted into digital pulses, which are then converted into counts per second (cps) at specific energy levels (Figure 14). Since atoms fluoresce at specific known energies when bombarded by x-rays, this technique can be used to determine the kind and concentration of elements present in a sample. However, because PXRF emitters and detectors vary in their ability to emit and detect x-rays, every PXRF device must be calibrated to known reference standards in order to verify what is actually being measured by the device.

For this analysis, two separate PXRF devices were used, a Niton XL3t 500 and a Niton GOLDD+ device. Both of these devices were used in their “Soil” modes with a 3 filter configuration. Filter composition and thicknesses are proprietary with both devices. Energies produced by the Niton XL3t 500 range from 20k to 50kVp@100uA utilizing a Au anode, and resultant backscatter x-rays are detected via an Si-Pin detector. The

NITON GOLDD+ device outputs from 6 to 50kV at currents up to 200uA with an Ag anode and resultant backscatter x-rays are detected by a silicon drift detector. Due to the design geometry of the NITON GOLDD+ device, lighter elements (up to Mg) can be detected without a helium purge system. However, since the Niton XL3t 500 device did not detect these elements, they were removed from these analyses.

Sample Preparation

Sample selection and preparation is less time consuming with XRF analysis than with INAA. Unlike INAA, precise mass measurements do not need to be taken, and samples do not need to be homogenized into powders. While PXRF is a bulk analysis technique, it functions via a directed beam. This allows for only a single area on an artifact to be subjected to cleaning as opposed to the entire artifact. Also, as long as one's hands are relatively clean, gloves do not need to be worn because, unlike INAA, sodium is not currently measured by PXRF. Finally, since solid objects were being analyzed instead of powders in this analysis (although the device is perfectly capable of examining powders), the risk of cross contamination between samples is minimal. Debitage was selected for analysis by assigning a random number to each piece of debitage from the 1997 Cooper's Ferry excavation classified as opal, ccs, chalcedony, jasper, red jasper, and Salmon River greenstone, then sorting by the random number and selecting the first 385. This number was arrived at as a tradeoff between getting a large enough sample to capture some of the nature of the variability of the dataset and the length of time required to process and analyze samples. If selected pieces

were of insufficient size for analyses (see below), they were returned and a replacement was randomly selected. Sample preparation steps for both artifacts and geologic samples follow:

1. Confirm that the selected sample that has an area of at least 1 cm in diameter with a thickness of at least 1mm that was free of any cortex or large inclusions.
2. Cleaned area to be sampled with a gentle dry brushing. If stubborn contaminants were present, then a second cleaning using DI water was performed.
3. Bombarded samples under three separate filter configurations for one minute per filter (one with a copper filter @ 40 keV, the second with an aluminum filter @ 15 keV, and the third unfiltered @ 40 keV.)

Reference Standard Selection

Standards used for device calibration were selected by estimating the relative elemental ratios of cherts as well as the minimum detection level of the device, and then bracketing these as much as possible. For example, previous research had shown that Fe in cherts ranges from a few hundred ppm to as much as two percent, while Cu ranged from below detection limits to a several hundred ppm. To accomplish this elemental bracketing, the following reference standards were used: USGS BCR-1 (basalt powder), USGS G-2 (granite powder), NRCCRM GBW07411 (soil powder), NBS SRM 91 (Opal Glass), USGS RGM-1 (rhyolite powder), GSC Tll-4 (till

powder), and NCS DC 73308 (soil powder). Left over powder from 15 chert samples tested via INAA from the preliminary study with known concentrations were also used to help calibrate the device. Two different internal standards were also used as standard constants to check against detector drift or malfunction, but not included in the calibration of the detector. The first was a piece of obsidian collected by the author from Glass Butte, Oregon. The second standard constant was USGS GSE-1G (basalt). Check standards were analyzed at the beginning of the project to create calibration curves and standard constants were run at the start of each batch to verify that the instrument was operating properly. Due to a hardware failure after approximately 600 samples had been processed, a second PXRF device (the Niton GOLDD+ described above) was obtained. Because of the large amount of time invested in the initial data collection, it was decided that the remaining 440 samples would be run on the replacement instrument instead of restarting the analysis of the entire dataset. To correct the different internal calibration of the new device, another run of the check standards was performed on the replacement Niton Goldd+ analyzer. Instead of calibrating to an external value however, the new instrument was calibrated to the failed Niton XL3t 500 device by using the values given for standards by the Niton XL3t 500 as “known” values instead of using published concentrations. This allowed for the direct incorporation of new data into the existing dataset. After the data was merged into a single dataset, standards ran on the old machine were calibrated to external values. Calibration curves were for the

most part linear in nature; however, potassium required a quadratic calibration curve for proper curve fitting (Appendix A: Calibration Curves). Standards used for this incorporation included the reference standards previously mentioned as well as 15 cherts that had been previously run via INAA as well as on the Niton XL3t 500 device. Not all samples had detectible concentrations of all elements tested; therefore, some calibration curves have a larger number of standards than others.

Data Examination, Preparation, and Transformations (PXRF)

One of the major obstacles when studying cherts with PXRF analysis is that some samples are almost pure silica, and contain many trace elements in quantities below detection limits of the device. Traditionally in geochemical analysis, variables that have many cases of missing data are discarded in order to simplify statistical analyses (Leah Minc, personal communication, 2010). In this research however, a different approach was used, with variables only being discarded if less than five percent of cases had detectible concentrations. Instead, when below detection limit results were obtained, a random number between .0001 and the detection limit of the device was used to replace missing data (Antweiler & Taylor, 2007). This retention of data allows for chert sources that are above detection limits on some variables to be discriminated from those which are below detection limits. For example, it two chert sources are similar on their amounts of Fe and K, but one has a detectible amount of Cu, and the second does not, this method would discriminate these two sources. If

instead Cu was removed because it was below detection limits for a source, then these two sources would not be discriminated.

Bivariate scatter plots of raw elemental ratios are also often used in geochemical studies of cherts to make group determinations. However, it was found that a more involved approach was needed to achieve group separation with this dataset. Since major, minor, and trace elements were being analyzed, a ratio matrix was created for those elements in which percent level quantities to help remove constant sum issues. This was followed by a logarithmic transformation to help data form normal distributions across variables as well as removing issues of scale. Data was then analyzed via multivariate scatter plots, principal component analysis, cluster analysis, and discriminant function analysis.

In total, Ba, Ca, Cd, Cr, Cu, Fe, K, Mn, Pb, Rb, Sr, Ti, V, and Zr were all detected in at least some of the cherts sampled. Once below level of detection measurements had been converted to random numbers below the detection limit of the device, the three elements with percent level concentrations (Ca, Fe, and K) were converted to ratios (Ca/Fe, Ca/K, and Fe/K). Using ratios of percent level concentrations helps with issues of scale between these elements versus trace elements, allows for cherts that had undergone similar formation or diagenesis processes to be grouped together even if raw element concentrations differed from sample to sample, and removes any constant sum issues in percent level data (Weltje, 2006); (Drew et al., 2010). Data

was then transformed via a base 10 logarithmic transformation. Logarithmic data transformation methods are a standard practice in geochemical analyses to correct for skewing and kurtosis (Leah Minc, personal communication, 2008), and helped reduce issues of scale between variables.

After the logarithmic and ratio transformations had been performed, each element and elemental ratio from each geologic group was analyzed for normality, outliers, and variance. Skewness and kurtosis were examined to assess normality, with values between -1 to 1 considered acceptable for skewness, and -3 to +3 for kurtosis. In all cases of high skewness/kurtosis, a few outliers were identified and removed. Outliers were quantified using the “Fourth Spread Method” (Devore, 2000); (Department of the Army, 2008, Appendix I - 13). In this method of outlier detection, any value that lies within 1.5 times the spread between the first and fourth quartiles is considered an outlier. This method of outlier detection is used in exploratory data analysis situations because the technique can be performed graphically via box and whisker plots and it has no innate requirements on sample size or distribution (Department of the Army, 2008, Appendix I-8). Given normally distributed data, this method will result in a distribution of roughly 2σ. Correlations between means and variances were tested by creating a series of regression plots of mean versus variance for each element.

Exploratory Data Analysis

Below is outlined the exploratory data analysis techniques used in the examination of chert sources as well as artifacts examined through INAA and PXRF.

Bi and Trivariate Scatterplots

A 14x14 scatterplot matrix of measured elements was created with known chert sources color coded and artifacts removed from view (Figure 15). This enables a visual assessment as to which elements were best able to separate known sources as well as allowing a check on discriminant function analysis and principal component analysis (PCA) element weighting. Elements that appeared to possibly separate groups were recorded and also examined via 3D scatter plots (Figure 16).

Principal Component Analysis

Principal Component Analysis (PCA) is a technique that is typically used to reduce the number of variables in a dataset by summarizing correlated variables into a single variable, leaving the resultant dataset as a smaller group of uncorrelated variables. The number of components initially created by PCA is the same as the number of variables being examined with each subsequent variable explaining less variation than the previous, leaving the analyst to choose how many components to retain for further analysis. There are a number of competing methods to determine how many components to save; for a detailed explanation of these different methods, please see Zwick & Velicer (1986).

While the typical usage of PCA is to reduce the dimensionality of a dataset, I chose instead to use it to remove collinearities between variables (Graham, 2003). This allows for both discriminant analysis as well as cluster analysis to be used without violating the assumption of minimal collinearities between variables (Jolliffe, 2002 pp. 200-210); (Graham, 2003).

The assumptions employed in principal component analysis vary depending on who is describing the technique. Some hold the view that nearly any data, regardless of distribution, can be examined via PCA as long as it is interval in nature. For example, Jolliffe (2002, p. 19) writes, "…*PCA and related techniques…have no need for explicit distributional assumptions,"* and Rencher (2002, p. 448) explains "*...principal component analysis requires essentially no assumptions"* (Rencher, 2002, p. 448). Others have a different interpretation. For instance, Surh (2005, p. 3) explains, that PCA must have a random sample of at least five cases per variable with at least 100 cases (preferably 10-20 cases per variable), a linear relationship between observed variables, a normal distribution for each observed variable, and that each pair of observed variables must have a bivariate normal distribution. For this analysis, I did not assume any specific distributions; however, in total, I examined 1024 cases with 14 variables, giving an end ratio of approximately 54 cases per variable.

Cluster Analysis

Cluster analysis refers to a collection of techniques used to separate a multivariate dataset into homogeneous groups when either no prior group information is known,

or when one wants to gain an understanding of how established groups relate to each other (Aldenderfer & Blashfield, 1995, p. 9). Cluster analysis requires that a dataset be representative, that variables are not collinear, and that extreme outliers have been removed (Hair et al., 1998, p. 490). Many different varieties of cluster analysis exist; in this study, Ward and Average techniques were used. Group agglomeration was performed using the Ward method on all artifacts and geologic samples using principal components extracted during PCA. Outliers were removed by doing two rounds of clustering, with individual cases that had large cluster differences being considered outliers and removed prior to the second cluster assignment (Hair et al., 1998, pp. 499:506, Figure 18). Clusters were visually assigned using a Euclidean distance graph (similar to the scree method of component selection in PCA) as well as a dendrogram, and then color coded/marked by cluster (Figure 17). These defined clusters are assumed to represent distinct chemical groups of cherts, and possibly distinct geologic sources or distinct groups of chert in a geologic source. The resulting clusters were then compared to PCA as well as DFA results by creating a 3D scatterplot of the top three principal components and discriminant functions and then examining the cluster codings on the resulting scatterplots (Figure 16). Since cluster analysis will create groupings no matter the dataset, group assignment and validation is vital. Retained Ward clusters were validated by performing a second cluster analysis using Average clustering and then by examining the cluster graphs for relative stability. Clusters that were stable across multiple different clustering

techniques were considered valid chemical groups, while clusters that were not stable were separated into an “unknown” group. Assigned clusters were used in later statistical tests. Separate cluster analyses were performed on known geologic sources, artifacts, and pooled artifacts/known sources.

Classical Statistical Tests

Analysis of Variance and Chi-Square

Assuming for a moment that cluster analysis groupings of chemical data represent distinct chemical groups and that these chemical groups may be a result of cherts coming from differing geologic sources, then an analysis of variance (ANOVA) test can be used to see if there are relationships between continuous variables measured in chert artifacts and geologic sources of chert. Both artifact mass as well as its distance below datum was tested against cluster assignment to see if any patterns existed between these variables. Chi-Square ($\chi 2$) was used with the same cluster/source assumption for categorical variables, including documented material type (i.e. red jasper, opal, chalcedony, agate, green stone, ccs), 1x1 meter quadrant of unit excavated from (i.e. NW, SW, SE, E, NE), artifact type (i.e. biface, uniface, blade, modified flake, debitage), lithostratigraphic unit (LU), and defined cultural component (Davis, 2001; Table 3) or pooled depending on their total amount in the analysis. For example, in the material $\chi 2$, “seam quartz” was removed from analysis because there were only two instances in the dataset. See the results section for a complete breakdown of variables removed and pooled during analysis.

Discriminant Function Analysis

Discriminant function analysis (DFA) is a Bayesian multivariate statistical technique used to highlight differences between known groups (descriptive DFA) as well as to assign unknown individuals into established groups (predictive DFA) (Hair et al., 1998 p. 1; Huberty et al., 1987). Descriptive DFA was used to determine if cherts that were collected *in situ* from known locations in the landscape (geologic sources) could be discriminated into distinct groups. Once this was established, predictive DFA was then used to examine whether unknown archaeological artifacts could be assigned to these groups. Assumptions for DFA include multivariate normality of independent variables, a lack of multicollinearity, equal variance/covariance matrices, and a lack of extreme outliers (Hair et al., 1998, p. 259; Shackley S. M., 1998). Variance, normality, and outliers were examined using the methods explained above in the "Data Examination, Preparation, Transformations" section, and issues of potential multicollinearity was rectified by using principal components as predictor variables, a technique dubbed by Jombart et al. (2010) as "DAPC" or discriminant analysis of principal components; see also (Fekedulegn et al., 2002). Sample size is also of import in discriminant analysis, with a ratio of 20:1 recommended for a sample to independent variable ratio, and a 5:1 ratio as an absolute minimum. Also, the smallest group examined by DFA must have more cases than the number of independent variables. Finally, group sizes cannot vary in the extreme from one to the next (Hair et al., 1998, p. 258). In this research, three descriptive DFA and one

predictive DFA were performed. All predictor variables were analyzed simultaneously, with separate group co-variances assumed on all four analyses. Squared Mahalanobis distances (D^2) were computed, and conditional probabilities for potential group membership were calculated by using the $\chi 2$ distribution.

When assigning unknown samples to known groups in predictive DFA, type 1, type 2, and type 3 errors can result (Luedtke, 1979); (Knippenberg, 2006). Type 1 errors occur when an unknown sample is assigned to a known group A, when it is actually from a known group B. Type 2 errors occur when an unknown sample is classified as coming from some unknown group not in the analysis, when in fact it came from group A or B, and type 3 errors occur when an unknown sample is assigned to a known group A or B, but is actually from some unknown sample (Figure 19). To address these issues, a methodology was implemented with cutoff values to determine unknown case membership. Luedtke (1979) computed the mean and standard deviation D^2 values based on descriptive DFA group results. From these results, she decided upon a cutoff D^2 value of 15 across all groups for her analyses, which in her dataset and methods included cases within two standard deviations for some groups, and up to eleven standard deviations from the group mean being included in others. While this cutoff value limited the number of type 2 errors, it raised the risk of type 3 errors, which are more serious in nature (Luedtke, 1979). Other researchers take a slightly different approach. For example, Knippenberg (2006) uses a maximum D^2 value from each group obtained in descriptive DFA to

establish a per group cutoff value. To combat the risk of type 3 errors occurring, I used a D^2 cutoff value that represented a single standard deviation from group means. However, instead of using the average and standard deviation D^2 values for known groups, I used the conditional probability of the D^2 statistic (determined by the $\chi 2$ distribution with k-1 degrees of freedom, with k representing groups) to establish the appropriate cutoff for group membership. This allowed for a single D^2 value to be used across all groups for group membership instead of differing values for each group. Posterior probabilities were then examined for "fence sitters" (i.e. cases that were within one standard deviation of more than one group), which were then documented as being unable to be assigned to any one group.

Preliminary INAA Study Statistical Methods

Because of the relatively small sample size of the chert groups in the pilot study (i.e. 76 samples in total across nine groups), multivariate statistical methods became more difficult to perform. As previously noted, there is some disagreement to the minimum amount of cases required for principal component analysis; however using Jolliffe's (2002) interpretation of having no specific distributional requirements, PCA is still a valid technique for use in the analysis of this dataset. Discriminant function analysis requires at least 15 individuals per group for proper group characterization and assignment, so it was not used for this analysis (some of the groups in this dataset have only 4 or 5 cases).

External Data Check

To test the effectiveness of the previously mentioned statistical approach, an external dataset was obtained. Data from four separate INAA analyses of cherts published by the University of Missouri Research Reactor (MURR) (http://archaeometry.missouri.edu/datasets/datasets.html, date of access 5/10/2011) were downloaded and combined into a single dataset. Archaeological artifacts were removed from the analysis as the goal was to determine the effectiveness of grouping known cherts into distinct chemical groups via descriptive discriminant analysis. After removal of archaeological artifacts, the dataset contained 267 cases and 15 separate groups (Table 4). Groups with fewer than 15 individuals per group were removed, leaving 213 samples in total. In the next chapter, I discuss the results of statistical tests, my preliminary INAA study, and the external INAA data from MURR as a precursor to the analysis of PXRF on collected geologic sources of chert as well as archaeological artifacts from the Cooper's Ferry site.

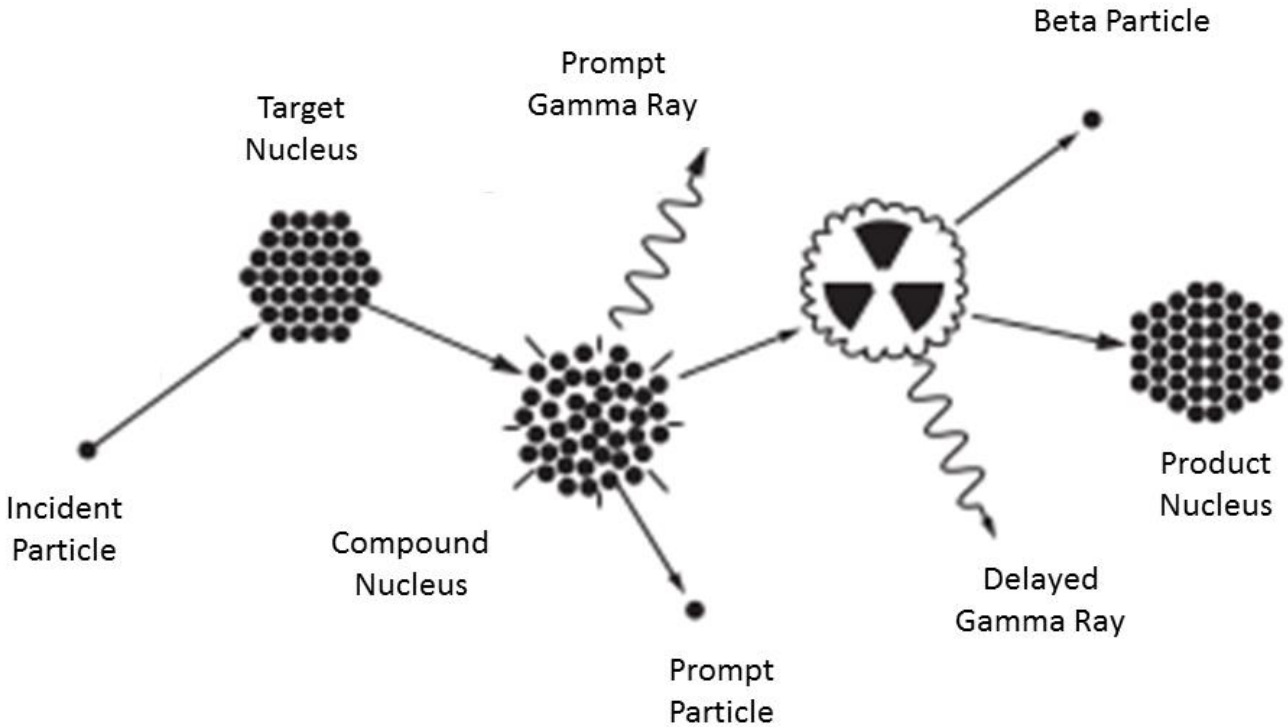

Figure 13 - Neutron Activation Analysis diagram - From Glascock & Heff (2003).

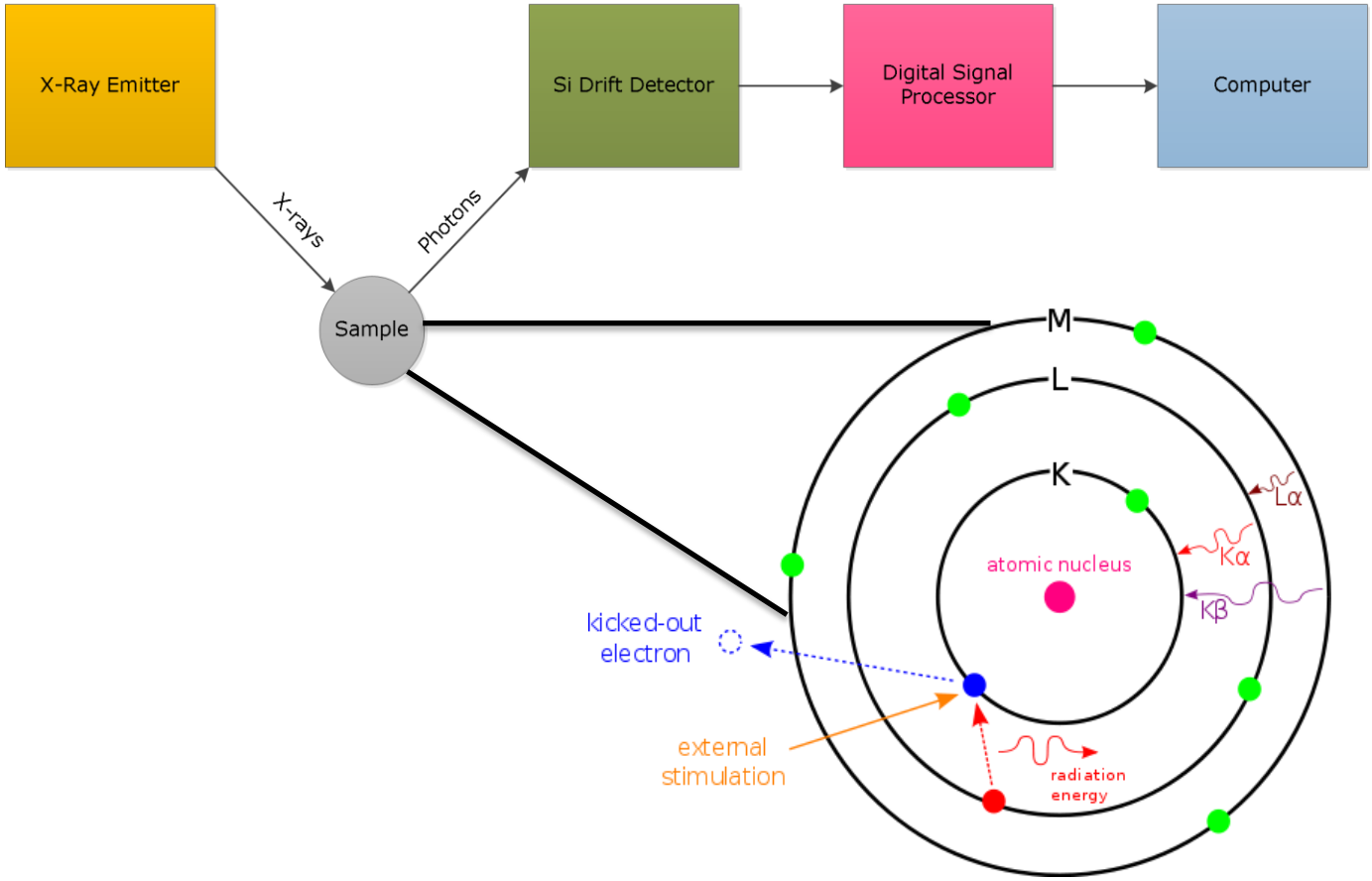

Figure 14 - Energy Dispersive X-ray Fluorescence Atomic Diagram. Modified from: "http://en.wikipedia.org/wiki/Energy-dispersive Xray Spectroscopy"

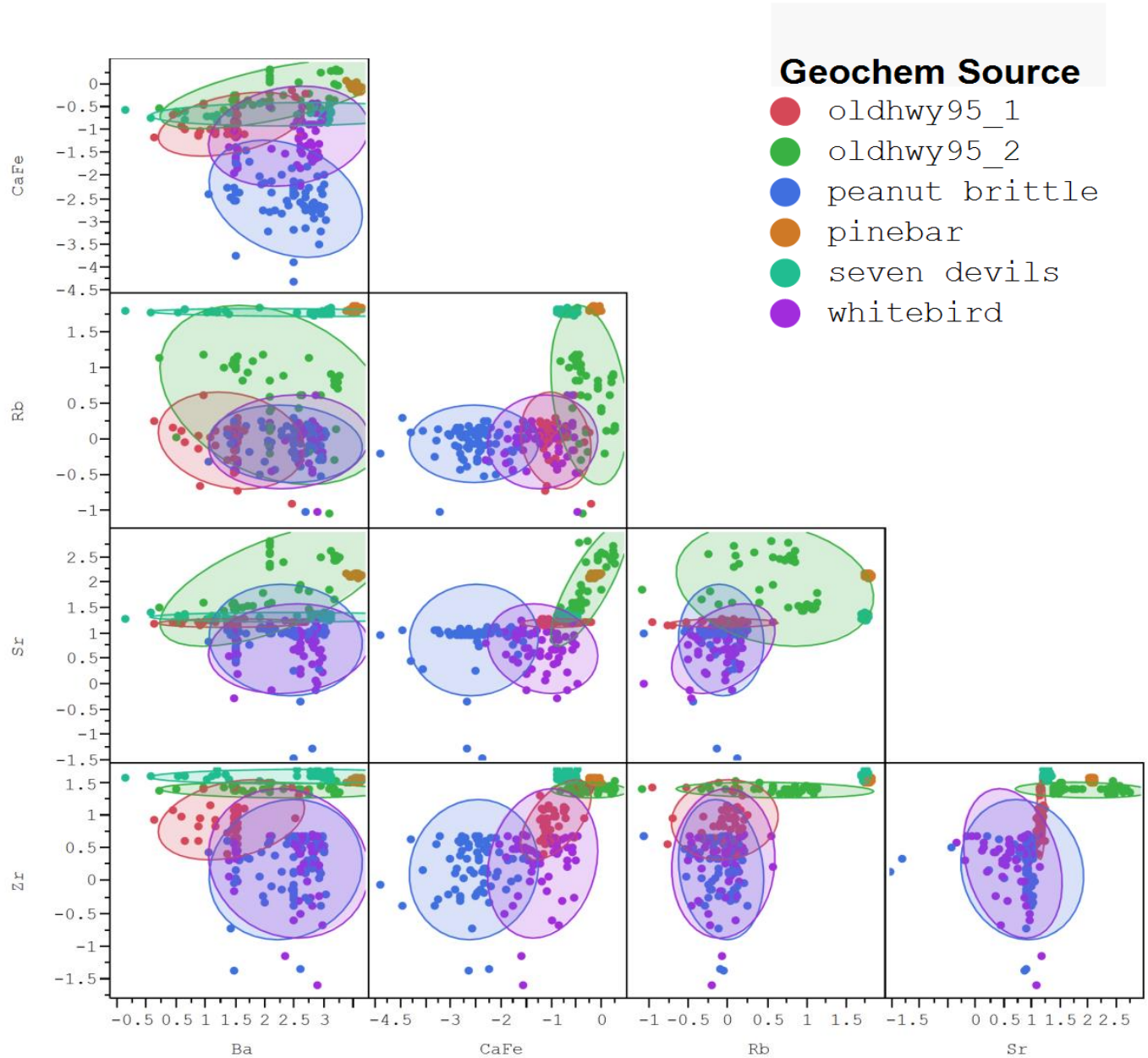

Figure 15 - Example scatterplot matrix. Colors designate different geologic sources. Ellipses are at the 95 percent confidence interval.

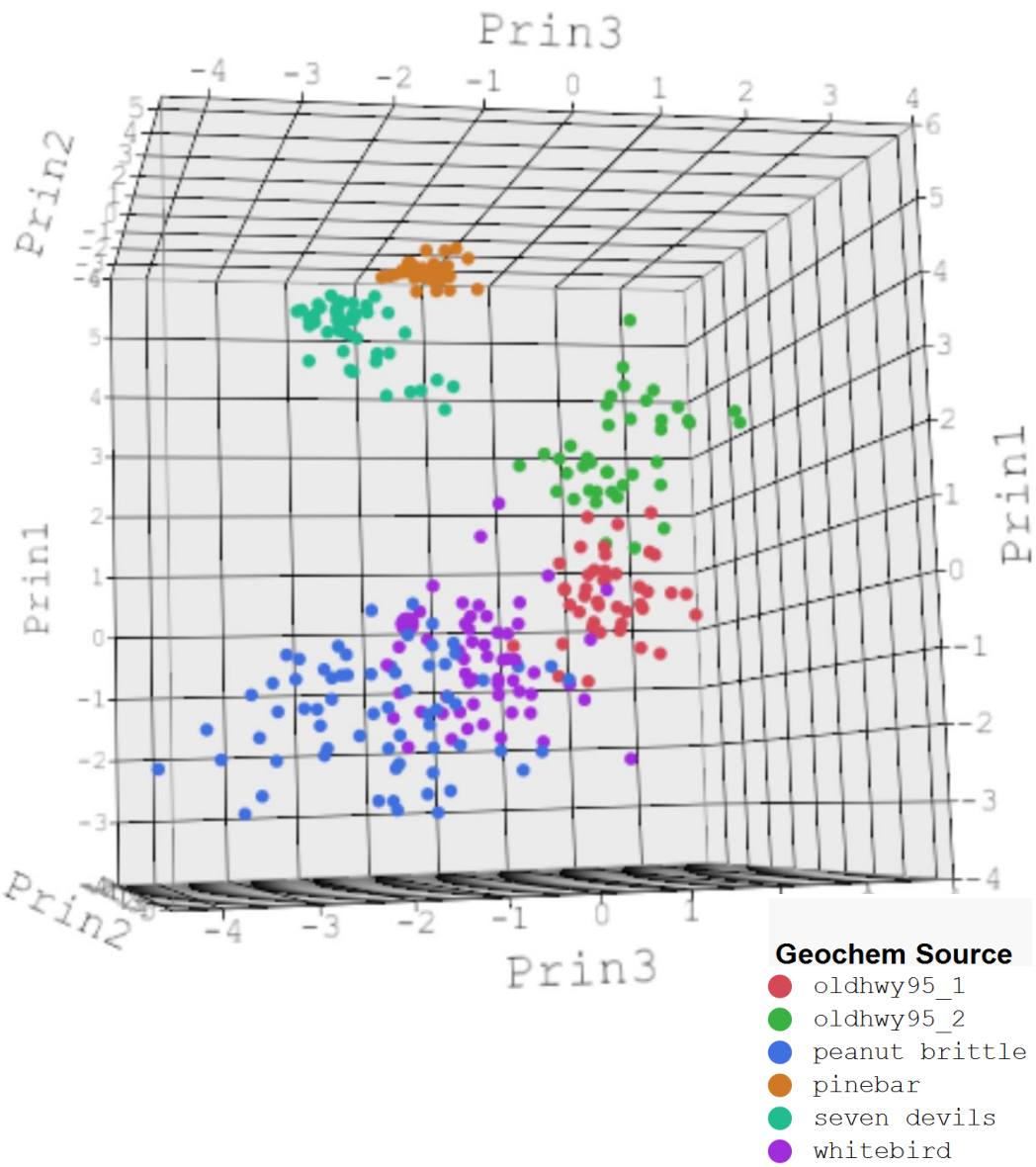

Figure 16 - 3D scatterplot of first three principal components, color coded by geologic source. Artifacts have been removed from this view for viewing simplicity, leaving known geologic sources.

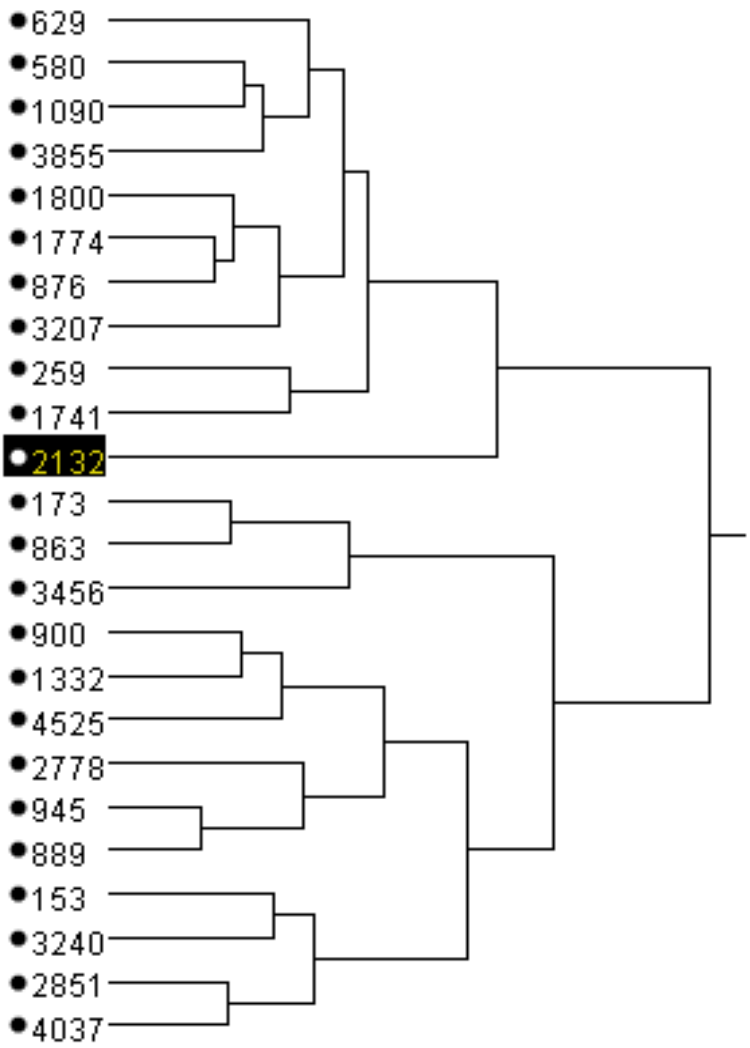

Figure 17 – Cluster Dendrogram. 2132 (the highlighted case) would be considered an outlier in this analysis.

Figure 18 – Distance plot example from cluster analysis

Description of Artifacts	Cultural Component	Lithostratigraphic Unit
Marked reduction in artifactual and faunal materials, absence of fire cracked rock.	A5 / A6	8b / 8a
Small leaf-shaped lanceolate points, a Bitterroot Side Notched point, hearths, debitage, modified flakes, unifaces, and bifaces	A4	6
Two stemmed Windust lanceolate points, one stemmed point fragment, debitage, modified flakes, unifaces, bifaces	A3	5
Lanceolate point fragment, hearth, debitage, unifaces, bifaces, multidirectional flake core, modified flakes	A2	4
Four Lind Coulee points, large scraper, blade found in cache pit extending downward from LU 6 surface; debitage found on and in surface of LU 6	A1	3

Table 3– Cultural components of unit A at Cooper's Ferry. Modified from Davis (2001 : Fig 108).

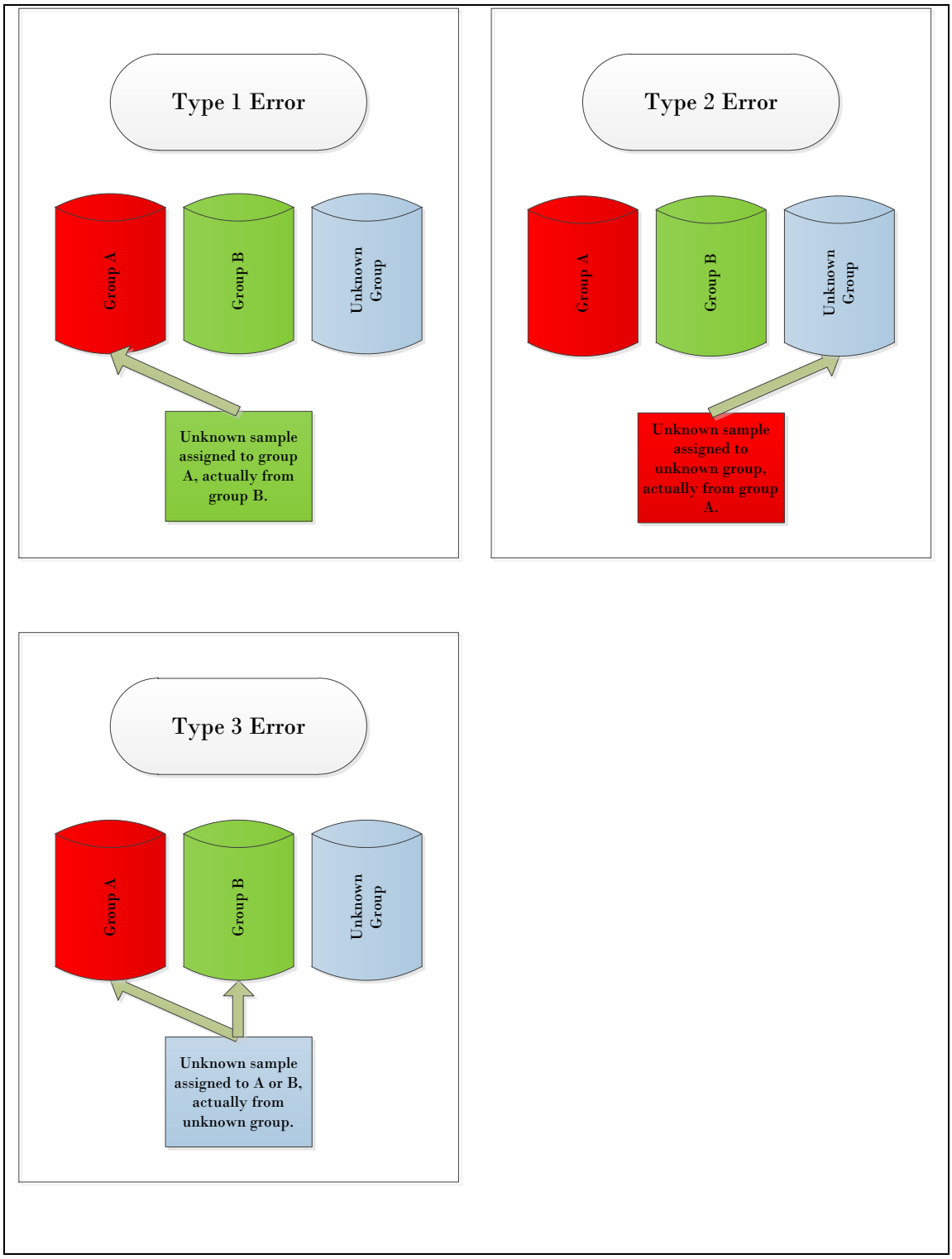

Figure 19 – Three types of classification errors as defined by Luedtke (1979).

Source Name	Count
Birch Creek Source, Malheur County, Oregon	17
Cobden-Dongola, Union County, Illinois	32
Flattop Butte, Colorado	36
Gering Formation, Nebraska*	10
Knife River, North Dakota	40
Mud Lake (Buena Vista Station), Oregon*	4
Mud Lake (Dog Mtn.), Oregon*	6
Mud Lake (Eagle's Nest), Oregon*	10
Nelson Butte, South Dakota	10
“other NV”*	4
Red Butte, Malheur Co., Oregon	15
Rome Beds, Malheur Co., Oregon*	10
Table Mountain, Wyoming	30
Tosawihi	18
West Horse Creek, South Dakota	25

Table 4 - Groups from combined MURR dataset. * Groups containing fewer than 15 members were removed from analysis.

Chapter 4: Results

In this chapter, an overview of the results from the survey for cherts in the LSRC is discussed. Results of the preliminary INAA study are presented, which is followed by an overview of the external data test. PXRF of geologic sources of cherts located in the LSRC are then covered, and the chapter is concluded with the results from PXRF analysis of artifacts from Cooper's Ferry.

Results of Survey for Geologic Sources of Cherts

In total, six geologic sources of chert were found by the author that were extensive enough for chemical characterization. Their descriptions follow below.

Pine Bar "Chert"

Originally dubbed Pine Bar "chert", this material is not a chert, but appears to be a silicified volcanic tuff. The exposure bearing this tuff is approximately 40 meters long by 20 meters wide and is located at the base of the canyon to the east of the Pine Bar Campground where it extends into the Salmon River at UTM 11T 552061, 5082063 (Figure 20). It lies directly on the contact region between the Wallowa Arc terrain and the Columbia River Basalt group. Pine Bar material is knappable, however it is more difficult to knap compared to other cherts recorded during survey. Cortex is pinkish-white in color and the matrix is grey-green (Appendix G. - Pine Bar Geologic Samples). Heat treating this material (400°C for seven hours) had no readily apparent effects on color or fracture patterns.

White Bird

White Bird chert is nodular in form and found in a decomposing Columbia River Basalt flow north of the town of White Bird at UTM 11T 556094, 5073524 (Figure 20). Nodules range in size from a few centimeters up to 15-20 centimeters in diameter. Cortex is typically white and yellow in color, with matrix colors ranging from semi-transparent blue-grey to yellow, white, and some red, and is easily knapped (Appendix G - White Bird Geologic Samples). Heat treatment of this chert (400 ^{o}C for seven hours) resulted in some color changes, with yellow and white colors being changed to red. This chert shattered upon cool-down from heat-treatment with two hour ramp-ups and downs; it is possible that extending the ramp times would have kept the chert from shattering.

Peanut Brittle

Peanut Brittle chert is found in veins within a decomposing basalt flow next to the town of Cottonwood UTM 11T551339, 5099069 (Figure 20). Dubbed “peanut brittle” due to its resemblance to the candy with the same name, it is glassy brown, opaque, and easily knapped. Veins run several meters long and are up to six cm in width. Heat treatment of this chert at 400° C for seven hours caused it to turn from a brown color to a burgundy color (Appendix G - Peanut Brittle Geologic Samples), resembling what is commonly called “red jasper” in the Columbia River Plateau (Loren Davis, personal communication, 2013), and also seemed to improve the knapping quality.

Seven Devils

Seven Devils chert is found as eroding horizontal lenses several meters wide and up to 20-30 cm thick in a weathered limestone deposit outside the town of Riggins, ID, approximately 55km to the south of Cooper's Ferry at UTM 11T 550910, 5099227 (Figure 20). Dubbed Seven Devils for its proximity to the mountains in which it is found, this chert lies in the Coon Hollow formation of the Wallowa Arc accreted terrain. Unlike the other cherts tested here, its parent silica is not volcanic in origin, but instead from a marine context, forming from silica contributed by the surrounding limestone (whether this limestone deposit was organic or inorganic in origin is not known at this time). Individual nodules have a thick, white cortex and gradate into multicolored greens, blues, and in some cases purple (Appendix G - Seven Devils Geologic Samples). Heat treatment did not cause any color changes in this chert. As with White Bird chert, it did shatter upon cool down. Experimentation with ramp times and temperature profiles may change these results.

Old Hwy 95_1 and Old Hwy 95_2

These two cherts will be included in the same description as they are very similar in macroscopic characteristics and were collected from similar deposits less than 1km apart from each other, near the town of White Bird, ID (UTM 11T 560909, 5078326 and UTM 11T 561228, 5079110 respectively, Figure 20). Discovered in a road cut of old US Highway 95, they were both expressed as irregularly angled veins within a highly decomposed basalt flow, ranging from approximately one to six centimeters

thick, and were also present as small nodules on the surface both above and below the road cut (Appendix G – Geologic Source Photographs). Veins were highly fractured, with the largest nodules being around five cm in diameter, but most being one to two centimeters in diameter. It is unclear if this fracturing is due to weathering or road construction. Heat treatment at 400°C did not cause any color changes in this chert. As with White Bird chert, both of these cherts shattered upon cool down.

Preliminary OSU INAA Study Results

Scatterplots – OSU INAA Data

Scatterplots of elements tested via INAA at Oregon State University showed some interesting patterning. First, the White Bird chert source appears to have a higher degree of variation compared to the other sources across all elements tested (Appendix C: Scatterplot Matrices). Second, the chert sources graphically separate fairly well in bivariate space. In this dataset, Selenium and Hafnium appear particularly well suited to resolving sources, though some overlap does occur (Figure 21). Also of note is that when viewing the entire scatterplot matrix (Appendix C: Scatterplot Matrices), multicollinearities between many elements tested are readily apparent, highlighting the need for PCA. This graphic representation is a clear indicator as to why using principal component analysis is critical when performing multivariate statistical analyses such as DFA on cherts, as these collinearities would violate the assumptions of cluster or discriminant analysis. Raw data was

transformed via log10 in order to remove any scaling issues as well as to enhance normality.

Principal Component Analysis – OSU INAA Data

Principal component analysis of the OSU INAA dataset (Figure 22) reveals that there is more variation within the White Bird chert source than the other sources . Chert sources also appear to be forming clusters, showing promise for sourcing if sample sizes were to be increased. Of note is that the Peanut Brittle, Seven Devils, and White Bird chert sources all separate well in this initial testing.

Cluster Analysis – OSU INAA Data

Cluster analysis was performed on principal components of INAA data to assess the sourcing potential of cherts collected in the field. As can be seen in Figure 23, clusters form around known geologic sources with fairly minimal intermixing and a good deal of cluster stability. This stability between clustering solutions and grouping of samples that matches geologic sources indicates that there is good potential to differentiate chert sources using geochemical methods.

External Data Test – MURR INAA Data

Scatterplots - MURR INAA Data

Scatterplot of elements tested in the INAA dataset obtained from MURR show good promise for discriminating chert sources; however no two - or three-element combinations can separate all sources simultaneously. As in the previous dataset, differing amounts of variation are seen between group means in log10 transformed

elemental data. Cesium, Rubidium, and Hafnium appear to resolve the different geologic groups best, although some overlap does occur between sources (Figure 24). Eleven different variable combinations have R^2 values above 0.8 (Table 5), indicating the presence multicollinearities within this dataset. Raw data was transformed via log10 in order to remove any scaling issues as well as enhance normality.

Principal Component Analysis - MURR INAA Data

Results of principal component analysis of the MURR dataset are shown below. As can be seen from the bivariate scatterplot of the first two principal components, there is some separation between groups; however overlaps exist between others (Figure 25). The Table Mountain, Flattop Butte, and West Horse Creek sources are completely overlapped in bivariate space, and Cobden-Dongola as well as Knife River also overlap considerably. Viewing the first three principal components simultaneously helps to further differentiate groups, but cannot resolve overlapping distributions (Figure 26). Upon generation, all principal components were retained for later discriminant analysis as well as cluster analysis.

Cluster Analysis – MURR INAA Data

Cluster analysis of principal components of the external MURR data is listed below (Figure 27), color coded by geologic source. The clustering algorithms grouped clusters by their geographic source, and as seen, as in principal component analysis, some intermixing occurs between Flattop Butte and West Horse Creek. As seen in

the cluster analysis performed on the preliminary INAA data generated by this author, clusters are stable across algorithms and are largely aligned with geologic sources.

Discriminant Function Analysis - MURR INAA Data

As previously discussed, one of the assumptions for DFA is that there is equal variance across groups (Hair et al., 1998). One method of testing variance in multivariate datasets is the Box's M test (Hair et al., 1998). Based on the high significance of Box's M results (Table 6) in this analysis, unequal group variances were assumed for DFA, dictating the need for the use of a quadratic as opposed to a linear classification model (Joachimsthale & Stam, 1988). Because group sizes were unequal in the analysis, prior probabilities were based on group size instead of being considered equal for all groups (Table 7). Using quadratic descriptive discriminant analysis and prior probabilities based on group membership, classification results show a 100% successful classification for all sources analyzed (Table 8). Bivariate and trivariate plots of retained discriminant canons graphically highlights the differences between sources (Figures 28 and 29).

PXRF Results – LSRC Geologic Chert Sources

Principal Component Analysis - LSRC Geologic Cherts

Results of principal component analysis of geochemical sources collected by the author in the study area show differentiation between sources (Appendix F – PXRF Principal Components of Geologic Sources), though some overlap occurs when

viewed via bivariate (Figure 30) scatterplots. As in the MURR dataset, viewing the data in trivariate form (Figure 31) helps different sources, but overlaps still do occur, especially with the Peanut Brittle and White Bird chert sources. This is somewhat expected as components are not being leveraged to maximize distances between groups, but instead to remove all collinearities between variables. All principal components generated were retained and used for later discriminant function analysis.

Cluster Analysis - LSRC Geologic Cherts

As with both the MURR data and the preliminary INAA study, cluster analysis of retained principal components grouped chert sources together both via ward as well as average cluster analysis (Figure 32). Clusters were relatively stable across algorithms, with some mixing between the Peanut Brittle and White Bird chert sources. This intermixing mirrors the intermixing seen in principal component analysis. Still, cluster analysis of known geologic sources was largely successful in grouping cherts according to their source.

Discriminant Function Analysis - LSRC Geologic Cherts

Based on the significance of Box's M test results (Table 9), unequal group variances were assumed for DFA. As in the previous discriminant analyses, a quadratic model was used in analysis instead of a linear classification model. Also, because group sizes were unequal in the analysis, prior probabilities were based on group size instead of being considered equal for all groups (Table 10). Using this methodology,

classification results showed 97.9% successful classification across sources (Table 11). When viewed on scatter plots (Figures 34-37), it becomes readily apparent that two chert sources (Pine Bar and Seven Devils) are different geochemically from the other four groups, which are fairly closely clustered together. Examination of D^2 values from casewise statistics back up this finding, with large secondary group D^2 values for these sources (Table 12). Since no artifacts were grouped within a single standard deviation of either Pine Bar or Seven Devils (except for a single piece of debitage, catalog number 2302, which was grouped with the Pine Bar source), they were removed and a second discriminant analysis was performed to better leverage the differences between the four remaining groups. When the descriptive DFA was performed with Pine Bar and Seven Devils removed, differences in variance between groups were reduced to the point that linear DFA was possible to use instead of quadratic DFA, allowing for a leave one out approach of cross validation (Table 13). Using cross validation, 95 percent of samples were correctly classified into their representative geologic sources (Table 13; Appendix – Geochemic Sources – Four Group Solution). Since discriminant analysis seeks to maximize the distances between groups, and Pine Bar as well as Seven Devils were very different from the other four chert sources, removal of these two has the effect of increasing the relative distance between the four remaining groups. This can be seen in bivariate and trivariate scatterplots (Figures 34-37).

PXRF Results – Cooper's Ferry Chert Artifacts

Principal Component Analysis – Cooper's Ferry Chert Artifacts

When examining bivariate plots of PCA results of artifactual data, combined with established source data, several traits stand out (Figure 37). First, most artifacts (shown below as black points) appear to cluster around a single centroid that is partially eclipsed by several geologic groups, but not centered in any. Second, as was stated in the previous section, artifacts are very different chemically from Pine Bar and Seven Devils, except for one artifact, number 2302 which is the black dot to the right of the Pine Bar ellipse.

Cluster Analysis – Cooper's Ferry Chert Artifacts

As in previous analyses, Ward and Average cluster analyses were performed on retained PCA components, with geologic sources color coded by their source (Figure 38). Note that the Seven Devils, Pine Bar, and Old Highway 95_2 sources group almost exclusively together. Old Highway 95_1 and Peanut Brittle are for the most part grouped together, while the White Bird source is mixed with the archaeological artifacts found. This suggests that most of the artifacts analyzed from the 1997 Cooper's Ferry archaeological excavation are of similar chemical composition to the White Bird chert source. One artifact, catalog number 2302, a piece of debitage found in LU 6, was grouped by cluster analysis as being similar to the Pine Bar source (Figure 38 and 39). To assign groups to artifacts, geologic samples were removed, and a new set of cluster analyses were performed. Clusters were retained based on

the relative distances between groups as well as by comparing both Ward and Average clustering algorithms concurrently to see when relative stability was achieved (Figure 40). Retained clusters were then used for later analyses.

Discriminant Function Analysis – Cooper's Ferry Chert Artifacts

After removing the Seven Devils and Pine Bar sources from the analysis due to a lack of geochemical similarity with other cherts tested, PDFA showed that 73.8% of artifacts (443 out of 600) did not fall within a single standard deviation of any tested geologic sources. Of the remaining 157 artifacts, 21 were grouped with Old Hwy95_1, five were grouped with Peanut Brittle, and the remaining 131 were grouped with the White Bird chert source.

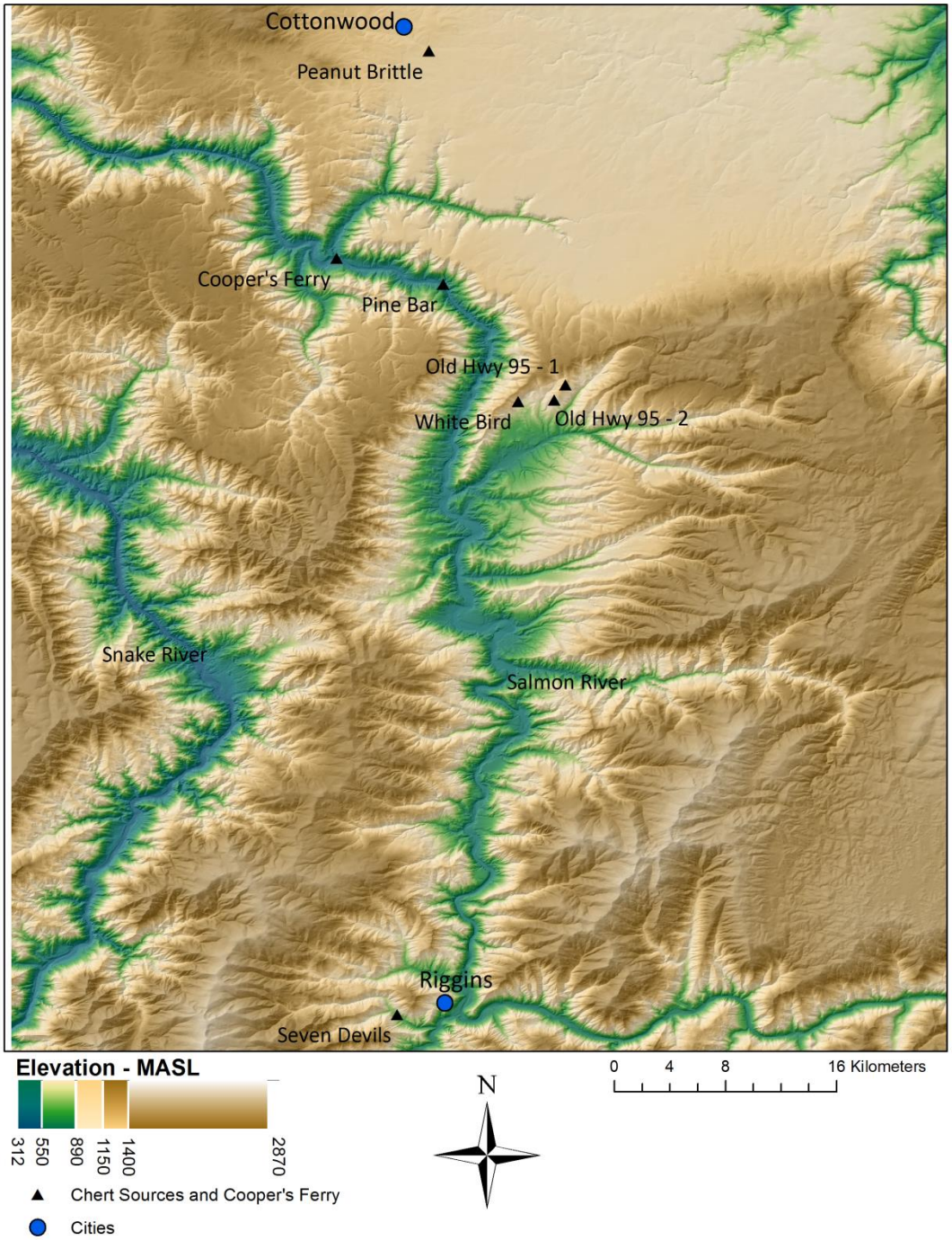

Figure 20 - Chert source locations in relation to Cooper's Ferry.

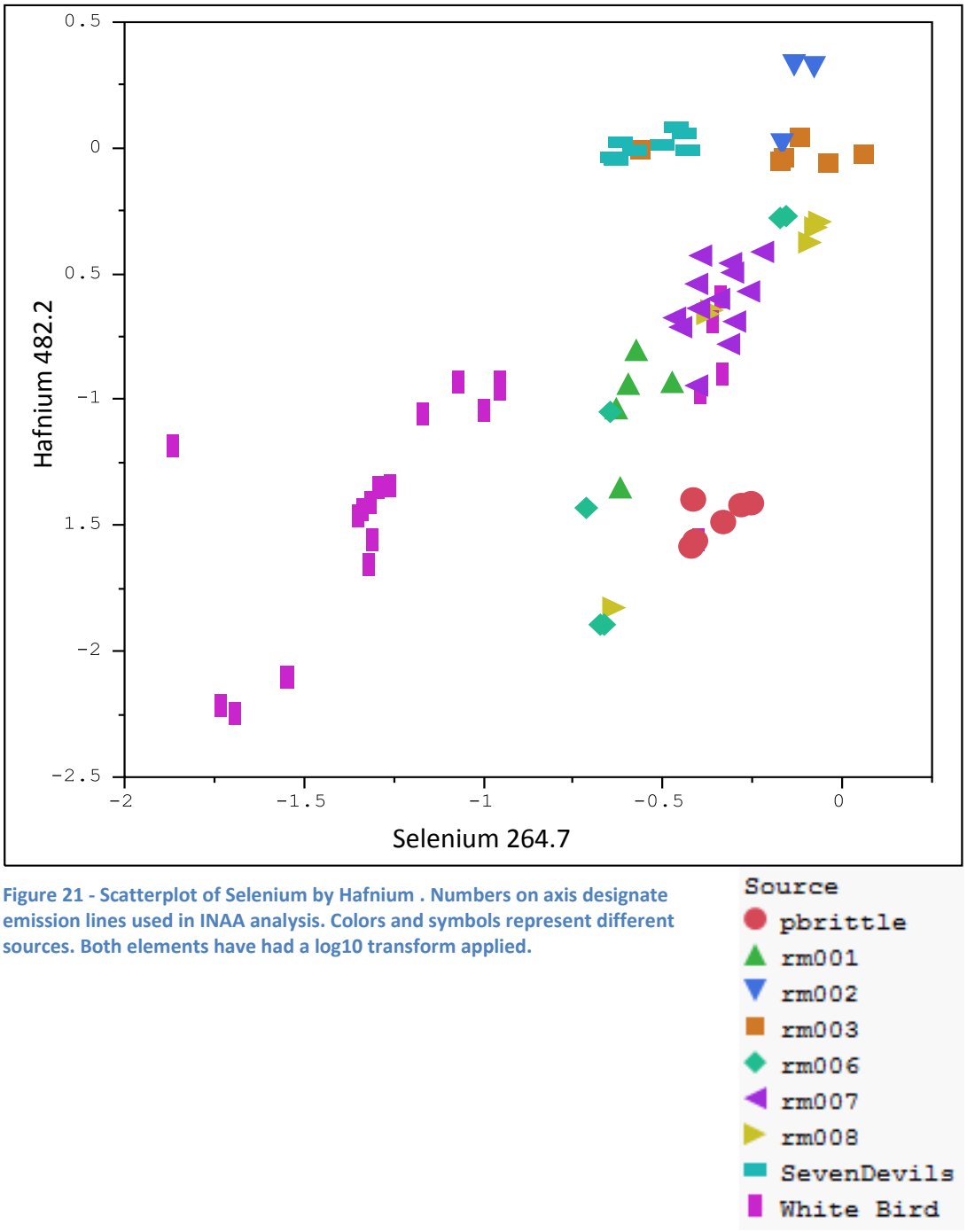

Figure 21 - Scatterplot of Selenium by Hafnium . Numbers on axis designate emission lines used in INAA analysis. Colors and symbols represent different sources. Both elements have had a log10 transform applied.

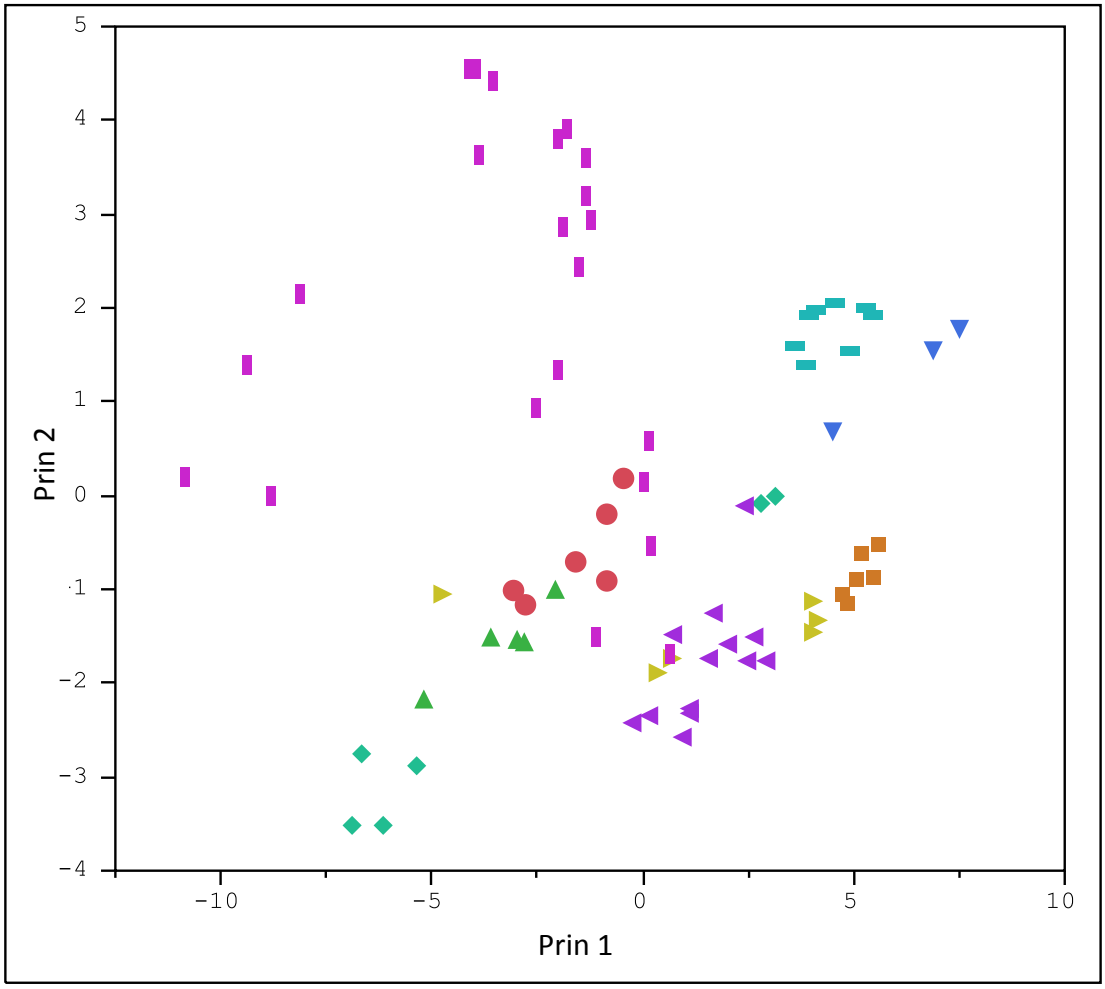

Figure 22 - First two principal components. Colors and symbols designate sources.

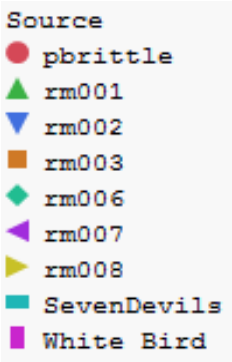

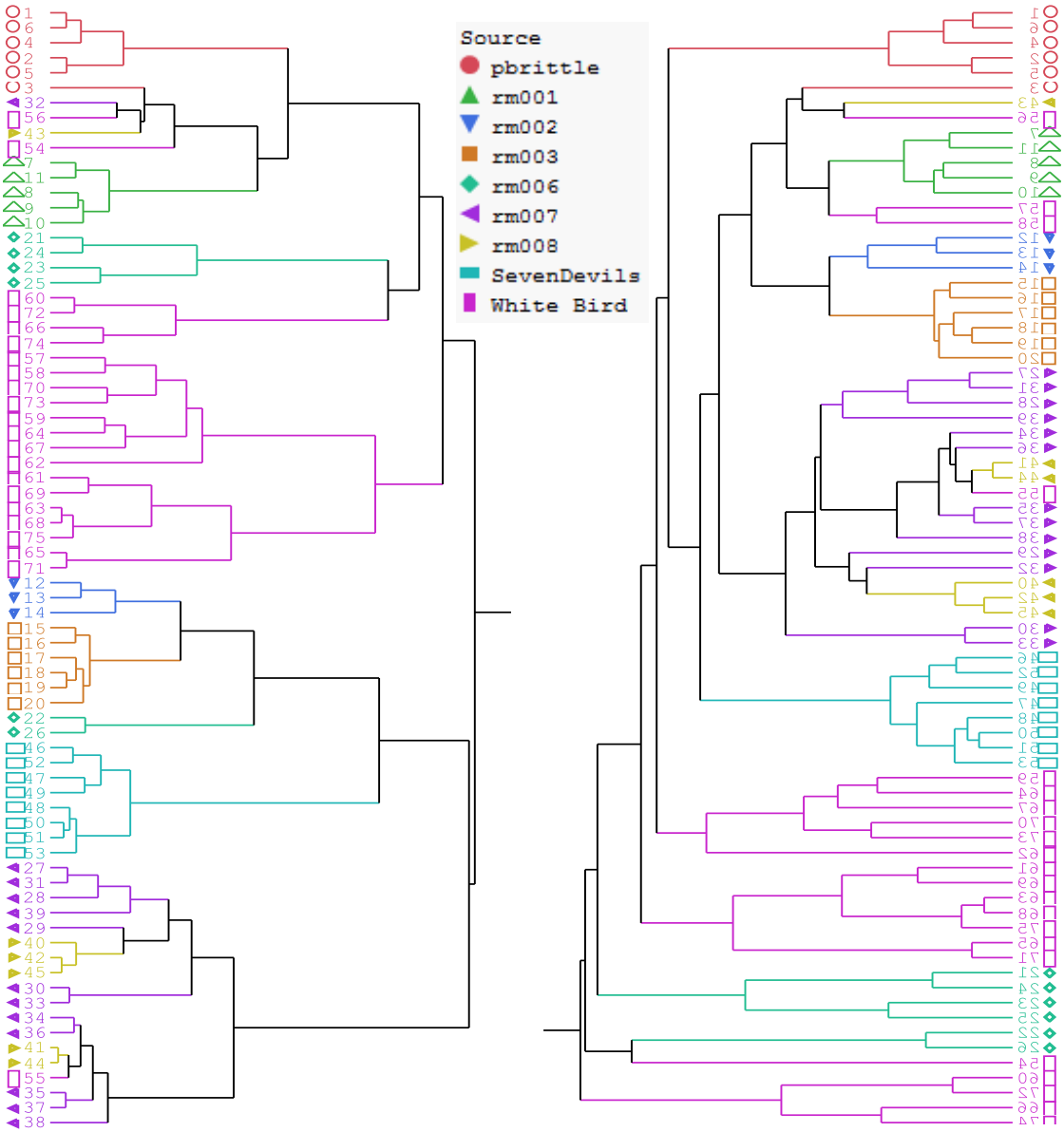

Figure 23 – Ward (left) and Average (right) clustering algorithms for Preliminary INAA data. Results are color and symbol coded to known geologic sources.

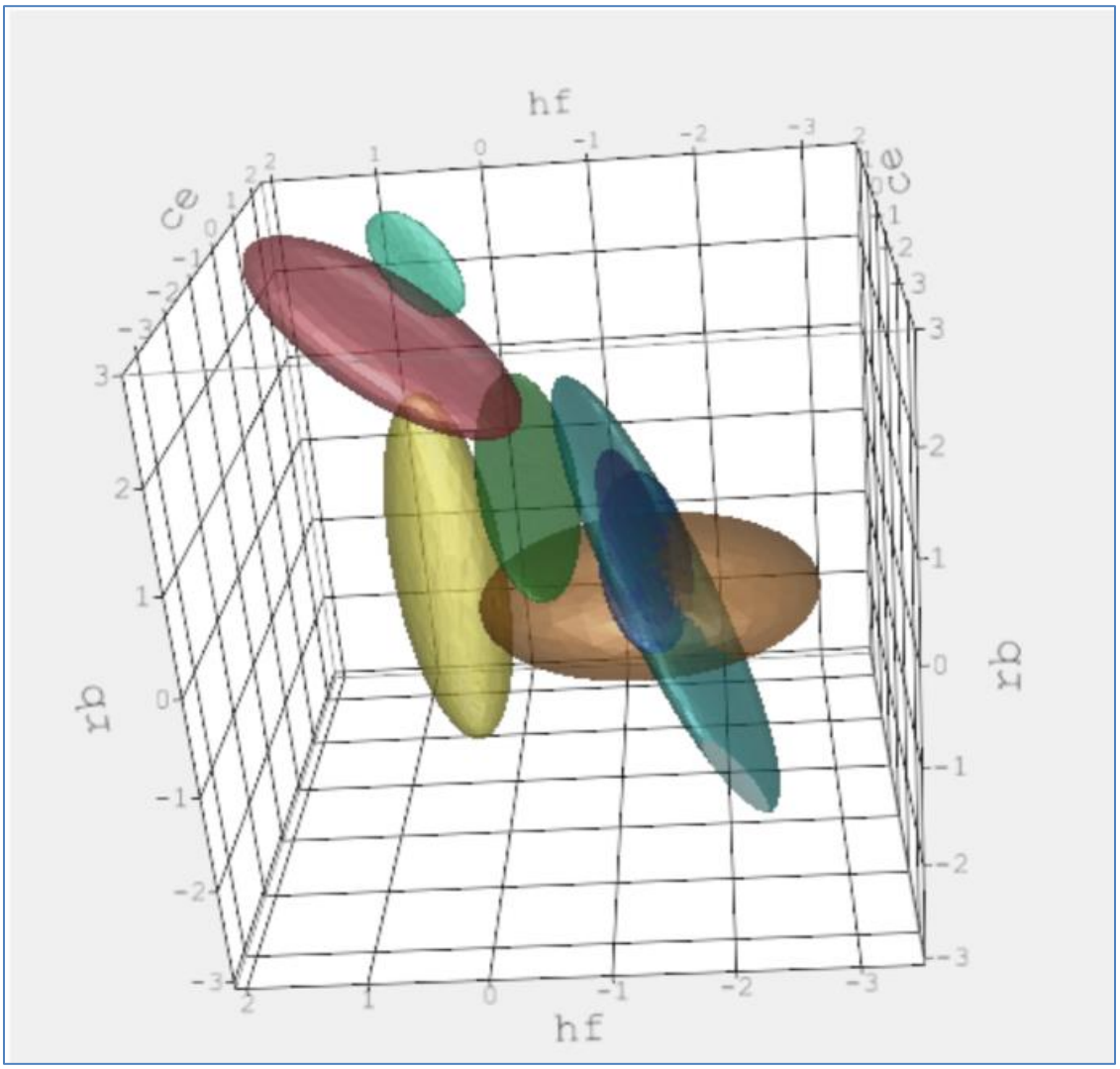

Figure 24 - 3D scatterplot of Rb, Hf, and Ce of MURR data. Ellipses represent 95% confidence intervals.

Site Name

- Birch Creek Source, Malheur County, Oregon
- Cobden-Dongola, Union County, Illinois
- Flattop Butte, Colorado
- Knife River, North Dakota
- Red Butte, Malheur Co., Oregon
- Table Mountain, Wyoming
- Tosawihi
- West Horse Creek, South Dakota

Co x Zn	Cs x Rb	Cs x Ta
La x Eu	Tb x Eu	Yb x Eu
Ta x Hf	Th x Hf	Yb x La
Zn x Rb	Yb x Tb	

Table 5 - Element combinations with R2 values above 0.8, indicating high levels of collinearities in the MURR external dataset.

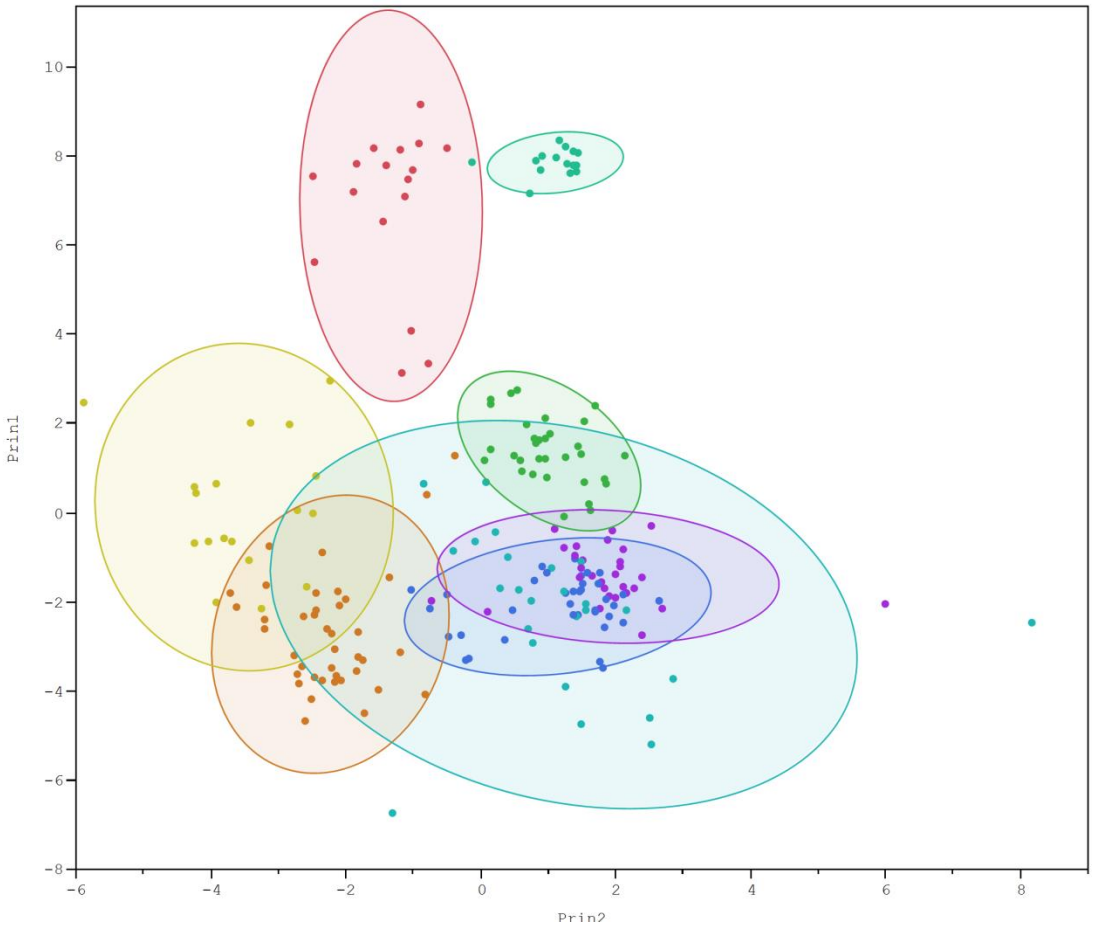

Site Name

- Birch Creek Source, Malheur County, Oregon
- Cobden-Dongola, Union County, Illinois
- Flattop Butte, Colorado
- Knife River, North Dakota
- Red Butte, Malheur Co., Oregon
- Table Mountain, Wyoming
- Tosawihi
- West Horse Creek, South Dakota

Figure 25 –First two principal components from principal component analysis of external MURR dataset.

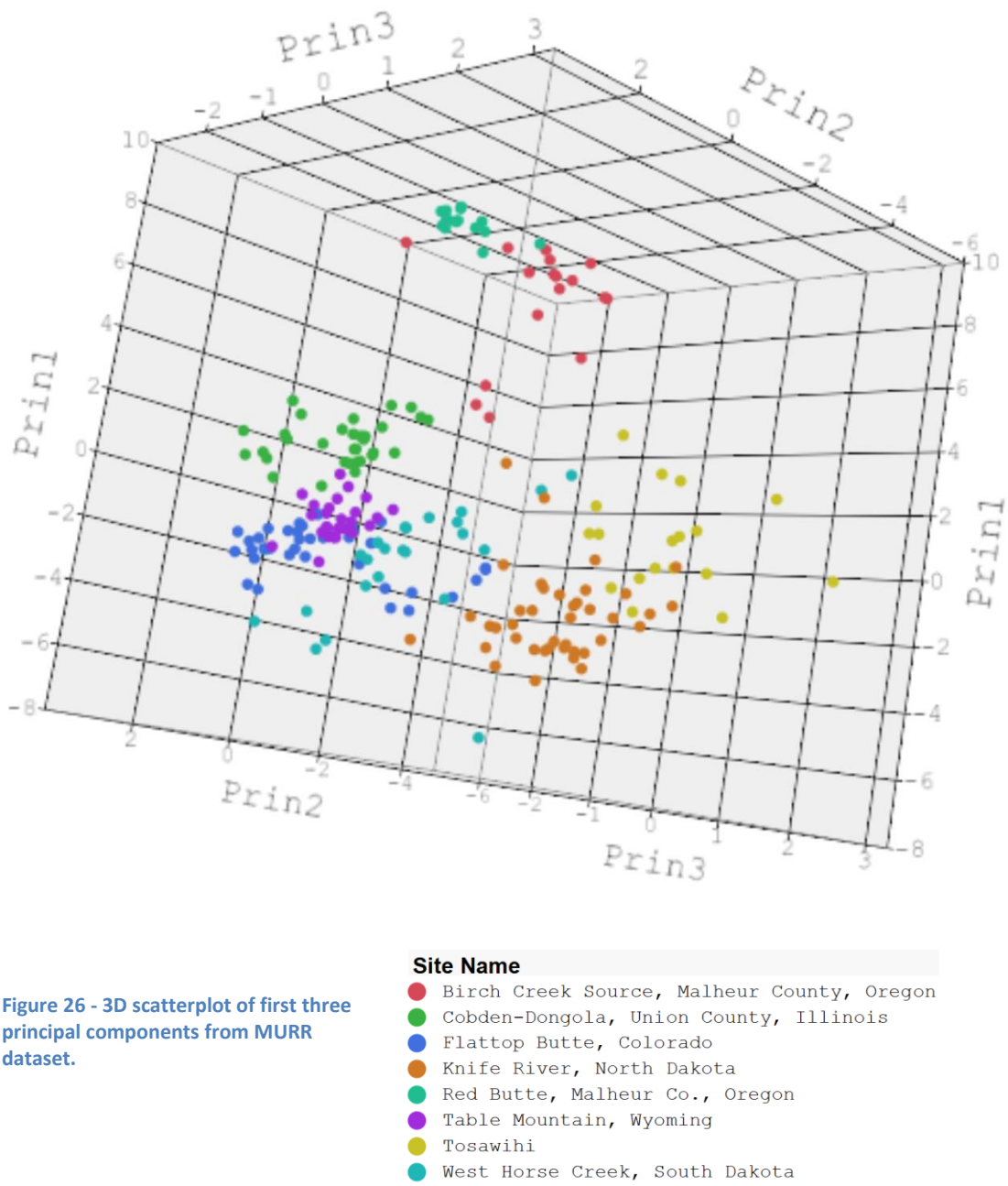

Figure 26 - 3D scatterplot of first three principal components from MURR dataset.

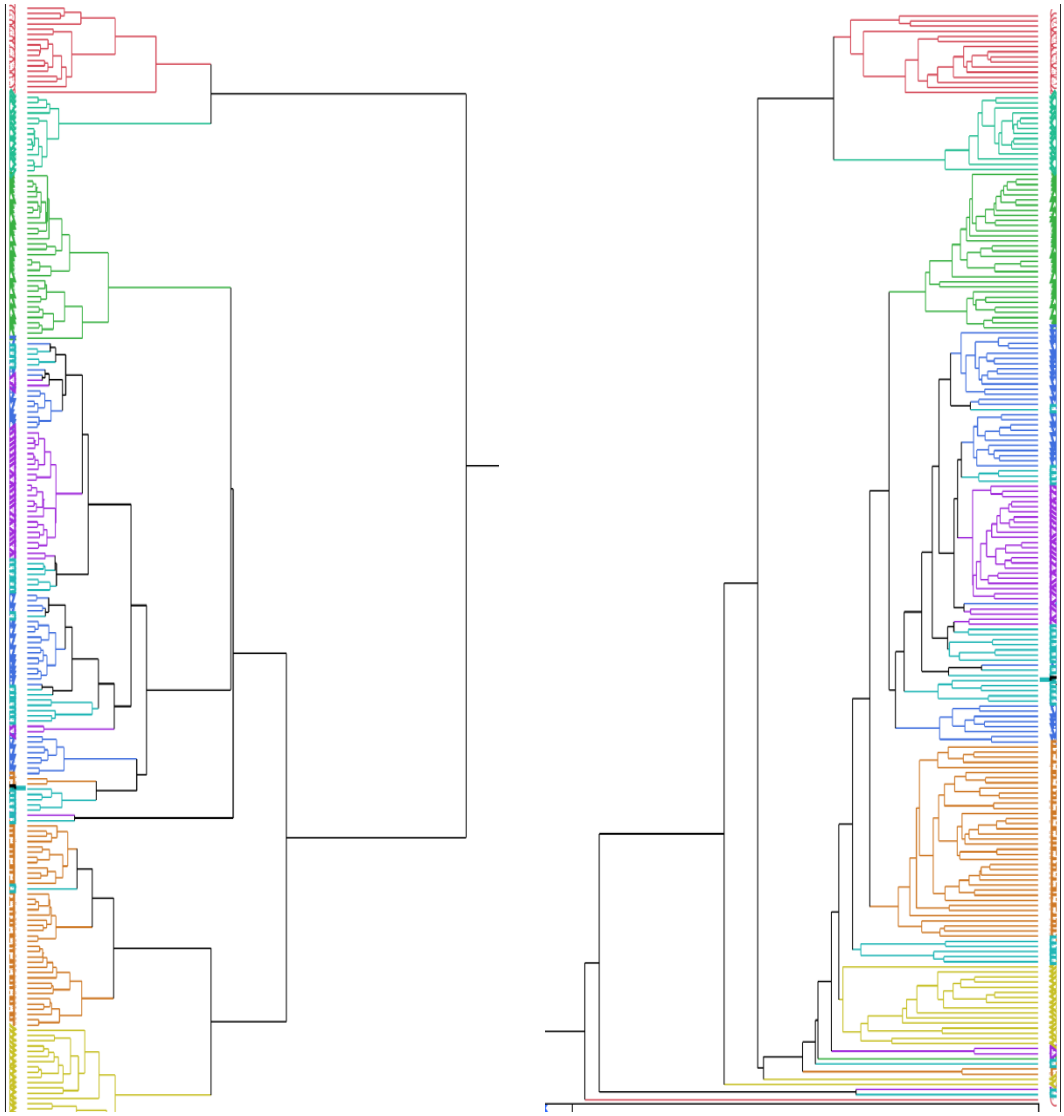

Site Name

- Birch Creek Source, Malheur County, Oregon
- Cobden-Dongola, Union County, Illinois
- Flattop Butte, Colorado
- Knife River, North Dakota
- Red Butte, Malheur Co., Oregon
- Table Mountain, Wyoming
- Tosawihi
- West Horse Creek, South Dakota

Figure 27 - Cluster analysis of external MURR dataset (Ward analysis on left, Average analysis on right).

Box's M

Box's M		7433
F	Approx.	6.773
	df1	561
	df2	16161
	Sig.	.000

Table 6 - Box's M test. Note the outlined Significance at 0.000. This dictates the need to perform quadratic DFA instead of linear for MURR dataset.

Prior Probabilities

		Cases Used in Analysis	
Source	Prior	Unweighted	Weighted
1	.080	17	17.000
2	.150	32	32.000
3	.169	36	36.000
4	.188	40	40.000
5	.070	15	15.000
6	.141	30	30.000
7	.085	18	18.000
8	.117	25	25.000
Total	1.000	213	213.000

Table 7 - Prior probabilities used for discriminant analysis of MURR dataset.

Classification Results[a]

			Predicted Group Membership								
		Source	1	2	3	4	5	6	7	8	Total
Original	Count	1	17	0	0	0	0	0	0	0	17
		2	0	32	0	0	0	0	0	0	32
		3	0	0	36	0	0	0	0	0	36
		4	0	0	0	40	0	0	0	0	40
		5	0	0	0	0	15	0	0	0	15
		6	0	0	0	0	0	30	0	0	30
		7	0	0	0	0	0	0	18	0	18
		8	0	0	0	0	0	0	0	25	25
	%	1	100.0	.0	.0	.0	.0	.0	.0	.0	100.0
		2	.0	100.0	.0	.0	.0	.0	.0	.0	100.0
		3	.0	.0	100.0	.0	.0	.0	.0	.0	100.0
		4	.0	.0	.0	100.0	.0	.0	.0	.0	100.0
		5	.0	.0	.0	.0	100.0	.0	.0	.0	100.0
		6	.0	.0	.0	.0	.0	100.0	.0	.0	100.0
		7	.0	.0	.0	.0	.0	.0	100.0	.0	100.0
		8	.0	.0	.0	.0	.0	.0	.0	100.0	100.0

a. 100.0% of original grouped cases correctly classified.

Numeric Source	Source Name
1	Birch Creek
2	Cobden-Dongola
3	Flattop Butte
4	Knife River
5	Red Butte
6	Table Mountain
7	Tosawihi
8	West Horse Creek

Table 8 - DFA predicted group membership for MURR dataset.

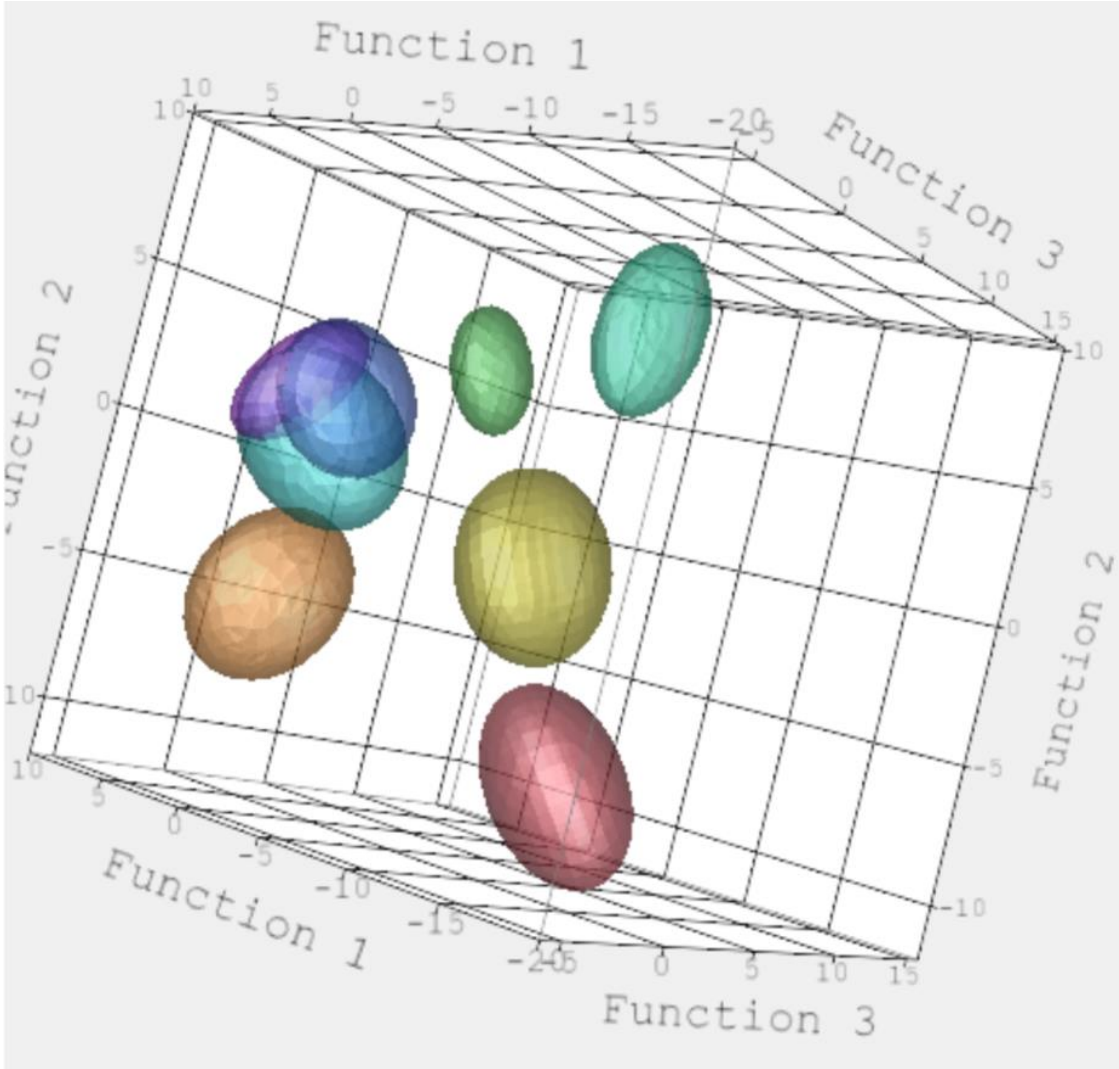

Source Name

- Birch Creek Source, Malheur County, Oregon
- Cobden-Dongola (Union County, Illinois
- Flattop Butte, Colorado
- Knife River, North Dakota
- Red Butte, Malheur Co., Oregon
- Table Mountain, Wyoming
- Tosawihi
- West Horse Creek, South Dakota

Figure 28 - Graph of first three discriminant functions from MURR data; ellipses represent 95% confidence interval.

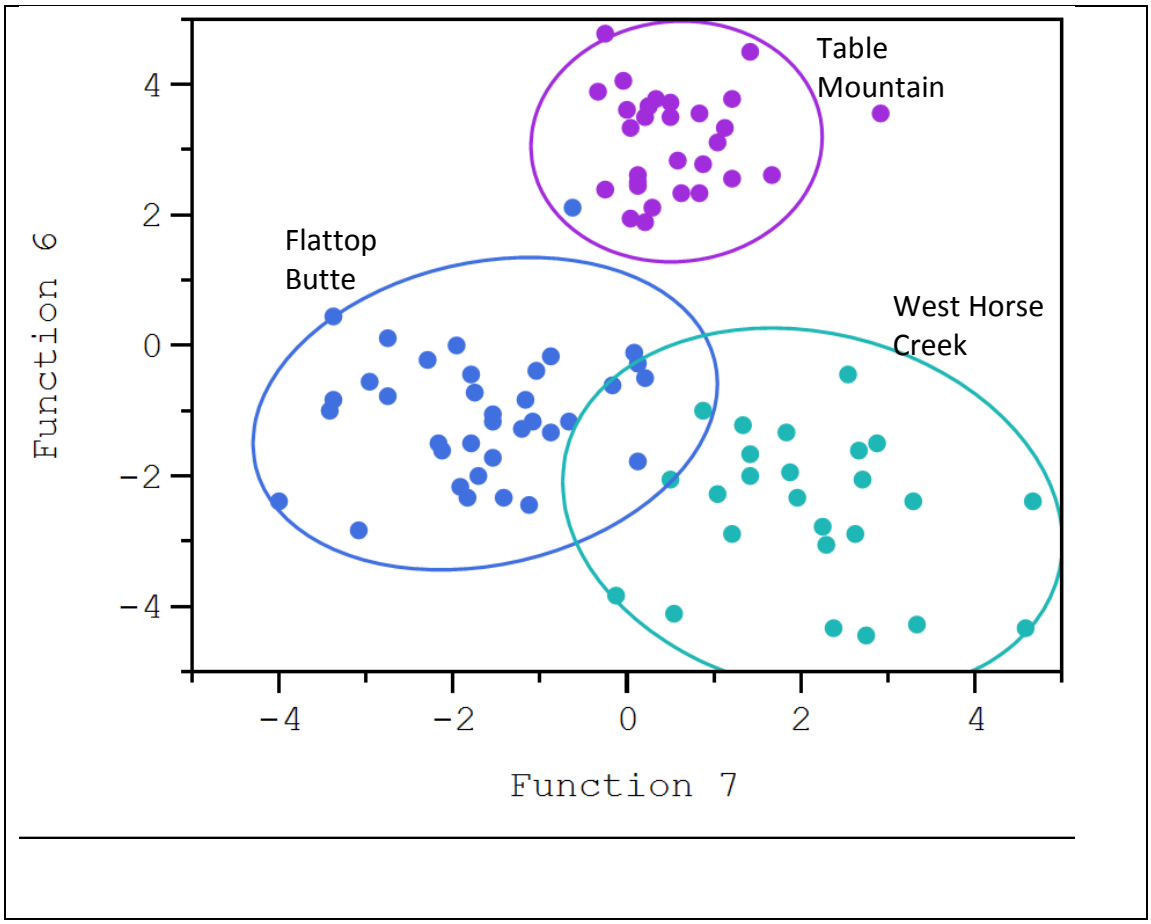

Figure 29- Discriminant functions six and seven from MURR dataset. Ellipses represent 95% confidence intervals.

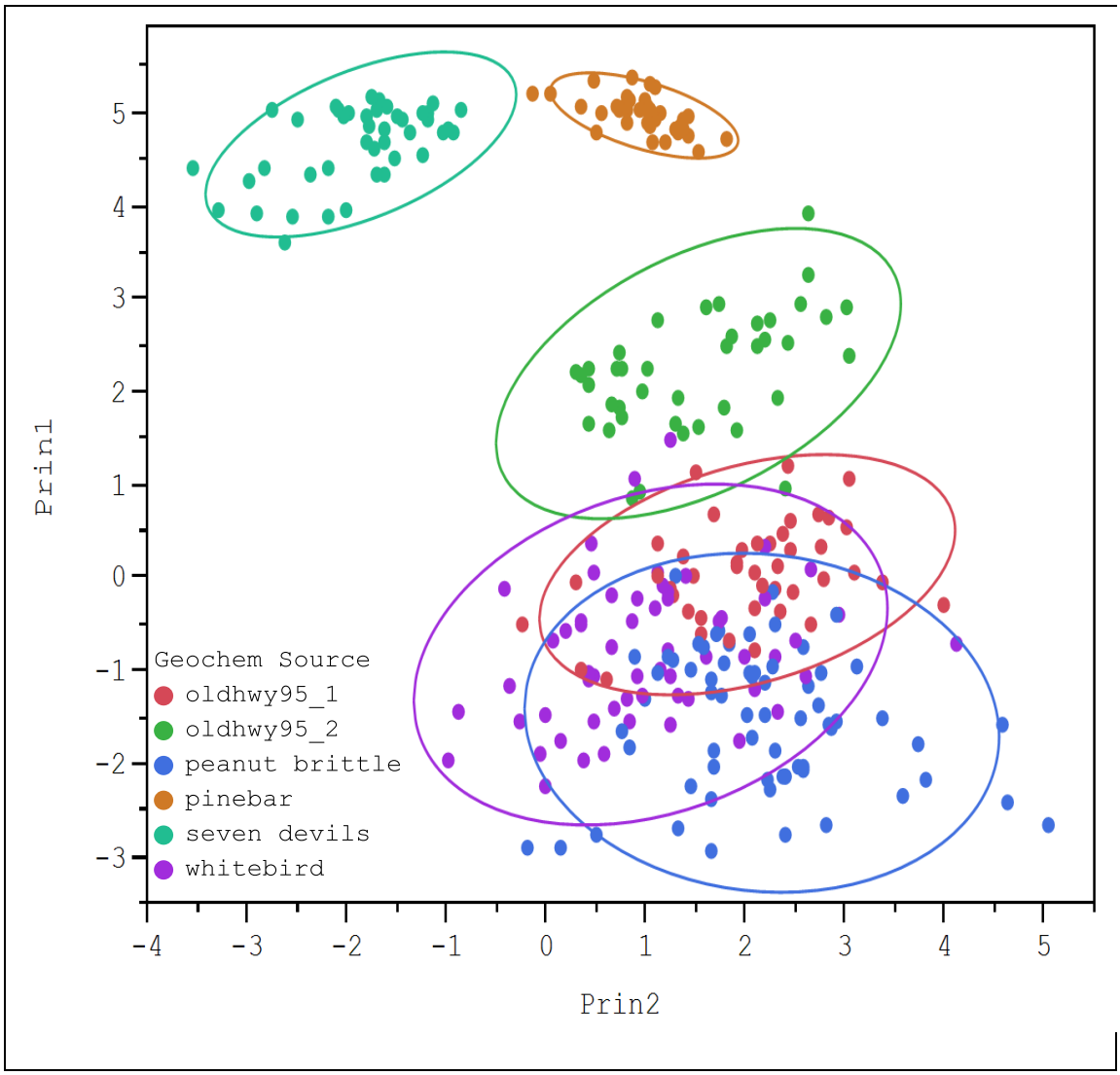

Figure 30- Principal component analysis of geologic samples from LSRC region. Cases are color coded to geologic source.

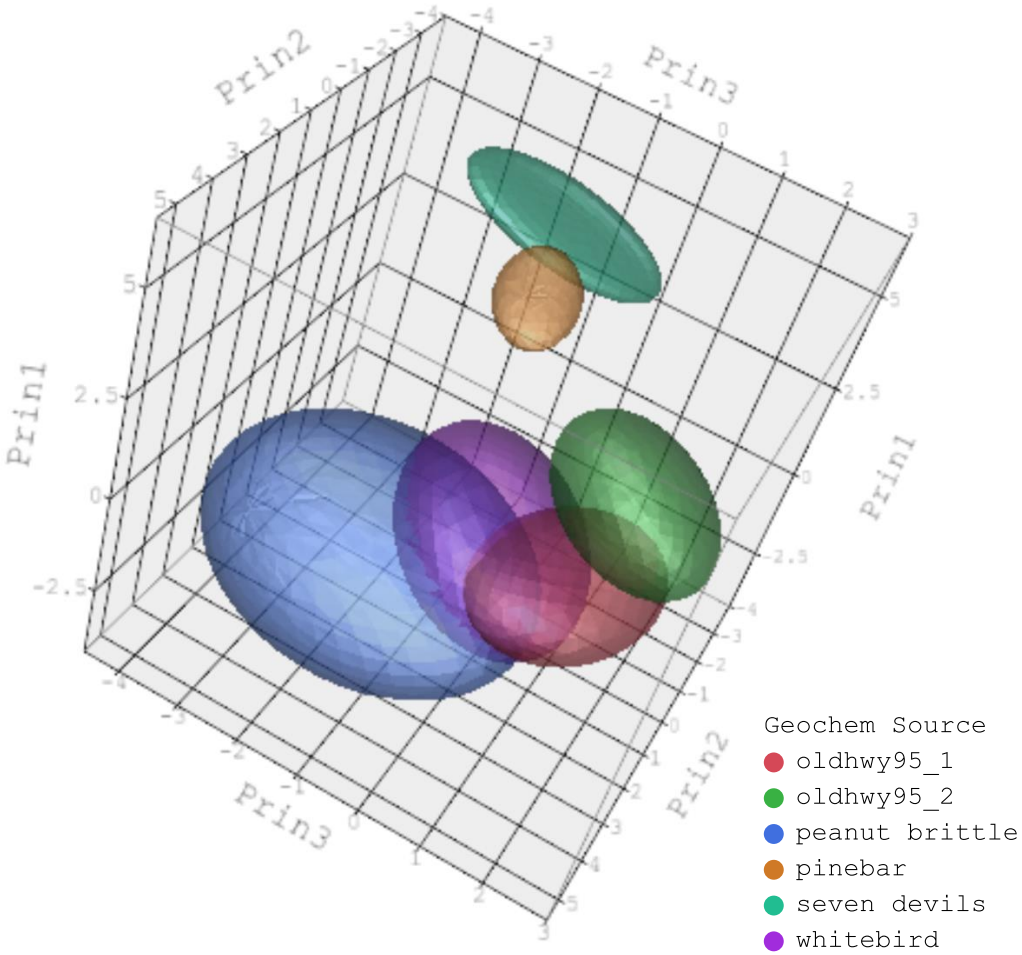

Figure 31 - First three principle components of geologic samples gathered from LSRC region. Cases are color coded to geologic source.

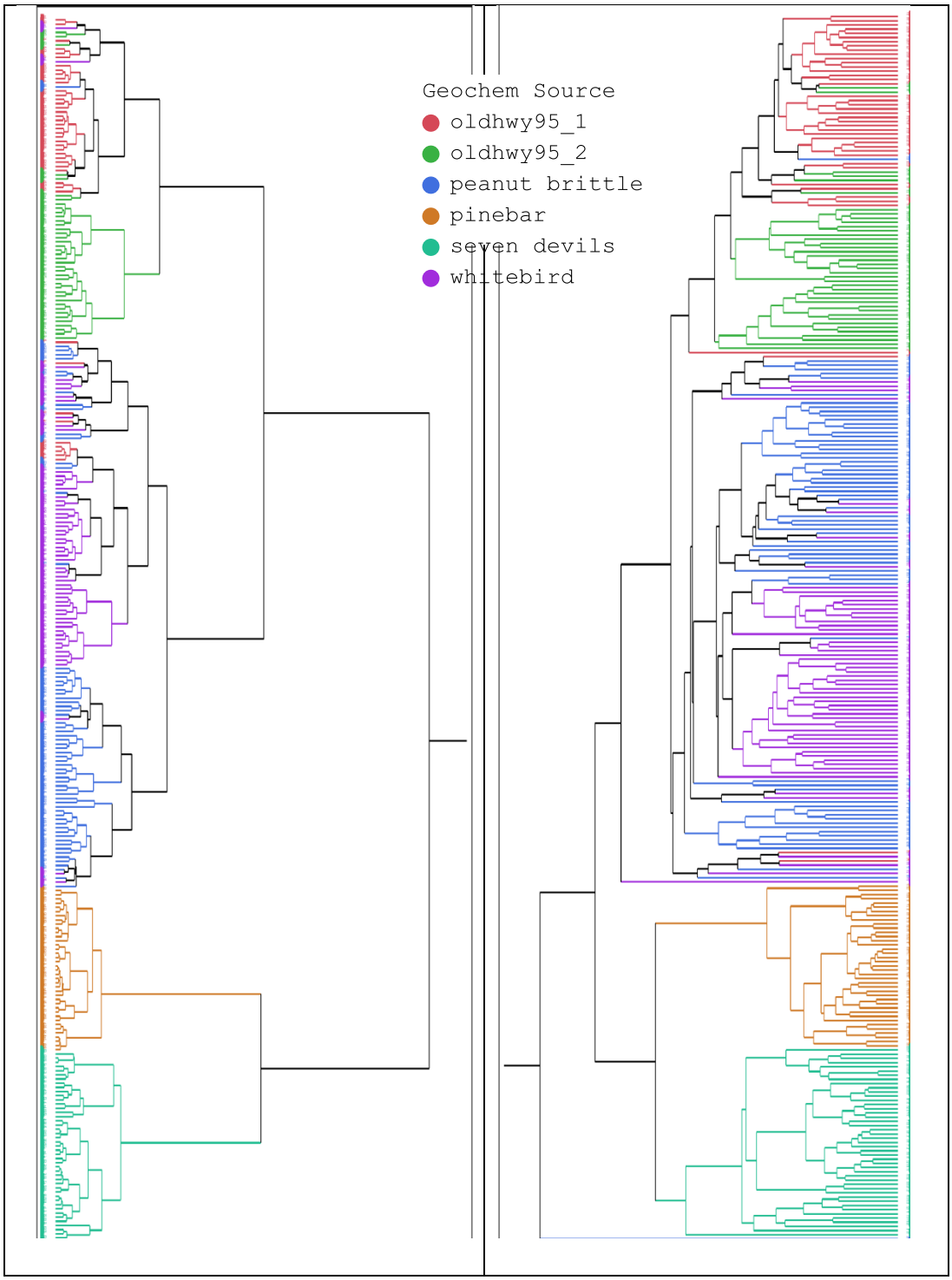

Figure 32 – Cluster analysis of LSRC geologic chert samples, color coded by geologic source. Ward cluster analysis is on left, Average cluster analysis is on right.

Box's M

Box's M		3954.770
F	**Approx.**	6.591
	df1	525
	df2	101369.935
	Sig.	.000

Table 9 - Box's M test of principal components from geologic sources. Note the outlined significance at 0.000. This dictates the need to perform quadratic DFA instead of linear

Prior Probabilities

Source	Prior	Cases Used in Analysis	
		Unweighted	Weighted
1.00	.143	43	43.000
2.00	.140	42	42.000
3.00	.233	70	70.000
4.00	.130	39	39.000
5.00	.157	47	47.000
6.00	.197	59	59.000
Total	1.000	300	300.000

Table 10 - Prior probabilities used for discriminant analysis of chert samples collected by the author.

Results	Source	Predicted Group Membership						Total
		Old Hwy 95_1	Old Hwy 95_2	Peanut Brittle	Pine Bar	Seven Devils	White Bird	
Count	Old Hwy 95_1	42	1	0	0	0	0	43
	Old Hwy 95_2	0	40	0	0	0	0	40
	Peanut Brittle	0	0	65	0	0	1	66
	Pine Bar	0	0	0	39	0	0	39
	Seven Devils	0	0	0	0	45	0	45
	White Bird	0	0	4	0	0	55	59
%	Old Hwy 95_1	97.7	2.3	.0	.0	.0	.0	100.0
	Old Hwy 95_2	.0	100.0	.0	.0	.0	.0	100.0
	Peanut Brittle	.0	.0	98.5	.0	.0	1.5	100.0
	Pine Bar	.0	.0	.0	100.0	.0	.0	100.0
	Seven Devils	.0	.0	.0	.0	100.0	.0	100.0
	White Bird	.0	.0	6.8	.0	.0	93.2	100.0

Table 11 - Classification Results for descriptive DFA on geologic chert sources from the LSRC.

Actual Group	Average Primary D^2	Average Secondary D^2	Next Closest Group
1	4.789325581	13.79110345	40% Group 6
2	4.880928571	42.71147619	62% Group 1
3	4.928571429	22.23462857	100% Group 6
4	4.87174359	45.16623077	60% Group 1
5	4.893659574	151.8732766	57% Group 2
6	4.618050847	18.55822034	92% Group 3

Table 12 - Primary and secondary group D^2 values for DDFA of PXRF dataset.

Results	Source	Total				
		Old Hwy 95_1	Old Hwy 95_2	Peanut Brittle	White Bird	Total
Count	Old Hwy 95_1	43	0	0	0	43
	Old Hwy 95_2	2	38	0	0	40
	Peanut Brittle	1	0	64	1	66
	White Bird	0	0	5	54	59
Cross Validated	Old Hwy 95_1	43	0	0	0	43
	Old Hwy 95_2	2	38	0	0	40
	Peanut Brittle	2	0	63	1	66
	White Bird	0	0	6	53	59

Table 13 - Classification results with Pine Bar and Seven Devils sources removed; linear descriptive DFA on geologic chert sources from the LSRC with cross validation.

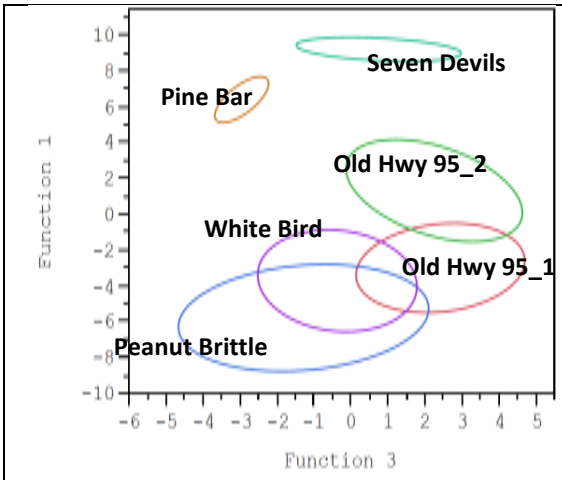

Figure 33 – Bivariate plot of first and third discriminant functions with all six groups. Note the overlaps between Peanut Brittle, White Bird, and Old Hwy95_1.

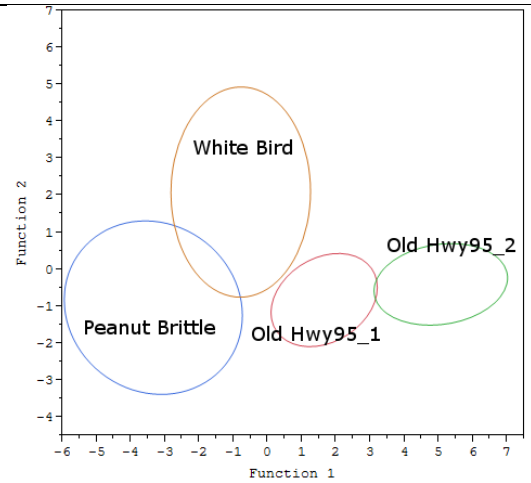

Figure 34 - Bivariate plot of first two discriminant functions without Seven Devils and Pine Bar. Note the increased separation between the remaining four groups.

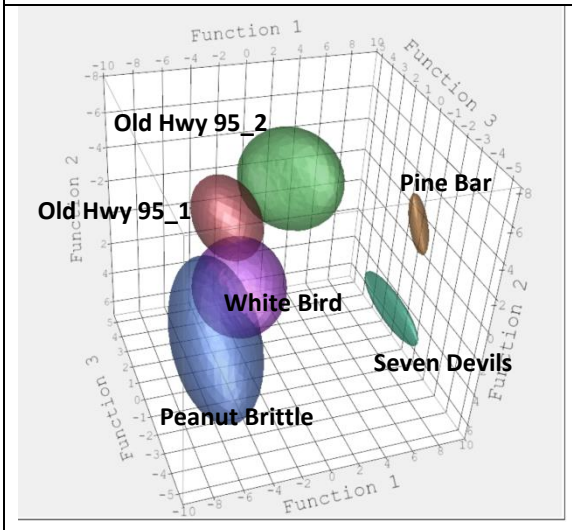

Figure 35 - Trivariate plot of first three discriminant functions with all six groups. Note the overlaps between Peanut Brittle, White Bird, and Old Hwy95_1.

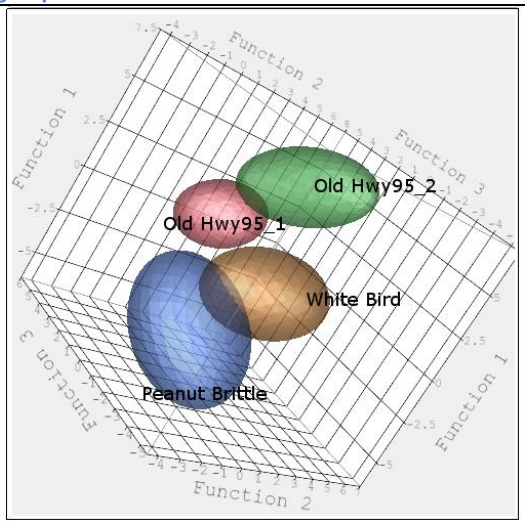

Figure 36 – Trivariate plot of first two discriminant functions without Seven Devils and Pine Bar. Note the increased separation between the remaining four groups.

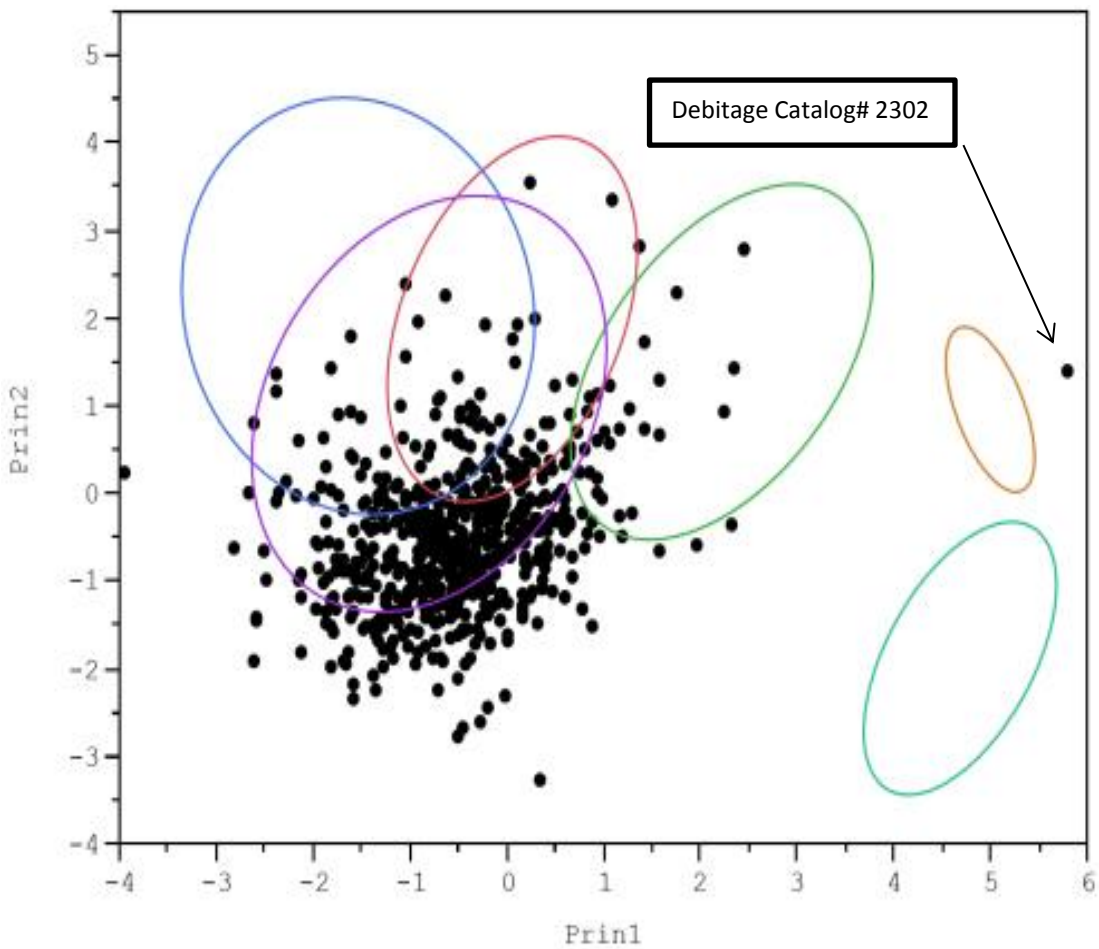

Figure 37 - Principal Component results of PXRF dataset. Artifacts are black points, colors represent geologic sources. The two clusters of points on the right side of the scatter plot are Seven Devils and Pine Bar. Ellipses represent 95 the percent confidence interval

Geologic Source
- Old Hwy 95_1
- Old Hwy 95_2
- Peanut Brittle
- Pine Bar
- Seven Devils
- White Bird

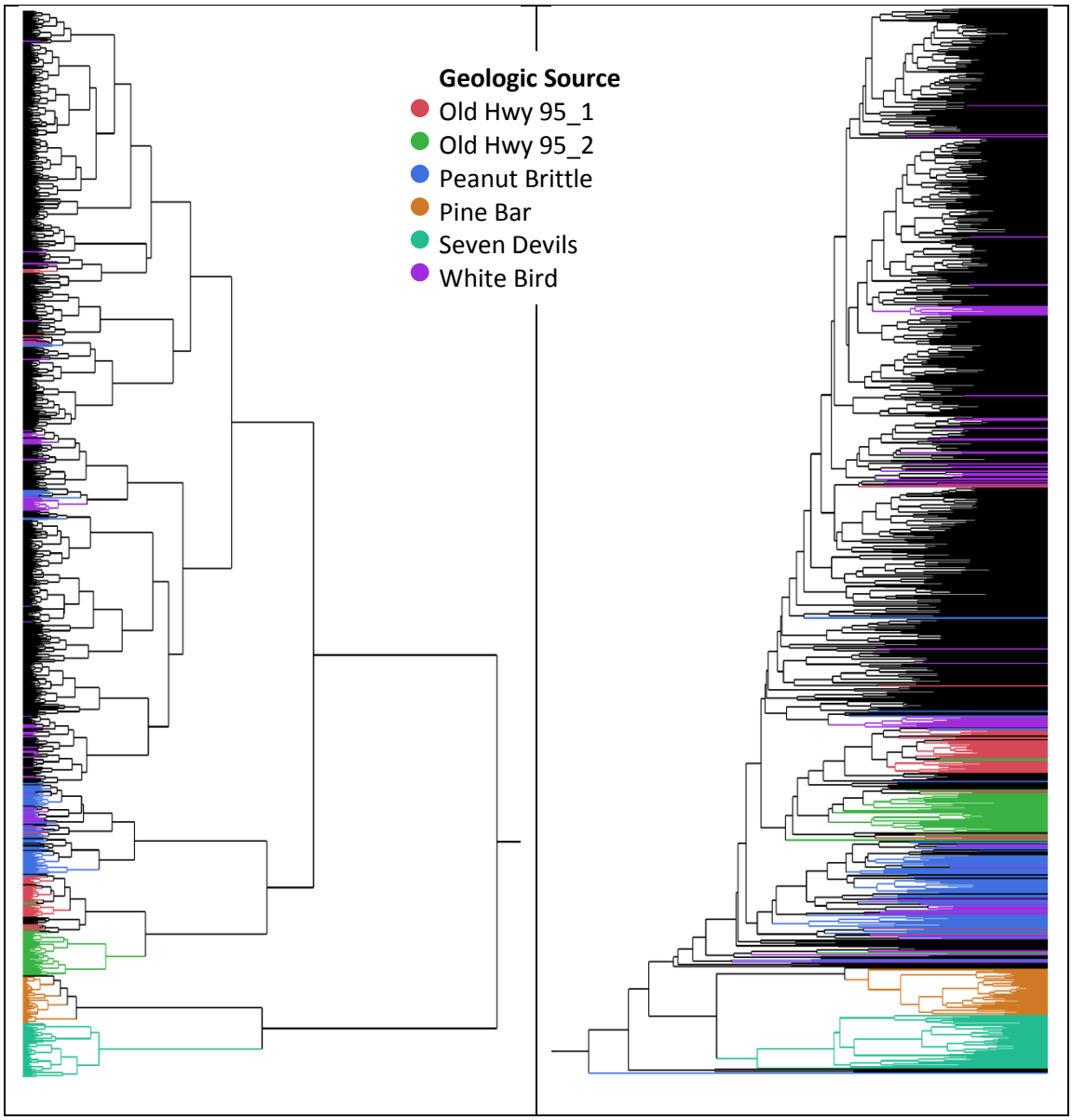

Figure 38 - Ward and Average cluster analysis with Cooper's Ferry artifacts (in black) and geologic sources.

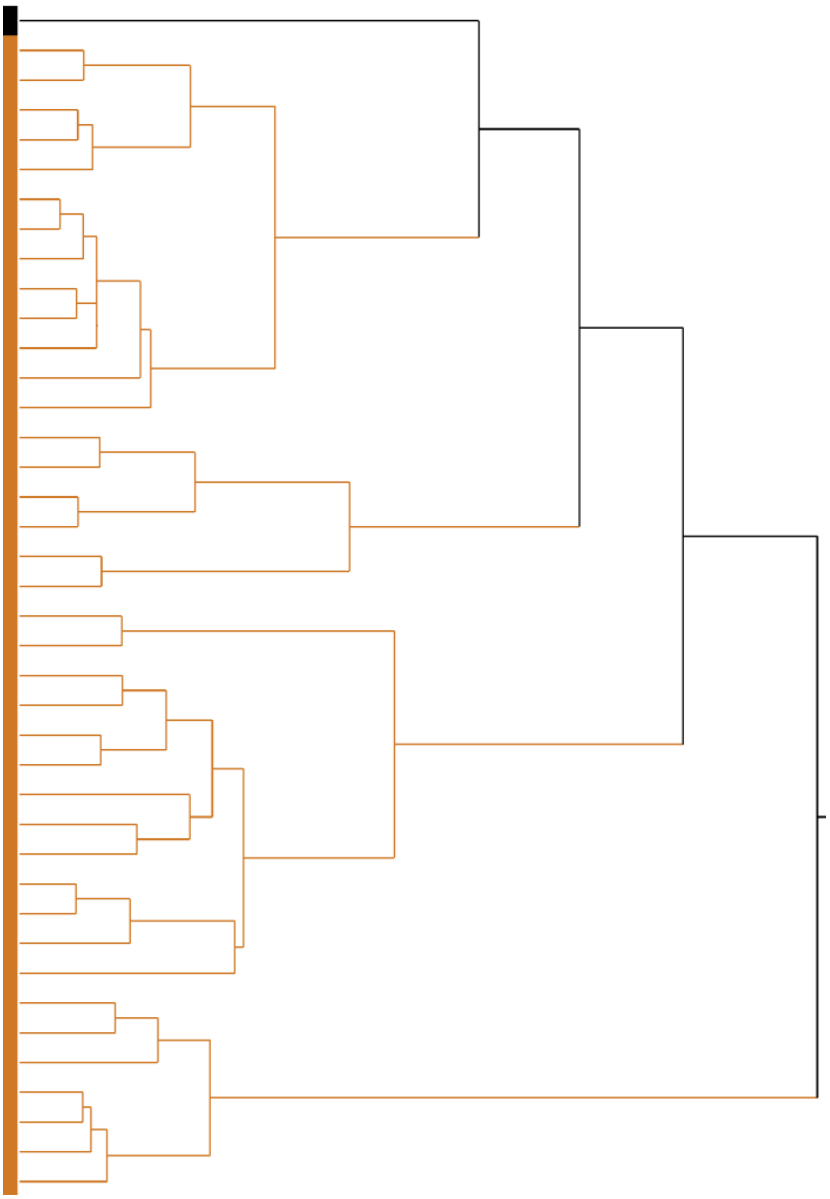

Figure 39 - Pine Bar cluster (orange cases) from Ward cluster analysis with Cooper's Ferry artifact - catalog number 2302 (the uppermost case in black).

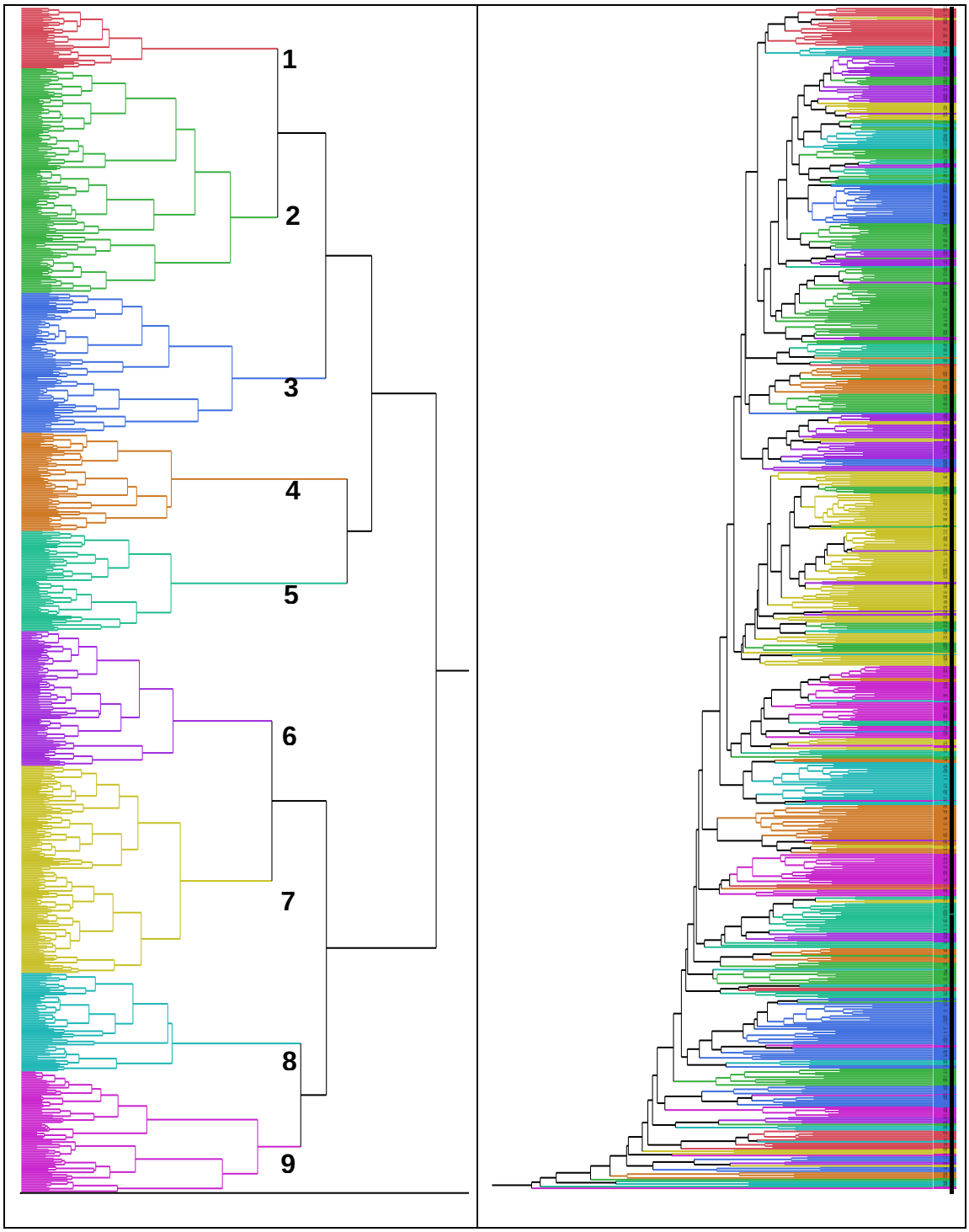

Figure 40 –Ward (left) and Average (right) cluster analysis of chert artifacts from Cooper's Ferry. Colors were set by Ward cluster analysis, nine cluster solution shown in on the left. Note that the red and yellow cases are grouped almost entirely together, indicating a high degree of stability in these groups. Dark blue, orange, and dark green clusters have been split into two or three separate groups using average clustering; however, individual cases within these splits are also still grouped together. This indicates that artifacts within these clusters are indeed more similar to each other geochemically than to the artifacts in differing clusters.

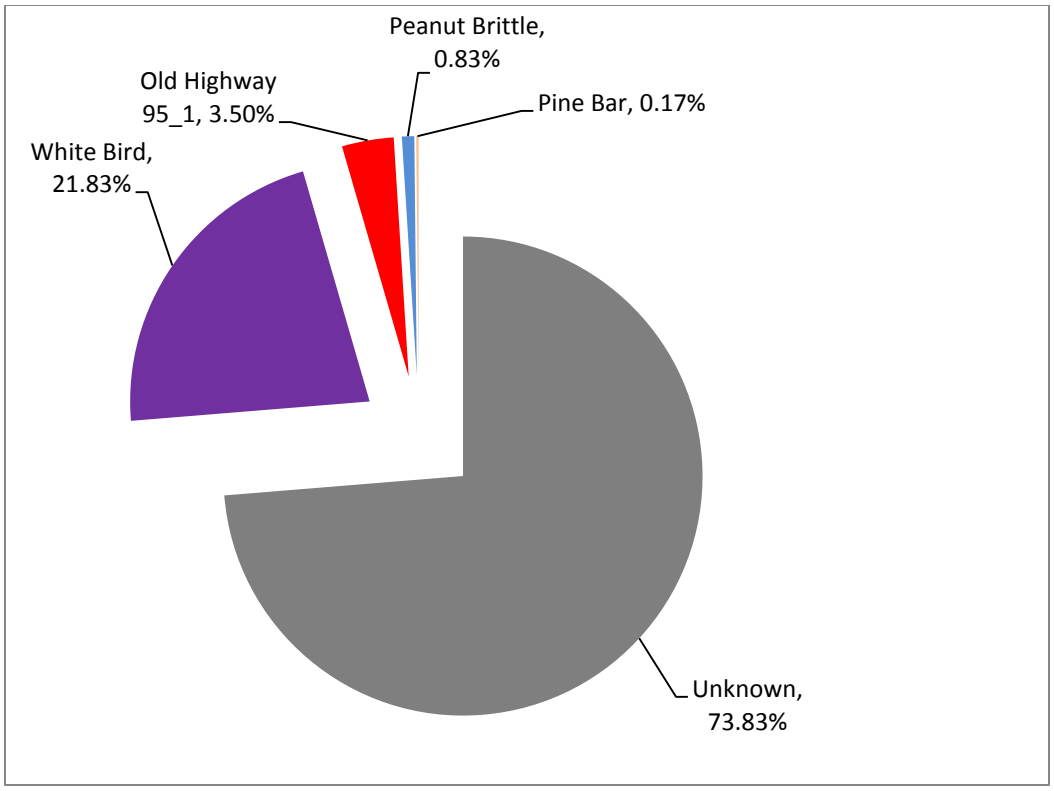

Figure 41 – Results of predictive discriminant function analysis of Cooper's Ferry artifacts. Artifacts were considered assigned to a geologic source if their PDFA conditional probability was within one standard deviation of their predicted group centroid. This shows that statistically, approximately 22% of artifacts tested were made from toolstone from the White Bird chert source 4% were from the Old Highway 95_1, and approximately 74% were from sources other than those tested during this research.

Chapter 5: Discussion of Results

This research was designed to determine the feasibility of sourcing cherts on the Columbia River Plateau through by studying chert artifacts from the Cooper's Ferry archaeological site. This study sought to address four main questions, each of which will be addressed below.

Are geologic chert sources located in the area surrounding the Cooper's Ferry site?
A survey was performed over several field seasons to locate possible chert sources around the Cooper's Ferry. Initially, nine possible sources were located and sampled, however upon further examination and revisiting the survey locality, only four of these were extensive enough in area to warrant further examination. Subsequent surveying found two more sources to test, bringing the total number of geologic sources sampled to six.

Can these chert sources be defined and differentiated on the basis of their inherent geochemistry?
To investigate this question, INAA as well as PXRF was used to investigate the elemental chemistry of cherts in the LSRC area to see if cherts could be resolved into distinct groups that matched their provenance in the landscape. As can be seen from the results of the preliminary INAA testing, discrimination of geologic sources using geochemical data was possible via both principal component analysis (Figure 22) as well as cluster analysis (Figure 23). While acknowledging that the sample size of this preliminary work was too small for vigorous statistical analysis, these results were

promising enough to merit continued research into elemental analyses of cherts from the LSRC region and the creation of a larger dataset using alternative methods.

A second benefit of performing the preliminary INAA study was that samples tested via INAA could be used as a calibration check for the PXRF device. Fifteen samples were selected from preliminary INAA testing with concentrations of elements that could also reasonably be resolved via PXRF and were run using the same procedures as the rest of the samples tested. These results were then used to create robust custom calibration curves for each element tested.

Also of note is the increased ability of INAA to resolve differences in crypto-crystalline silicates. INAA is more precise, more accurate, and has lower levels of detection than PXRF. This increased accuracy and precision leads to less missing data which corresponds with more differentiating power and the ability to separate sources with increased levels of accuracy. Because of this, the author recommends that when a provenance study of cherts is undertaken, INAA be strongly considered for the initial examination of geologic chert sources in the area. This investigation also has the byproduct of creating internal chert reference standards that can be used to help calibrate other devices (such as PXRF) that may be used in the analysis.

To test the statistical approach used in this study, an external data check from other chert sourcing research was compiled and examined to determine if the statistical methods outlined above could differentiate chert sources. The results of the external

data test showed good separation of geochemical source using the methodological approach proposed in previous chapters, with all groups being separated with a one hundred percent group validation rate.

After INAA results showed promise for differentiating cherts in the LSRC, and I was able to apply my analytical methods to successfully discriminate the MURR dataset, the next step was to determine if PXRF could resolve the 300 geologic samples selected for analysis from the study area. An examination of the distributions of retained principal components by chert sources shows that sources are indeed differentiated by principal components, with bivariate plots showing groupings, though some overlap is also present (Figure 30).

Cluster analysis, which does not have any *a priori* knowledge of group assignment, also showed distinct separations between groups with relative stability between clustering algorithms. This strengthens the case that the known samples are distinguishable into separate chemical groups that correlate to their provenance in the landscape. Using cluster analysis on a known dataset prior to examination of unknowns also allows researchers to examine the distances between known chert groups and then apply a heuristic based approach when examining artifact assemblages.

Discriminant analysis was able to leverage principal components to distinguish geologic groups with a high degree of accuracy, with 98% of all samples classified

correctly when examining all six sources simultaneously. With Seven Devils and Pine Bar removed, 95% of cases were able to be classified correctly under cross validation.

Can chert artifacts from the Cooper's Ferry site be statistically correlated to geologic chert sources in the Lower Salmon River Canyon?

To examine this question, artifacts from Cooper's Ferry were examined via predictive discriminant function analysis to determine if any artifacts grouped successfully with established chert sources (Figure 41). Secondarily, artifact geochemistry was examined for possible groupings, with any apparent groupings being compared to recorded artifact metrics such as size, provenience within the excavation unit, cultural component, and artifact classification (i.e., debitage, formed tool). Cluster analysis of artifacts without geologic sources showed two main groups of artifacts stable across clustering algorithms, cluster one and seven, with several other groups being relatively stable[7] (Figure 38). While this does not necessarily point to separate geologic sources of chert being present in the artifacts analyzed, it does show that there are, at a minimum, discernible geochemical groups of cherts that can be seen in the artifact assemblage. Comparison of retained clusters versus other metrics (e.g., weight, length, width, thickness, lithostratigraphic unit, depth below datum) showed no statistical groupings (Appendix D - Clusters vs. Artifact Metrics). Cluster analysis of artifacts pooled with geologic sources (Figures 39 and 41) show that the majority of artifacts are geochemically most similar to the White Bird chert source. While this

[7] Cluster stability refers to individual cases (in this case artifacts) being grouped together across different clustering algorithms. For more information on clustering, page 28.

similarity does not quantitatively indicate artifacts are from the White Bird source, it does point to White Bird being of similar chemical makeup to the artifacts found within 10IH73. Since the geochemistry of chert is set by geologic formation processes and subsequent weathering/diagenesis effects, it is reasonable to infer that the cherts used in the creation of many of these artifacts share a common formation and weathering history to those of the White Bird source, indicating that they are possibly from a nearby location. Comparison of retained clusters against artifact metrics shows two interesting patterns. First, artifact type by cluster shows that two clusters differentiate from the norm; cluster one has a high degree of debitage, while cluster seven is skewed heavily towards formed tools. The second pattern seen again relates to clusters one and seven, with cluster one being most similar to the White Bird chert source, and cluster seven being the most dissimilar to the White Bird chert source.

Some may argue that the above shows that cherts can only be differentiated into those from Columbia River Basalt formations versus other formations such as the Wallowa Arc terrain. This interpretation was refuted however by both descriptive discriminant analysis as well as cluster analysis of geologic sources performed by this author, in which nearly all cases from four separate geologic sources of chert were successfully assigned to their sources of origin - two of which are only a few hundred meters apart (Figures 32-36 and Tables 9-13)

Using the conservative measure of one standard deviation to reduce the risk of type one errors, predictive discriminant analysis assigned roughly 21% of artifacts examined to the White Bird chert source. Whether this measure is too liberal or conservative can be debated, however, as with interpreting cluster analysis results, if these cherts did not come from the White Bird source, then they at least came from a source with a very similar formation, diagenesis, and subsequent weathering history. This points to these artifacts either being from the White Bird chert source, or some other nearby location.

The evidence presented in the previous chapters makes a strong argument that cherts can indeed be discriminated into specific geologic source locations via chemical analysis if appropriate attention is given to analytical methodologies. Specifically, PXRF devices cannot be treated as “black box” devices. Calibration issues and matrix effects are very real problems in PXRF analyses, and must be carefully examined – see Shackley (2010) for an in-depth discussion of these issues. Just because a PXRF unit is portable and usable in the field does not mean that laboratory standards for issues such as cleanliness can be ignored. Small amounts of sediments can drastically throw off a chemical analysis, especially when analyzing silicates where the differences between sources are measured in a few ppm. As such, especially when used in the field, rigorous laboratory methods must still be adhered to. This of course does not preclude its use for in-field analyses; it just reinforces that one must be cognizant of the limitations of the device.

Also of note in this research is that when working with some types of materials in elemental based provenance analyses, bivariate plots of raw data can be useful in differentiating separate groups. Indeed, in this analysis, two of the sources tested (i.e. Pine Bar and Seven Devils cherts) could be easily separated by individual bivariate plots of raw data. To separate chert sources that are more similar in elemental properties however, where no single ratio of two elements will successfully discriminate sources, more robust multivariate methodologies are needed. Positive results were obtained using the methodology presented in this work to discriminate between geologic chert sources, both with data collected by this author using INAA as well as PXRF, as well as with external data sets downloaded from the MURR.

While cluster analysis is sometimes attacked by as generating useless data (e.g. differing clustering solutions depending on algorithm used or creating clusters from randomly distributed data) it can be a useful technique, as long as one is cognizant of its limitations (Templ et al., 2008). Specifically, analysts should perform and compare multiple different clustering methods and examine their output for relative stability. Issues of scale between variables as well as possible multicollinearities also need to be investigated for and corrected if present (Kettenring, 2006). When cluster analyses were performed on the samples from known sources in this analysis, good separation between most chert sources was achieved using principal components as input variables, as well as relative stability between clustering techniques - again

both with the data collected by this author as well as with external datasets. It is important to reiterate that PCA was not used to reduce the dimensionality of the dataset in these analyses but used to remove any multicollinearities that could skew cluster analysis results. This research shows that cluster analysis is a valid technique for differentiating sources of cherts and can be a valuable method of exploratory data analysis in elemental provenance studies of crypto-crystalline silicates.

Of course, just because there are clusters of elemental data does not necessarily mean that they represent distinct geographic source locations. Interpretations of the presence of these chemical groups (besides different geographic/geologic origins) could be, but are not limited to:

- Sediment contamination on sample
- Artifact angle in relation to the x-ray detector
- Samples being too thin to get a good reading
- Post formation heat treatment
- Post depositional weathering[8]
- Inclusions within the chert matrix

Still, many of these interpretations can be tested for and ruled out completely or considered exceedingly unlikely, as discussed below.

[8] In this case, the term “post depositional” refers to archaeological artifacts after they have been discarded, not after their initial deposition from geologic processes.

Methodologically, artifacts were only examined via PXRF if they met a specific size requirement, in this analysis 1 cm in length x 1 cm in width x 1 mm in thickness[9]. Randomly selected debitage that did not meet this size requirement were removed with replacement, while tools were removed and not replaced (since 100 percent of tools were analyzed from the 1997 catalog). Ignoring for a moment that there were specific size requirements for this analysis, if size or mass was an issue, one would expect to see correlation between one of the aforementioned clusters when compared with artifact size. However, examinations of artifact metrics (i.e. weight, thickness, length, and width) show no correlations with cluster assignments.

Sediment contamination could also cause distinct geochemical groupings. In this scenario, sediments, which are typically much higher in trace elements than cherts, would throw off measurements of some artifacts. This would have the effect of assigning the “dirty” artifacts to distinct geochemical groups separate from the “clean” artifacts. Because all artifacts were cleaned by the same analyst in the same manner and were visually examined for sediment contamination prior to analysis, this scenario can be rejected. Angle of artifacts in relation to the detector could possibly also be an issue, with the angle of the artifact (or the presence of large flake scars) possibly causing errors in the data. However, the method of artifact placement

[9] One mm in thickness. was chosen as a tradeoff between being able to get a large sample of debitage and having a minimum sample size for accurate and precise results. Both of the instruments used in this analysis had a detector window of 1cm in diameter. See (Davis, Jackson, Shackley, Teague, & Hampel, 1998) for an in-depth discussion on minimum sample sizes when performing PXRF analysis.

on the detector did not change throughout the analysis, and the same analyst collected all the readings, so this explanation is rejected.

Post depositional weathering is another issue that could potentially affect chert geochemistry. As discussed in Chapter 2: Background, the pH of groundwater as well as temperature and pressure does have an effect on the silica matrix of cherts. It is not unreasonable to assume that some minerals locked within the outer edges of chert nodules may be preferentially removed while other minerals maybe deposited thereby creating a weathering rind or cortex around nodules of cherts as well as artifacts (Gauthier et al., 2012). If post depositional weathering were responsible for shifting chert geochemistry at the Coopers Ferry site, one would expect to see a correlation between clusters and depth below surface or lithostratigraphic units. These different units would act as different weathering environments (as well as with increased time spent in the weathering environment). Upon examination of the total dataset, (Appendix D – Clusters vs. Artifact Metrics) no strong correlations are seen between either depth or lithostratigraphic units and clustering solutions. Even if correlations were seen, other, explanations besides post depositional weathering could be called into play, such as different sources of chert being used at different periods of time.

Heat treatment is a topic often discussed in geochemical research of cherts (Luedtke, 1979, 1992), (Lyons, et al., 2003) with most research showing that heat treatment

has little to no effect on bulk elemental analysis, though chert color themselves can vary greatly under high heat due to elements such as iron changing oxidation states Some limited analysis on heat treatment was performed by this author on one source of chert during this research. Two pieces of Peanut Brittle chert were tested via PXRF, then baked in a kiln at 400° c for seven hours[10], then examined again via PXRF. Pre and post heat treatment measurements of all elements detected were within a few ppm of each other, suggesting that no geochemical changes occurred with heat treatment that could be detected via PXRF analysis. Heat treatment did change chert color as brown (7.5 YR 5/6) cherts changed to dusky red (10 R 3/4) (Figure 42). Though color and luster changes such as this are common in cherts (Luedtke, 1992), it is unreliable, at least within the LSRC, to use color alone to detect if cherts have been heat treated because cherts from a single LSRC source can come in almost any color. Further testing of the properties of cherts found in the study area however could help illuminate the nature of heat treatment in LSRC cherts.

With cluster analysis being able to differentiate separate sources of cherts *a priori* of any group knowledge in LSRC cherts, as well as in the external dataset downloaded from the MURR, the next step was to apply cluster analysis to Cooper's Ferry chert artifact assemblage elemental data. Nine distinct clusters were seen within the assemblage with a good degree of stability displayed between clustering algorithms.

---

[10] Seven hours @ 400° c, however including ramp up and down the total time was eleven hours using a linear two hour ramp up / down. Cherts were heated uncovered in unglazed ceramic cups.

These nine clusters were retained as possible chert sources within the assemblage, and a series of ANOVA and $\chi 2$ tests were applied between these retained clusters and recorded artifact metrics such as tool type or size.

How does studying chert artifact provenance at Cooper's Ferry inform our understanding of early human use of chert toolstone, and what are the larger implications of this study?

Comparison of chert sources assigned via cluster analysis with lithostratigraphic unit, depth below datum, and previously established cultural components show no statistical correlations. Two main points can be gathered from these results. First, if these groups truly represent distinct sources, it implies that there is no evidence of a distinct "founding curate set" (Schiffer, 1987, p. 90) at Cooper's Ferry. While there must obviously be a learning and experimentation period for people coming into a new landscape, it appears that raw materials are found rapidly enough, at least at Cooper's Ferry, to not be differentiated in the archaeological record or that a founding curate set might be present in cultural occupations that predate the initial occupation of Cooper's Ferry. If a founding curate set were present in any quantity, then changes in the ratios of chert sources seen in the archaeological record would appear either at the earliest cultural component, at the deepest levels below surface, or at the lowest lithostratigraphic units, yet none are seen. Furthermore, no observable changes in chert source use are seen diachronically. This lack of diachronic diversity in chert source usage implies that the same cultural group of people occupied the site throughout the site occupation history as well as a lack of

change in regional mobility patterns. These results suggest that a long period of generationally transmitted traditional ecological knowledge of chert sources existed at the Cooper's Ferry site.

The DAPC technique implemented in the previous chapters has also been shown in this research to be effective in the analysis of elemental data, as long as the requirements for data distribution are met. DAPC was able to correctly assign between 95% and 98% of cases correctly in geologic LSRC chert samples, and between 95% to 100% percent of cases in the MURR dataset, depending on how groups are merged together. Cross validation of known samples also had excellent results.

Comparison of Ward cluster groupings was also performed versus Mahalanobis distances retained via discriminant analysis from known chert sources to gain an understanding as to the average degree of similarity of different groups of artifacts to known chert sources (Figure 43). Two of the clusters (one and three) had an average Mahalanobis distance of 8.4 and 8.1, which is within two standard deviations of the closest chert source (White Bird in almost all cases). While admittedly speculative, one possibility is that these artifacts came from a source somewhere nearby the White Bird chert source that had similar formation and subsequent weathering processes. Clusters seven and nine were more dissimilar from any known chert sources, with average Mahalanobis scores of 24.2 and 24.3 respectively -

approximately four standard deviations from the nearest chert source group centroid (Figure 43). Continuing the previous line of speculative reasoning, these sources, being more dissimilar from established sources, may well be from geographically more distant locations. As more sources are located and examined in the region, this pattern should become better understood.

Another interesting pattern was observed when comparing artifact classification with assigned chert source (Figure 44). Clusters one and three (and two, to a lesser degree) contain a high percentage of debitage, while cluster seven contains a high percentage of formed tools (χ^2 (8, N = 600) = 49.05, p = < .0001). When tools are broken into their various typological sub-categories (Figure 45) cluster nine contains 50% of the unifaces examined, and 61% of the cores (χ^2 results not available due to small quantitates of some categories). This is interesting when compared with the average D^2 values of retained clusters, which are low for clusters one and three, and high for cluster seven. If, as proposed above, cherts from cluster seven were obtained from sources further afield from tested sources, and one and three were close to the tested sources, then one possible conclusion is that the chert used in cores found at the site were obtained from sources farther from established chert sources than debitage, which was in much higher percentages from groups one through three. Somewhat paradoxically, this pattern could actually be reversed, with the cherts in groups seven and nine being from sources closer to Cooper's Ferry than groups one and three. This is because the White Bird chert source, which is the

closest geochemically to the majority of the artifacts found in the site, is over 10 km from Cooper's Ferry. In the years since this study was undertaken, subsequent chert surveys have found several more chert sources closer to the site, several within one to two km. It could be that these sources are the point of origin for the cores found in the site, while a source near the White Bird cherts maybe the point of origin of for groups one and three, which have much higher concentrations of debitage. Again, it must be stressed that this is conjecture however, and that only more research will help resolve this question.

Figure 42 - Effects of heat treatment on Peanut Brittle chert. Nodules on right side (framed in white box) have been heat treated at 400°c for seven hours. Note the color change from brown to dusky red.

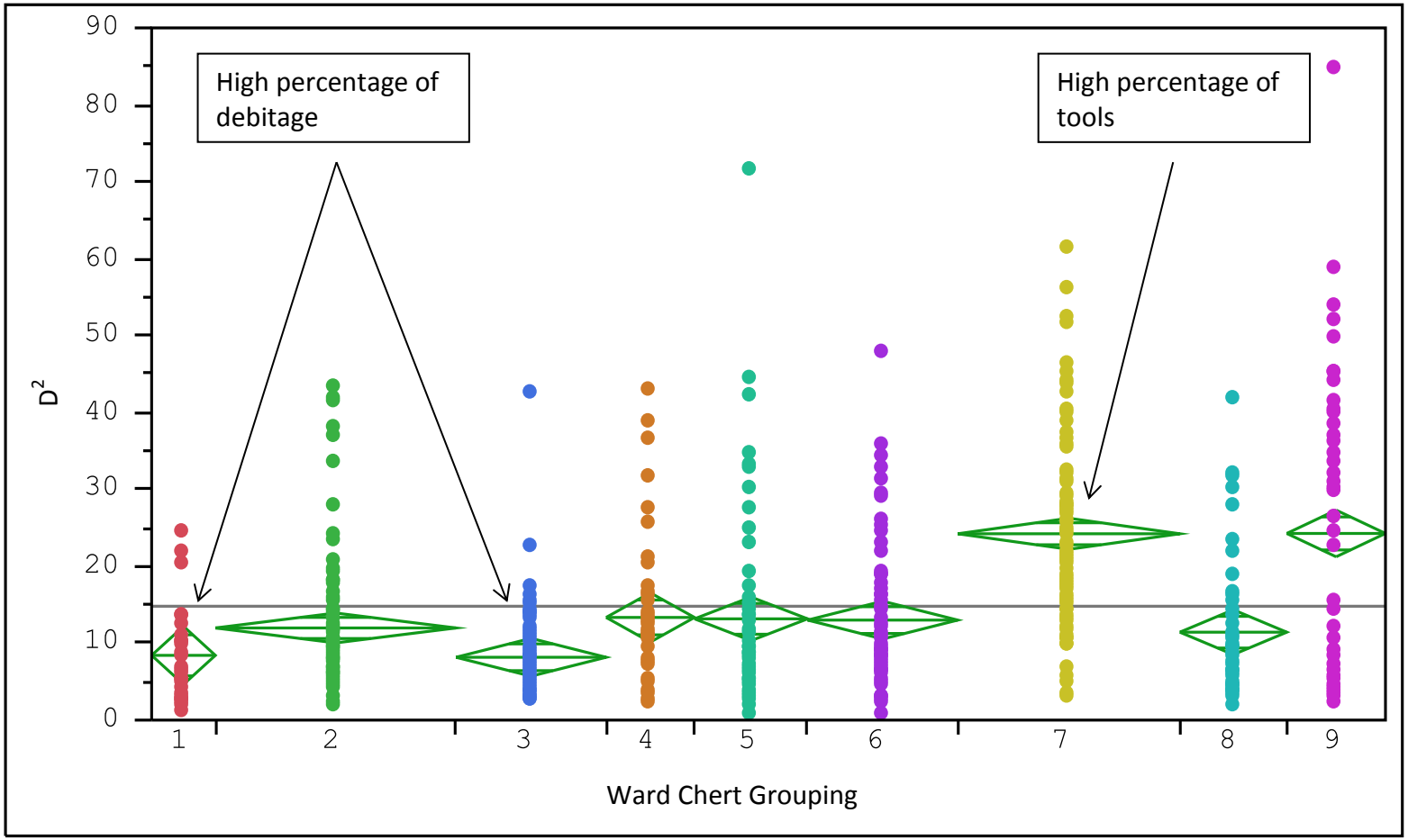

Figure 43 - Mahalanobis distance measures of Ward chert groupings. Clusters 1 and 3, which are more similar to tested chert sources, also are correlated with higher ratios of debitage, while cluster 7 has a higher ratio of tools and is more distant geochemically from tested chert sources.

One-way ANOVA

Rsquare	0.196395
Adj Rsquare	0.186899
Root Mean Square Error	11.02916
Mean of Response	15.00215
Observations (or Sum Wgts)	686

Source	DF	Sum of Squares	Mean Square	F Ratio	Prob > F
Ward Chert Grouping	8	20126.21	2515.78	20.6818	<.0001*
Error	677	82351.85	121.64		
C. Total	685	102478.06			

Level	Number	Mean	Std Error	Lower 95%	Upper 95%
1	35	8.9718	1.8643	5.311	12.632
2	130	11.8478	0.9673	9.949	13.747
3	81	8.6846	1.2255	6.278	11.091
4	57	14.1454	1.4608	11.277	17.014
5	58	13.0000	1.4482	10.156	15.843
6	78	13.1749	1.2488	10.723	15.627
7	120	24.1434	1.0068	22.167	26.120
8	57	12.4687	1.4608	9.600	15.337
9	70	21.9705	1.3182	19.382	24.559

Comparisons for each pair using Student's t
Confidence Quantile

T	Alpha
1.96347	0.05

Connecting Letters Report

Level					Mean
7	A				24.143413
9	A				21.970496
4		B			14.145360
6		B	C		13.174949
5		B	C		12.999976
8		B	C		12.468710
2		B	C		11.847820
1			C	D	8.971845
3				D	8.684628

Levels not connected by same letter are significantly different.

Table 14 - Test results of Mahalanobis distance by ward chert groupings.

Level	-Level	Difference	Std Err Dif	Lower CL	Upper CL	p-Value
7	3	15.46	1.59	12.35	18.58	<.0001*
7	1	15.18	2.12	11.02	19.34	<.0001*
9	3	13.29	1.8	9.76	16.82	<.0001*
9	1	13	2.29	8.52	17.49	<.0001*
7	2	12.3	1.4	9.56	15.04	<.0001*
7	8	11.68	1.78	8.2	15.16	<.0001*
7	5	11.15	1.77	7.69	14.61	<.0001*
7	6	10.97	1.61	7.82	14.12	<.0001*
9	2	10.13	1.64	6.92	13.34	<.0001*
7	4	10	1.78	6.52	13.49	<.0001*
9	8	9.51	1.97	5.64	13.37	<.0001*
9	5	8.98	1.96	5.13	12.82	<.0001*
9	6	8.8	1.82	5.24	12.37	<.0001*
9	4	7.83	1.97	3.97	11.69	<.0001*
4	3	5.47	1.91	1.72	9.21	0.0043*
4	1	5.18	2.37	0.53	9.83	0.0293*
6	3	4.5	1.75	1.06	7.93	0.0105*
5	3	4.32	1.9	0.6	8.05	0.0232*

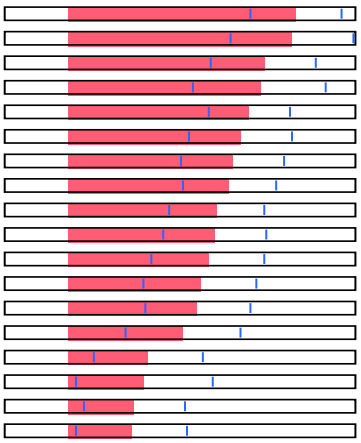

6	1	4.21	2.25	-0.21	8.61	0.0615
5	1	4.03	2.37	-0.61	8.67	0.0884
8	3	3.79	1.91	0.05	7.53	0.0476*
8	1	3.5	2.37	-1.16	8.15	0.1403
2	3	3.17	1.57	0.1	6.23	0.0431*
2	1	2.88	2.11	-1.25	7	0.1714
4	2	2.3	1.76	-1.15	5.74	0.1902
7	9	2.18	1.66	-1.09	5.43	0.1906
4	8	1.68	2.07	-2.38	5.74	0.4173
6	2	1.33	1.58	-1.78	4.43	0.4011
5	2	1.16	1.75	-2.27	4.58	0.5085
4	5	1.15	2.06	-2.9	5.19	0.5778
4	6	0.98	1.93	-2.81	4.75	0.6138
6	8	0.71	1.93	-3.07	4.48	0.7134
8	2	0.63	1.76	-2.82	4.07	0.7232
5	8	0.54	2.06	-3.51	4.58	0.7963
1	3	0.29	2.24	-4.1	4.67	0.8976
6	5	0.18	1.92	-3.58	3.93	0.9271

Table 15 - Test results of Mahalanobis distance by ward chert groupings (cont.).

Debitage or Tool

Ward Chert Grouping

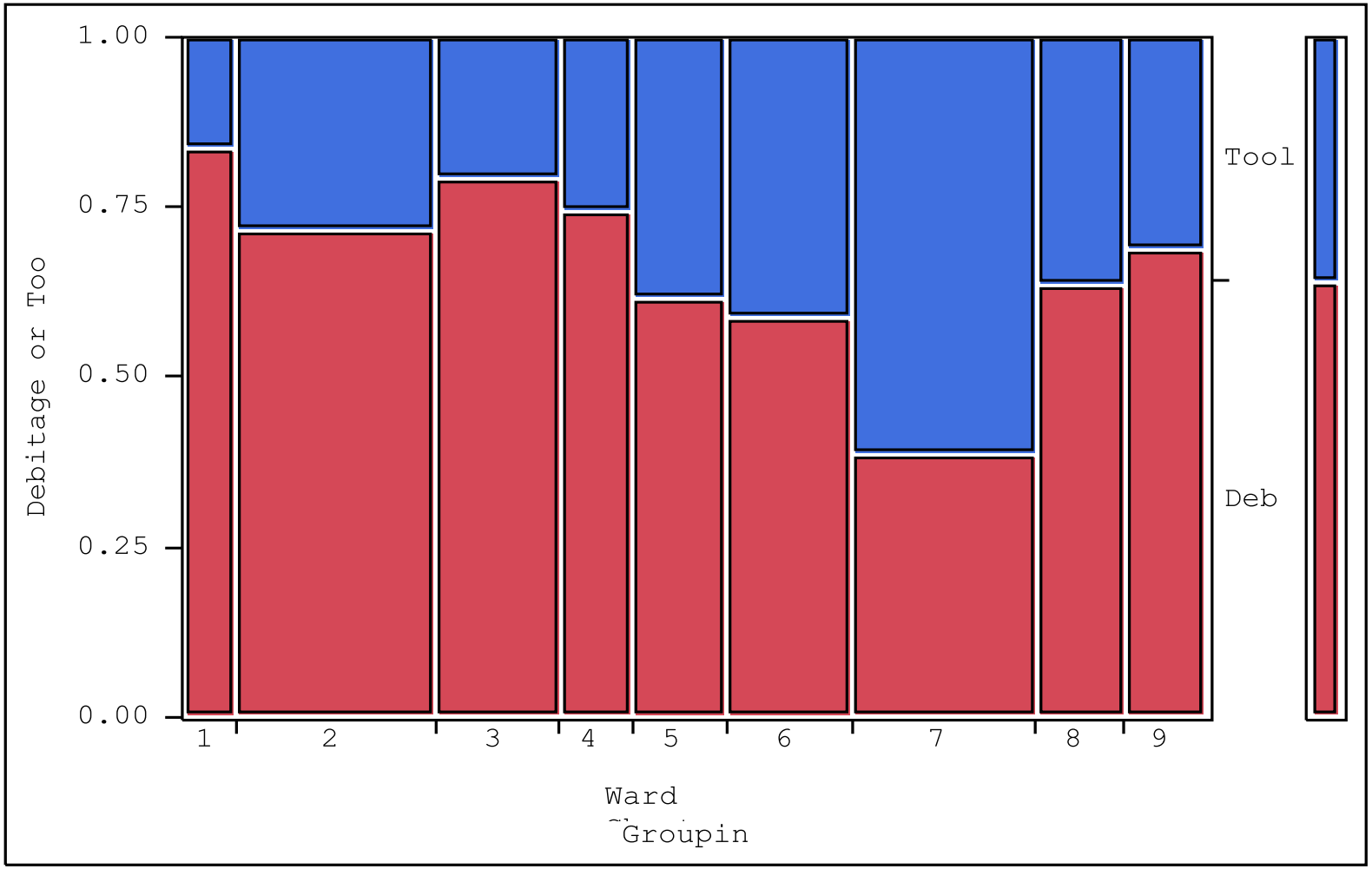

Figure 44 – Cooper's Ferry tool to debitage ratios by Ward chert grouping.

Count Expected Deviation Cell Chi^2	Deb	Tool	Total
1	26 19.8917 6.10833 1.8757	5 11.1083 -6.1083 3.3589	31
2	84 75.075 8.925 1.0610	33 41.925 -8.925 1.9000	117
3	58 46.8417 11.1583 2.6581	15 26.1583 -11.158 4.7598	73
4	32 27.5917 4.40833 0.7043	11 15.4083 -4.4083 1.2612	43
5	34 35.2917 -1.2917 0.0473	21 19.7083 1.29167 0.0847	55
6	43 46.8417 -3.8417 0.3151	30 26.1583 3.84167 0.5642	73
7	42 69.3 -27.3 10.7545	66 38.7 27.3 19.2581	108
8	33 33.3667 -0.3667 0.0040	19 18.6333 0.36667 0.0072	52
9	33 30.8 2.2 0.1571	15 17.2 -2.2 0.2814	48
	385	215	600

N	DF	-LogLike	RSquare (U)
600	8	24.520066	0.0626
Test		ChiSquare	Prob>ChiSq
Likelihood Ratio		49.040	<.0001*
Pearson		49.053	<.0001*

Table 16 - Chi-Squre results of CCS artifact type by retained cluster from Cooper's Ferry.

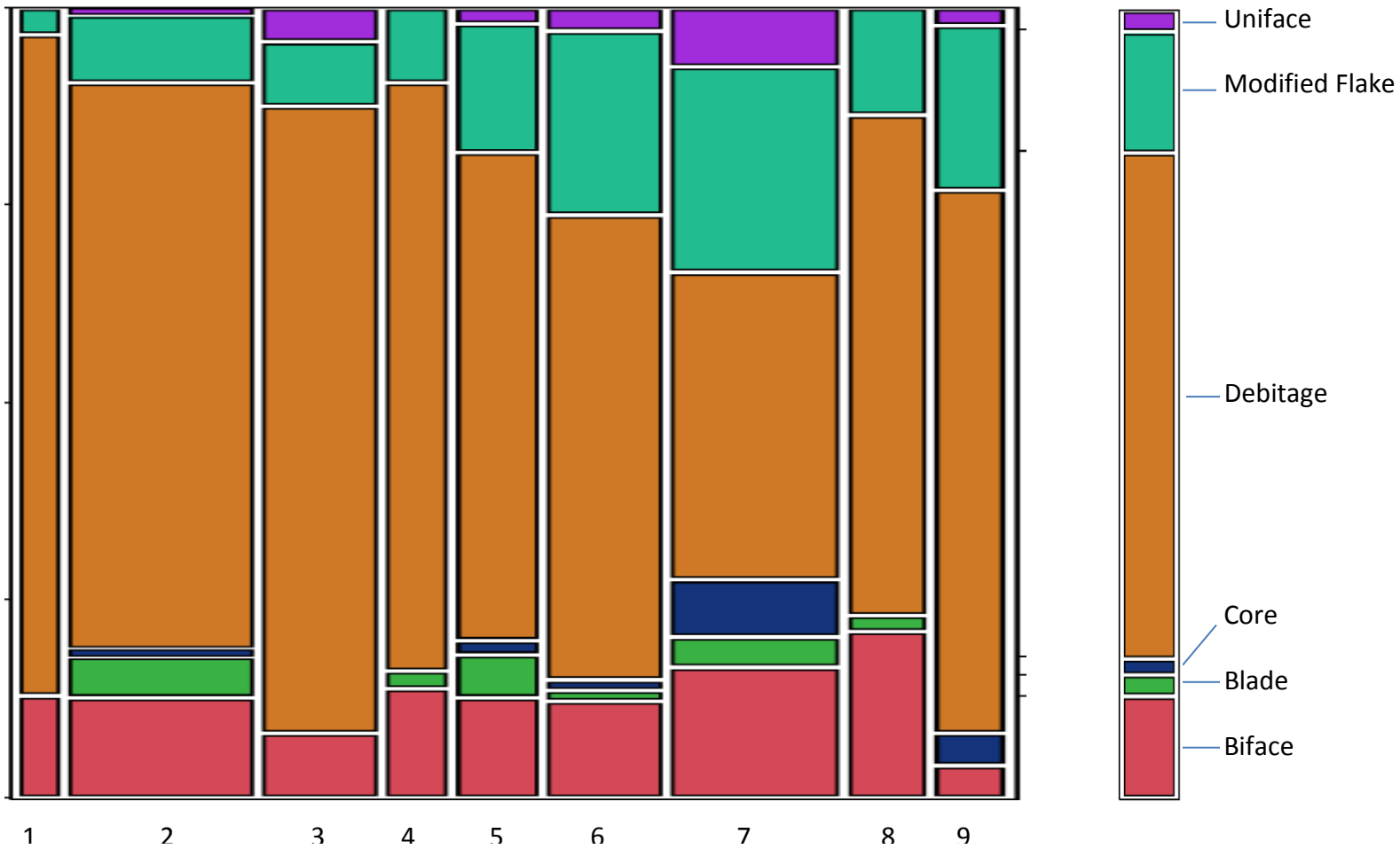

Figure 45 –Cooper's Ferry artifact type by Ward chert grouping.

Chapter 6: Conclusions

When this research began, little was known about the nature of chert geochemistry on the Columbia River Plateau. Only a single study, Hess (1996) had been performed on cherts in archaeological contexts, with a second study by Cummins et al. (1988) examining opal found within five tree-casts in in the Grand Ronde Columbia river basalt flow. In total, the sum of these two studies totals to 55 geologic samples and four archaeological samples tested geochemically for an area well over 100,000 km^2 in area. This research adds an additional 600 archaeological artifacts to that number, as well as 300 geologic samples.

This research has also shown that it is likely that there were at least five separate chert sources in use at Cooper's Ferry, and that three of these sources showed interesting patterning when examining the ratio of debitage to tools. Two of these proposed sources, (groups 1 and 3), are mainly represented as debitage at the site, while group 7 is mainly represented in formed tools. One possible explanation for this pattern is that the artifacts represented in group 7 are being knapped at some other location and then brought to the site, while artifacts in groups 1 and 3 are being mainly knapped at Cooper's Ferry and their finished products are then transported to other locations. Also of interest is that artifacts from groups 1 and 3 tended to be closer geochemically to the sources tested by the author, while the geochemistry of group 7 chemically was more distinct from any tested chert source. It is difficult to say with any degree of certainty if this degree of chemical differences

in chert sources also corresponds to greater spatial distance to sources; however a more thorough sampling of chert sources in the area should help resolve this question.

We have learned through the research presented here that knowledge of local chert sources likely was passed down from generation to generation for several thousand years at the Cooper's Ferry site. The ratio of chert source usage remains relatively constant from the earliest artifacts tested, possibly in excess of 11,000 RCYBP (Davis, 2001) through to the latest, dated approximately to 8,400 RCYBP (Davis, 2001; Figure 46). This long term transmission of cultural knowledge is consistent with the current view of early plateau cultural connections. Leonhardy and Rice (1970), Rice (1972), and Ames (1998), outline a single cultural phase that spans the timeframe of artifacts excavated at the Cooper's Ferry site. Dubbed "Windust" by Leonhardy and Rice, and "Period 1B" by Ames, this phase is defined by low population densities, stemmed and lancolate projectile points produced using a Levallois-like reduction strategy and use of chert as the primary toolstone of choice (Rice, 1972:213-215). Davis (2001) argues that three separate cultural phases present at Cooper's Ferry, "Cooper's Ferry 1", "Cooper's Ferry 2", and the beginnings of "Craig Mountain". While Cooper's Ferry 1 and "Craig Mountain" are present at the site, the majority of artifacts fall within Cooper's Ferry 2, which is roughly contemporaneous with the Windust phase defined by Leonhardy and Rice (1970) (Davis, 2001).

Future Directions

The next step in this research has already begun. Over the last two years, four new chert sources have been located in the LSRC near Cooper's Ferry and are awaiting chemical characterization. Over the 2013 summer field season, Oregon State University will work with the Idaho BLM and local land owners to conduct an intensive survey around Cooper's Ferry for new chert sources. Projectile points from across the Columbia River Plateau are currently being scanned via PXRF analysis using the methodologies outlined in this research as part of a larger projectile point typology project; at the time of this writing over 100 points have been analyzed, with another 150 to be completed by June, 2013. In 2009, Cooper's Ferry was reopened as a large block excavation (currently 12 x 6 meters) with plans to examine all formed tools as well as large samples of debitage recovered via PXRF. This will drastically increase the sample sizes of artifacts examined from the site and will aid our understanding of how people are using cherts through time. Formal lithic analysis of the artifacts recovered from Cooper's Ferry is ongoing, the results of which, when combined with knowledge of chert provenance, technology, subsistence patterns, and logistical strategies pursued by early foragers of the LSRC.

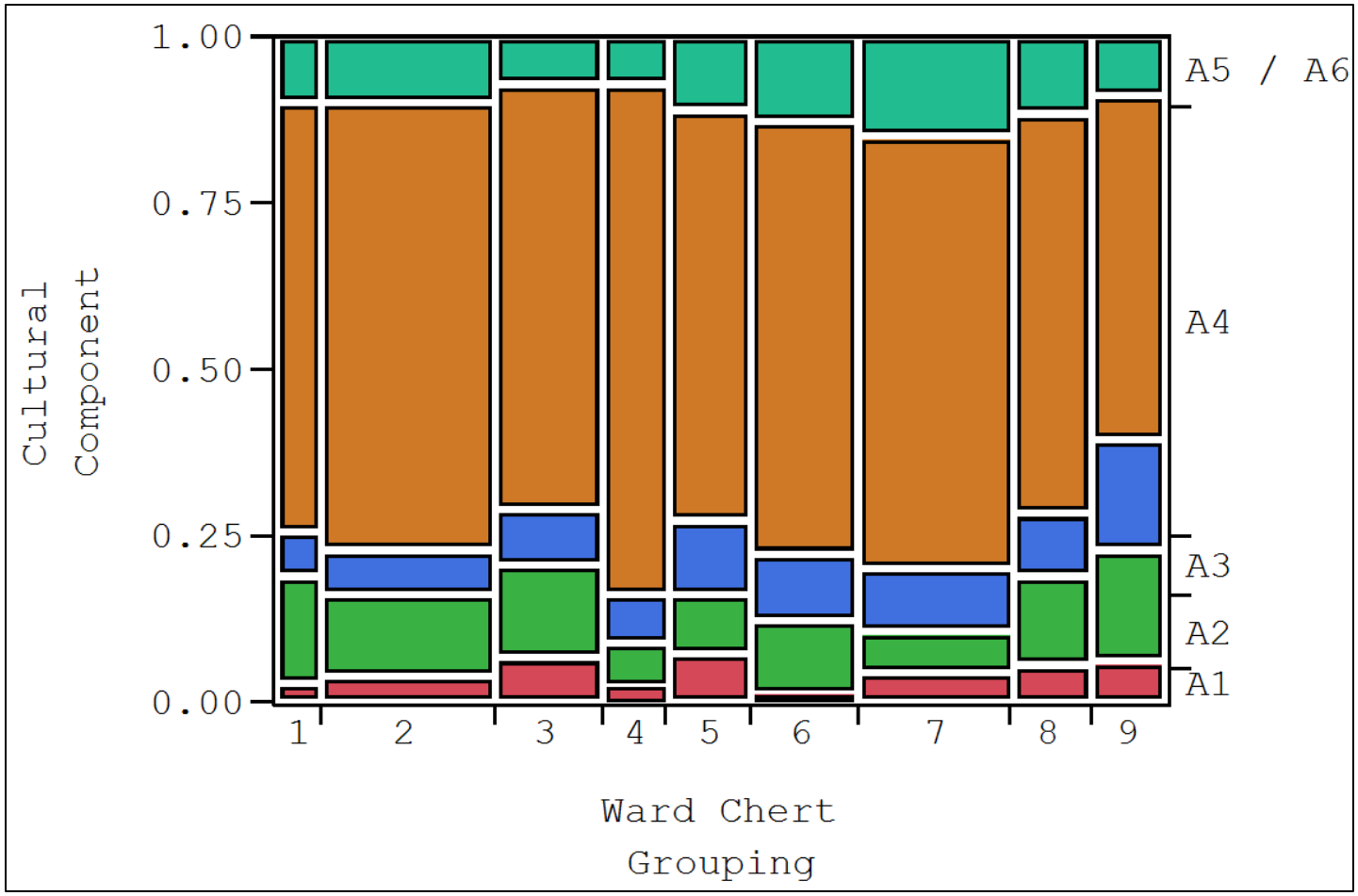

Figure 46 - Cultural Components at Cooper's Ferry by Ward Chert Grouping. Note the lack of any strong correlations between chert groupings and components.

Bibliography

Aldenderfer, M., & Blashfield, R. (1995). *Cluster Analysis* (Vol. 44). Sage Publishing.

Allwood, A., Kamber, B., Walter, M., Burch, I., & Kanik, I. (2010). Trace Elements Record Depositional History of an Early Archean Stromatolitic Carbonate Platform. *Chemical Geology, 270*, 148-163.

Ames, K. G., Dumond, D. E., Galm, J. R., & Minor, R. (1998). Prehistory of the Southern Plateau. In D. Walker, *Handbook of North American Indians* (Vol. 9, pp. 103-119). Washington, DC: Smithsonian Institution Press.

Antweiler, R. C., & Taylor, H. E. (2007). Evaluation of Statistical Treatments of Left-Censored Environmental Data using Coincident Uncensored Data Sets: I. Summary Statistics. *Environmental Science and Technology, 42*(10), 3732-3738.

Biagi, P., & Nisbet, R. (2010). The Prehistoric Flint Mines at Jhimpir in Lower Sindh (Pakistan). *Antiquity, 084*(325).

Cottrell, M. (1985). Tomato Springs: The Identification of a Jasper Trade and Production Center in Southern California. *American Antiquity, 50*(4), 833-849.

Cummings, M., Trone, P., & Pollock, J. (1989). Geochemistry of Colloidal Silica Precipitates in Altered Grande Ronde Basalt, Northeastern Oregon, USA. *Chemical Geology, 75*, 61-79.

Davis, K., Jackson, T., Shackley, S., Teague, T., & Hampel, J. (1998). Factors Affecting the Energy-Dispersive X-Ray Flourescence (EDXRF) Analysis of Archaeological Obsidian. In S. Shackley, *Archaeological Obsidian Studies. Method and Theory* (pp. 159-180). New York: Plenum Press.

Davis, L. G. (2001). *The Coevolution of Early Hunter-Gatherer Culture and Riparian Ecosystems in the Southern Columbia River Plateau, PH. D Dissertation.* Edmonton: University of Alberta.

Davis, L. G., & Schweger, C. E. (2004). Geoarchaeological Context of Late Pleistocene and Early Holocene Occupation at the Cooper's Ferry Site, Western Idaho, USA. *Geoarchaeoogy, 19*(7), 685-704.

DeMaster, D. (2005). The Diagenesis of Biogenic Silica: Chemical Transformations Occuring in the Water Columnm, Seabed, and Crust. In F. Mackenzie, *Sediments, Diagenesis, and Sedimentary rocks* (Vol. 7, pp. 87-96). Amsterdam: Elsevier.

Department of the Army. (2008). *Environmental Statistics - CEMP-CE Manual 1110-1-4014.* Washington, DC: U.S. Army Corps of Engineers.

Devore, J. (2000). *Probability and statistics for engineering and the sciences.* Pacific Grove, CA: Thomson Learning.

Drennan, R. D. (1996). *Statistics for Archaeologists: A Common sence Approach.* (M. Jochim, & R. Dickens, Eds.) New York, New York, United States: Springer Science + Business Media, LLC.

Drew, L. J., Grunsky, E. C., Sutphin, D. M., & Woodruff, L. G. (2010). Multivariate Analysis of the Geochemistry and Mineralogy of Soils Along Two Continental-scale Transects in North America. *Science of the Total Environment, 409*, 218-227.

Eugster, H. (1967). Hydrous Sodium Silicates from Lake Magadi, Kenya: Precursors of Bedded Chert. *Science, 157*, 1177-1180.

Evans, A., Wolframm, Y., Donahue, R., & Lovis, W. (2007). A Pilot Study of "Black Chert" Sourcing and Implications for Assessing Hunter-Gatherer Mobility Strategies in Northern England. *Journal of Archaeological Science, 34*(12), 2161-2169.

Evans, K., Aleinikoff, J., Obradovich, J., & Fanning, C. (2000). SHRIMP U-Pb Geochronology of Volcanic Rocks, Belt Supergroup, Western Montana; Evidence for Rapid Deposition of Sedimentary Strata. *Canadian Journal of Earth Sciences, 37*(9), 1287-1300.

Fekedulegn, B. D., Colbert, J., Hicks, R. J., & Schuckers, M. E. (2002). *Coping with Multicollinearity: An Example on Application of Principal Components*

Regression in Dendroecology. Forest Service, Northeastern Research Station. Newton Square, PA: Department of Agriculture.

Gauthier, G., Burke, A., & Lecler, M. (2012). Assessing XRF for the Geochemical Characterization of Radiolarian Chert Artifacts. *Journal of Archaeological Science*, 1-16 (In press).

Gauze, G. (2003). *The Struggle for Existence.* Mineola, New York: Courier Dover Publications.

Glascock, M. (2004). Neutron Activation Analysis of Chert Artifacts From a Hopewell Mound. *Journal of Radioanalytical and Nuclear Chemistry, 262*(1), 97-102.

Glascock, M., & Neff, H. (2003). Neutron Activation Analysis and Provenance Research in Archaeology. *Measurement Science and Technology, 14*, 1516-1526.

Graham, M. (2003). Confronting Multicollinearity in Ecological Multiple Regression. *Ecology, 84*(11), 2809-2815.

Gregorio, B., & Sharp, T. (2006). The Structure and Distribution of Carbon in 3.5 Ga Apex chert: Implications for the Biogenicity of Earth's Oldest Putative Microfossils. *American Mineralogist, 91*, 784-789.

Grenne, T., & Slack, J. (2003). Paleozoic and Mesozoic Silica-Rich Seawater: Evidence from Hematitic Chert (Jasper) Deposits. *Geology, 31*, 319-322.

Hair, J. F., Anderson, R. E., Tatham, R. L., & Black, W. C. (1998). *Multivariate Data Analysis* (5th ed.). Upper Saddle River, New Jersey, United States: Prentice Hall.

Hess, S. (1996). Chert Provenance Analysis at the Mack Canyon Site, Sherman County, Oregon: An Evaluative Study. *Geoarchaeology, 11*, 51-81.

Hesse, R. (1989). Silica Diagenesis: Origin of Inorganic and Replacement Cherts. *Earth Science Reviews, 26*, 253-284.

Hoard, R., Bozell, J., Holen, S., Glascock, M., Neff, H., & Elam, M. (1993). Archaeology Source Determination of White River Group Silicates from Two Archaeological Sites in the Great Plains. *American Antiquity, 58*(4), 698-710.

Hostermann, J. (1960). Geology of the Clay Deposits in Parts of Washington and Idaho. *Clays and Clay Minerals*, *7*, pp. 285-294.

Huberty, C., Wisenbaker, J., & Smith, J. (1987). Assessing Predictive Accuracy in Discriminant Analysis. *Multivariate Behavioral Research, 22*, 307-329.

Huckell, B., Kilby, D., Boulanger, M., & Glascock, M. (2011). Sentinel Butte: Neutron Activation Analysis of White River Group Chert from a Primary Source and Artifacts from a Clovis Cache in North Dakota, USA. *Journal of Archaeological Science, 38*(5), 965-976.

Jarvis, H. W. (1988). *INAA Characterization of Onodaga Chert: A Preliminary Study in Western New York (Masters Thesis).* Buffalo: New York State University at Buffalo.

Joachimsthale, E. A., & Stam, A. (1988). Four Approaches to the Classification Problem in Discriminant Analysis: An Experimental Study. *Decision Sciences, 19*(2), 322-333.

Jolliffe, I. (2002). *Principal Component Analysis* (2nd ed.). New York, New York, USA: Springer-Verlag.

Jombart, T. D. (2010). Discriminant Analysis of Principal Components: A New Method for the Analysis of Genetically Structured Populations. *BMC genetics, 11:94*. doi:10.1186/1471-2156-11-94

Jones, G. T., Beck, C., Jones, E. E., & Hughs, R. E. (2003). Lithic Source Use and Paleoarchaic Foraging Territories in the Great Basin. *American Antiquity, 68*(1), 5-38.

Kendell, H. (2010). To Measure or not to Measure: Geochemical Analysis of Siliceous Materials in the Interior Plateau of British Columbia. *Explorations in Anthropology, 10*(2), 8-21.

Kettenring, J. (2006). The Practice of Cluster Analysis. *Journal of Classification, 23*, 3-30. doi:10.1007/s00357-006-0002-6

Kirkham, V., & Melville, M. (1929). The Latah Formation. *Journal of Geology, 37*(5), 483-504.

Knauth, P. (1979). A Model for the Origin of Chert in Limestone. *Geology*, 274-277.

Knauth, P. (1994). Petrogenesis of chert. *Reviews in Mineralogy and Geochemistry, 29*, 233-258.

Knippenberg, S. (2006). *Stone Artefact Production and Exchange Among the Northern Lesser Antilles.* Utrecht, Netherlands: DPP.

Ledesma, R., & Valero-Mora, P. (2007). Determining the Number of Factors to Retain in EFA: An Easy-to-use Computer Program for Carrying out Parallel Analysis. *Practical Assessment, Research & Evaluation, 12*(2), 1-11.

Leonhardy, F. C., & Rice, D. G. (1970). A Proposed Culture Typology for the Lower Snake River Region, Southeastern Washington. *Northwest Anthropological Research Notes*, 1-29.

Link, P., Fanning, C., Lund, K., & and Aleinikoff, J. (2007). Detrital Zircons, Correlation and Provenance of Mesoproterozoic Belt Supergroup and Correlative Strata of East-Central Idaho and Southwest Montana. *SEPM Special Publication 86, Proterozoic geology of western North America and Siberia*, 101-128.

Luedtke, B. (1978). Chert Sources and Trace-Element Analysis. *American Antiquity, 43*(3), 413-423.

Luedtke, B. (1979, Oct). The Identification of Sources of Chert Artifacts. *American Antiquity*, 744-757.

Luedtke, B. (1992). *An Archaeologists Guide to Chert and Flint.* Los Angeles: University of California.

Lyons, W., Glascock, M., & Mehringer, P. (2003, September). Silica from Sources to Site: Ultraviolet Fluorescence and Trace Elements Identify Cherts from Lost Dune, Southeastern Oregon, USA. *Journal of Archaeological Science, 30*(9), 1139-1159.

Maliva, R. (2001). Silicification in the Belt Supergroup (Mesoproterozoic), Glacier National Park, Montana, USA. *Sedimentology*(48), 887-896.

Malyk-Selivanova, N., Ashley, G., Gal, R., Glascock, M., & Neff, H. (1998). Geological-Geochemical Approach to "Sourcing" of Prehistoric Chert Artiacts, Northwestern Alaska. *Geoarchaeology, 13*(7), 673-708.

Meyers, G., & Guarino, A. (2006). *Applied Multivariate Research: Design and Interpretation.* Thousand Oaks: Sage Publications.

Mierendorf, R. (n.d.). Chert Procurement in the Upper Skagit River Valley of the Northern Cascade Range, Ross Lake National Recreation Area, Washington. *US Department of the interior, NPS.*

Minc, L. (2009). Style and Substance: Evidence for Regionalism Within the Aztec Market System. *Latin American Antiquity, 20*(2), 343-374.

Murray, R. (1993). Chemical Criteria to Identify the Depositional Environment of Chert: General Principles and Applications. *Sedimentary Geology, 90*(3-4), 213-232.

Murray, R. W., Buchholtz Ten Brink, M. R., Gerlach, D. C., Price Russ III, G., & Jones, D. L. (1991). Rare Earth, Major, and Trace Elements in Chert from the Franciscan Complex and Monterey Group, California: Assessing REE Sources to Fine-Grained Marine Sediments. *Geochimica et Cosmochimica Acta, 55*(7), 1875-1895.

Murray, R., Jones, D., & Brink, B. t. (1992). Diagenetic Formation of Bedded Chert: Evidence from Chemistry of the Chert-Shale Couplet. *Geology, 20*, 271-274.

Nadooshan, F. K., Abedi, A., Glascock, M. D., Eskandari, N., & Khazaee, M. (2013). Provenance of Prehistoric Obsidian Artefacts from Kul Tepe, Northwestern Iran Using X-ray Ffluorescence (XRF) analysis. *Journal of Archaeological Science*(40), 1956-1965.

Owen, A., Armstrong, H., & Floyd, J. (1999). Rare Earth Elements in Chert Clasts as Provenance Indicators in the Ordovician and Silurian of the Southern Uploads of Scotland. *Sedientary Geology, 124*(1-4), 185-186.

Pufahl, P., & Hiatt, E. (2012). Oxygenation of the Earth's Atmosphere–Ocean System: A Review of Physical and Chemical Sedimentologic Responses. *Marine and Petroleum Geology, 32*(1), 1-20.

Racki, G. (2000). Radiolarian Palaeoecology and Radiolarites: Is the Present the Key to the Past? *Earth-Science Reviews, 52*(1-3), 83-120.

Rafferty, S., Wood, C., & Rieth, C. (2007). A Trace Element Analysis of New York Chert Sources. *North American Archaeologist, 28*(2), 167-186.

Reidel, S., Martin, B., & Petcovic, H. (2003). The Columbia River Flood Basalts and the Yakima Fold Belt. In T. Swanson, *Western Cordillera and Adjacent Areas* (pp. 87-92). Geologic Society of America.

Rencher, A. C. (2002). *Methods of Multivariate Analysis* (2nd ed.). John Whiley and Sons.

Rice, D. G. (1972). The Windust Phase in Lower Snake River Prehistory. *Report of Investigations no. 50. Laboratory of Anthropology*.

Rollinson, H. (1992). Another Look at the Constant Sum Problem in Geochemistry. *Mineralogical Magazine, 56*, 469-475.

Schiffer, M. (1987). *Formation Processes of the Archaeological Record.* Albuquerque: University of Utah Press.

Shackley, M. S. (2010). Is There Reliability and Validity in Portable X-ray Fluorescence Spectrometry (PXRF). *The SAA Archaeological Record, 10*(5), 17-20.

Shackley, S. (1987). Comment on "Tomato Springs: The Identification of a Jasper Trade and Production Center in Southern California. *American Antiquity, 52*(3), 616-623.

Shackley, S. (2012). An Introduction to X-Ray Flourescence (XRF) Analysis in Archaeology. In S. Shackley, *X-Ray Flourescene Spectrometry (XRF) in Geoarchaelogy* (pp. 7-44). New York, New York: Springer.

Shackley, S. M. (1998). *Archaeological Obsidian Studies: Method and Theory* (Vol. 3). New York, New York: Plenum Press.

Sheppard, P., Trichereau, B., & Milicich, C. (2010). Pacific Obsidian Sourcing by Portable XRF. *Archaeology in Oceania, 45*(1), 21-30.

Skala, W. (1979). Some Effects of the Constant-Sum Problem in Geochemistry. *Chemical Geology, 27*(1-2), 1-9.

Spinden, H. J. (1908). *The Nez Percé Indians.* Lancaster, Pa: The New era printing company.

Straub, K., & Link, P. (2013, May). *Columbia River Basalt Province*. Retrieved from Digital Geology of Idaho: http://geology.isu.edu/Digital_Geology_Idaho/Module10/mod10.htm

Suhr, D. D. (2005). Principal Component Analysis vs. Exploratory Factor Analysis. *Proceedings of the Thirtieth Annual SAS® Users Group International Conference.* Cary: SAS Institute Inc.

Templ, M., Filzmoser, P., & Reimann, C. (2008). Cluster Analysis Applied to Regional Geochemical Data: Problems and Possibilities. *Applied Geochemistry, 23*(8), 2198-2213.

Vallier, T. (1998). *Island and Rapids A Geological Story of Hells Canyon.* lewiston: Confluence Press.

Van den Boorn, S., Van Bergen, M., Vroon, P., De Vries, S., & Nijman, W. (2010). Silicon Isoptope and Trace Element Constraints on the Origin of ~3.5 Ga Cherts: Implications for Early Archaen Marine Environments. *Geochimica et Cosmochimica Acta, 74*, 1077-1103.

Watkins, M. W. (2006, November). Determining Parallel Analysis Criteria. *Journal of Modern Applied Statistical Methods, 5*(2), 344-346.

Weltje, G. J. (2006). Ternary Sandstone Composition and Provenance: An Evaluation of the 'Dickinson Model'. In A. Buccianti, G. Mateu-Figueras, & V. P. Glahn, *Compositional data analysis in the geosciences: from theory to practice* (pp. 79-99). Geological Society of London.

White, J., White, D., Vallier, T., Stanley, G., & Ash, S. (1992). Middle Jurassic Strata Link Wallowa, Olds Ferry, and Izee Terranes in the Accreted Blue Mountains Island Arc, Northeastern Oregon. *Geology, 20*, 729-732.

Williams, L. A., & Crerar, D. (1985). Silica Diagenesis, II. General Mechanisms. *Journal of Sedimentary Petrology, 55*(3), 0312-0321.

Zwick, W. R., & Velicer, W. F. (1986, May). Comparison of Five Rules for Determining the Number of Components to Retain. *Psychological Bulletin, 99*(3), 432-442.

Appendices

Appendix A: Calibration Curves

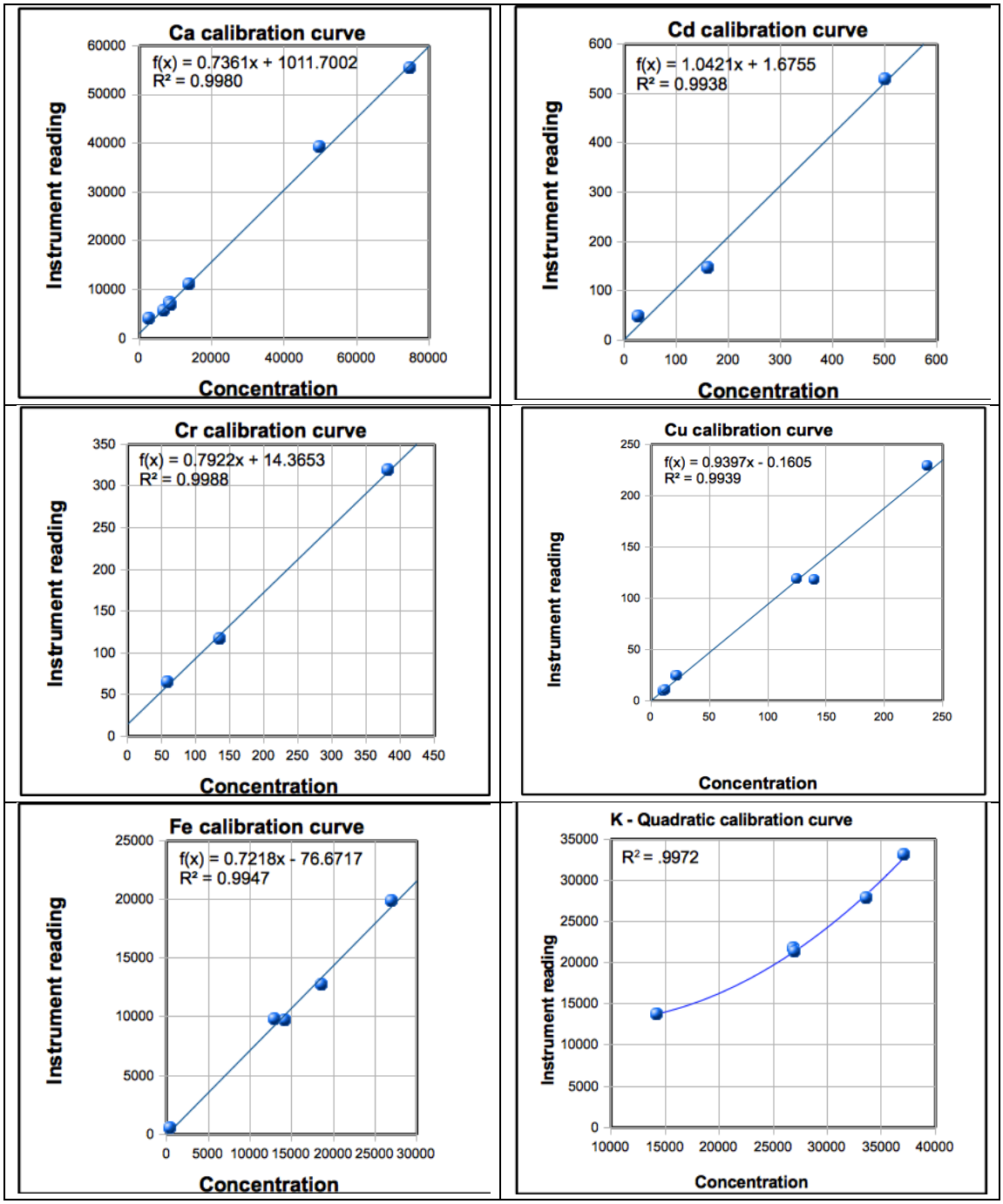

Figure A 1 - Calibration Curves for PXRF Device.

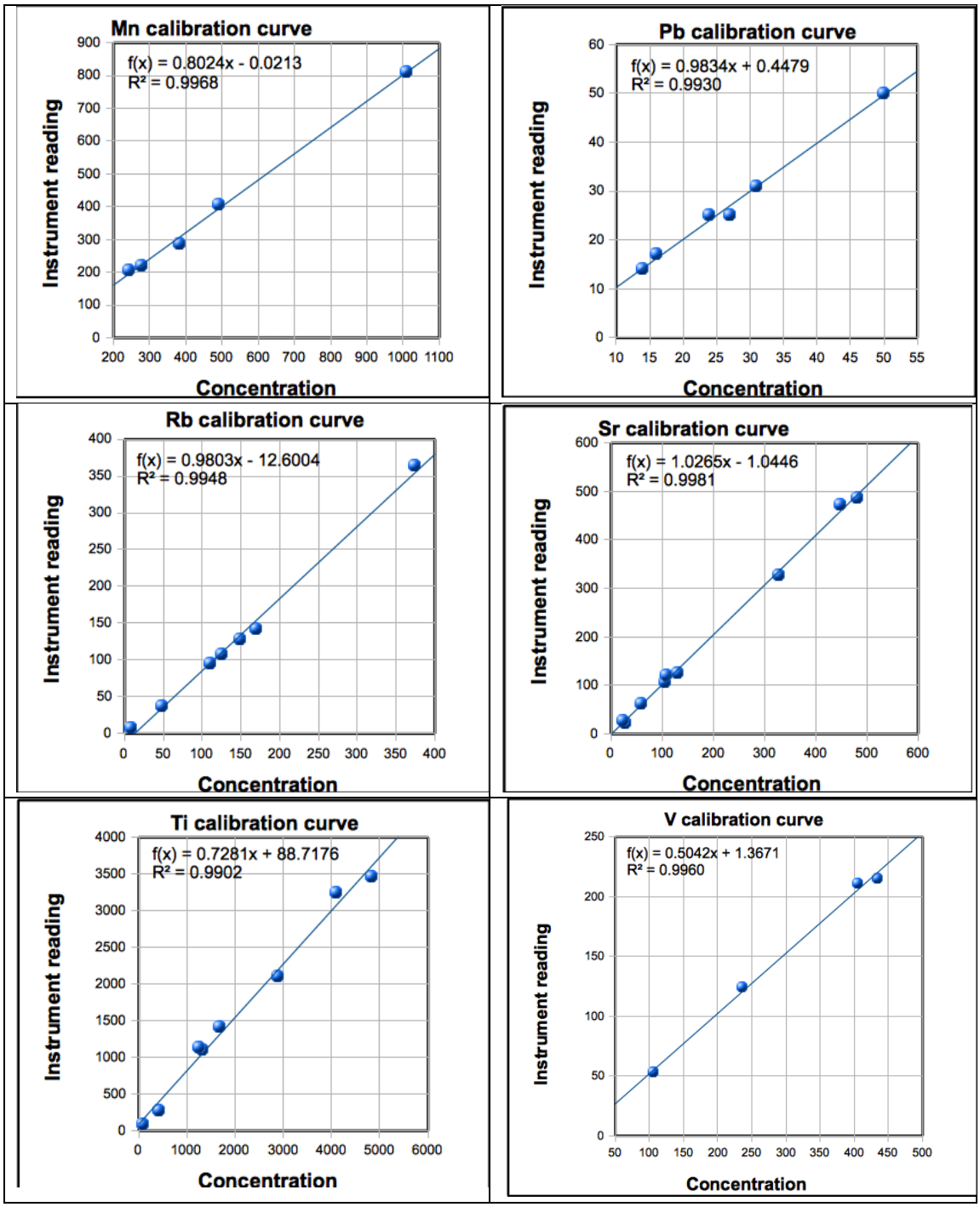

Figure A 1 - Calibration Curves for PXRF Device (cont.).

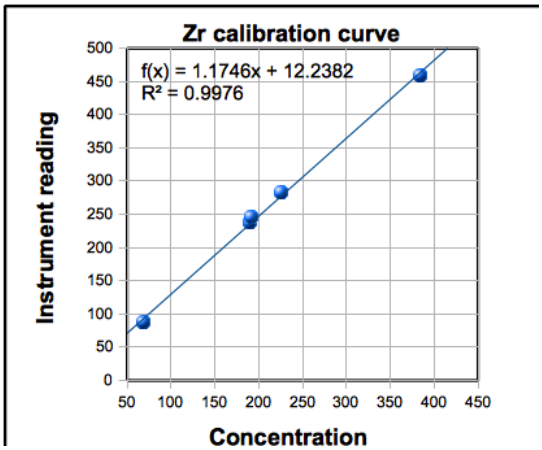

Figure A 1 - Calibration Curves for PXRF Device (cont.).

Appendix B: Analytical Methodology Flowchart

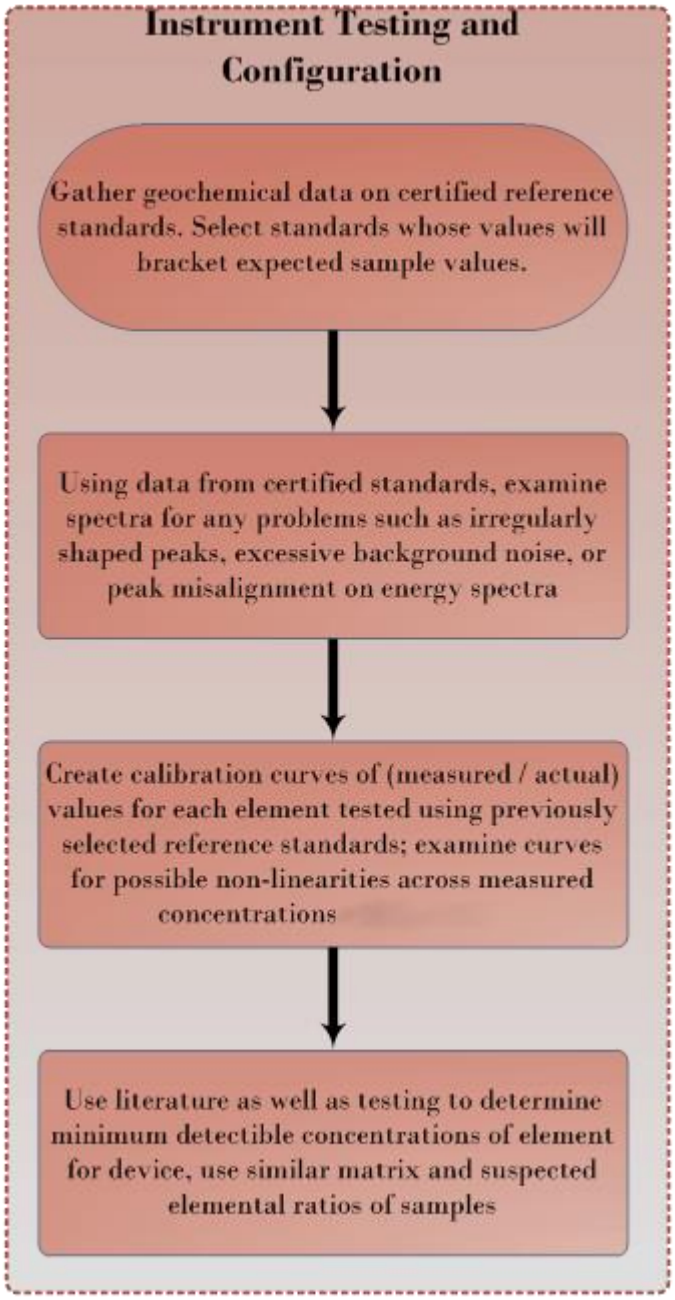

Figure B 1 - Analytical Methodology Flowchart.

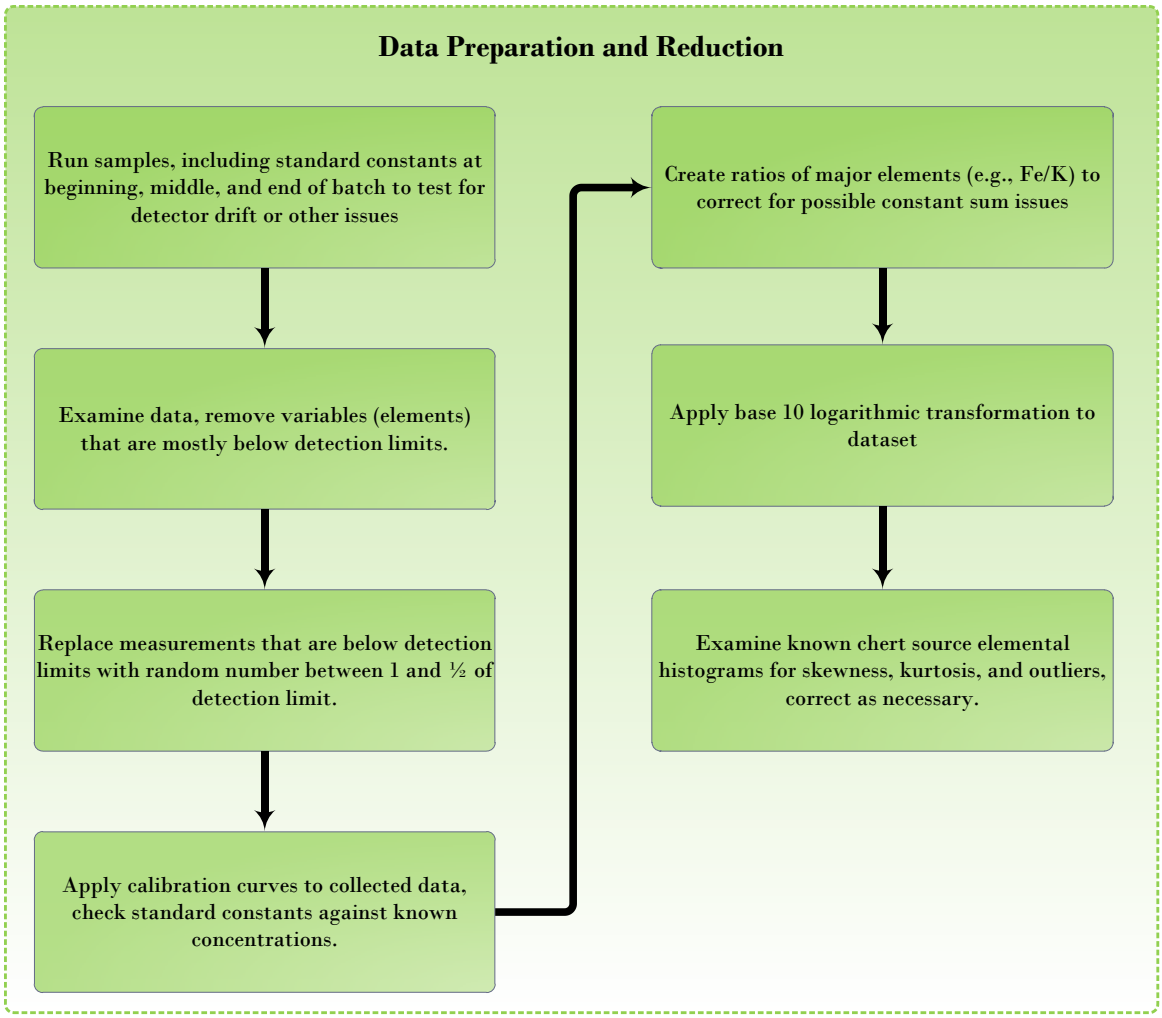

Figure B 1 - Analytical Methodology Flowchart (cont.).

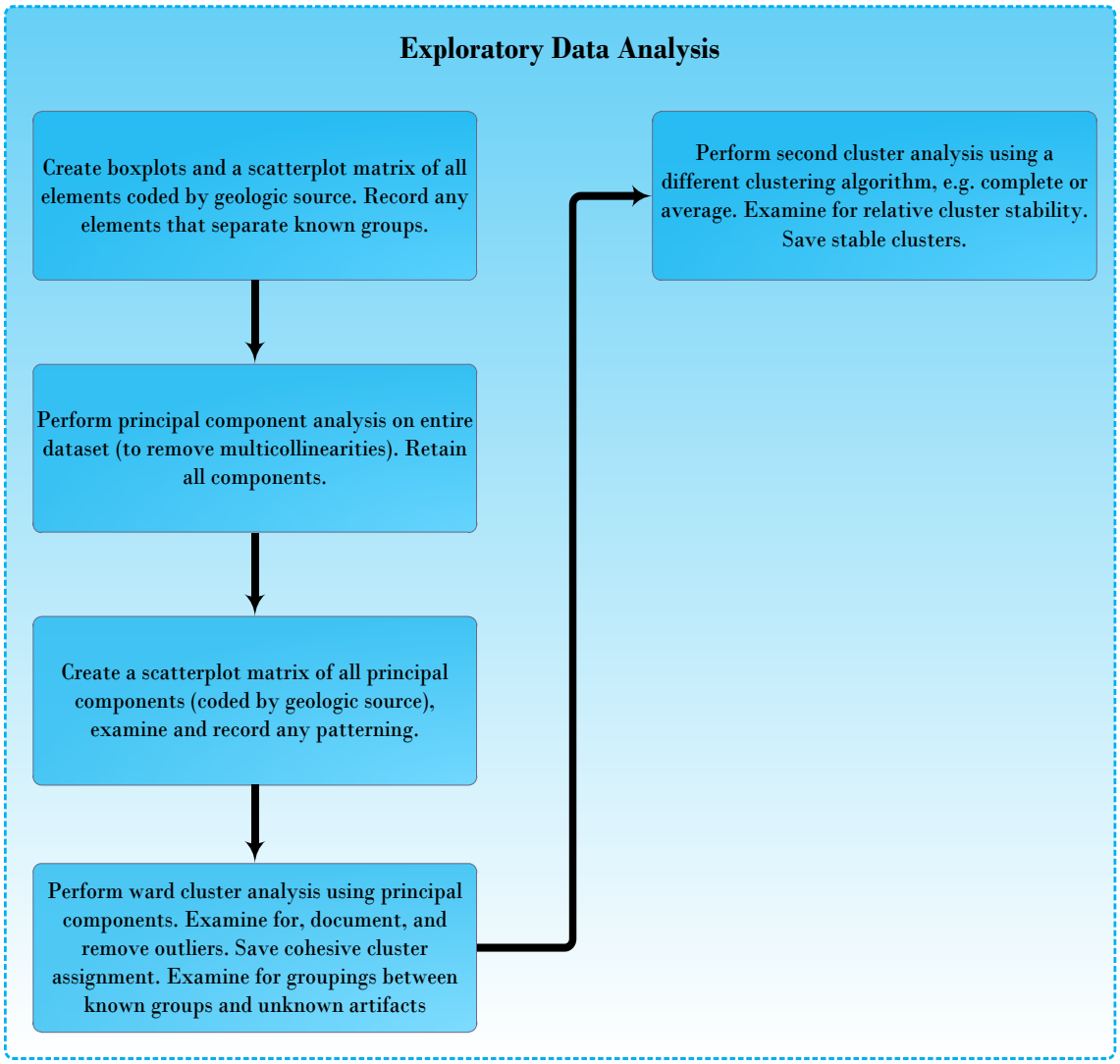

Figure B 1 - Analytical Methodology Flowchart (cont.).

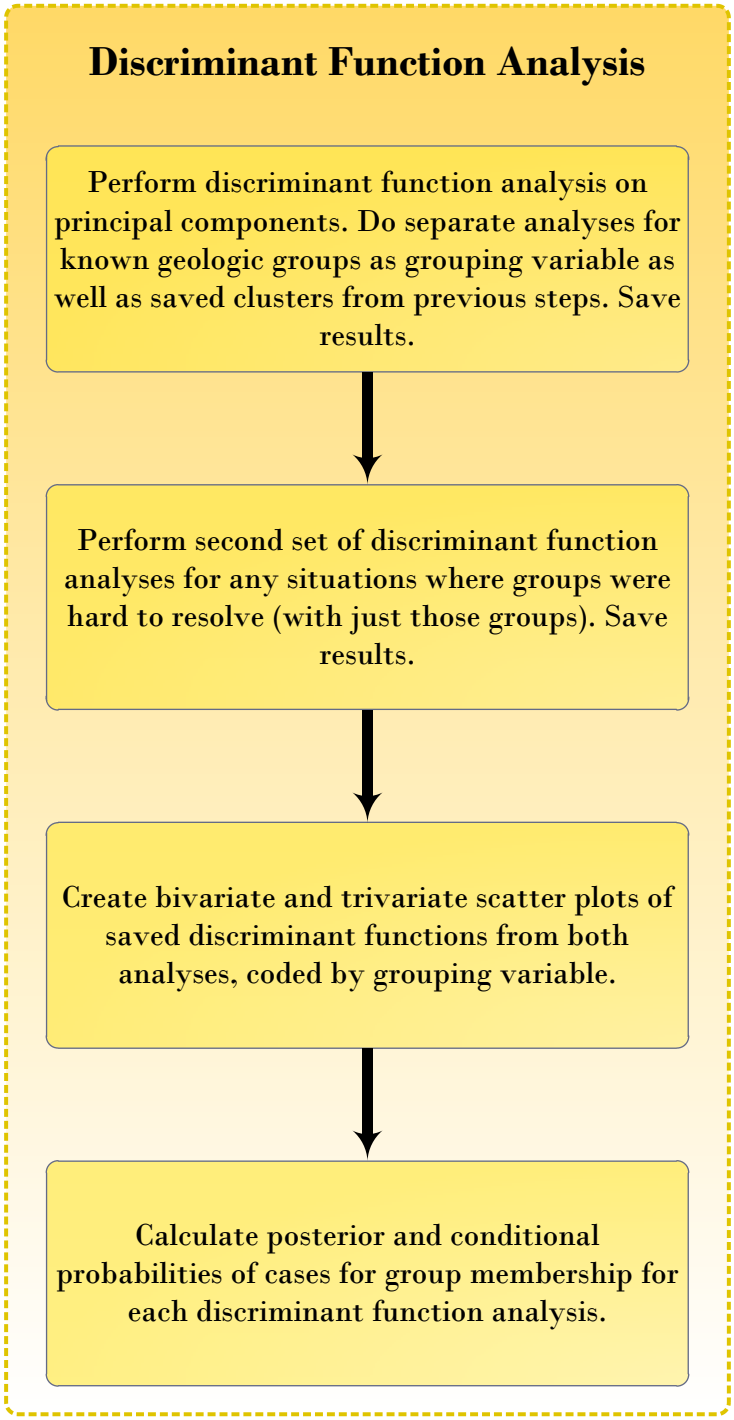

Figure B 1 - Analytical Methodology Flowchart (cont.).

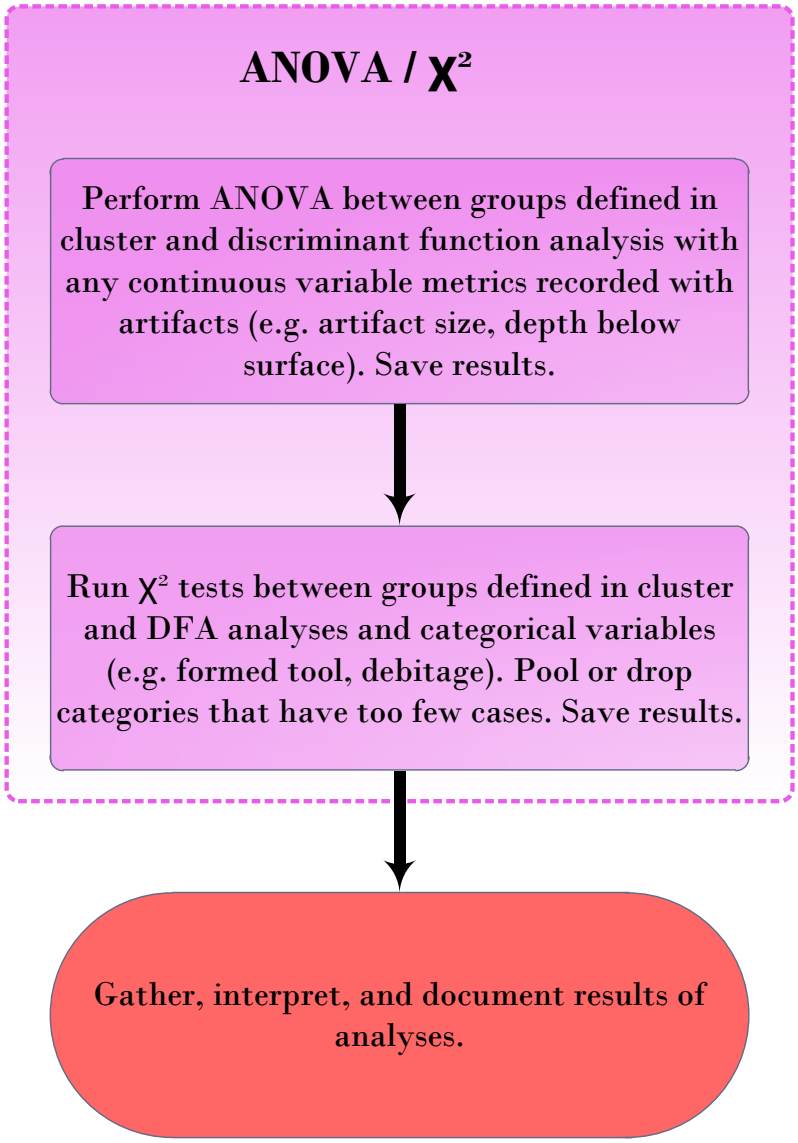

Figure B 1 - Analytical Methodology Flowchart (cont.).

Appendix C: Scatterplot Matrices

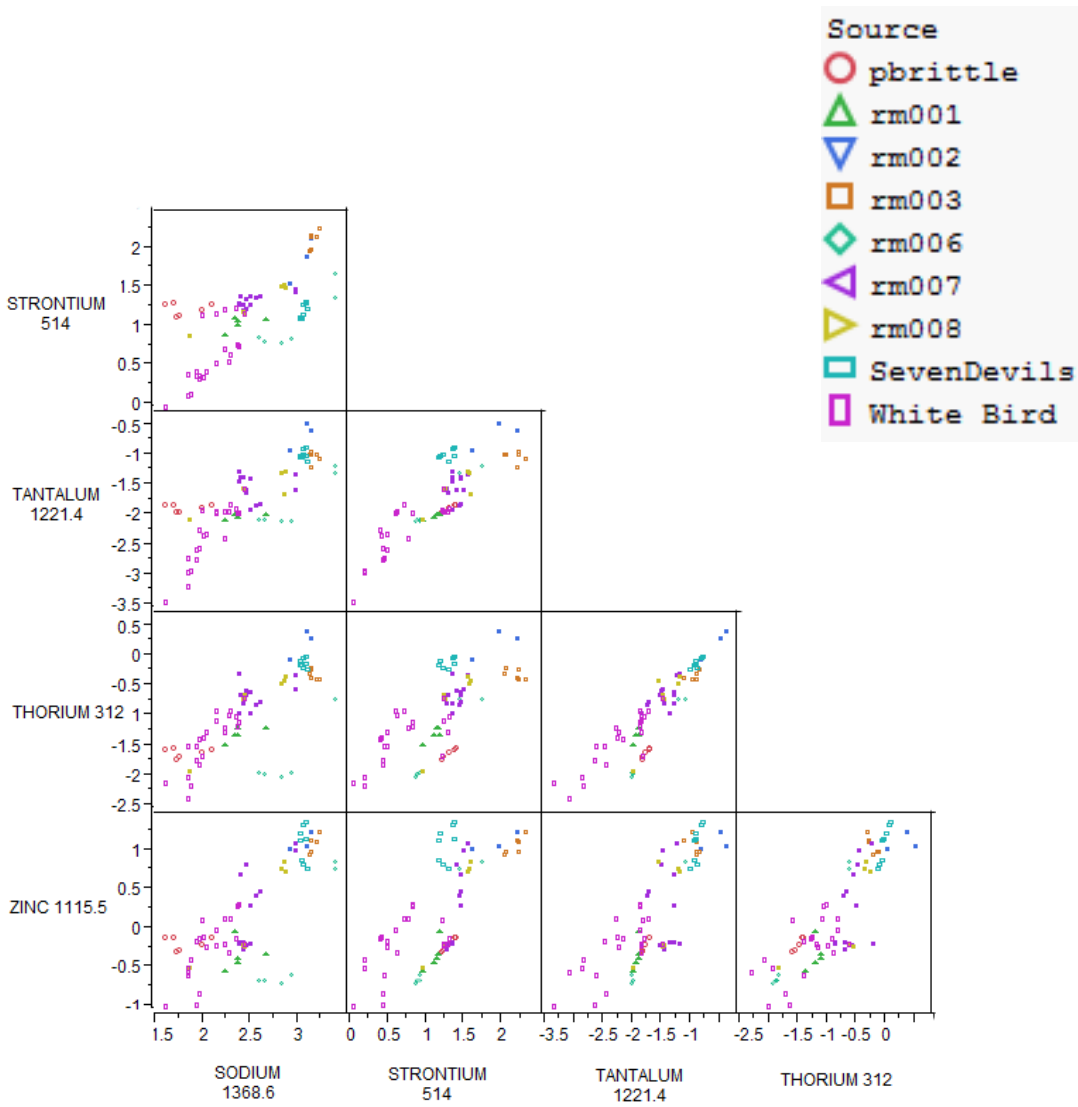

Figure C 1 - Scatterplot matrix of log10 INAA geologic source data.

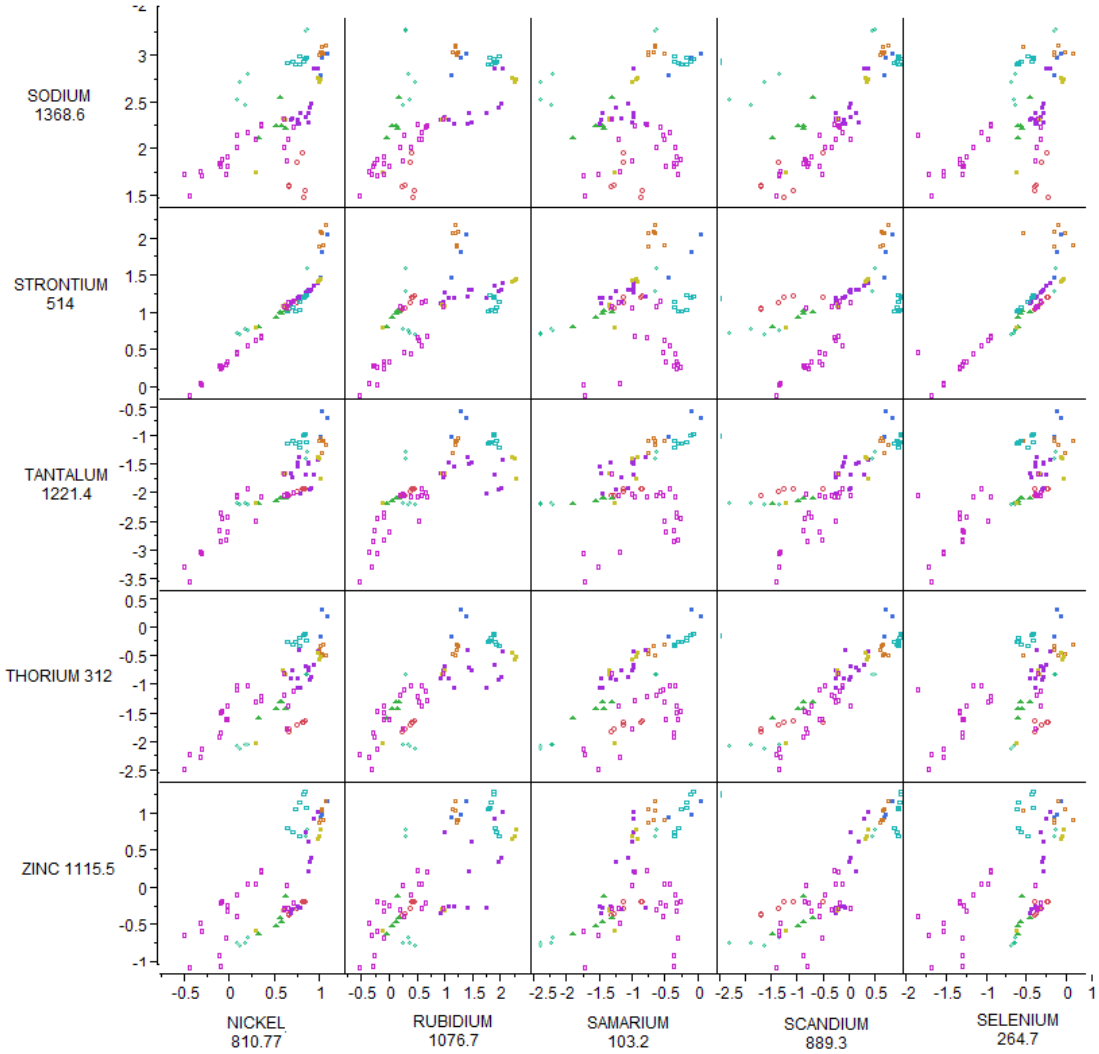

Figure C 1 - Scatterplot matrix of log10 INAA geologic source data (cont.).

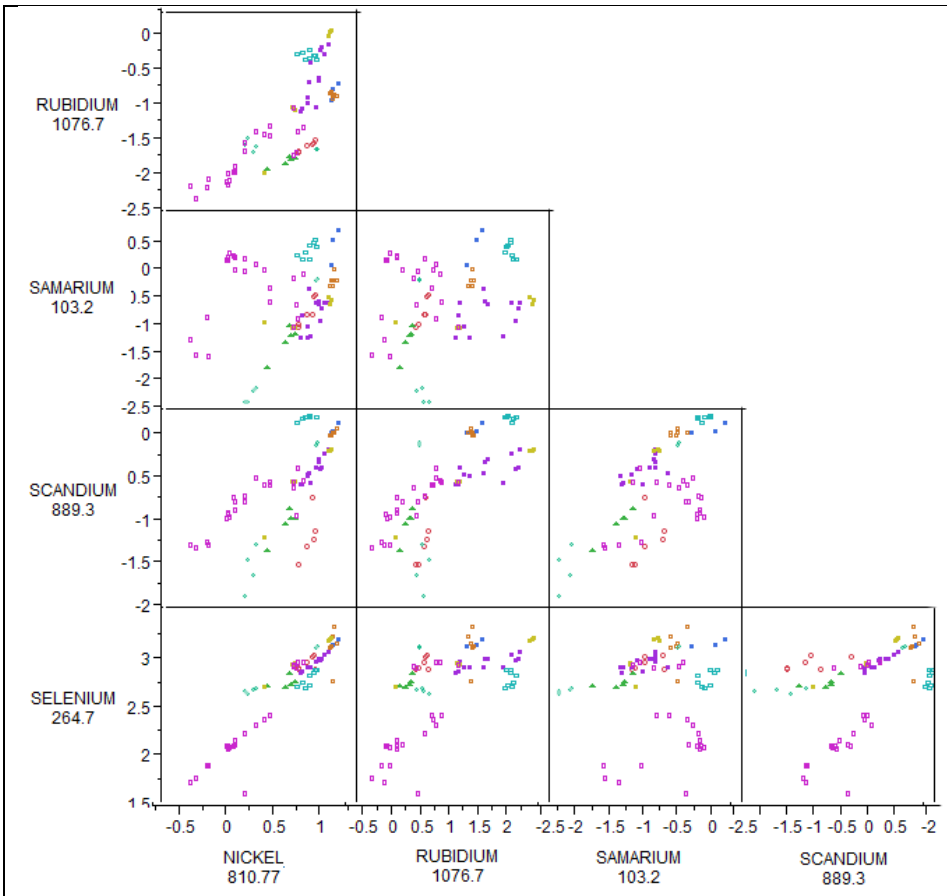

Figure C 1 - Scatterplot matrix of log10 INAA geologic source data (cont.).

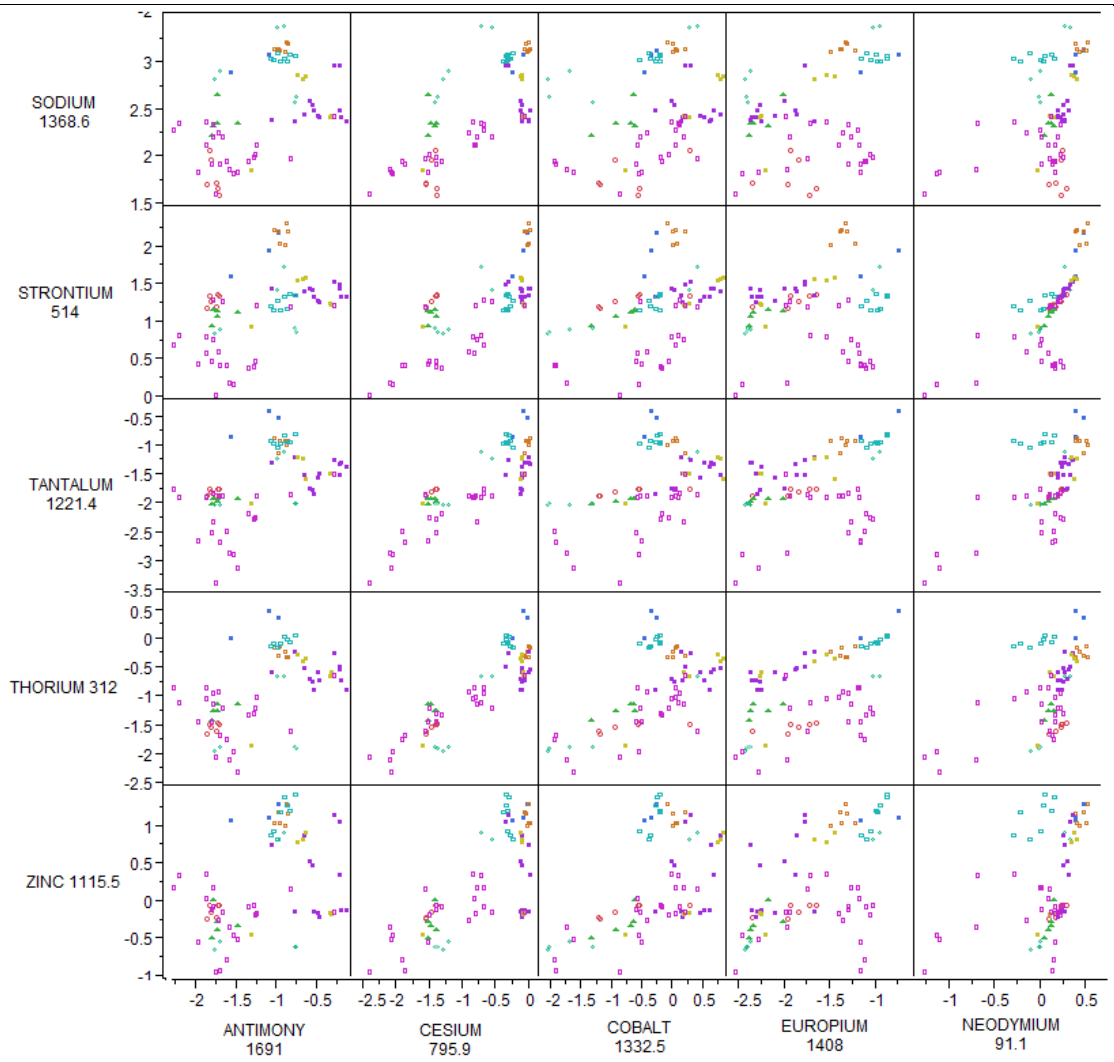

Figure C 2 - Scatterplot matrix of log10 INAA geologic source data (cont.).

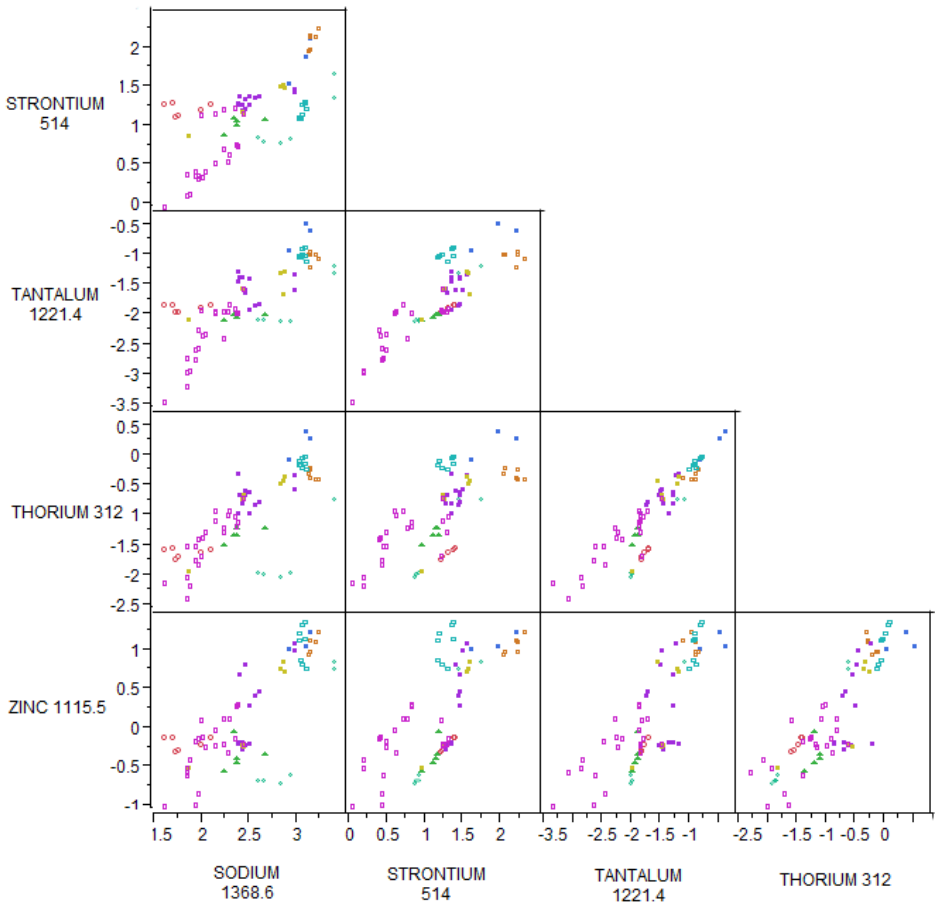

Figure C 1 - Scatterplot matrix of log10 INAA geologic source data (cont.).

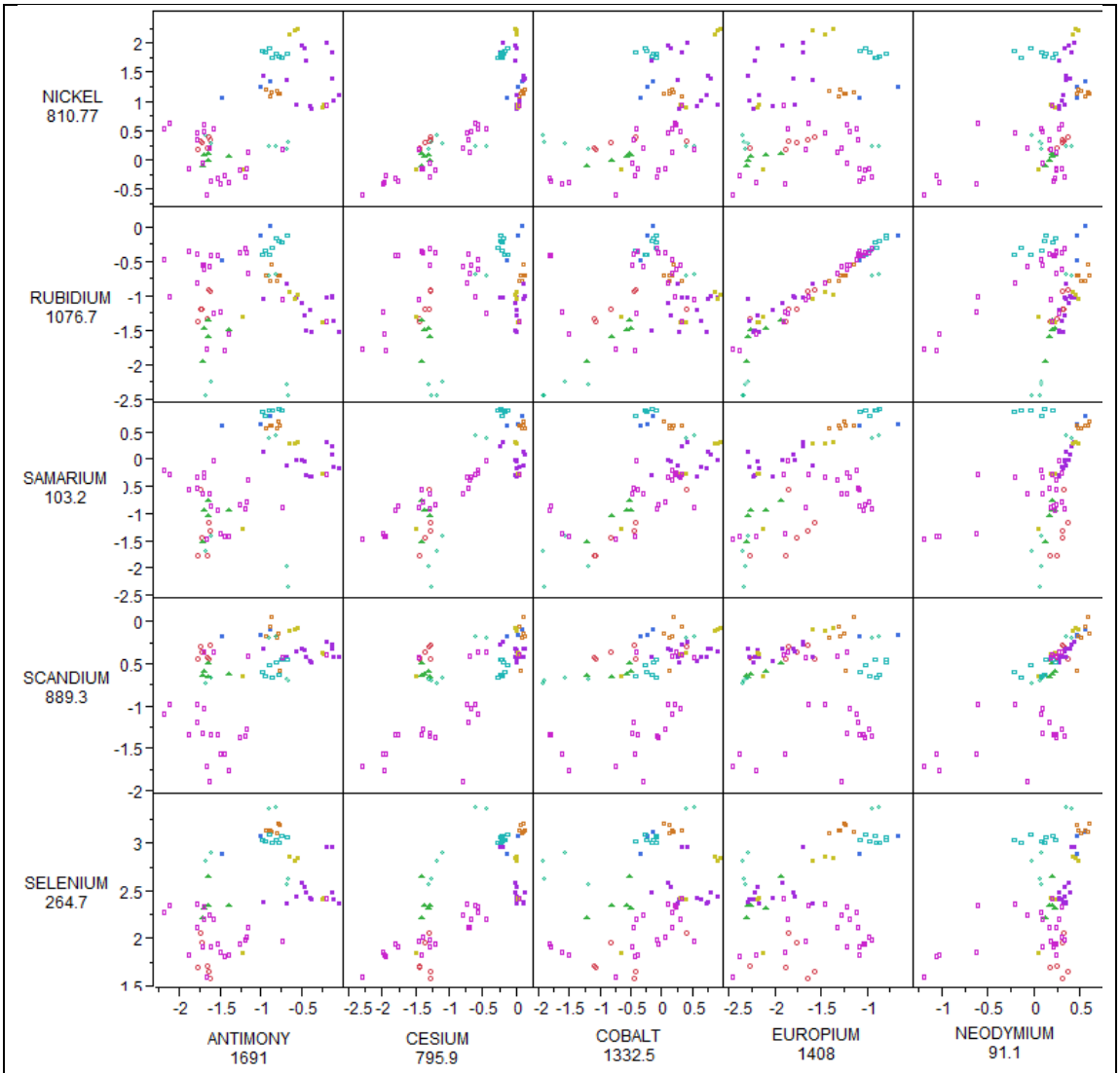

Figure C 1 - Scatterplot matrix of log10 INAA geologic source data (cont.).

Appendix D: Clusters vs. Artifact Metrics

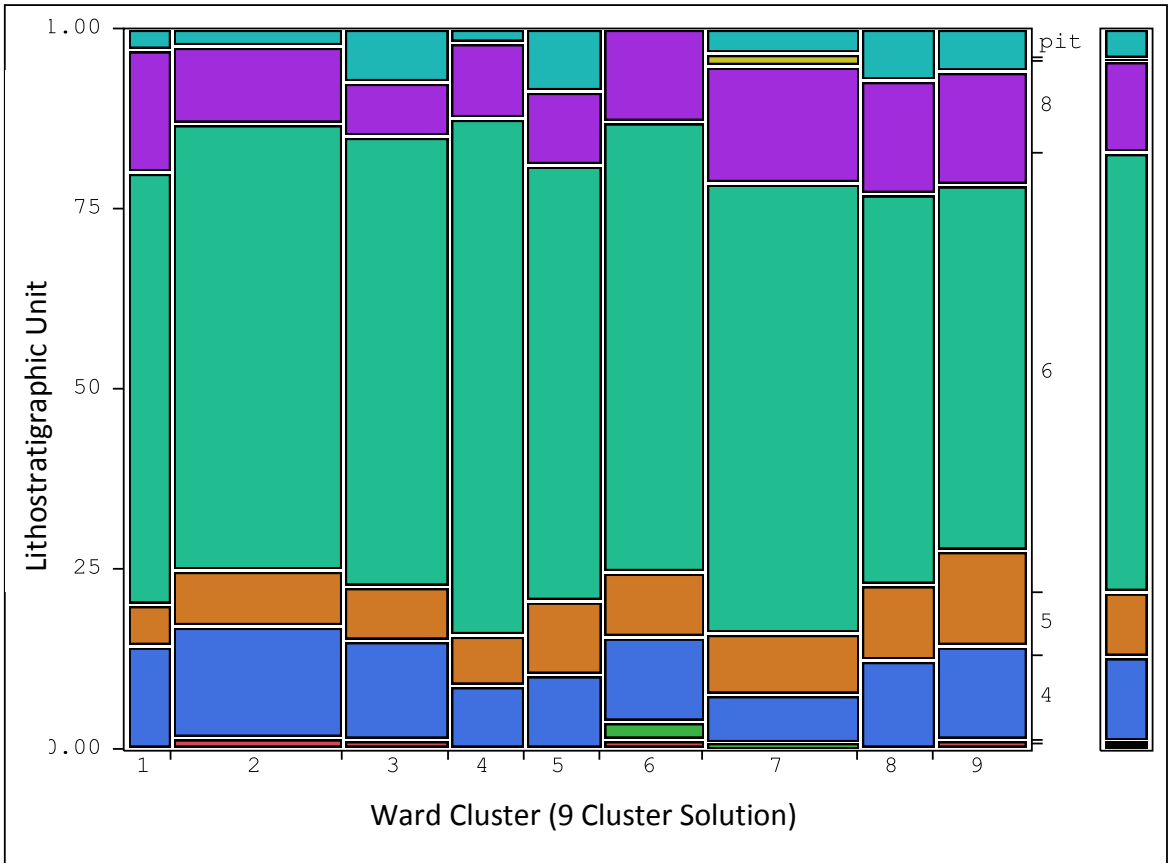

Figure D 1 – Retained cluster by lithostratigraphic unit from Cooper's Ferry excavation.

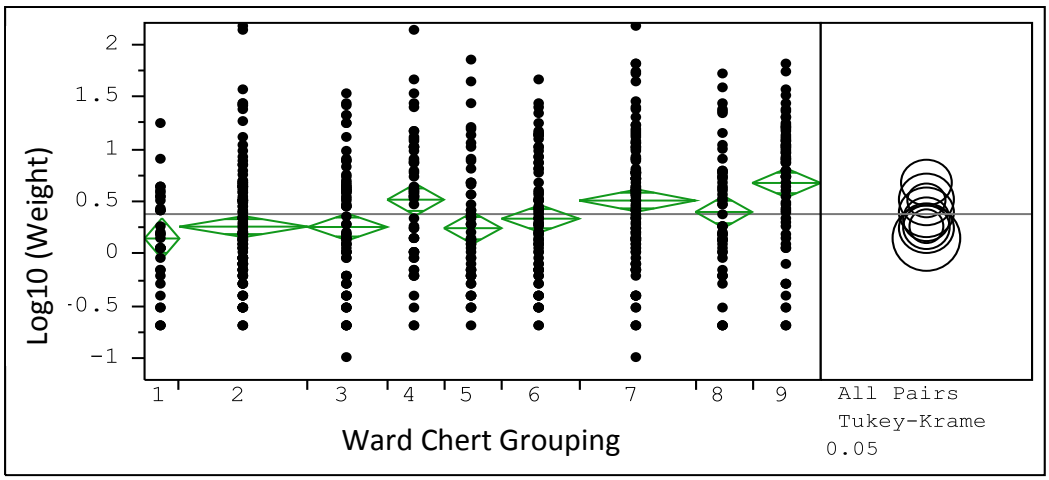

Figure D 2 - Retained cluster by artifact weight from Cooper's Ferry excavation.

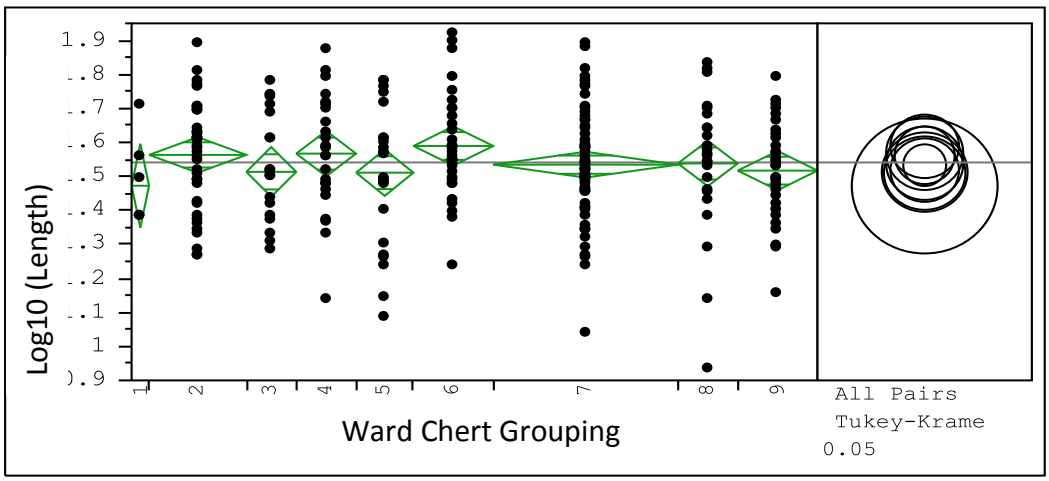

Figure D 3 - Retained cluster by artifact length from Cooper's Ferry excavation.

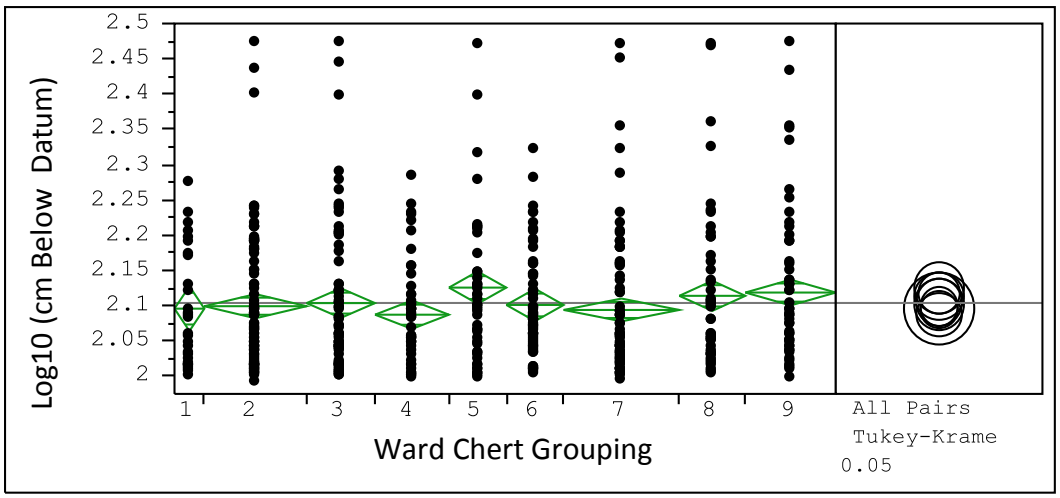

Figure D 4 - Retained cluster by artifact depth below datum from Cooper's Ferry excavation.

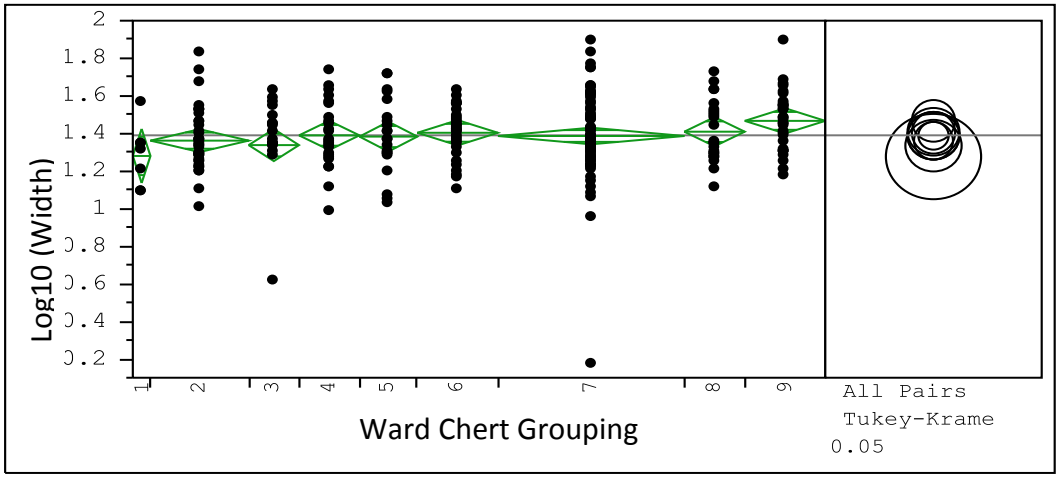

Figure D 5 - Retained cluster by artifact width from Cooper's Ferry excavation.

Appendix E: Discriminant Function Analysis Results

External Dataset

Casewise results for geologic sources of cherts using the MURR dataset are listed below. Less than one, one to 1.5, and 1.5 to two standard deviations are highlighted by color (pink, green, and blue respectively). Cases color-coded red are entries where either predicted and actual sources do not match, or that where secondary group posterior probabilities were within one standard deviation of their group centroid. Table is sorted primarily by "Actual Group" and secondarily by "D^2".

Source Name	Source Number
Birch Creek Source, Malheur County, Oregon	1
Cobden-Dongola (Union County, Illinois	2
Flattop Butte, Colorado	3
Knife River, North Dakota	4
Mud Lake	5
Red Butte, Malheur Co., Oregon	6
Signal Butte, Nebraska	7
Table Mountain, Wyoming	8
Tosawihi	9
West Horse Creek, South Dakota	10

Table E 1 - Name to number conversion of external dataset DFA analysis.

Actual Group	Predicted Group	Cond. Prob	Post. Prob	D^2	2nd group	2nd Post. Prob	2nd Group D^2
1	1	.872	1.000	4.541	5	.000	250.433
1	1	.783	1.000	5.565	5	.000	225.359
1	1	.704	1.000	6.354	5	.000	227.322
1	1	.627	1.000	7.100	5	.000	184.148
1	1	.622	1.000	7.148	5	.000	208.821
1	1	.594	1.000	7.411	5	.000	327.773
1	1	.566	1.000	7.690	5	.000	303.090
1	1	.565	1.000	7.692	5	.000	208.732
1	1	.541	1.000	7.933	5	.000	235.970
1	1	.496	1.000	8.385	5	.000	148.322

Table E 2 - Casewise results of external MURR INAA descriptive discriminant function analysis.

Actual Group	Predicted Group	Cond. Prob	Post. Prob	D^2	2nd group	2nd Post. Prob	2nd Group D^2
1	1	.487	1.000	8.476	5	.000	295.213
1	1	.316	1.000	10.441	5	.000	343.988
1	1	.280	1.000	10.934	5	.000	246.108
1	1	.254	1.000	11.332	5	.000	384.788
1	1	.215	1.000	11.972	5	.000	282.475
1	1	.212	1.000	12.028	5	.000	239.818
2	2	.999	1.000	.983	4	.000	120.951
2	2	.992	1.000	1.938	4	.000	115.297
2	2	.992	1.000	1.997	4	.000	122.783
2	2	.952	1.000	3.281	4	.000	139.657
2	2	.893	1.000	4.271	4	.000	128.376
2	2	.880	1.000	4.444	3	.000	136.560
2	2	.873	1.000	4.532	4	.000	118.872
2	2	.859	1.000	4.709	4	.000	126.558
2	2	.780	1.000	5.592	4	.000	121.503
2	2	.742	1.000	5.981	4	.000	132.199
2	2	.681	1.000	6.582	4	.000	114.207
2	2	.646	1.000	6.916	4	.000	151.983
2	2	.641	1.000	6.967	4	.000	140.035
2	2	.637	1.000	6.999	4	.000	129.588
2	2	.628	1.000	7.090	4	.000	112.371
2	2	.597	1.000	7.388	4	.000	114.126
2	2	.429	1.000	9.092	4	.000	139.724
2	2	.406	1.000	9.349	4	.000	127.966
2	2	.401	1.000	9.400	10	.000	157.555
2	2	.378	1.000	9.673	4	.000	145.368
2	2	.367	1.000	9.799	4	.000	140.859
2	2	.268	1.000	11.110	4	.000	129.467
2	2	.265	1.000	11.161	4	.000	143.510
2	2	.203	1.000	12.181	4	.000	97.311
2	2	.200	1.000	12.245	3	.000	173.750
2	2	.119	1.000	14.107	10	.000	126.644
2	2	.103	1.000	14.597	3	.000	94.690
2	2	.066	1.000	16.038	4	.000	162.752
2	2	.052	1.000	16.797	4	.000	140.516
2	2	.050	1.000	16.936	10	.000	102.217
2	2	.037	1.000	17.844	10	.000	87.759
3	3	.983	1.000	2.432	10	.000	20.590
3	3	.980	1.000	2.540	9	.000	101.506
3	3	.973	1.000	2.761	10	.000	88.079
3	3	.946	1.000	3.399	10	.000	68.632
3	3	.920	1.000	3.868	10	.000	100.052
3	3	.902	1.000	4.134	7	.000	32.132
3	3	.898	1.000	4.190	10	.000	74.385
3	3	.857	1.000	4.737	9	.000	102.229

Table E 2 - Casewise results of external MURR INAA descriptive discriminant function analysis (cont.).

Actual Group	Predicted Group	Cond. Prob	Post. Prob	D^2	2nd group	2nd Post. Prob	2nd Group D^2
3	3	.820	1.000	5.165	10	.000	33.917
3	3	.815	1.000	5.217	9	.000	97.881
3	3	.812	1.000	5.247	10	.000	40.243
3	3	.757	1.000	5.827	9	.000	95.749
3	3	.630	1.000	7.068	10	.000	60.888
3	3	.626	1.000	7.110	9	.000	107.223
3	3	.554	1.000	7.806	10	.000	100.100
3	3	.506	1.000	8.279	9	.000	90.720
3	3	.504	1.000	8.298	10	.000	24.261
3	3	.463	.999	8.725	10	.001	18.831
3	3	.447	1.000	8.893	10	.000	96.686
3	3	.432	1.000	9.061	9	.000	107.987
3	3	.427	.998	9.113	10	.002	17.721
3	3	.405	1.000	9.354	10	.000	21.715
3	3	.379	.999	9.661	10	.001	20.934
3	3	.298	1.000	10.688	10	.000	55.502
3	3	.281	1.000	10.920	10	.000	63.610
3	3	.257	1.000	11.280	7	.000	40.145
3	3	.186	1.000	12.518	5	.000	124.833
3	3	.147	1.000	13.369	10	.000	100.012
3	3	.135	1.000	13.670	10	.000	35.449
3	3	.120	1.000	14.076	10	.000	39.324
3	3	.119	1.000	14.081	10	.000	85.108
3	3	.117	.990	14.151	10	.010	19.841
3	3	.101	1.000	14.664	10	.000	57.012
3	3	.096	1.000	14.823	10	.000	44.902
3	3	.026	1.000	18.873	10	.000	67.508
4	4	.996	1.000	1.605	3	.000	157.880
4	4	.990	1.000	2.114	3	.000	142.927
4	4	.980	1.000	2.534	3	.000	198.799
4	4	.908	1.000	4.052	3	.000	195.327
4	4	.892	1.000	4.280	10	.000	120.443
4	4	.888	1.000	4.329	3	.000	191.831
4	4	.866	1.000	4.620	3	.000	169.623
4	4	.851	1.000	4.801	3	.000	180.793
4	4	.704	1.000	6.355	10	.000	115.145
4	4	.701	1.000	6.386	3	.000	199.466
4	4	.693	1.000	6.461	3	.000	125.805
4	4	.665	1.000	6.728	3	.000	160.066
4	4	.648	1.000	6.899	3	.000	141.250
4	4	.645	1.000	6.926	10	.000	133.986
4	4	.633	1.000	7.042	3	.000	121.841
4	4	.624	1.000	7.130	3	.000	175.787
4	4	.621	1.000	7.152	3	.000	190.434
4	4	.582	1.000	7.529	3	.000	197.941

Table E 2 - Casewise results of external MURR INAA descriptive discriminant function analysis (cont.).

Actual Group	Predicted Group	Cond. Prob	Post. Prob	D^2	2nd group	2nd Post. Prob	2nd Group D^2
4	4	.547	1.000	7.869	3	.000	183.342
4	4	.540	1.000	7.946	3	.000	150.604
4	4	.524	1.000	8.097	3	.000	223.718
4	4	.519	1.000	8.147	3	.000	158.026
4	4	.517	1.000	8.176	3	.000	157.764
4	4	.514	1.000	8.202	3	.000	177.049
4	4	.504	1.000	8.305	10	.000	144.358
4	4	.502	1.000	8.321	10	.000	140.082
4	4	.493	1.000	8.413	3	.000	151.319
4	4	.453	1.000	8.832	3	.000	169.834
4	4	.403	1.000	9.381	3	.000	214.806
4	4	.292	1.000	10.765	10	.000	182.089
4	4	.273	1.000	11.040	3	.000	163.584
4	4	.257	1.000	11.274	3	.000	142.574
4	4	.180	1.000	12.625	3	.000	110.246
4	4	.143	1.000	13.462	3	.000	201.634
4	4	.111	1.000	14.329	3	.000	259.476
4	4	.078	1.000	15.497	3	.000	246.840
4	4	.033	1.000	18.200	3	.000	138.069
4	4	.023	1.000	19.243	3	.000	211.759
4	4	.001	1.000	26.932	3	.000	138.632
5	5	.972	1.000	2.786	10	.000	95.881
5	5	.892	1.000	4.283	4	.000	99.541
5	5	.848	1.000	4.839	2	.000	105.471
5	5	.826	1.000	5.092	4	.000	108.433
5	5	.762	1.000	5.778	10	.000	113.468
5	5	.751	1.000	5.891	10	.000	95.441
5	5	.680	1.000	6.587	4	.000	135.556
5	5	.679	1.000	6.599	10	.000	149.451
5	5	.627	1.000	7.097	10	.000	68.324
5	5	.520	1.000	8.145	10	.000	101.830
5	5	.518	1.000	8.157	4	.000	88.852
5	5	.331	1.000	10.245	2	.000	101.838
5	5	.319	1.000	10.402	10	.000	75.907
5	5	.283	1.000	10.895	10	.000	45.478
5	5	.279	1.000	10.948	10	.000	108.176
5	5	.265	1.000	11.160	10	.000	91.726
5	5	.211	1.000	12.036	4	.000	104.398
5	5	.195	1.000	12.342	10	.000	92.959
5	5	.128	1.000	13.835	4	.000	112.487
5	5	.127	1.000	13.883	10	.000	84.053
6	6	.777	1.000	5.620	5	.000	103.361
6	6	.713	1.000	6.262	5	.000	154.348
6	6	.676	1.000	6.624	5	.000	93.977
6	6	.628	1.000	7.088	5	.000	91.090

Table E 2 - Casewise results of external MURR INAA descriptive discriminant function analysis (cont.).

Actual Group	Predicted Group	Cond. Prob	Post. Prob	D^2	2nd group	2nd Post. Prob	2nd Group D^2
6	6	.578	1.000	7.569	5	.000	151.456
6	6	.511	1.000	8.231	5	.000	96.073
6	6	.459	1.000	8.767	5	.000	160.661
6	6	.454	1.000	8.825	5	.000	99.397
6	6	.447	1.000	8.893	5	.000	186.996
6	6	.386	1.000	9.577	5	.000	194.383
6	6	.356	1.000	9.932	5	.000	94.339
6	6	.330	1.000	10.257	5	.000	107.515
6	6	.323	1.000	10.355	5	.000	86.588
7	7	.993	.905	1.902	8	.095	9.512
7	7	.990	.556	2.090	8	.444	5.644
7	7	.871	1.000	4.560	8	.000	25.752
7	7	.829	1.000	5.059	3	.000	26.684
7	7	.810	.981	5.273	8	.019	16.254
7	8**	.800	.945	5.381	7	.055	7.946
7	7	.797	.937	5.408	8	.063	13.921
7	7	.721	1.000	6.183	8	.000	24.540
7	7	.674	.999	6.641	3	.001	14.319
7	7	.673	.913	6.655	8	.087	14.475
7	7	.669	.999	6.695	3	.001	13.863
7	7	.657	1.000	6.809	8	.000	26.045
7	7	.594	1.000	7.411	3	.000	25.476
7	7	.587	1.000	7.484	3	.000	28.713
7	8**	.529	.843	8.052	7	.157	8.303
7	7	.488	.999	8.463	3	.001	16.732
7	7	.463	1.000	8.721	3	.000	29.057
7	7	.447	1.000	8.896	3	.000	32.203
7	7	.431	1.000	9.067	3	.000	20.045
7	7	.312	1.000	10.497	8	.000	58.027
7	7	.288	.999	10.819	8	.001	28.988
7	7	.287	1.000	10.843	3	.000	30.596
7	8**	.243	.753	11.501	7	.247	10.621
7	7	.164	1.000	12.970	3	.000	37.597
7	7	.134	.650	13.688	8	.317	18.227
7	7	.124	.974	13.965	8	.026	24.310
7	7	.086	.975	15.185	3	.024	16.062
7	7	.071	1.000	15.829	10	.000	40.190
7	8**	.050	.525	16.924	7	.475	14.017
8	8	.982	.960	2.473	7	.040	5.733
8	8	.943	.849	3.462	7	.151	3.811
8	8	.840	1.000	4.940	7	.000	18.301
8	8	.801	.840	5.367	7	.160	5.575
8	8	.763	.946	5.770	7	.054	8.405
8	8	.733	.919	6.065	7	.081	7.811
8	8	.709	1.000	6.306	7	.000	26.835

Table E 2 - Casewise results of external MURR INAA descriptive discriminant function analysis (cont.).

Actual Group	Predicted Group	Cond. Prob	Post. Prob	D^2	2nd group	2nd Post. Prob	2nd Group D^2
8	8	.702	.998	6.370	7	.002	15.779
8	8	.685	.565	6.540	7	.435	3.958
8	8	.683	.847	6.561	7	.153	6.880
8	8	.678	.990	6.610	7	.010	12.654
8	8	.659	.949	6.794	7	.051	9.528
8	8	.652	.961	6.859	7	.039	10.159
8	8	.538	.964	7.958	7	.036	11.406
8	8	.534	.923	7.999	7	.076	9.875
8	8	.503	1.000	8.310	7	.000	20.495
8	8	.493	1.000	8.417	7	.000	23.441
8	8	.459	1.000	8.769	7	.000	35.356
8	8	.285	.565	10.862	7	.435	8.277
8	8	.220	.987	11.879	7	.013	17.447
8	8	.209	.729	12.080	7	.266	10.994
8	8	.171	1.000	12.821	3	.000	22.603
8	8	.136	1.000	13.627	7	.000	36.739
8	8	.111	.877	14.325	7	.123	15.142
8	8	.054	.844	16.706	7	.156	16.980
8	8	.047	1.000	17.130	10	.000	28.082
9	9	.980	1.000	2.533	4	.000	193.048
9	9	.833	1.000	5.017	10	.000	190.614
9	9	.539	1.000	7.950	4	.000	193.959
9	9	.537	1.000	7.970	4	.000	261.863
9	9	.482	1.000	8.529	10	.000	211.943
9	9	.464	1.000	8.719	4	.000	212.426
9	9	.457	1.000	8.791	4	.000	144.109
9	9	.444	1.000	8.928	4	.000	187.255
9	9	.435	1.000	9.020	4	.000	235.656
9	9	.376	1.000	9.696	4	.000	260.093
9	9	.367	1.000	9.796	4	.000	185.077
9	9	.332	1.000	10.227	4	.000	182.009
9	9	.288	1.000	10.826	4	.000	348.166
10	10	.951	1.000	3.304	3	.000	29.878
10	10	.945	1.000	3.434	7	.000	31.261
10	10	.918	.995	3.896	7	.005	24.457
10	10	.889	1.000	4.321	3	.000	24.150
10	10	.887	1.000	4.342	7	.000	87.022
10	10	.786	1.000	5.530	3	.000	59.339
10	10	.669	1.000	6.696	7	.000	43.686
10	10	.659	1.000	6.793	3	.000	38.195
10	10	.620	1.000	7.163	7	.000	59.816
10	10	.603	1.000	7.332	7	.000	54.438
10	10	.493	1.000	8.416	7	.000	56.851
10	10	.468	1.000	8.674	7	.000	148.448
10	10	.443	1.000	8.943	7	.000	112.097

Table E 2 - Casewise results of external MURR INAA descriptive discriminant function analysis (cont.).

Actual Group	Predicted Group	Cond. Prob	Post. Prob	D^2	2nd group	2nd Post. Prob	2nd Group D^2
10	10	.412	1.000	9.276	4	.000	87.846
10	10	.401	1.000	9.407	3	.000	49.982
10	10	.360	1.000	9.879	3	.000	55.621
10	10	.300	1.000	10.651	3	.000	47.833
10	10	.149	1.000	13.303	3	.000	121.922
10	10	.146	1.000	13.382	4	.000	163.355
10	10	.112	1.000	14.288	4	.000	135.255
10	10	.108	.999	14.422	3	.001	31.278
10	10	.088	1.000	15.110	4	.000	84.717
10	7**	.031	.624	18.399	10	.357	9.438

Table E 2 - Casewise results of external MURR INAA descriptive discriminant function analysis (cont.).

Geochemical Sources –Six Groups

Casewise results for geochemical sources analyzed are listed below. Data are sorted primarily by actual group, and secondarily by D^2 values. Primary D^2 values below one standard deviation are highlighted in pink, values between one and 1.5 standard deviations are highlighted in blue, values between 1.5 and two standard deviations are green. Cases beyond two standard deviations are white. Additionally, cases where the second group D^2 value is below one standard deviation from the secondary group centroid as well as cases in which the predicted group does not match the actual group are listed in red. See Table E 3 - Group name to number key for PXRF analysis of geochemical sources, six group solution for group to number conversion.

Source Name	Source Number
Old Hwy 95_1	1
Old Hwy 95_2	2
Peanut Brittle	3
Pine Bar	4
Seven Devils	5
White Bird	6

Table E 3 - Group name to number key for PXRF analysis of geochemical sources, six group solution.

Actual Group	Predicted Group	Cond. Prob	Post. Prob	D^2	2nd group	2nd Post. Prob	2nd Group D^2
1	1	.988	1.000	.597	2	.000	17.056
1	1	.963	1.000	.999	6	.000	16.138
1	1	.942	1.000	1.227	2	.000	15.849
1	1	.937	.997	1.284	2	.003	12.383
1	1	.927	1.000	1.374	3	.000	15.104
1	1	.919	.998	1.452	6	.002	11.999
1	1	.916	.998	1.474	6	.001	12.998
1	1	.901	1.000	1.604	3	.000	14.733

Table E 4 - Casewise results from PXRF analysis of geochemical sources.

Actual Group	Predicted Group	Cond. Prob	Post. Prob	D^2	2nd group	2nd Post. Prob	2nd Group D^2
1	1	.883	.998	1.748	6	.002	12.197
1	1	.860	.999	1.918	6	.000	15.202
1	1	.851	.981	1.983	2	.019	9.064
1	1	.849	1.000	2.001	3	.000	17.494
1	1	.796	.997	2.372	6	.002	12.860
1	1	.777	.999	2.495	2	.000	17.024
1	1	.766	.995	2.568	6	.003	11.952
1	1	.754	1.000	2.647	3	.000	19.092
1	1	.735	.999	2.775	6	.001	15.267
1	1	.681	.992	3.126	6	.008	10.759
1	1	.640	.978	3.389	2	.022	10.157
1	1	.555	.999	3.963	3	.001	15.685
1	1	.526	.992	4.164	6	.007	11.937
1	1	.455	.984	4.689	6	.013	11.302
1	2	.448	.832	4.743	1	.168	8.801
1	1	.421	.997	4.961	3	.003	13.681
1	1	.375	1.000	5.347	3	.000	17.450
1	1	.365	1.000	5.440	6	.000	19.282
1	1	.344	.945	5.628	6	.053	9.395
1	1	.341	.999	5.657	2	.001	18.317
1	1	.340	.726	5.668	2	.274	6.764
1	1	.314	1.000	5.920	3	.000	20.843
1	1	.300	1.000	6.062	6	.000	22.095
1	1	.286	.997	6.218	6	.002	17.011
1	1	.277	1.000	6.307	3	.000	26.867
1	1	.273	1.000	6.360	3	.000	22.398
1	1	.255	.998	6.567	3	.002	16.197
1	1	.226	.547	6.931	2	.453	6.449
1	1	.113	.959	8.911	3	.033	12.481
1	1	.094	.999	9.395	3	.001	21.231
1	1	.084	1.000	9.710	2	.000	24.489
1	1	.075	.823	10.024	2	.177	12.237
1	1	.049	.982	11.145	6	.013	17.739
1	1	.031	.998	12.281	6	.002	22.950
1	1	.025	1.000	12.817	3	.000	28.018
2	2	.987	1.000	.625	6	.000	40.135
2	2	.968	1.000	.929	1	.000	32.320
2	2	.941	1.000	1.242	1	.000	35.450
2	2	.897	1.000	1.634	1	.000	38.416
2	2	.894	1.000	1.662	6	.000	47.354
2	2	.876	1.000	1.803	6	.000	53.528
2	2	.828	1.000	2.148	1	.000	52.814
2	2	.826	1.000	2.164	1	.000	38.956
2	2	.822	1.000	2.189	1	.000	19.468
2	2	.815	1.000	2.242	1	.000	23.629
2	2	.773	1.000	2.525	6	.000	46.520

Table E 4 - Casewise results from PXRF analysis of geochemical sources (cont.).

Actual Group	Predicted Group	Cond. Prob	Post. Prob	D^2	2nd group	2nd Post. Prob	2nd Group D^2
2	2	.749	1.000	2.680	1	.000	35.841
2	2	.684	1.000	3.102	6	.000	45.811
2	2	.666	1.000	3.221	6	.000	63.542
2	2	.644	1.000	3.361	1	.000	31.652
2	2	.619	1.000	3.529	1	.000	53.678
2	2	.601	1.000	3.648	1	.000	36.499
2	2	.596	.991	3.685	1	.009	13.992
2	2	.574	1.000	3.829	6	.000	66.342
2	2	.551	1.000	3.986	1	.000	24.249
2	2	.509	1.000	4.283	1	.000	25.588
2	2	.503	1.000	4.329	1	.000	38.778
2	2	.495	1.000	4.388	1	.000	33.068
2	2	.477	1.000	4.519	1	.000	33.376
2	2	.466	1.000	4.603	1	.000	31.248
2	2	.457	1.000	4.677	6	.000	67.711
2	2	.409	1.000	5.054	1	.000	43.027
2	2	.409	1.000	5.056	6	.000	66.923
2	2	.408	.959	5.068	1	.041	12.249
2	2	.344	1.000	5.630	6	.000	57.063
2	2	.318	1.000	5.882	6	.000	61.901
2	2	.285	1.000	6.221	6	.000	64.712
2	2	.283	1.000	6.242	1	.000	47.784
2	2	.221	1.000	6.994	1	.000	54.242
2	2	.177	1.000	7.639	6	.000	54.664
2	2	.166	1.000	7.835	1	.000	46.285
2	2	.115	.676	8.864	1	.324	11.188
2	2	.104	1.000	9.142	6	.000	36.590
2	2	.092	.878	9.453	1	.122	14.264
2	2	.051	.989	11.037	1	.011	20.856
2	2	.050	1.000	11.060	6	.000	95.163
2	2	.005	1.000	16.819	6	.000	77.006
3	3	.997	.997	.325	6	.003	12.853
3	3	.973	.993	.866	6	.007	11.989
3	3	.962	1.000	1.009	6	.000	22.873
3	3	.960	.990	1.034	6	.010	11.398
3	3	.960	.997	1.035	6	.003	13.709
3	3	.947	.960	1.175	6	.040	8.702
3	3	.928	.975	1.362	6	.025	9.876
3	3	.923	.962	1.408	6	.038	9.019
3	3	.921	.995	1.433	6	.005	13.033
3	3	.910	1.000	1.523	6	.000	26.892
3	3	.898	.988	1.623	6	.012	11.571
3	3	.895	1.000	1.653	6	.000	23.305
3	3	.885	.999	1.731	6	.001	18.071
3	3	.876	.999	1.797	6	.001	16.791
3	3	.844	.995	2.039	6	.005	13.759

Table E 4 - Casewise results from PXRF analysis of geochemical sources (cont.).

Actual Group	Predicted Group	Cond. Prob	Post. Prob	D^2	2nd group	2nd Post. Prob	2nd Group D^2
3	3	.843	1.000	2.045	6	.000	23.174
3	3	.815	.978	2.237	6	.022	10.959
3	3	.812	.999	2.262	6	.001	16.849
3	3	.810	.961	2.272	6	.039	9.881
3	3	.786	.917	2.434	6	.083	8.408
3	3	.756	1.000	2.637	6	.000	26.554
3	3	.755	.997	2.645	6	.003	15.413
3	3	.752	.987	2.660	6	.013	12.550
3	3	.715	.988	2.901	6	.012	12.900
3	3	.713	.994	2.916	6	.006	14.286
3	3	.707	1.000	2.952	6	.000	38.015
3	3	.703	1.000	2.983	6	.000	28.167
3	3	.694	1.000	3.039	6	.000	28.431
3	3	.680	1.000	3.128	6	.000	24.479
3	3	.661	1.000	3.255	6	.000	19.868
3	3	.652	.824	3.310	6	.176	7.575
3	3	.650	.871	3.327	6	.129	8.325
3	3	.631	1.000	3.450	6	.000	20.504
3	3	.628	1.000	3.470	6	.000	21.440
3	3	.580	1.000	3.788	6	.000	32.478
3	3	.567	1.000	3.882	6	.000	29.241
3	3	.549	.735	4.003	6	.265	7.219
3	3	.529	1.000	4.142	6	.000	22.784
3	3	.525	.985	4.169	6	.015	13.765
3	3	.524	.847	4.178	6	.135	9.030
3	3	.515	.999	4.241	6	.001	19.340
3	3	.502	.794	4.336	6	.183	8.450
3	3	.495	.993	4.390	6	.007	15.530
3	3	.494	.508	4.398	6	.488	5.653
3	3	.484	.999	4.468	6	.001	19.717
3	3	.472	.957	4.561	6	.043	11.946
3	3	.468	1.000	4.591	6	.000	31.167
3	3	.444	.735	4.776	6	.265	7.990
3	3	.408	.999	5.065	6	.001	19.303
3	3	.402	1.000	5.113	6	.000	35.827
3	3	.392	.999	5.204	6	.001	21.285
3	3	.360	1.000	5.480	6	.000	45.782
3	3	.356	1.000	5.522	6	.000	42.775
3	3	.328	.999	5.778	6	.001	22.010
3	3	.298	1.000	6.085	6	.000	24.518
3	3	.262	1.000	6.482	6	.000	28.628
3	3	.256	1.000	6.551	6	.000	43.736
3	3	.215	.997	7.079	6	.003	19.674
3	3	.209	1.000	7.163	6	.000	26.294
3	3	.131	.906	8.495	6	.094	14.209
3	3	.102	1.000	9.187	6	.000	26.633

Table E 4 - Casewise results from PXRF analysis of geochemical sources (cont.).

Actual Group	Predicted Group	Cond. Prob	Post. Prob	D^2	2nd group	2nd Post. Prob	2nd Group D^2
3	3	.096	1.000	9.348	6	.000	30.375
3	3	.089	1.000	9.562	6	.000	64.335
3	3	.072	1.000	10.115	6	.000	36.369
3	3	.038	1.000	11.750	6	.000	50.324
3	3	.029	1.000	12.461	6	.000	29.429
3	3	.012	1.000	14.560	6	.000	46.813
3	3	.003	1.000	18.308	6	.000	39.476
3	3	.001	1.000	20.726	6	.000	40.808
3	3	.001	1.000	21.107	6	.000	41.892
4	4	.997	1.000	.335	2	.000	43.641
4	4	.988	1.000	.593	2	.000	42.338
4	4	.977	1.000	.807	2	.000	44.159
4	4	.914	1.000	1.491	2	.000	46.071
4	4	.888	1.000	1.709	2	.000	45.467
4	4	.864	1.000	1.888	2	.000	44.366
4	4	.841	1.000	2.057	2	.000	44.885
4	4	.840	1.000	2.063	2	.000	45.099
4	4	.828	1.000	2.151	2	.000	43.645
4	4	.806	1.000	2.303	2	.000	44.722
4	4	.779	1.000	2.486	2	.000	41.844
4	4	.773	1.000	2.526	2	.000	46.791
4	4	.753	1.000	2.654	2	.000	46.771
4	4	.716	1.000	2.893	2	.000	42.460
4	4	.715	1.000	2.903	2	.000	47.058
4	4	.702	1.000	2.989	2	.000	48.057
4	4	.692	1.000	3.051	2	.000	45.924
4	4	.665	1.000	3.226	2	.000	42.829
4	4	.639	1.000	3.397	2	.000	45.625
4	4	.567	1.000	3.876	2	.000	44.477
4	4	.539	1.000	4.074	2	.000	46.475
4	4	.530	1.000	4.134	2	.000	44.011
4	4	.525	1.000	4.174	2	.000	47.282
4	4	.494	1.000	4.397	2	.000	46.266
4	4	.382	1.000	5.287	2	.000	42.987
4	4	.299	1.000	6.075	2	.000	43.069
4	4	.298	1.000	6.082	2	.000	46.834
4	4	.263	1.000	6.470	2	.000	45.375
4	4	.240	1.000	6.746	2	.000	41.339
4	4	.223	1.000	6.966	2	.000	44.872
4	4	.222	1.000	6.984	2	.000	46.761
4	4	.222	1.000	6.985	2	.000	47.048
4	4	.191	1.000	7.424	2	.000	49.982
4	4	.179	1.000	7.611	2	.000	42.377
4	4	.156	1.000	8.008	2	.000	46.282
4	4	.102	1.000	9.173	2	.000	44.795
4	4	.017	1.000	13.791	2	.000	51.629

Table E 4 - Casewise results from PXRF analysis of geochemical sources (cont.).

Actual Group	Predicted Group	Cond. Prob	Post. Prob	D^2	2nd group	2nd Post. Prob	2nd Group D^2
4	4	.016	1.000	14.000	2	.000	45.360
4	4	.006	1.000	16.219	2	.000	42.510
5	5	.990	1.000	.549	2	.000	157.676
5	5	.977	1.000	.798	2	.000	159.997
5	5	.972	1.000	.879	2	.000	154.712
5	5	.966	1.000	.955	3	.000	157.986
5	5	.966	1.000	.961	3	.000	159.842
5	5	.954	1.000	1.106	3	.000	159.253
5	5	.945	1.000	1.198	3	.000	162.958
5	5	.889	1.000	1.703	3	.000	158.285
5	5	.881	1.000	1.761	2	.000	155.575
5	5	.836	1.000	2.096	3	.000	153.035
5	5	.740	1.000	2.739	3	.000	159.063
5	5	.739	1.000	2.744	2	.000	150.582
5	5	.719	1.000	2.876	2	.000	142.908
5	5	.714	1.000	2.911	2	.000	137.805
5	5	.652	1.000	3.315	2	.000	151.303
5	5	.634	1.000	3.431	2	.000	142.599
5	5	.612	1.000	3.579	2	.000	146.124
5	5	.595	1.000	3.688	3	.000	149.729
5	5	.595	1.000	3.690	3	.000	161.470
5	5	.572	1.000	3.843	2	.000	161.159
5	5	.569	1.000	3.863	3	.000	161.678
5	5	.566	1.000	3.882	2	.000	149.849
5	5	.498	1.000	4.366	2	.000	158.076
5	5	.460	1.000	4.651	3	.000	169.978
5	5	.457	1.000	4.671	3	.000	153.989
5	5	.431	1.000	4.874	2	.000	164.323
5	5	.405	1.000	5.088	3	.000	167.954
5	5	.390	1.000	5.216	2	.000	148.881
5	5	.383	1.000	5.278	3	.000	156.502
5	5	.330	1.000	5.759	3	.000	169.260
5	5	.322	1.000	5.840	2	.000	154.527
5	5	.314	1.000	5.926	3	.000	158.606
5	5	.311	1.000	5.954	2	.000	135.609
5	5	.309	1.000	5.967	3	.000	159.292
5	5	.303	1.000	6.038	2	.000	147.523
5	5	.295	1.000	6.115	2	.000	124.550
5	5	.253	1.000	6.592	2	.000	153.121
5	5	.247	1.000	6.656	2	.000	119.799
5	5	.208	1.000	7.174	2	.000	144.755
5	5	.195	1.000	7.357	3	.000	166.760
5	5	.194	1.000	7.380	2	.000	155.622
5	5	.090	1.000	9.517	2	.000	127.849
5	5	.083	1.000	9.728	3	.000	162.151
5	5	.068	1.000	10.266	2	.000	115.543

Table E 4 - Casewise results from PXRF analysis of geochemical sources (cont.).

Actual Group	Predicted Group	Cond. Prob	Post. Prob	D^2	2nd group	2nd Post. Prob	2nd Group D^2
5	5	.062	1.000	10.531	2	.000	126.716
5	5	.021	1.000	13.234	3	.000	155.703
5	5	.021	1.000	13.257	2	.000	147.367
6	6	.996	1.000	.377	3	.000	16.269
6	6	.979	1.000	.764	3	.000	15.542
6	6	.958	.993	1.055	3	.007	9.932
6	6	.956	1.000	1.082	3	.000	22.450
6	6	.955	1.000	1.089	3	.000	16.210
6	6	.947	1.000	1.179	3	.000	24.291
6	6	.943	1.000	1.218	3	.000	21.072
6	6	.932	1.000	1.325	3	.000	23.435
6	6	.929	1.000	1.356	3	.000	23.571
6	6	.927	1.000	1.377	3	.000	21.887
6	6	.913	1.000	1.502	3	.000	19.949
6	6	.809	1.000	2.279	3	.000	16.726
6	6	.809	1.000	2.284	3	.000	27.366
6	6	.805	.999	2.311	3	.001	15.593
6	6	.799	.999	2.353	3	.001	15.060
6	6	.792	1.000	2.394	3	.000	23.862
6	6	.753	.999	2.654	3	.001	15.953
6	3	.752	.969	2.662	6	.031	10.738
6	6	.746	1.000	2.699	3	.000	28.244
6	6	.729	1.000	2.811	3	.000	27.024
6	3	.720	.618	2.872	6	.382	5.006
6	6	.717	1.000	2.888	3	.000	25.307
6	6	.716	1.000	2.895	3	.000	27.195
6	6	.704	.991	2.976	3	.009	11.225
6	6	.703	.970	2.977	3	.030	8.786
6	6	.688	.997	3.077	3	.003	13.496
6	6	.664	1.000	3.231	3	.000	21.126
6	6	.650	1.000	3.322	3	.000	20.488
6	6	.647	.995	3.344	3	.003	13.863
6	6	.646	.996	3.350	3	.004	13.424
6	6	.639	.953	3.397	3	.047	8.252
6	6	.627	1.000	3.473	3	.000	17.694
6	6	.621	1.000	3.519	3	.000	18.785
6	6	.611	.933	3.582	3	.067	7.666
6	6	.599	.822	3.660	3	.178	5.546
6	6	.560	.997	3.928	3	.003	14.715
6	6	.543	.890	4.047	3	.110	7.046
6	6	.489	1.000	4.435	3	.000	28.445
6	6	.476	.587	4.527	3	.413	4.054
6	6	.459	.993	4.655	3	.007	13.459
6	3	.437	.897	4.827	6	.100	10.384
6	3	.408	.573	5.061	6	.426	6.826
6	6	.363	.999	5.457	3	.001	17.453

Table E 4 - Casewise results from PXRF analysis of geochemical sources (cont.).

Actual Group	Predicted Group	Cond. Prob	Post. Prob	D^2	2nd group	2nd Post. Prob	2nd Group D^2
6	6	.332	.991	5.741	3	.009	13.991
6	6	.270	1.000	6.386	3	.000	29.299
6	6	.263	1.000	6.470	3	.000	34.012
6	6	.262	.857	6.485	1	.140	12.111
6	6	.237	.677	6.789	3	.323	7.094
6	6	.225	1.000	6.948	3	.000	23.390
6	6	.223	.983	6.965	3	.017	13.951
6	6	.179	1.000	7.614	3	.000	28.334
6	6	.152	.997	8.082	3	.003	18.795
6	6	.068	.997	10.255	3	.003	20.617
6	6	.065	1.000	10.372	3	.000	32.219
6	6	.056	.856	10.790	3	.144	13.183
6	6	.053	1.000	10.927	3	.000	31.871
6	6	.038	1.000	11.792	3	.000	27.756
6	6	.035	1.000	11.966	3	.000	26.767
6	6	.000	1.000	24.612	3	.000	46.130

Table E 4 - Casewise results from PXRF analysis of geochemical sources (cont.).

Geochemical Sources – Four group solution

Casewise results for geochemical sources Old Hwy95_1, Old Hwy95_2, Peanut Brittle, and White Bird group analysis are listed below. Cases are primarily sorted by their actual group, an secondarily by their conditional probability. Note that no second cases fall within a single standard deviation of both the primary and secondary groups simultaneously. Groups are color coded by conditional probability, with red cases being within a single standard deviation of its predicted sources, tan being between one and 1.5, green being between 1.5 and two, and no color for greater than two. Blue cases represent misclassified cases.

Cat#	Actual Group	Predicted Group	Cond. Prob.	Post. Prob.	D^2	2nd Group	2nd Cond. Prob.	2nd Post. Prob.	2nd Group D^2
oldhwy95_1.43	Old Hwy 95_1	Old Hwy 95_1	1.00	1.00	0.06	6.00	0.00	0.00	15.90
oldhwy95_1.39	Old Hwy 95_1	Old Hwy 95_1	0.98	1.00	0.18	6.00	0.00	0.00	15.21
oldhwy95_1.6	Old Hwy 95_1	Old Hwy 95_1	0.98	1.00	0.21	6.00	0.00	0.00	18.19
oldhwy95_1.10	Old Hwy 95_1	Old Hwy 95_1	0.97	1.00	0.26	6.00	0.00	0.00	13.71
oldhwy95_1.14	Old Hwy 95_1	Old Hwy 95_1	0.97	1.00	0.27	2.00	0.00	0.00	18.32
oldhwy95_1.33	Old Hwy 95_1	Old Hwy 95_1	0.96	1.00	0.32	6.00	0.00	0.00	16.82
oldhwy95_1.20	Old Hwy 95_1	Old Hwy 95_1	0.95	1.00	0.34	2.00	0.00	0.00	20.61
oldhwy95_1.22	Old Hwy 95_1	Old Hwy 95_1	0.95	1.00	0.35	6.00	0.00	0.00	15.04
oldhwy95_1.38	Old Hwy 95_1	Old Hwy 95_1	0.94	1.00	0.40	6.00	0.00	0.00	14.36

Table E 5 - Casewise results from PXRF analysis of geochemical sources using four group solution.

oldhwy95_1.5	Old Hwy 95_1	Old Hwy 95_1	0.94	1.00	0.41	2.00	0.00	0.00	19.24
oldhwy95_1.41	Old Hwy 95_1	Old Hwy 95_1	0.93	1.00	0.45	6.00	0.00	0.00	13.65
oldhwy95_1.2	Old Hwy 95_1	Old Hwy 95_1	0.92	1.00	0.49	6.00	0.00	0.00	15.70
oldhwy95_1.16	Old Hwy 95_1	Old Hwy 95_1	0.91	1.00	0.52	2.00	0.00	0.00	14.22
oldhwy95_1.9	Old Hwy 95_1	Old Hwy 95_1	0.89	1.00	0.62	2.00	0.00	0.00	18.62
oldhwy95_1.28	Old Hwy 95_1	Old Hwy 95_1	0.89	1.00	0.64	6.00	0.00	0.00	18.62
oldhwy95_1.27	Old Hwy 95_1	Old Hwy 95_1	0.88	1.00	0.65	6.00	0.00	0.00	14.70
oldhwy95_1.24	Old Hwy 95_1	Old Hwy 95_1	0.88	0.99	0.69	6.00	0.01	0.01	11.13
oldhwy95_1.37	Old Hwy 95_1	Old Hwy 95_1	0.87	1.00	0.73	6.00	0.00	0.00	14.25
oldhwy95_1.7	Old Hwy 95_1	Old Hwy 95_1	0.86	1.00	0.74	6.00	0.00	0.00	23.01
oldhwy95_1.18	Old Hwy 95_1	Old Hwy 95_1	0.85	0.99	0.80	6.00	0.01	0.01	11.21
oldhwy95_1.31	Old Hwy 95_1	Old Hwy 95_1	0.83	0.99	0.87	6.00	0.01	0.01	10.66
oldhwy95_1.42	Old Hwy 95_1	Old Hwy 95_1	0.82	1.00	0.91	6.00	0.00	0.00	21.13
oldhwy95_1.29	Old Hwy 95_1	Old Hwy 95_1	0.80	0.99	0.99	6.00	0.02	0.01	10.37
oldhwy95_1.17	Old Hwy 95_1	Old Hwy 95_1	0.80	1.00	1.03	6.00	0.00	0.00	12.85
oldhwy95_1.40	Old Hwy 95_1	Old Hwy 95_1	0.80	0.99	1.03	6.00	0.01	0.01	11.03
oldhwy95_1.32	Old Hwy 95_1	Old Hwy 95_1	0.76	0.99	1.15	2.00	0.01	0.01	10.98
oldhwy95_1.3	Old Hwy 95_1	Old Hwy 95_1	0.76	1.00	1.19	6.00	0.00	0.00	20.20
oldhwy95_1.1	Old Hwy 95_1	Old Hwy 95_1	0.72	0.99	1.33	2.00	0.01	0.00	12.34
oldhwy95_1.30	Old Hwy 95_1	Old Hwy 95_1	0.69	1.00	1.49	2.00	0.00	0.00	24.58
oldhwy95_1.25	Old Hwy 95_1	Old Hwy 95_1	0.68	1.00	1.53	6.00	0.00	0.00	17.09
oldhwy95_1.15	Old Hwy 95_1	Old Hwy 95_1	0.63	1.00	1.71	2.00	0.00	0.00	24.75
oldhwy95_1.36	Old Hwy 95_1	Old Hwy 95_1	0.61	1.00	1.82	2.00	0.00	0.00	13.96
oldhwy95_1.13	Old Hwy 95_1	Old Hwy 95_1	0.57	1.00	2.01	2.00	0.00	0.00	15.51
oldhwy95_1.19	Old Hwy 95_1	Old Hwy 95_1	0.51	0.99	2.30	6.00	0.01	0.01	11.66
oldhwy95_1.21	Old Hwy 95_1	Old Hwy 95_1	0.50	1.00	2.38	6.00	0.00	0.00	27.04
oldhwy95_1.12	Old Hwy 95_1	Old Hwy 95_1	0.44	0.99	2.73	2.00	0.01	0.01	11.72
oldhwy95_1.35	Old Hwy 95_1	Old Hwy 95_1	0.44	1.00	2.73	6.00	0.00	0.00	15.71

Table E 5 - Casewise results from PXRF analysis of geochemical sources using four group solution (cont.).

oldhwy95_1.11	Old Hwy 95_1	Old Hwy 95_1	0.42	1.00	2.80	6.00	0.00	0.00	26.00
oldhwy95_1.26	Old Hwy 95_1	Old Hwy 95_1	0.41	1.00	2.89	6.00	0.00	0.00	25.59
oldhwy95_1.23	Old Hwy 95_1	Old Hwy 95_1	0.32	0.91	3.51	2.00	0.05	0.09	8.04
oldhwy95_1.8	Old Hwy 95_1	Old Hwy 95_1	0.29	1.00	3.72	2.00	0.00	0.00	15.05
oldhwy95_1.34	Old Hwy 95_1	Old Hwy 95_1	0.29	0.86	3.72	2.00	0.06	0.14	7.23
oldhwy95_1.4	Old Hwy 95_1	Old Hwy 95_1	0.28	0.84	3.81	2.00	0.07	0.16	6.92
oldhwy95_2.37	Old Hwy 95_2	Old Hwy 95_2	1.00	1.00	0.03	1.00	0.00	0.00	18.89
oldhwy95_2.18	Old Hwy 95_2	Old Hwy 95_2	0.99	1.00	0.11	1.00	0.00	0.00	16.61
oldhwy95_2.24	Old Hwy 95_2	Old Hwy 95_2	0.98	1.00	0.18	1.00	0.00	0.00	21.02
oldhwy95_2.36	Old Hwy 95_2	Old Hwy 95_2	0.98	1.00	0.19	1.00	0.00	0.00	20.80
oldhwy95_2.22	Old Hwy 95_2	Old Hwy 95_2	0.97	1.00	0.23	1.00	0.00	0.00	17.38
oldhwy95_2.40	Old Hwy 95_2	Old Hwy 95_2	0.97	1.00	0.23	1.00	0.00	0.00	15.27
oldhwy95_2.23	Old Hwy 95_2	Old Hwy 95_2	0.92	1.00	0.49	1.00	0.00	0.00	17.43
oldhwy95_2.17	Old Hwy 95_2	Old Hwy 95_2	0.90	1.00	0.58	1.00	0.00	0.00	18.45
oldhwy95_2.35	Old Hwy 95_2	Old Hwy 95_2	0.90	1.00	0.58	1.00	0.00	0.00	12.91
oldhwy95_2.21	Old Hwy 95_2	Old Hwy 95_2	0.86	1.00	0.77	1.00	0.00	0.00	25.54
oldhwy95_2.19	Old Hwy 95_2	Old Hwy 95_2	0.85	1.00	0.79	1.00	0.00	0.00	16.30
oldhwy95_2.12	Old Hwy 95_2	Old Hwy 95_2	0.84	1.00	0.85	1.00	0.00	0.00	22.81
oldhwy95_2.31	Old Hwy 95_2	Old Hwy 95_2	0.81	1.00	0.98	1.00	0.00	0.00	25.36
oldhwy95_2.25	Old Hwy 95_2	Old Hwy 95_2	0.80	1.00	1.01	1.00	0.00	0.00	15.12
oldhwy95_2.32	Old Hwy 95_2	Old Hwy 95_2	0.78	1.00	1.08	1.00	0.00	0.00	24.92
oldhwy95_2.15	Old Hwy 95_2	Old Hwy 95_2	0.76	1.00	1.16	1.00	0.00	0.00	24.93
oldhwy95_2.6	Old Hwy 95_2	Old Hwy 95_2	0.76	1.00	1.17	1.00	0.00	0.00	14.42
oldhwy95_2.29	Old Hwy 95_2	Old Hwy 95_2	0.76	0.99	1.17	1.00	0.01	0.01	11.23
oldhwy95_2.20	Old Hwy 95_2	Old Hwy 95_2	0.67	0.98	1.53	1.00	0.02	0.02	9.73
oldhwy95_2.2	Old Hwy 95_2	Old Hwy 95_2	0.67	0.99	1.54	1.00	0.02	0.01	10.43
oldhwy95_2.1	Old Hwy 95_2	Old Hwy 95_2	0.63	0.99	1.72	1.00	0.01	0.01	11.63
oldhwy95_2.27	Old Hwy 95_2	Old Hwy 95_2	0.61	1.00	1.81	1.00	0.00	0.00	22.60

Table E 5 - Casewise results from PXRF analysis of geochemical sources using four group solution (cont.).

oldhwy95_2.11	Old Hwy 95_2	Old Hwy 95_2	0.60	1.00	1.86	1.00	0.00	0.00	27.35
oldhwy95_2.8	Old Hwy 95_2	Old Hwy 95_2	0.59	1.00	1.90	1.00	0.00	0.00	28.59
oldhwy95_2.13	Old Hwy 95_2	Old Hwy 95_2	0.56	1.00	2.06	1.00	0.00	0.00	24.90
oldhwy95_2.7	Old Hwy 95_2	Old Hwy 95_2	0.54	1.00	2.14	1.00	0.00	0.00	32.40
oldhwy95_2.3	Old Hwy 95_2	Old Hwy 95_2	0.50	1.00	2.37	1.00	0.00	0.00	27.78
oldhwy95_2.30	Old Hwy 95_2	Old Hwy 95_2	0.49	0.93	2.44	1.00	0.05	0.07	7.87
oldhwy95_2.14	Old Hwy 95_2	Old Hwy 95_2	0.48	1.00	2.45	1.00	0.00	0.00	22.35
oldhwy95_2.4	Old Hwy 95_2	Old Hwy 95_2	0.39	1.00	2.99	1.00	0.00	0.00	33.93
oldhwy95_2.28	Old Hwy 95_2	Old Hwy 95_2	0.35	1.00	3.29	1.00	0.00	0.00	23.54
oldhwy95_2.38	Old Hwy 95_2	Old Hwy 95_1	0.33	0.81	3.46	2.00	0.10	0.19	6.18
oldhwy95_2.33	Old Hwy 95_2	Old Hwy 95_2	0.32	1.00	3.50	1.00	0.00	0.00	37.28
oldhwy95_2.5	Old Hwy 95_2	Old Hwy 95_2	0.27	0.87	3.91	1.00	0.05	0.13	7.82
oldhwy95_2.39	Old Hwy 95_2	Old Hwy 95_1	0.26	0.99	4.04	2.00	0.00	0.01	13.62
oldhwy95_2.16	Old Hwy 95_2	Old Hwy 95_2	0.26	0.79	4.05	1.00	0.08	0.21	6.89
oldhwy95_2.10	Old Hwy 95_2	Old Hwy 95_2	0.22	1.00	4.41	1.00	0.00	0.00	38.17
oldhwy95_2.26	Old Hwy 95_2	Old Hwy 95_2	0.22	1.00	4.47	1.00	0.00	0.00	40.13
oldhwy95_2.34	Old Hwy 95_2	Old Hwy 95_2	0.11	1.00	6.00	1.00	0.00	0.00	45.14
oldhwy95_2.9	Old Hwy 95_2	Old Hwy 95_2	0.10	1.00	6.21	1.00	0.00	0.00	41.89
peanut_brittle_48	Peanut Brittle	Peanut Brittle	0.98	1.00	0.20	6.00	0.00	0.00	14.26
peanut_brittle_8	Peanut Brittle	Peanut Brittle	0.96	1.00	0.29	6.00	0.00	0.00	13.72
peanut_brittle_36	Peanut Brittle	Peanut Brittle	0.95	1.00	0.36	6.00	0.00	0.00	16.85
peanut_brittle_35	Peanut Brittle	Peanut Brittle	0.87	1.00	0.70	6.00	0.00	0.00	14.19
peanut_brittle_54	Peanut Brittle	Peanut Brittle	0.86	1.00	0.74	6.00	0.00	0.00	12.86
peanut_brittle_18	Peanut Brittle	Peanut Brittle	0.84	1.00	0.84	6.00	0.01	0.00	12.37
peanut_brittle_2	Peanut Brittle	Peanut Brittle	0.83	0.99	0.88	6.00	0.01	0.01	11.22
peanut_brittle_19	Peanut Brittle	Peanut Brittle	0.83	1.00	0.88	6.00	0.00	0.00	24.73
peanut_brittle_22	Peanut Brittle	Peanut Brittle	0.81	1.00	0.97	6.00	0.00	0.00	22.38
peanut_brittle_34	Peanut Brittle	Peanut Brittle	0.80	0.99	1.01	6.00	0.02	0.01	10.45

Table E 5 - Casewise results from PXRF analysis of geochemical sources using four group solution (cont.).

peanut_brittle_41	Peanut Brittle	Peanut Brittle	0.79	0.99	1.05	6.00	0.01	0.01	10.86
peanut_brittle_39	Peanut Brittle	Peanut Brittle	0.75	1.00	1.19	6.00	0.00	0.00	17.54
peanut_brittle_45	Peanut Brittle	Peanut Brittle	0.75	0.99	1.22	6.00	0.01	0.01	11.39
peanut_brittle_33	Peanut Brittle	Peanut Brittle	0.74	1.00	1.24	6.00	0.00	0.00	18.07
peanut_brittle_64	Peanut Brittle	Peanut Brittle	0.74	1.00	1.25	6.00	0.00	0.00	19.62
peanut_brittle_27	Peanut Brittle	Peanut Brittle	0.73	1.00	1.29	6.00	0.00	0.00	13.36
peanut_brittle_4	Peanut Brittle	Peanut Brittle	0.72	1.00	1.36	6.00	0.00	0.00	25.62
peanut_brittle_60	Peanut Brittle	Peanut Brittle	0.70	1.00	1.42	6.00	0.00	0.00	21.95
peanut_brittle_61	Peanut Brittle	Peanut Brittle	0.67	1.00	1.54	6.00	0.00	0.00	27.47
peanut_brittle_25	Peanut Brittle	Peanut Brittle	0.66	1.00	1.60	6.00	0.00	0.00	19.51
peanut_brittle_40	Peanut Brittle	Peanut Brittle	0.64	1.00	1.67	6.00	0.00	0.00	14.88
peanut_brittle_10	Peanut Brittle	Peanut Brittle	0.61	0.99	1.85	6.00	0.01	0.01	11.16
peanut_brittle_57	Peanut Brittle	Peanut Brittle	0.60	1.00	1.85	6.00	0.00	0.00	21.02
peanut_brittle_9	Peanut Brittle	Peanut Brittle	0.57	1.00	1.99	6.00	0.00	0.00	20.09
peanut_brittle_17	Peanut Brittle	Peanut Brittle	0.57	1.00	2.02	6.00	0.00	0.00	14.07
peanut_brittle_59	Peanut Brittle	Peanut Brittle	0.56	1.00	2.04	6.00	0.00	0.00	21.25
peanut_brittle_65	Peanut Brittle	Peanut Brittle	0.55	1.00	2.09	6.00	0.00	0.00	21.55
peanut_brittle_1	Peanut Brittle	Peanut Brittle	0.52	0.99	2.29	6.00	0.01	0.01	10.88
peanut_brittle_24	Peanut Brittle	Peanut Brittle	0.50	1.00	2.35	6.00	0.00	0.00	17.53
peanut_brittle_58	Peanut Brittle	Peanut Brittle	0.49	1.00	2.42	6.00	0.00	0.00	24.87
peanut_brittle_28	Peanut Brittle	Peanut Brittle	0.46	0.99	2.56	6.00	0.01	0.01	12.13
peanut_brittle_46	Peanut Brittle	Peanut Brittle	0.46	0.88	2.61	6.00	0.09	0.12	6.46
peanut_brittle_29	Peanut Brittle	Peanut Brittle	0.43	1.00	2.76	6.00	0.00	0.00	29.40
peanut_brittle_42	Peanut Brittle	Peanut Brittle	0.38	0.97	3.07	6.00	0.02	0.02	10.39
peanut_brittle_52	Peanut Brittle	Peanut Brittle	0.36	1.00	3.20	6.00	0.00	0.00	13.67
peanut_brittle_21	Peanut Brittle	Peanut Brittle	0.34	1.00	3.38	6.00	0.00	0.00	34.96
peanut_brittle_55	Peanut Brittle	Peanut Brittle	0.33	1.00	3.45	6.00	0.00	0.00	26.91
peanut_brittle_51	Peanut Brittle	Peanut Brittle	0.32	0.99	3.47	6.00	0.01	0.01	12.83

Table E 5 - Casewise results from PXRF analysis of geochemical sources using four group solution (cont.).

peanut_brittle_30	Peanut Brittle	Peanut Brittle	0.31	1.00	3.60	6.00	0.00	0.00	20.58
peanut_brittle_12	Peanut Brittle	Peanut Brittle	0.30	1.00	3.65	6.00	0.00	0.00	14.72
peanut_brittle_43	Peanut Brittle	Peanut Brittle	0.27	1.00	3.94	6.00	0.00	0.00	18.58
peanut_brittle_47	Peanut Brittle	Peanut Brittle	0.27	1.00	3.96	6.00	0.00	0.00	34.00
peanut_brittle_38	Peanut Brittle	Peanut Brittle	0.27	0.95	3.96	6.00	0.02	0.04	10.28
peanut_brittle_49	Peanut Brittle	Peanut Brittle	0.27	1.00	3.97	6.00	0.00	0.00	18.27
peanut_brittle_26	Peanut Brittle	Peanut Brittle	0.24	1.00	4.18	6.00	0.00	0.00	22.51
peanut_brittle_3	Peanut Brittle	Peanut Brittle	0.24	1.00	4.23	6.00	0.00	0.00	14.73
peanut_brittle_63	Peanut Brittle	Peanut Brittle	0.24	0.98	4.23	6.00	0.01	0.02	12.13
peanut_brittle_56	Peanut Brittle	Peanut Brittle	0.23	1.00	4.36	6.00	0.00	0.00	34.25
peanut_brittle_32	Peanut Brittle	Peanut Brittle	0.19	0.92	4.78	6.00	0.02	0.06	10.19
peanut_brittle_53	Peanut Brittle	Peanut Brittle	0.18	1.00	4.83	1.00	0.00	0.00	29.93
peanut_brittle_31	Peanut Brittle	Peanut Brittle	0.14	1.00	5.42	6.00	0.00	0.00	35.14
peanut_brittle_37	Peanut Brittle	Peanut Brittle	0.12	1.00	5.83	6.00	0.00	0.00	31.49
peanut_brittle_5	Peanut Brittle	Peanut Brittle	0.11	1.00	5.97	6.00	0.00	0.00	42.11
peanut_brittle_7	Peanut Brittle	Peanut Brittle	0.09	1.00	6.41	1.00	0.00	0.00	22.63
peanut_brittle_15	Peanut Brittle	Peanut Brittle	0.08	0.59	6.65	6.00	0.04	0.25	8.18
peanut_brittle_20	Peanut Brittle	Old Hwy 95_1	0.08	0.71	6.81	3.00	0.02	0.26	9.71
peanut_brittle_23	Peanut Brittle	Peanut Brittle	0.06	0.68	7.49	1.00	0.04	0.28	8.42
peanut_brittle_6	Peanut Brittle	Peanut Brittle	0.05	1.00	7.82	6.00	0.00	0.00	26.50
peanut_brittle_44	Peanut Brittle	Peanut Brittle	0.03	1.00	9.16	6.00	0.00	0.00	36.15
peanut_brittle_66	Peanut Brittle	Peanut Brittle	0.03	1.00	9.31	6.00	0.00	0.00	34.74
peanut_brittle_13	Peanut Brittle	White Bird	0.02	0.77	9.62	3.00	0.01	0.19	12.61
peanut_brittle_62	Peanut Brittle	Peanut Brittle	0.01	1.00	10.51	6.00	0.00	0.00	25.17
peanut_brittle_11	Peanut Brittle	Peanut Brittle	0.01	1.00	10.81	1.00	0.00	0.00	40.08
peanut_brittle_14	Peanut Brittle	Peanut Brittle	0.01	1.00	11.00	6.00	0.00	0.00	49.23
peanut_brittle_50	Peanut Brittle	Peanut Brittle	0.00	1.00	14.93	6.00	0.00	0.00	45.92
peanut_brittle_16	Peanut Brittle	Peanut Brittle	0.00	0.99	15.13	6.00	0.00	0.01	24.40

Table E 5 - Casewise results from PXRF analysis of geochemical sources using four group solution (cont.).

White Bird_17	White Bird	White Bird	0.99	1.00	0.13	1.00	0.00	0.00	16.98
White Bird_53	White Bird	White Bird	0.98	1.00	0.17	3.00	0.00	0.00	17.84
White Bird_35	White Bird	White Bird	0.97	1.00	0.23	3.00	0.00	0.00	15.12
White Bird_30	White Bird	White Bird	0.96	1.00	0.32	1.00	0.00	0.00	18.59
White Bird_56	White Bird	White Bird	0.94	1.00	0.40	3.00	0.00	0.00	17.90
White Bird_26	White Bird	White Bird	0.92	1.00	0.51	3.00	0.01	0.00	11.59
White Bird_7	White Bird	White Bird	0.91	1.00	0.55	1.00	0.00	0.00	13.25
White Bird_39	White Bird	White Bird	0.83	1.00	0.86	1.00	0.00	0.00	14.47
White Bird_33	White Bird	White Bird	0.83	0.99	0.88	1.00	0.01	0.00	11.37
White Bird_18	White Bird	White Bird	0.82	0.99	0.93	1.00	0.01	0.00	11.18
White Bird_3	White Bird	White Bird	0.78	1.00	1.09	3.00	0.00	0.00	24.41
White Bird_27	White Bird	White Bird	0.75	1.00	1.19	3.00	0.00	0.00	14.30
White Bird_55	White Bird	White Bird	0.74	1.00	1.26	1.00	0.00	0.00	14.42
White Bird_2	White Bird	White Bird	0.71	1.00	1.37	3.00	0.00	0.00	21.47
White Bird_32	White Bird	White Bird	0.70	1.00	1.43	3.00	0.00	0.00	18.26
White Bird_15	White Bird	White Bird	0.69	1.00	1.49	3.00	0.00	0.00	24.43
White Bird_31	White Bird	Peanut Brittle	0.68	0.98	1.50	6.00	0.03	0.02	8.79
White Bird_43	White Bird	White Bird	0.66	1.00	1.58	1.00	0.01	0.00	12.16
White Bird_50	White Bird	White Bird	0.66	1.00	1.59	1.00	0.00	0.00	24.47
White Bird_24	White Bird	White Bird	0.66	1.00	1.60	1.00	0.00	0.00	18.74
White Bird_16	White Bird	White Bird	0.63	1.00	1.73	1.00	0.00	0.00	20.90
White Bird_36	White Bird	White Bird	0.62	1.00	1.79	1.00	0.00	0.00	18.99
White Bird_52	White Bird	White Bird	0.60	1.00	1.88	1.00	0.00	0.00	16.52
White Bird_34	White Bird	White Bird	0.59	1.00	1.93	1.00	0.00	0.00	21.59
White Bird_47	White Bird	White Bird	0.58	0.94	1.96	3.00	0.05	0.06	7.87
White Bird_1	White Bird	White Bird	0.57	1.00	2.02	1.00	0.00	0.00	19.85
White Bird_28	White Bird	White Bird	0.56	0.99	2.05	1.00	0.01	0.01	10.74
White Bird_12	White Bird	White Bird	0.56	1.00	2.07	3.00	0.00	0.00	18.83

Table E 5 - Casewise results from PXRF analysis of geochemical sources using four group solution (cont.).

White Bird_4	White Bird	White Bird	0.51	0.99	2.32	3.00	0.01	0.01	10.96
White Bird_51	White Bird	White Bird	0.51	0.99	2.33	3.00	0.01	0.01	11.54
White Bird_37	White Bird	White Bird	0.47	1.00	2.51	1.00	0.00	0.00	23.87
White Bird_20	White Bird	White Bird	0.47	0.99	2.53	3.00	0.01	0.01	12.53
White Bird_45	White Bird	Peanut Brittle	0.43	0.94	2.78	6.00	0.04	0.06	8.21
White Bird_46	White Bird	White Bird	0.43	0.91	2.79	1.00	0.08	0.09	6.74
White Bird_14	White Bird	White Bird	0.41	0.90	2.87	3.00	0.06	0.10	7.54
White Bird_8	White Bird	White Bird	0.38	1.00	3.10	1.00	0.00	0.00	17.36
White Bird_25	White Bird	White Bird	0.37	1.00	3.14	3.00	0.00	0.00	30.55
White Bird_19	White Bird	White Bird	0.37	1.00	3.14	1.00	0.00	0.00	29.04
White Bird_11	White Bird	White Bird	0.36	1.00	3.22	3.00	0.00	0.00	28.66
White Bird_40	White Bird	White Bird	0.34	0.81	3.38	1.00	0.13	0.19	5.71
White Bird_13	White Bird	White Bird	0.34	0.94	3.38	3.00	0.03	0.05	9.31
White Bird_49	White Bird	White Bird	0.32	0.72	3.54	3.00	0.13	0.28	5.69
White Bird_23	White Bird	White Bird	0.29	1.00	3.71	3.00	0.00	0.00	31.30
White Bird_5	White Bird	Peanut Brittle	0.21	0.68	4.50	6.00	0.12	0.31	5.86
White Bird_38	White Bird	White Bird	0.21	0.90	4.56	1.00	0.04	0.10	8.42
White Bird_54	White Bird	White Bird	0.19	0.79	4.73	3.00	0.05	0.19	7.83
White Bird_44	White Bird	White Bird	0.16	0.68	5.24	3.00	0.06	0.26	7.39
White Bird_48	White Bird	White Bird	0.15	1.00	5.35	3.00	0.00	0.00	28.80
White Bird_6	White Bird	Peanut Brittle	0.13	0.84	5.62	6.00	0.02	0.11	9.41
White Bird_21	White Bird	White Bird	0.13	0.99	5.65	1.00	0.00	0.01	14.96
White Bird_42	White Bird	White Bird	0.13	1.00	5.72	3.00	0.00	0.00	33.97
White Bird_29	White Bird	White Bird	0.11	1.00	5.98	1.00	0.00	0.00	23.55
White Bird_58	White Bird	White Bird	0.11	1.00	6.06	3.00	0.00	0.00	35.36
White Bird_59	White Bird	White Bird	0.08	0.99	6.88	1.00	0.00	0.01	15.98
White Bird_10	White Bird	White Bird	0.07	1.00	7.18	3.00	0.00	0.00	36.30
White Bird_57	White Bird	White Bird	0.06	0.94	7.50	3.00	0.00	0.06	13.11

Table E 5 - Casewise results from PXRF analysis of geochemical sources using four group solution (cont.).

White Bird_9	White Bird	Peanut Brittle	0.06	0.74	7.51	6.00	0.02	0.17	10.23
White Bird_22	White Bird	White Bird	0.04	0.87	8.60	1.00	0.00	0.08	12.86
White Bird_41	White Bird	White Bird	0.03	1.00	8.72	1.00	0.00	0.00	33.56

Table E 5 - Casewise results from PXRF analysis of geochemical sources using four group solution (cont.).

Casewise Results – Artifacts

Casewise results for artifacts of PXRF analysis using four group solution up analysis are listed below. Cases are primarally sorted by their actual group, and secondarily by their conditional probability. Note that no second cases fall within a single standard deviation of both the primary and secondary groups simultaneously. Groups are color coded by conditional probability, with red cases being within a single standard deviation of its predicted sources, tan being between one and 1.5, green being between 1.5 and two, and no color for greater than two.

Cat#	Predicted Group	Cond. Prob.	Post. Prob.	D^2	2nd Group	2nd Cond. Prob.	2nd Post. Prob.	2nd Group D^2
2028	Old Hwy 95_1	0.90	0.99	0.59	6.00	0.01	0.01	11.43
1230	Old Hwy 95_1	0.71	0.98	1.36	6.00	0.02	0.02	10.16
707	Old Hwy 95_1	0.71	0.97	1.37	6.00	0.03	0.03	8.91
681	Old Hwy 95_1	0.60	1.00	1.87	2.00	0.01	0.00	12.48
912	Old Hwy 95_1	0.58	0.93	1.94	6.00	0.05	0.07	7.70
4776	Old Hwy 95_1	0.56	0.97	2.08	6.00	0.02	0.03	9.60
3842	Old Hwy 95_1	0.54	0.98	2.16	2.00	0.02	0.02	10.38
1253	Old Hwy 95_1	0.48	0.93	2.49	6.00	0.04	0.07	8.43
4008	Old Hwy 95_1	0.45	0.94	2.64	2.00	0.05	0.06	7.92
2861	Old Hwy 95_1	0.43	0.92	2.78	6.00	0.04	0.07	8.46
203	Old Hwy 95_1	0.41	0.99	2.88	6.00	0.01	0.01	12.67

Table E 6 - Casewise results from predictive discriminant function analysis of PXRF analysis of artifacts from Cooper's Ferry. Results are color coded by distance from group centroid (cont.).

Cat#	Predicted Group	Cond. Prob.	Post. Prob.	D^2	2nd Group	2nd Cond. Prob.	2nd Post. Prob.	2nd Group D^2
2621	Old Hwy 95_1	0.40	0.99	2.92	6.00	0.00	0.01	13.73
3039	Old Hwy 95_1	0.40	0.99	2.94	6.00	0.00	0.01	13.83
904	Old Hwy 95_1	0.39	0.77	2.99	6.00	0.11	0.23	6.01
2068	Old Hwy 95_1	0.39	1.00	2.99	6.00	0.00	0.00	16.97
3799	Old Hwy 95_1	0.37	0.95	3.13	6.00	0.02	0.04	10.13
3078	Old Hwy 95_1	0.37	0.78	3.16	6.00	0.10	0.22	6.35
2248	Old Hwy 95_1	0.35	0.75	3.26	6.00	0.11	0.25	6.06
4088	Old Hwy 95_1	0.35	1.00	3.31	6.00	0.00	0.00	18.54
4621	Old Hwy 95_1	0.33	0.65	3.46	6.00	0.15	0.35	5.31
1831	Old Hwy 95_1	0.32	1.00	3.47	3.00	0.00	0.00	17.65
2805	Old Hwy 95_1	.296	.925	3.701	2.000	0.03	.073	8.626
3006	Old Hwy 95_1	.282	.687	3.814	6.000	0.11	.312	6.024
2970	Old Hwy 95_1	.281	.925	3.822	6.000	0.02	.072	9.564
3422	Old Hwy 95_1	.277	.990	3.856	2.000	0.00	.005	14.167
2077	Old Hwy 95_1	.257	.851	4.039	6.000	0.04	.136	8.339
2278	Old Hwy 95_1	.252	.951	4.088	2.000	0.02	.038	10.409
4049	Old Hwy 95_1	.248	.915	4.127	6.000	0.02	.081	9.606
4138	Old Hwy 95_1	.248	.972	4.132	6.000	0.01	.028	11.891
4486	Old Hwy 95_1	.237	.874	4.232	6.000	0.03	.124	8.777
253	Old Hwy 95_1	.231	.963	4.303	6.000	0.01	.037	11.478
2250	Old Hwy 95_1	.224	.779	4.371	6.000	0.06	.218	7.552
1098	Old Hwy 95_1	.224	.860	4.374	6.000	0.03	.101	9.290
4006	Old Hwy 95_1	.222	.545	4.394	6.000	0.14	.450	5.413
913	Old Hwy 95_1	.199	.980	4.656	6.000	0.00	.010	14.442
2651	Old Hwy 95_1	.172	.883	4.997	6.000	0.02	.082	10.390
2605	Old Hwy 95_1	.171	.840	5.010	6.000	0.03	.160	8.961
2879	Old Hwy 95_1	.157	.609	5.208	6.000	0.08	.389	6.733
329	Old Hwy 95_1	.155	.920	5.246	6.000	0.01	.078	10.801

Table E 6 - Casewise results from predictive discriminant function analysis of PXRF analysis of artifacts from Cooper's Ferry. Results are color coded by distance from group centroid (cont.).

Cat#	Predicted Group	Cond. Prob.	Post. Prob.	D^2	2nd Group	2nd Cond. Prob.	2nd Post. Prob.	2nd Group D^2
2743	Old Hwy 95_1	.154	.787	5.257	6.000	0.03	.200	8.632
4488	Old Hwy 95_1	.121	.958	5.823	3.000	0.00	.038	13.154
3239	Old Hwy 95_1	.113	.962	5.965	6.000	0.00	.035	13.218
1939	Old Hwy 95_1	.110	.641	6.040	6.000	0.05	.357	7.844
895	Old Hwy 95_1	.104	.743	6.155	6.000	0.03	.250	8.967
1288	Old Hwy 95_1	.100	.984	6.261	6.000	0.00	.016	15.171
4615	Old Hwy 95_1	.090	.812	6.492	6.000	0.01	.147	10.544
194	Old Hwy 95_1	.082	.974	6.696	6.000	0.00	.016	15.509
5074	Old Hwy 95_1	.082	.575	6.710	6.000	0.05	.423	7.960
5092	Old Hwy 95_1	.079	.939	6.778	6.000	0.00	.060	12.896
3399	Old Hwy 95_1	.077	.817	6.848	6.000	0.01	.182	10.484
1237	Old Hwy 95_1	.077	.498	6.856	6.000	0.06	.498	7.489
4365	Old Hwy 95_1	.077	.737	6.859	6.000	0.02	.261	9.565
2920	Old Hwy 95_1	.069	.559	7.103	2.000	0.06	.441	7.435
841	Old Hwy 95_1	.065	.852	7.223	6.000	0.01	.147	11.365
421	Old Hwy 95_1	.053	.679	7.684	6.000	0.02	.320	9.822
2616	Old Hwy 95_1	.050	.615	7.795	2.000	0.03	.348	8.786
670	Old Hwy 95_1	.050	.936	7.818	6.000	0.00	.064	13.832
763	Old Hwy 95_1	.050	.993	7.822	2.000	0.00	.007	17.459
3447	Old Hwy 95_1	.048	.787	7.914	2.000	0.02	.213	10.384
2245	Old Hwy 95_1	.043	.779	8.161	6	0.01	.207	11.443
2945	Old Hwy 95_1	.041	.979	8.237	2	0.00	.021	15.775
666	Old Hwy 95_1	.040	.721	8.315	6	0.01	.279	10.843
250	Old Hwy 95_1	.038	.987	8.410	2	0.00	.007	18.138
3887	Old Hwy 95_1	.035	.996	8.594	2	0.00	.004	19.516
2019	Old Hwy 95_1	.035	.537	8.621	6	0.02	.463	9.546
1170	Old Hwy 95_1	.031	.551	8.857	2	0.03	.449	9.126
3855	Old Hwy 95_1	.026	.626	9.289	6	0.01	.374	10.953

Table E 6 - Casewise results from predictive discriminant function analysis of PXRF analysis of artifacts from Cooper's Ferry. Results are color coded by distance from group centroid (cont.).

Cat#	Predicted Group	Cond. Prob.	Post. Prob.	D^2	2nd Group	2nd Cond. Prob.	2nd Post. Prob.	2nd Group D^2
1779	Old Hwy 95_1	.026	.722	9.291	2	0.01	.274	11.084
3385	Old Hwy 95_1	.025	.984	9.381	6	0.00	.016	18.280
853	Old Hwy 95_1	.018	.824	10.081	6	0.00	.176	13.795
4190	Old Hwy 95_1	.016	.929	10.340	6	0.00	.071	16.113
3291	Old Hwy 95_1	.015	.708	10.402	6	0.01	.289	12.828
3207	Old Hwy 95_1	.015	.989	10.513	6	0.00	.011	20.115
2910	Old Hwy 95_1	.013	.972	10.708	2	0.00	.028	17.690
970	Old Hwy 95_1	.013	.996	10.746	2	0.00	.004	21.499
5113	Old Hwy 95_1	.013	.796	10.751	6	0.00	.204	14.110
186	Old Hwy 95_1	.010	.925	11.343	6	0.00	.075	17.000
4563	Old Hwy 95_1	.007	.593	12.083	2	0.00	.365	12.909
1684	Old Hwy 95_1	.006	.933	12.502	2	0.00	.067	17.628
3990	Old Hwy 95_1	.004	.996	13.320	6	0.00	.003	25.262
2959	Old Hwy 95_1	.004	.513	13.363	6	0.00	.487	14.102
2977	Old Hwy 95_1	.004	.974	13.381	2	0.00	.026	20.481
1074	Old Hwy 95_1	.004	1.000	13.430	2	0.00	.000	29.588
880	Old Hwy 95_1	.003	.590	13.668	6	0.00	.318	15.536
5026	Old Hwy 95_1	.003	.979	13.711	6	0.00	.020	22.086
3775	Old Hwy 95_1	.003	.999	13.857	6	0.00	.001	29.202
2717	Old Hwy 95_1	.003	.987	13.861	2	0.00	.012	22.466
822	Old Hwy 95_1	.003	.581	13.925	6	0.00	.412	15.247
303	Old Hwy 95_1	.003	.902	13.961	6	0.00	.050	20.393
4191	Old Hwy 95_1	.003	.459	14.037	6	0.00	.410	14.893
5115	Old Hwy 95_1	.002	.552	14.606	6	0.00	.444	15.678
568	Old Hwy 95_1	.002	.598	14.736	6	0.00	.392	16.216
3002	Old Hwy 95_1	.002	.546	15.218	2	0.00	.423	15.582
214	Old Hwy 95_1	.001	.990	15.659	6	0.00	.008	25.869
4760	Old Hwy 95_1	.001	.958	15.659	6	0.00	.036	22.852

Table E 6 - Casewise results from predictive discriminant function analysis of PXRF analysis of artifacts from Cooper's Ferry. Results are color coded by distance from group centroid (cont.).

Cat#	Predicted Group	Cond. Prob.	Post. Prob.	D^2	2nd Group	2nd Cond. Prob.	2nd Post. Prob.	2nd Group D^2
3400	Old Hwy 95_1	.001	.905	16.020	6	0.00	.073	21.680
3857	Old Hwy 95_1	.001	.738	16.263	2	0.00	.262	18.193
86	Old Hwy 95_1	.001	.517	16.272	6	0.00	.482	17.044
1344	Old Hwy 95_1	.001	.589	16.628	6	0.00	.411	17.983
2918	Old Hwy 95_1	.001	.615	16.656	6	0.00	.383	18.236
4632	Old Hwy 95_1	.001	.829	16.672	2	0.00	.110	20.563
1921	Old Hwy 95_1	.001	.586	16.726	6	0.00	.384	18.203
960	Old Hwy 95_1	.001	.922	17.202	6	0.00	.078	22.777
5095	Old Hwy 95_1	.001	.669	17.237	6	0.00	.331	19.276
5175	Old Hwy 95_1	.001	.977	17.266	6	0.00	.021	25.555
1133	Old Hwy 95_1	.000	.969	17.818	6	0.00	.026	25.691
5288	Old Hwy 95_1	.000	.538	17.853	6	0.00	.458	18.808
1108	Old Hwy 95_1	.000	.895	18.273	6	0.00	.105	23.196
1742	Old Hwy 95_1	.000	.647	18.282	2	0.00	.352	19.357
5174	Old Hwy 95_1	.000	.976	18.353	6	0.00	.024	26.399
2623	Old Hwy 95_1	.000	.903	18.569	6	0.00	.071	24.278
325	Old Hwy 95_1	.000	.528	18.714	2	0.00	.467	18.817
3518	Old Hwy 95_1	.000	.552	18.967	2	0.00	.441	19.270
3464	Old Hwy 95_1	.000	.883	19.777	2	0.00	.116	23.683
784	Old Hwy 95_1	.000	.518	20.075	2	0.00	.480	20.082
2570	Old Hwy 95_1	.000	.636	20.230	6	0.00	.287	22.456
819	Old Hwy 95_1	.000	.999	20.391	6	0.00	.001	35.988
3550	Old Hwy 95_1	.000	.985	20.533	6	0.00	.014	29.717
808	Old Hwy 95_1	.000	.486	20.877	6	0.00	.271	22.679
3317	Old Hwy 95_1	.000	.822	20.931	6	0.00	.170	24.720
5062	Old Hwy 95_1	.000	.991	21.574	6	0.00	.006	32.441
2741	Old Hwy 95_1	.000	.657	21.580	6	0.00	.340	23.531
1866	Old Hwy 95_1	.000	.874	22.368	2	0.00	.122	26.168

Table E 6 - Casewise results from predictive discriminant function analysis of PXRF analysis of artifacts from Cooper's Ferry. Results are color coded by distance from group centroid (cont.).

Cat#	Predicted Group	Cond. Prob.	Post. Prob.	D^2	2nd Group	2nd Cond. Prob.	2nd Post. Prob.	2nd Group D^2
5292	Old Hwy 95_1	.000	.626	22.709	6	0.00	.313	24.732
967	Old Hwy 95_1	.000	.997	23.079	6	0.00	.003	35.451
5093	Old Hwy 95_1	.000	.804	23.444	6	0.00	.196	26.895
5294	Old Hwy 95_1	.000	.608	24.709	6	0.00	.390	26.230
1196	Old Hwy 95_1	.000	.668	25.030	6	0.00	.332	27.059
4601	Old Hwy 95_1	.000	.584	25.071	6	0.00	.395	26.486
3977	Old Hwy 95_1	.000	.997	25.928	2	0.00	.003	37.366
5289	Old Hwy 95_1	.000	.972	26.512	6	0.00	.014	35.602
5291	Old Hwy 95_1	.000	.982	27.638	2	0.00	.009	36.836
834	Old Hwy 95_1	.000	.883	29.823	6	0.00	.116	34.521
149	Old Hwy 95_1	.000	.967	42.463	6	0.00	.021	50.723
830	Old Hwy 95_1	.000	.673	46.304	6	0.00	.273	48.739
4328	Old Hwy 95_2	.098	.548	6.286	1.000	0.08	.449	6.830
2628	Old Hwy 95_2	.060	.917	7.421	1.000	0.01	.083	12.365
817	Old Hwy 95_2	.047	.978	7.948	1.000	0.00	.022	15.656
1274	Old Hwy 95_2	.003	.699	14.025	1	0.00	.256	16.177
598	Old Hwy 95_2	.000	.685	17.986	1	0.00	.263	20.047
2302	Old Hwy 95_2	.000	1.000	18.426	1	0.00	.000	64.162
368	Peanut Brittle	0.52	0.94	2.25	6.00	0.06	0.06	7.59
556	Peanut Brittle	0.48	0.92	2.47	6.00	0.07	0.08	7.07
411	Peanut Brittle	0.39	0.88	2.99	6.00	0.08	0.12	6.77
4052	Peanut Brittle	0.34	0.99	3.32	6.00	0.01	0.01	11.88
2778	Peanut Brittle	0.33	0.99	3.41	6.00	0.01	0.01	12.13
2269	Peanut Brittle	.266	1.000	3.960	6.000	0.00	.000	23.846
2348	Peanut Brittle	.243	.935	4.180	6.000	0.03	.065	9.298
901	Peanut Brittle	.212	.529	4.499	6.000	0.21	.469	4.516
153	Peanut Brittle	.208	.999	4.554	6.000	0.00	.001	18.383
838	Peanut Brittle	.196	.953	4.690	6.000	0.01	.047	10.483

Table E 6 - Casewise results from predictive discriminant function analysis of PXRF analysis of artifacts from Cooper's Ferry. Results are color coded by distance from group centroid (cont.).

Cat#	Predicted Group	Cond. Prob.	Post. Prob.	D^2	2nd Group	2nd Cond. Prob.	2nd Post. Prob.	2nd Group D^2
1157	Peanut Brittle	.161	.991	5.148	6.000	0.00	.009	14.373
375	Peanut Brittle	.135	.990	5.553	6.000	0.00	.010	14.575
818	Peanut Brittle	.090	.735	6.491	6.000	0.04	.265	8.309
3943	Peanut Brittle	.083	.949	6.675	1.000	0.01	.047	11.819
794	Peanut Brittle	.059	.440	7.434	1.000	0.06	.287	7.430
3602	Peanut Brittle	.028	.998	9.118	6	0.00	.002	21.780
4464	Peanut Brittle	.010	.394	11.400	1	0.01	.373	10.655
1767	Peanut Brittle	.006	.595	12.278	6	0.00	.313	13.337
3779	Peanut Brittle	.003	.999	13.746	6	0.00	.001	28.660
1956	Peanut Brittle	.000	.969	19.341	6	0.00	.031	26.005
471	White Bird	1.00	1.00	0.07	3.00	0.00	0.00	15.25
2153	White Bird	0.99	1.00	0.12	1.00	0.00	0.00	15.08
504	White Bird	0.97	1.00	0.22	3.00	0.00	0.00	19.32
561	White Bird	0.97	1.00	0.25	1.00	0.00	0.00	13.31
4767	White Bird	0.96	1.00	0.28	1.00	0.00	0.00	14.64
128	White Bird	0.94	1.00	0.38	3.00	0.01	0.00	12.61
3133	White Bird	0.94	1.00	0.41	3.00	0.00	0.00	14.25
944	White Bird	0.93	1.00	0.47	1.00	0.01	0.00	12.13
2370	White Bird	0.92	1.00	0.51	3.00	0.00	0.00	17.85
4183	White Bird	0.91	1.00	0.52	1.00	0.01	0.00	11.86
3479	White Bird	0.90	1.00	0.59	3.00	0.01	0.00	12.54
4161	White Bird	0.89	1.00	0.64	1.00	0.00	0.00	14.80
2410	White Bird	0.88	1.00	0.69	1.00	0.00	0.00	22.30
3153	White Bird	0.86	1.00	0.76	1.00	0.00	0.00	17.47
322	White Bird	0.86	1.00	0.76	1.00	0.00	0.00	15.74
1055	White Bird	0.86	1.00	0.76	1.00	0.01	0.00	11.55
831	White Bird	0.86	1.00	0.77	1.00	0.00	0.00	18.63
3190	White Bird	0.85	1.00	0.82	3.00	0.00	0.00	17.17

Table E 6 - Casewise results from predictive discriminant function analysis of PXRF analysis of artifacts from Cooper's Ferry. Results are color coded by distance from group centroid (cont.).

Cat#	Predicted Group	Cond. Prob.	Post. Prob.	D^2	2nd Group	2nd Cond. Prob.	2nd Post. Prob.	2nd Group D^2
2306	White Bird	0.83	1.00	0.88	1.00	0.00	0.00	20.77
878	White Bird	0.83	1.00	0.89	1.00	0.00	0.00	17.15
1022	White Bird	0.82	1.00	0.92	3.00	0.00	0.00	13.14
3287	White Bird	0.80	1.00	1.00	1.00	0.00	0.00	15.34
835	White Bird	0.78	1.00	1.08	1.00	0.00	0.00	20.94
2254	White Bird	0.78	0.99	1.10	1.00	0.01	0.01	10.95
127	White Bird	0.77	1.00	1.12	1.00	0.00	0.00	14.63
157	White Bird	0.77	0.99	1.15	1.00	0.01	0.01	10.67
1214	White Bird	0.75	1.00	1.23	1.00	0.00	0.00	16.83
3758	White Bird	0.74	1.00	1.25	1.00	0.00	0.00	13.78
336	White Bird	0.74	1.00	1.26	1.00	0.00	0.00	16.31
1741	White Bird	0.71	1.00	1.37	1.00	0.00	0.00	23.12
4438	White Bird	0.70	1.00	1.42	1.00	0.00	0.00	24.42
1774	White Bird	0.69	1.00	1.48	1.00	0.00	0.00	15.03
885	White Bird	0.68	0.99	1.50	3.00	0.00	0.00	12.89
564	White Bird	0.67	1.00	1.57	1.00	0.00	0.00	16.22
2877	White Bird	0.67	0.99	1.57	1.00	0.02	0.01	10.07
3991	White Bird	0.66	1.00	1.59	1.00	0.00	0.00	14.23
934	White Bird	0.66	0.99	1.61	1.00	0.02	0.01	10.21
3745	White Bird	0.65	1.00	1.66	1.00	0.00	0.00	18.96
545	White Bird	0.64	1.00	1.67	1.00	0.01	0.00	11.84
3240	White Bird	0.64	1.00	1.70	3.00	0.00	0.00	22.55
4109	White Bird	0.64	0.99	1.71	3.00	0.01	0.01	12.07
1257	White Bird	0.63	1.00	1.74	1.00	0.00	0.00	13.97
887	White Bird	0.62	1.00	1.77	3.00	0.00	0.00	27.08
3272	White Bird	0.62	1.00	1.78	1.00	0.00	0.00	15.76
1178	White Bird	0.62	0.99	1.78	1.00	0.01	0.01	10.74
2528	White Bird	0.62	1.00	1.79	3.00	0.00	0.00	23.39

Table E 6 - Casewise results from predictive discriminant function analysis of PXRF analysis of artifacts from Cooper's Ferry. Results are color coded by distance from group centroid (cont.).

Cat#	Predicted Group	Cond. Prob.	Post. Prob.	D^2	2nd Group	2nd Cond. Prob.	2nd Post. Prob.	2nd Group D^2
1240	White Bird	0.62	1.00	1.79	1.00	0.00	0.00	14.12
1036	White Bird	0.59	0.99	1.92	3.00	0.01	0.01	11.76
2132	White Bird	0.59	0.99	1.93	1.00	0.01	0.01	10.96
662	White Bird	0.57	0.96	2.01	1.00	0.05	0.04	7.74
4325	White Bird	0.56	0.99	2.07	1.00	0.01	0.01	11.57
3274	White Bird	0.53	0.95	2.23	1.00	0.05	0.05	7.62
2385	White Bird	0.53	1.00	2.23	1.00	0.00	0.00	13.68
311	White Bird	0.52	0.95	2.24	3.00	0.04	0.05	8.48
3165	White Bird	0.52	1.00	2.25	3.00	0.00	0.00	20.02
897	White Bird	0.51	0.99	2.29	1.00	0.01	0.01	11.55
173	White Bird	0.51	1.00	2.32	1.00	0.00	0.00	20.04
3053	White Bird	0.51	1.00	2.33	1.00	0.00	0.00	20.80
124	White Bird	0.50	1.00	2.35	3.00	0.00	0.00	14.81
4355	White Bird	0.50	1.00	2.36	1.00	0.00	0.00	17.28
832	White Bird	0.50	1.00	2.39	3.00	0.00	0.00	26.49
1155	White Bird	0.49	1.00	2.40	1.00	0.00	0.00	15.61
2417	White Bird	0.49	1.00	2.41	1.00	0.00	0.00	19.41
2246	White Bird	0.49	0.98	2.43	1.00	0.02	0.01	10.46
952	White Bird	0.48	1.00	2.45	1.00	0.00	0.00	18.15
139	White Bird	0.48	1.00	2.46	1.00	0.00	0.00	19.39
1554	White Bird	0.48	1.00	2.46	3.00	0.00	0.00	21.47
2309	White Bird	0.47	0.95	2.52	1.00	0.05	0.05	7.81
906	White Bird	0.47	1.00	2.53	1.00	0.00	0.00	24.53
3009	White Bird	0.47	1.00	2.55	1.00	0.00	0.00	15.24
3461	White Bird	0.46	0.97	2.57	3.00	0.02	0.03	10.03
4646	White Bird	0.46	1.00	2.59	1.00	0.00	0.00	18.97
248	White Bird	0.46	0.94	2.60	1.00	0.05	0.05	7.80
2397	White Bird	0.46	1.00	2.61	1.00	0.00	0.00	21.42

Table E 6 - Casewise results from predictive discriminant function analysis of PXRF analysis of artifacts from Cooper's Ferry. Results are color coded by distance from group centroid (cont.).

Cat#	Predicted Group	Cond. Prob.	Post. Prob.	D^2	2nd Group	2nd Cond. Prob.	2nd Post. Prob.	2nd Group D^2
2508	White Bird	0.45	0.97	2.62	3.00	0.01	0.02	10.67
4346	White Bird	0.44	1.00	2.68	1.00	0.00	0.00	22.20
4164	White Bird	0.44	1.00	2.68	1.00	0.00	0.00	22.19
4634	White Bird	0.44	1.00	2.70	3.00	0.00	0.00	26.12
4265	White Bird	0.44	0.98	2.71	1.00	0.02	0.02	9.91
2532	White Bird	0.43	0.93	2.73	1.00	0.06	0.07	7.37
4403	White Bird	0.43	0.99	2.75	1.00	0.01	0.01	11.38
340	White Bird	0.43	1.00	2.75	1.00	0.00	0.00	18.25
1590	White Bird	0.43	1.00	2.75	1.00	0.00	0.00	15.65
5047	White Bird	0.42	1.00	2.80	1.00	0.00	0.00	14.99
2701	White Bird	0.42	1.00	2.81	1.00	0.00	0.00	15.26
1012	White Bird	0.42	1.00	2.82	1.00	0.00	0.00	13.69
4326	White Bird	0.42	0.96	2.82	1.00	0.03	0.04	8.61
2377	White Bird	0.42	0.99	2.83	1.00	0.01	0.01	11.54
1123	White Bird	0.42	1.00	2.83	1.00	0.00	0.00	21.17
882	White Bird	0.42	1.00	2.84	1.00	0.00	0.00	18.32
258	White Bird	0.41	1.00	2.88	1.00	0.00	0.00	19.54
1531	White Bird	0.41	0.99	2.89	1.00	0.01	0.01	10.78
876	White Bird	0.41	1.00	2.89	1.00	0.00	0.00	13.45
650	White Bird	0.41	0.93	2.90	3.00	0.03	0.06	8.72
631	White Bird	0.40	0.94	2.93	1.00	0.05	0.06	7.77
378	White Bird	0.40	1.00	2.96	1.00	0.00	0.00	13.75
993	White Bird	0.40	0.99	2.96	1.00	0.01	0.01	11.47
4259	White Bird	0.40	0.98	2.97	1.00	0.02	0.02	9.82
642	White Bird	0.39	1.00	2.98	1.00	0.00	0.00	28.70
2555	White Bird	0.39	1.00	2.98	1.00	0.00	0.00	22.04
870	White Bird	0.39	0.95	2.98	1.00	0.04	0.05	8.35
899	White Bird	0.39	1.00	3.04	1.00	0.00	0.00	17.30

Table E 6 - Casewise results from predictive discriminant function analysis of PXRF analysis of artifacts from Cooper's Ferry. Results are color coded by distance from group centroid (cont.).

Cat#	Predicted Group	Cond. Prob.	Post. Prob.	D^2	2nd Group	2nd Cond. Prob.	2nd Post. Prob.	2nd Group D^2
945	White Bird	0.38	0.99	3.07	1.00	0.01	0.01	12.59
1090	White Bird	0.38	1.00	3.07	1.00	0.00	0.00	16.60
2164	White Bird	0.38	1.00	3.07	1.00	0.00	0.00	20.65
907	White Bird	0.38	1.00	3.09	1.00	0.00	0.00	24.94
3315	White Bird	0.37	1.00	3.13	1.00	0.00	0.00	17.59
629	White Bird	0.37	1.00	3.16	3.00	0.00	0.00	30.34
1151	White Bird	0.37	1.00	3.16	1.00	0.00	0.00	14.63
2513	White Bird	0.37	1.00	3.17	1.00	0.00	0.00	18.16
3783	White Bird	0.36	0.89	3.18	1.00	0.08	0.11	6.75
2113	White Bird	0.36	0.90	3.19	1.00	0.08	0.10	6.87
1756	White Bird	0.36	1.00	3.20	1.00	0.00	0.00	13.98
2821	White Bird	0.36	1.00	3.21	1.00	0.00	0.00	22.75
1726	White Bird	0.36	0.97	3.24	1.00	0.02	0.03	9.83
4481	White Bird	0.36	0.88	3.24	1.00	0.08	0.11	6.69
4536	White Bird	0.35	1.00	3.27	1.00	0.00	0.00	20.58
222	White Bird	0.35	1.00	3.28	1.00	0.00	0.00	16.31
4404	White Bird	0.35	0.99	3.29	1.00	0.01	0.01	12.80
3665	White Bird	0.34	0.91	3.32	1.00	0.06	0.09	7.37
920	White Bird	0.34	1.00	3.33	1.00	0.00	0.00	13.99
1828	White Bird	0.34	1.00	3.33	1.00	0.00	0.00	13.32
2041	White Bird	0.34	0.98	3.33	3.00	0.01	0.02	11.21
4525	White Bird	0.34	1.00	3.33	3.00	0.00	0.00	16.19
3968	White Bird	0.34	1.00	3.37	1.00	0.00	0.00	19.65
889	White Bird	0.33	1.00	3.42	3.00	0.00	0.00	15.37
3971	White Bird	0.32	0.98	3.48	1.00	0.02	0.02	10.43
4762	White Bird	0.32	1.00	3.48	1.00	0.00	0.00	25.09
399	White Bird	0.32	1.00	3.51	1.00	0.00	0.00	13.75
84	White Bird	0.32	0.96	3.51	1.00	0.02	0.04	9.41

Table E 6 - Casewise results from predictive discriminant function analysis of PXRF analysis of artifacts from Cooper's Ferry. Results are color coded by distance from group centroid (cont.).

Cat#	Predicted Group	Cond. Prob.	Post. Prob.	D^2	2nd Group	2nd Cond. Prob.	2nd Post. Prob.	2nd Group D^2
3301	White Bird	0.32	0.99	3.52	3.00	0.00	0.01	13.86
3910	White Bird	.317	.986	3.532	1.000	0.01	.014	11.452
915	White Bird	.311	.999	3.573	1.000	0.00	.000	18.284
2781	White Bird	.308	.970	3.603	1.000	0.02	.030	9.953
4038	White Bird	.307	1.000	3.606	3.000	0.00	.000	25.004
2837	White Bird	.304	.998	3.629	1.000	0.00	.002	15.264
1419	White Bird	.303	.844	3.640	3.000	0.06	.156	7.242
3961	White Bird	.302	1.000	3.646	1.000	0.00	.000	18.400
4155	White Bird	.300	.911	3.662	1.000	0.05	.089	7.684
2433	White Bird	.300	.983	3.666	1.000	0.01	.017	11.103
809	White Bird	.296	.742	3.701	3.000	0.11	.256	6.056
4227	White Bird	.292	.756	3.730	1.000	0.15	.244	5.363
2298	White Bird	.291	.961	3.736	1.000	0.02	.039	9.526
1954	White Bird	.285	.752	3.791	1.000	0.15	.248	5.377
5596	White Bird	.285	1.000	3.792	1.000	0.00	.000	23.579
863	White Bird	.284	.963	3.795	3.000	0.01	.037	10.553
1758	White Bird	.283	.995	3.805	1.000	0.00	.005	13.584
4187	White Bird	.283	.998	3.807	1.000	0.00	.002	15.971
1854	White Bird	.275	.711	3.879	1.000	0.17	.289	5.046
2757	White Bird	.272	1.000	3.902	1.000	0.00	.000	20.220
145	White Bird	.271	.685	3.911	1.000	0.18	.315	4.834
4306	White Bird	.269	.822	3.929	1.000	0.10	.178	6.354
3080	White Bird	.269	.998	3.935	1.000	0.00	.002	15.897
2035	White Bird	.268	.934	3.937	1.000	0.03	.047	9.287
2949	White Bird	.268	.897	3.938	1.000	0.03	.061	8.672
900	White Bird	.265	.997	3.965	1.000	0.00	.003	15.047
2327	White Bird	.257	.647	4.043	1.000	0.20	.352	4.628
3446	White Bird	.256	1.000	4.050	1.000	0.00	.000	20.341

Table E 6 - Casewise results from predictive discriminant function analysis of PXRF analysis of artifacts from Cooper's Ferry. Results are color coded by distance from group centroid (cont.).

Cat#	Predicted Group	Cond. Prob.	Post. Prob.	D^2	2nd Group	2nd Cond. Prob.	2nd Post. Prob.	2nd Group D^2
633	White Bird	.256	.847	4.053	1.000	0.05	.086	7.997
2898	White Bird	.244	.940	4.167	1.000	0.03	.057	9.128
1212	White Bird	.244	.999	4.172	3.000	0.00	.001	17.833
4503	White Bird	.234	.972	4.272	1.000	0.01	.028	10.707
4234	White Bird	.230	.824	4.312	1.000	0.06	.129	7.397
3929	White Bird	.228	.962	4.328	1.000	0.02	.037	10.187
1850	White Bird	.223	1.000	4.387	1.000	0.00	.000	25.160
827	White Bird	.222	.999	4.389	1.000	0.00	.001	17.876
412	White Bird	.222	1.000	4.394	3.000	0.00	.000	30.887
977	White Bird	.221	.995	4.409	1.000	0.00	.005	14.180
147	White Bird	.219	1.000	4.422	1.000	0.00	.000	20.545
926	White Bird	.219	.961	4.425	1.000	0.02	.038	10.239
541	White Bird	.215	1.000	4.472	3.000	0.00	.000	33.200
241	White Bird	.213	.773	4.488	1.000	0.10	.227	6.311
4248	White Bird	.210	.592	4.522	1.000	0.20	.408	4.636
4250	White Bird	.209	.749	4.541	1.000	0.10	.219	6.364
4490	White Bird	.207	.879	4.561	3.000	0.03	.121	8.755
877	White Bird	.206	1.000	4.566	1.000	0.00	.000	29.644
1802	White Bird	.206	.996	4.569	1.000	0.00	.004	15.070
632	White Bird	.192	1.000	4.741	1.000	0.00	.000	23.605
4424	White Bird	.189	.993	4.770	1.000	0.00	.006	14.327
2926	White Bird	.188	.989	4.785	1.000	0.00	.011	13.079
152	White Bird	.188	.610	4.789	3.000	0.11	.384	5.938
2775	White Bird	.186	1.000	4.816	3.000	0.00	.000	21.470
4091	White Bird	.183	1.000	4.855	1.000	0.00	.000	19.745
150	White Bird	.182	.871	4.867	1.000	0.03	.087	8.849
3407	White Bird	.179	1.000	4.907	3.000	0.00	.000	27.920
4237	White Bird	.176	.829	4.949	1.000	0.06	.171	7.478

Table E 6 - Casewise results from predictive discriminant function analysis of PXRF analysis of artifacts from Cooper's Ferry. Results are color coded by distance from group centroid (cont.).

Cat#	Predicted Group	Cond. Prob.	Post. Prob.	D^2	2nd Group	2nd Cond. Prob.	2nd Post. Prob.	2nd Group D^2
3276	White Bird	.176	.937	4.949	3.000	0.01	.063	10.588
5084	White Bird	.175	1.000	4.959	1.000	0.00	.000	26.733
898	White Bird	.175	.882	4.961	1.000	0.04	.118	8.346
3402	White Bird	.175	.942	4.963	1.000	0.02	.057	9.954
985	White Bird	.173	1.000	4.989	1.000	0.00	.000	25.132
2494	White Bird	.172	.991	4.998	1.000	0.00	.009	13.727
2921	White Bird	.172	.973	5.004	1.000	0.01	.027	11.542
211	White Bird	.170	.677	5.019	1.000	0.12	.323	5.864
385	White Bird	.170	.968	5.020	1.000	0.01	.032	11.182
851	White Bird	.166	.952	5.085	1.000	0.02	.048	10.437
821	White Bird	.165	.999	5.089	1.000	0.00	.001	17.990
4129	White Bird	.165	1.000	5.090	3.000	0.00	.000	23.743
2737	White Bird	.164	.998	5.105	1.000	0.00	.002	17.080
864	White Bird	.163	.951	5.129	1.000	0.01	.048	10.469
2230	White Bird	.162	.584	5.138	1.000	0.16	.415	5.187
528	White Bird	.162	.987	5.139	1.000	0.00	.013	13.157
3927	White Bird	.161	1.000	5.158	1.000	0.00	.000	22.643
454	White Bird	.159	.885	5.182	1.000	0.03	.115	8.637
388	White Bird	.157	1.000	5.206	1.000	0.00	.000	30.280
699	White Bird	.156	1.000	5.223	1.000	0.00	.000	23.118
1844	White Bird	.155	.747	5.239	1.000	0.08	.253	6.772
3839	White Bird	.154	.742	5.250	1.000	0.08	.258	6.727
2133	White Bird	.154	1.000	5.253	1.000	0.00	.000	21.296
643	White Bird	.153	.955	5.266	3.000	0.01	.044	11.625
829	White Bird	.150	.987	5.321	1.000	0.00	.013	13.338
592	White Bird	.150	.634	5.322	3.000	0.07	.317	6.933
418	White Bird	.147	.998	5.359	1.000	0.00	.002	17.623
857	White Bird	.143	1.000	5.420	1.000	0.00	.000	35.465

Table E 6 - Casewise results from predictive discriminant function analysis of PXRF analysis of artifacts from Cooper's Ferry. Results are color coded by distance from group centroid (cont.).

Cat#	Predicted Group	Cond. Prob.	Post. Prob.	D^2	2nd Group	2nd Cond. Prob.	2nd Post. Prob.	2nd Group D^2
249	White Bird	.142	.653	5.447	1.000	0.11	.346	6.084
4208	White Bird	.142	.994	5.451	1.000	0.00	.006	15.107
341	White Bird	.141	.960	5.454	1.000	0.01	.038	11.291
2448	White Bird	.141	.993	5.466	1.000	0.00	.007	14.706
833	White Bird	.138	.994	5.508	3.000	0.00	.006	15.828
2225	White Bird	.136	.818	5.551	1.000	0.05	.181	7.932
843	White Bird	.135	.521	5.566	1.000	0.16	.478	5.107
85	White Bird	.131	.879	5.628	1.000	0.03	.121	8.956
4314	White Bird	.129	1.000	5.672	3.000	0.00	.000	37.137
2169	White Bird	.125	.730	5.732	1.000	0.07	.269	7.095
2869	White Bird	.125	.984	5.737	1.000	0.00	.016	13.349
2991	White Bird	.123	.796	5.768	1.000	0.05	.201	7.890
1912	White Bird	.123	.842	5.770	1.000	0.04	.158	8.482
465	White Bird	.123	.701	5.779	1.000	0.08	.299	6.849
3834	White Bird	.123	.812	5.786	1.000	0.04	.187	8.088
125	White Bird	.122	.977	5.793	1.000	0.01	.023	12.686
2576	White Bird	.121	.997	5.823	1.000	0.00	.003	17.130
4260	White Bird	.120	.640	5.841	1.000	0.10	.359	6.365
1805	White Bird	.119	.928	5.853	1.000	0.02	.072	10.331
179	White Bird	.118	.996	5.878	1.000	0.00	.004	16.077
1688	White Bird	.113	.995	5.980	1.000	0.00	.005	16.014
3781	White Bird	.112	.991	5.986	1.000	0.00	.009	14.862
1800	White Bird	.108	.713	6.069	3.000	0.04	.268	8.249
636	White Bird	.107	.999	6.090	1.000	0.00	.001	18.862
1122	White Bird	.107	1.000	6.091	1.000	0.00	.000	21.830
627	White Bird	.107	.995	6.093	1.000	0.00	.005	16.121
908	White Bird	.106	.936	6.113	1.000	0.01	.063	10.878
3765	White Bird	.105	.842	6.146	1.000	0.03	.157	8.874

Table E 6 - Casewise results from predictive discriminant function analysis of PXRF analysis of artifacts from Cooper's Ferry. Results are color coded by distance from group centroid (cont.).

Cat#	Predicted Group	Cond. Prob.	Post. Prob.	D^2	2nd Group	2nd Cond. Prob.	2nd Post. Prob.	2nd Group D^2
3908	White Bird	.105	.498	6.148	1.000	0.12	.424	5.836
959	White Bird	.104	.982	6.169	1.000	0.00	.018	13.505
3381	White Bird	.100	.923	6.260	1.000	0.01	.074	10.686
4786	White Bird	.094	.998	6.404	1.000	0.00	.002	18.313
2856	White Bird	.092	.985	6.452	3.000	0.00	.015	15.078
936	White Bird	.090	.927	6.491	1.000	0.01	.071	10.986
3456	White Bird	.089	.859	6.515	1.000	0.02	.141	9.491
5346	White Bird	.089	.988	6.520	1.000	0.00	.012	14.709
3212	White Bird	.088	.536	6.533	1.000	0.10	.461	6.205
4037	White Bird	.088	1.000	6.555	1.000	0.00	.000	30.970
2727	White Bird	.086	.898	6.583	1.000	0.01	.063	11.255
635	White Bird	.086	.967	6.589	1.000	0.01	.033	12.683
259	White Bird	.083	1.000	6.685	3.000	0.00	.000	32.632
771	White Bird	.082	.992	6.702	3.000	0.00	.008	16.672
3894	White Bird	.080	.754	6.750	1.000	0.04	.245	8.363
1189	White Bird	.080	1.000	6.770	1.000	0.00	.000	26.389
2328	White Bird	.079	.958	6.773	3.000	0.00	.025	14.295
3383	White Bird	.079	1.000	6.785	1.000	0.00	.000	27.959
2241	White Bird	.078	.915	6.812	1.000	0.01	.085	10.939
580	White Bird	.078	.983	6.830	1.000	0.00	.017	14.295
2610	White Bird	.077	.737	6.850	1.000	0.04	.255	8.337
932	White Bird	.075	.872	6.908	1.000	0.02	.128	10.119
700	White Bird	.073	.908	6.956	1.000	0.01	.092	10.904
950	White Bird	.073	.888	6.963	1.000	0.01	.112	10.468
918	White Bird	.073	.999	6.978	1.000	0.00	.001	21.460
132	White Bird	.072	.937	6.984	1.000	0.01	.063	11.756
338	White Bird	.070	.996	7.049	1.000	0.00	.004	17.619
4331	White Bird	.070	.897	7.060	1.000	0.01	.102	10.776

Table E 6 - Casewise results from predictive discriminant function analysis of PXRF analysis of artifacts from Cooper's Ferry. Results are color coded by distance from group centroid (cont.).

Cat#	Predicted Group	Cond. Prob.	Post. Prob.	D^2	2nd Group	2nd Cond. Prob.	2nd Post. Prob.	2nd Group D^2
919	White Bird	.069	.970	7.107	1.000	0.00	.030	13.408
2263	White Bird	.068	.891	7.123	1.000	0.01	.107	10.721
225	White Bird	.068	1.000	7.139	1.000	0.00	.000	29.499
2725	White Bird	.066	.993	7.190	1.000	0.00	.006	16.633
436	White Bird	.066	.999	7.206	1.000	0.00	.001	19.612
4329	White Bird	.065	1.000	7.213	1.000	0.00	.000	29.758
506	White Bird	.065	.657	7.215	3.000	0.02	.188	9.943
220	White Bird	.065	.991	7.239	1.000	0.00	.009	15.902
4192	White Bird	.064	1.000	7.252	1.000	0.00	.000	25.626
4244	White Bird	.064	.930	7.268	1.000	0.01	.070	11.816
3055	White Bird	.060	.995	7.425	1.000	0.00	.005	17.479
891	White Bird	.059	.988	7.430	1.000	0.00	.012	15.699
931	White Bird	.059	.988	7.438	1.000	0.00	.012	15.630
2702	White Bird	.058	.998	7.498	1.000	0.00	.001	20.694
1807	White Bird	.058	.949	7.501	1.000	0.01	.051	12.709
5027	White Bird	.056	.955	7.543	1.000	0.00	.045	13.024
1181	White Bird	.056	.973	7.573	1.000	0.00	.027	14.096
98	White Bird	.056	.776	7.577	1.000	0.02	.222	9.446
2036	White Bird	.053	.799	7.705	1.000	0.02	.192	9.920
221	White Bird	.049	.665	7.857	1.000	0.03	.331	8.620
3413	White Bird	.048	.999	7.903	1.000	0.00	.001	20.596
4277	White Bird	.047	.835	7.943	1.000	0.01	.164	10.561
2262	White Bird	.046	1.000	7.995	1.000	0.00	.000	41.724
660	White Bird	.046	.995	8.018	1.000	0.00	.005	17.990
510	White Bird	.045	.802	8.064	1	0.02	.198	10.224
4780	White Bird	.044	.981	8.079	1	0.00	.019	15.344
2354	White Bird	.043	.993	8.130	1	0.00	.007	17.459
4777	White Bird	.043	1.000	8.147	1	0.00	.000	25.575

Table E 6 - Casewise results from predictive discriminant function analysis of PXRF analysis of artifacts from Cooper's Ferry. Results are color coded by distance from group centroid (cont.).

Cat#	Predicted Group	Cond. Prob.	Post. Prob.	D^2	2nd Group	2nd Cond. Prob.	2nd Post. Prob.	2nd Group D^2
1107	White Bird	.042	1.000	8.197	1	0.00	.000	31.507
224	White Bird	.041	.996	8.278	1	0.00	.004	18.647
4137	White Bird	.040	1.000	8.325	1	0.00	.000	34.938
3262	White Bird	.039	.796	8.350	1	0.02	.204	10.446
2203	White Bird	.039	.899	8.371	1	0.01	.099	12.156
2266	White Bird	.037	1.000	8.507	1	0.00	.000	32.165
3472	White Bird	.035	.995	8.578	1	0.00	.005	18.575
4074	White Bird	.034	.935	8.639	1	0.00	.065	13.353
269	White Bird	.034	.999	8.661	1	0.00	.001	22.183
148	White Bird	.034	.627	8.702	1	0.03	.371	9.118
5098	White Bird	.033	.999	8.732	1	0.00	.001	22.567
3598	White Bird	.033	.975	8.733	1	0.00	.025	15.398
1182	White Bird	.032	.993	8.785	1	0.00	.007	18.103
213	White Bird	.031	1.000	8.861	3	0.00	.000	31.827
4617	White Bird	.030	.987	8.956	1	0.00	.013	17.038
4256	White Bird	.027	1.000	9.208	1	0.00	.000	29.497
856	White Bird	.027	.999	9.213	1	0.00	.001	22.861
312	White Bird	.026	1.000	9.222	1	0.00	.000	25.579
4319	White Bird	.026	.941	9.295	1	0.00	.052	14.446
3191	White Bird	.025	.913	9.347	1	0.00	.087	13.412
278	White Bird	.025	1.000	9.371	1	0.00	.000	25.102
939	White Bird	.025	.998	9.372	1	0.00	.002	21.206
2935	White Bird	.024	.971	9.466	1	0.00	.029	15.869
481	White Bird	.022	.994	9.645	1	0.00	.006	19.284
1342	White Bird	.022	.692	9.650	1	0.01	.307	10.642
859	White Bird	.022	1.000	9.670	1	0.00	.000	33.956
628	White Bird	.020	.981	9.876	1	0.00	.019	17.132
4045	White Bird	.019	.993	9.977	1	0.00	.007	19.324

Table E 6 - Casewise results from predictive discriminant function analysis of PXRF analysis of artifacts from Cooper's Ferry. Results are color coded by distance from group centroid (cont.).

Cat#	Predicted Group	Cond. Prob.	Post. Prob.	D^2	2nd Group	2nd Cond. Prob.	2nd Post. Prob.	2nd Group D^2
5347	White Bird	.018	.569	10.048	1	0.02	.431	9.971
497	White Bird	.016	.844	10.263	1	0.00	.153	13.049
893	White Bird	.016	.452	10.339	1	0.01	.285	10.631
852	White Bird	.015	.996	10.401	2	0.00	.003	21.037
2311	White Bird	.015	1.000	10.525	3	0.00	.000	38.298
3542	White Bird	.015	1.000	10.538	1	0.00	.000	43.649
560	White Bird	.015	.992	10.539	3	0.00	.007	20.542
2281	White Bird	.014	.520	10.577	1	0.02	.431	10.317
172	White Bird	.014	.598	10.630	1	0.01	.401	10.798
1221	White Bird	.014	.735	10.681	1	0.01	.263	12.106
2862	White Bird	.013	.985	10.703	3	0.00	.015	19.265
121	White Bird	.013	1.000	10.712	1	0.00	.000	25.958
3541	White Bird	.013	1.000	10.812	1	0.00	.000	30.926
372	White Bird	.012	.999	10.923	1	0.00	.001	25.469
552	White Bird	.012	.997	11.023	1	0.00	.003	21.816
5076	White Bird	.011	.843	11.076	1	0.00	.156	13.813
3965	White Bird	.011	.665	11.112	1	0.01	.326	11.908
820	White Bird	.011	.744	11.121	1	0.01	.256	12.620
2954	White Bird	.011	.944	11.163	1	0.00	.038	16.931
2851	White Bird	.011	.996	11.192	3	0.00	.004	22.369
4441	White Bird	.010	.630	11.263	1	0.01	.370	11.692
4041	White Bird	.010	.982	11.404	1	0.00	.016	18.999
3167	White Bird	.009	1.000	11.519	1	0.00	.000	34.071
1597	White Bird	.009	1.000	11.556	1	0.00	.000	42.793
3818	White Bird	.008	1.000	11.705	1	0.00	.000	28.585
837	White Bird	.008	.997	11.814	1	0.00	.003	22.695
951	White Bird	.008	.790	11.919	2	0.00	.139	14.617
3108	White Bird	.006	1.000	12.344	1	0.00	.000	46.782

Table E 6 - Casewise results from predictive discriminant function analysis of PXRF analysis of artifacts from Cooper's Ferry. Results are color coded by distance from group centroid (cont.).

Cat#	Predicted Group	Cond. Prob.	Post. Prob.	D^2	2nd Group	2nd Cond. Prob.	2nd Post. Prob.	2nd Group D^2
5293	White Bird	.006	.998	12.380	1	0.00	.002	24.218
1148	White Bird	.006	.925	12.401	1	0.00	.075	16.794
928	White Bird	.006	.929	12.401	1	0.00	.051	17.570
5091	White Bird	.006	.999	12.406	1	0.00	.001	25.392
3998	White Bird	.006	.998	12.480	1	0.00	.002	24.007
1281	White Bird	.006	.996	12.485	1	0.00	.004	22.765
453	White Bird	.006	1.000	12.532	1	0.00	.000	32.143
3056	White Bird	.006	.916	12.574	1	0.00	.084	16.714
5229	White Bird	.006	.727	12.604	1	0.00	.268	13.970
2953	White Bird	.005	.928	12.830	1	0.00	.072	17.316
3143	White Bird	.005	1.000	12.853	1	0.00	.000	37.008
634	White Bird	.005	.999	12.861	1	0.00	.001	26.253
4418	White Bird	.005	.866	12.889	1	0.00	.134	15.988
948	White Bird	.005	.994	12.952	1	0.00	.006	22.575
302	White Bird	.005	1.000	13.011	1	0.00	.000	31.500
223	White Bird	.004	.985	13.343	1	0.00	.015	21.117
1127	White Bird	.004	1.000	13.409	1	0.00	.000	28.506
2126	White Bird	.004	.797	13.474	1	0.00	.202	15.583
3835	White Bird	.003	.999	13.615	1	0.00	.001	26.494
2514	White Bird	.003	1.000	14.214	3	0.00	.000	45.849
187	White Bird	.003	1.000	14.292	1	0.00	.000	31.714
3466	White Bird	.002	.842	14.421	1	0.00	.158	17.138
1675	White Bird	.002	1.000	14.593	1	0.00	.000	36.975
949	White Bird	.002	1.000	14.873	1	0.00	.000	45.707
5272	White Bird	.002	.962	15.127	1	0.00	.038	20.979
5072	White Bird	.002	.995	15.337	1	0.00	.005	25.368
4221	White Bird	.001	.582	15.815	1	0.00	.407	15.896
129	White Bird	.001	1.000	15.857	1	0.00	.000	43.547

Figure E 6 - Casewise results from predictive discriminant function analysis of PXRF analysis of artifacts from Cooper's Ferry. Results are color coded by distance from group centroid (cont.).

Cat#	Predicted Group	Cond. Prob.	Post. Prob.	D^2	2nd Group	2nd Cond. Prob.	2nd Post. Prob.	2nd Group D^2
3468	White Bird	.001	.560	16.209	1	0.00	.433	16.093
228	White Bird	.001	.969	16.833	1	0.00	.031	23.086
151	White Bird	.001	.612	17.007	1	0.00	.388	17.288
5305	White Bird	.001	.765	17.017	1	0.00	.235	18.740
295	White Bird	.001	1.000	17.141	1	0.00	.000	38.211
3448	White Bird	.001	.968	17.248	1	0.00	.032	23.433
1847	White Bird	.001	1.000	17.509	1	0.00	.000	39.690
5114	White Bird	.001	.959	17.687	1	0.00	.040	23.401
1399	White Bird	.000	.568	17.765	1	0.00	.337	18.180
1021	White Bird	.000	.535	17.793	1	0.00	.465	17.441
5295	White Bird	.000	.994	18.030	1	0.00	.006	27.707
4078	White Bird	.000	1.000	18.419	1	0.00	.000	33.362
796	White Bird	.000	.900	18.476	1	0.00	.100	22.238
131	White Bird	.000	.988	18.618	1	0.00	.012	26.755
237	White Bird	.000	1.000	18.846	1	0.00	.000	34.969
5285	White Bird	.000	.886	18.858	1	0.00	.113	22.335
243	White Bird	.000	.920	18.989	1	0.00	.080	23.238
326	White Bird	.000	.936	19.319	1	0.00	.064	24.066
2909	White Bird	.000	.593	19.451	1	0.00	.398	19.615
927	White Bird	.000	1.000	19.538	1	0.00	.000	47.869
2193	White Bird	.000	1.000	19.795	1	0.00	.000	37.882
2039	White Bird	.000	1.000	20.240	3	0.00	.000	59.705
4535	White Bird	.000	1.000	20.521	1	0.00	.000	38.471
4603	White Bird	.000	.553	20.760	1	0.00	.446	20.557
5153	White Bird	.000	.848	20.979	1	0.00	.151	23.792
5089	White Bird	.000	.999	21.086	1	0.00	.001	34.889
3812	White Bird	.000	.484	21.395	1	0.00	.460	20.865
1695	White Bird	.000	1.000	21.418	1	0.00	.000	37.101

Table E 6 - Casewise results from predictive discriminant function analysis of PXRF analysis of artifacts from Cooper's Ferry. Results are color coded by distance from group centroid (cont.).

Cat#	Predicted Group	Cond. Prob.	Post. Prob.	D^2	2nd Group	2nd Cond. Prob.	2nd Post. Prob.	2nd Group D^2
113	White Bird	.000	.999	21.538	1	0.00	.001	33.961
1373	White Bird	.000	1.000	21.568	1	0.00	.000	36.217
1803	White Bird	.000	.991	21.790	1	0.00	.009	30.640
328	White Bird	.000	.726	22.088	2	0.00	.274	23.259
626	White Bird	.000	.850	22.300	1	0.00	.150	25.142
903	White Bird	.000	.948	22.323	1	0.00	.050	27.594
5063	White Bird	.000	.859	22.361	1	0.00	.140	25.352
304	White Bird	.000	.901	22.683	1	0.00	.063	27.372
4644	White Bird	.000	1.000	22.692	3	0.00	.000	59.315
108	White Bird	.000	1.000	23.048	1	0.00	.000	46.586
2285	White Bird	.000	.729	23.198	1	0.00	.270	24.548
4211	White Bird	.000	.573	23.220	1	0.00	.426	23.179
294	White Bird	.000	1.000	23.475	1	0.00	.000	45.776
3782	White Bird	.000	1.000	24.396	1	0.00	.000	41.659
1101	White Bird	.000	.997	24.517	1	0.00	.003	35.399
2071	White Bird	.000	.636	24.726	2	0.00	.235	25.942
3874	White Bird	.000	.861	25.033	1	0.00	.128	28.213
4033	White Bird	.000	.856	25.111	1	0.00	.144	28.046
123	White Bird	.000	.624	25.551	1	0.00	.358	26.025
4212	White Bird	.000	.689	25.889	1	0.00	.270	27.131
826	White Bird	.000	.940	26.492	1	0.00	.031	32.705
573	White Bird	.000	.848	27.347	1	0.00	.152	30.154
4085	White Bird	.000	1.000	28.132	1	0.00	.000	42.971
71	White Bird	.000	.755	28.521	1	0.00	.245	30.138
256	White Bird	.000	.986	33.427	1	0.00	.014	41.371
2015	White Bird	.000	.754	34.060	1	0.00	.246	35.669
5094	White Bird	.000	.636	35.142	1	0.00	.362	35.638
1860	White Bird	.000	.549	35.543	1	0.00	.402	35.532
5701	White Bird	.000	.991	38.861	1	0.00	.009	47.625

Table E 6 - Casewise results from predictive discriminant function analysis of PXRF analysis of artifacts from Cooper's Ferry (cont.)

Appendix F: PXRF Principal Components of Geologic Sources

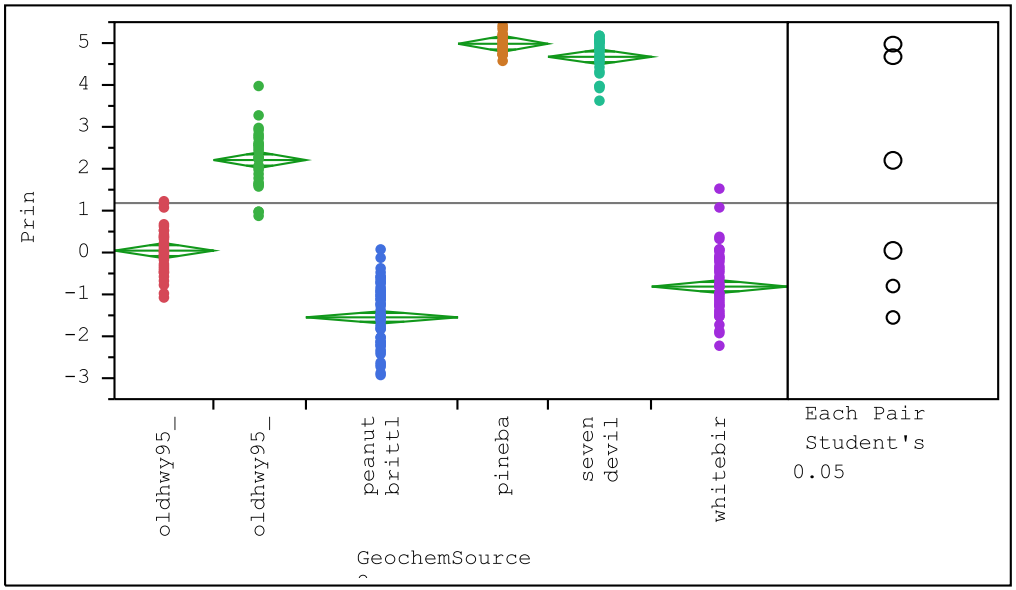

One-way ANOVA

Summary of Fit

Rsquare	0.948631
Adj Rsquare	0.947733
Root Mean Square Error	0.605422
Mean of Response	1.18069
Observations (or Sum Wgts)	292

Table F 1 – Principal component one by LSRC geologic chert sources examined via PXRF.

Analysis of Variance

Source	DF	Sum of Squares	Mean Square	F Ratio	Prob > F
Geologic Source	5	1935.8708	387.174	1056.307	<.0001*
Error	286	104.8292	0.367		
C. Total	291	2040.6999			

Means for One-way ANOVA

Level	Number	Mean	Std Error	Lower 95%	Upper 95%
oldhwy95_1	43	0.0451	0.09233	-0.137	0.227
oldhwy95_2	40	2.2083	0.09573	2.020	2.397
peanut brittle	66	-1.5470	0.07452	-1.694	-1.400
Pine Bar	39	4.9835	0.09695	4.793	5.174
Seven Devils	45	4.6719	0.09025	4.494	4.850
White Bird	59	-0.8136	0.07882	-0.969	-0.658

Std Error uses a pooled estimate of error variance

Means Comparisons

Comparisons for each pair using Student's t

Confidence Quantile

t	Alpha
1.96829	0.05

LSD Threshold Matrix

Abs(Dif)-LSD	Pine Bar	Seven Devils	oldhwy95_2	oldhwy95_1	White Bird	peanut brittle
Pine Bar	-0.2699	0.0509	2.5070	4.6749	5.5512	6.2898
Seven Devils	0.0509	-0.2512	2.2046	4.3727	5.2497	5.9885
oldhwy95_2	2.5070	2.2046	-0.2665	1.9015	2.7779	3.5165
oldhwy95_1	4.6749	4.3727	1.9015	-0.2570	0.6197	1.3585
White Bird	5.5512	5.2497	2.7779	0.6197	-0.2194	0.5199
peanut brittle	6.2898	5.9885	3.5165	1.3585	0.5199	-0.2074

Positive values show pairs of means that are significantly different.

Table F 1 – Principal component one by LSRC geologic chert sources examined via PXRF (cont.).

Connecting Letters Report

Level							Mean
Pine Bar	A						4.983487
Seven Devils		B					4.671907
oldhwy95_2			C				2.208322
oldhwy95_1				D			0.045089
White Bird					E		-0.813596
peanut brittle						F	-1.546968

Levels not connected by same letter are significantly different.

Ordered Differences Report

Level	- Level	Difference	Std Err Dif	Lower CL	Upper CL	p-Value
Pine Bar	peanut brittle	6.530455	0.1222780	6.289776	6.771134	<.0001*
Seven Devils	peanut brittle	6.218875	0.1170419	5.988502	6.449248	<.0001*
Pine Bar	White Bird	5.797082	0.1249432	5.551158	6.043007	<.0001*
Seven Devils	White Bird	5.485502	0.1198236	5.249654	5.721350	<.0001*
Pine Bar	oldhwy95_1	4.938398	0.1338747	4.674893	5.201902	<.0001*
Seven Devils	oldhwy95_1	4.626818	0.1291097	4.372692	4.880943	<.0001*
oldhwy95_2	peanut brittle	3.755290	0.1213135	3.516510	3.994071	<.0001*
oldhwy95_2	White Bird	3.021917	0.1239994	2.777850	3.265985	<.0001*
Pine Bar	oldhwy95_2	2.775165	0.1362415	2.507002	3.043328	<.0001*
Seven Devils	oldhwy95_2	2.463585	0.1315622	2.204632	2.722538	<.0001*
oldhwy95_2	oldhwy95_1	2.163233	0.1329943	1.901461	2.425004	<.0001*
oldhwy95_1	peanut brittle	1.592058	0.1186493	1.358521	1.825594	<.0001*
oldhwy95_1	White Bird	0.858685	0.1213942	0.619745	1.097624	<.0001*
White Bird	peanut brittle	0.733373	0.1084714	0.519869	0.946876	<.0001*
Pine Bar	Seven Devils	0.311580	0.1324522	0.050875	0.572285	0.0193*

Table F 1 – Principal component one by LSRC geologic chert sources examined via PXRF (cont.).

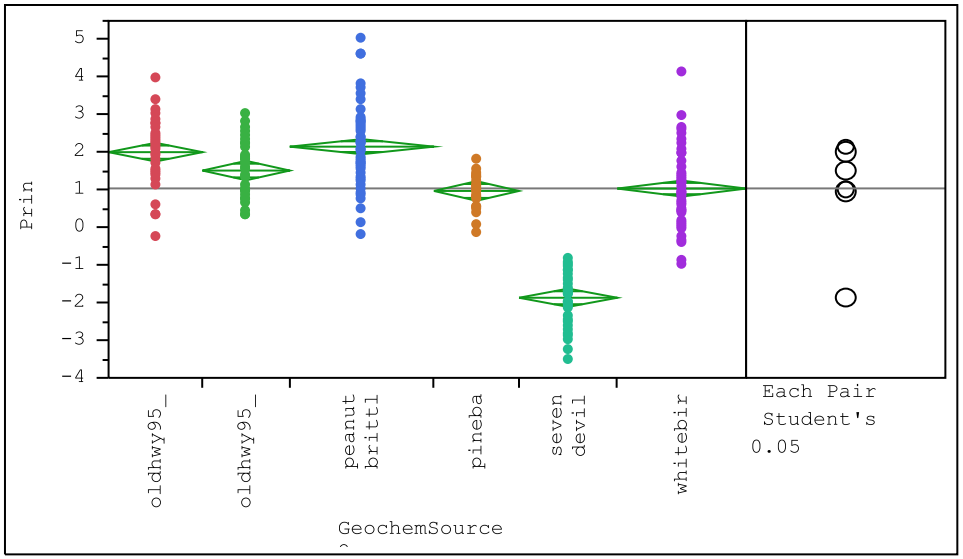

One-way ANOVA

Summary of Fit

Rsquare	0.722244
Adj Rsquare	0.717388
Root Mean Square Error	0.829451
Mean of Response	1.041397
Observations (or Sum Wgts)	292

Table F 2 – Principal component two by LSRC geologic chert sources examined via PXRF.

Analysis of Variance

Source	DF	Sum of Squares	Mean Square	F Ratio	Prob > F
Geologic Source	5	511.64364	102.329	148.7361	<.0001*
Error	286	196.76470	0.688		
C. Total	291	708.40834			

Means for One-way ANOVA

Level	Number	Mean	Std Error	Lower 95%	Upper 95%
oldhwy95_1	43	2.0061	0.12649	1.757	2.255
oldhwy95_2	40	1.5165	0.13115	1.258	1.775
peanut brittle	66	2.1524	0.10210	1.951	2.353
Pine Bar	39	0.9738	0.13282	0.712	1.235
Seven Devils	45	-1.8682	0.12365	-2.112	-1.625
White Bird	59	1.0373	0.10799	0.825	1.250

Std Error uses a pooled estimate of error variance

Means Comparisons

Comparisons for each pair using Student's t

Confidence Quantile

t	Alpha
1.96829	0.05

LSD Threshold Matrix

Abs(Dif)-LSD	peanut brittle	oldhwy95_1	oldhwy95_2	White Bird	Pine Bar	Seven Devils
peanut brittle	-0.2842	-0.1737	0.3087	0.8226	0.8489	3.7049
oldhwy95_1	-0.1737	-0.3521	0.1309	0.6415	0.6713	3.5261
oldhwy95_2	0.3087	0.1309	-0.3651	0.1449	0.1754	3.0299
White Bird	0.8226	0.6415	0.1449	-0.3006	-0.2735	2.5823
Pine Bar	0.8489	0.6713	0.1754	-0.2735	-0.3697	2.4848
Seven Devils	3.7049	3.5261	3.0299	2.5823	2.4848	-0.3442

Table F 2 – Principal component two by LSRC geologic chert sources examined via PXRF (cont.).

Connecting Letters Report

Level					Mean
peanut brittle	A				2.152372
oldhwy95_1	A				2.006112
oldhwy95_2		B			1.516535
White Bird			C		1.037251
Pine Bar			C		0.973777
Seven Devils				D	-1.868179

Levels not connected by same letter are significantly different.

Ordered Differences Report

Level	- Level	Difference	Std Err Dif	Lower CL	Upper CL	p-Value
peanut brittle	Seven Devils	4.020551	0.1603518	3.70493	4.336171	<.0001*
oldhwy95_1	Seven Devils	3.874291	0.1768852	3.52613	4.222453	<.0001*
oldhwy95_2	Seven Devils	3.384714	0.1802452	3.02994	3.739490	<.0001*
White Bird	Seven Devils	2.905431	0.1641629	2.58231	3.228551	<.0001*
Pine Bar	Seven Devils	2.841956	0.1814645	2.48478	3.199131	<.0001*
peanut brittle	Pine Bar	1.178595	0.1675255	0.84886	1.508334	<.0001*
peanut brittle	White Bird	1.115121	0.1486099	0.82261	1.407628	<.0001*
oldhwy95_1	Pine Bar	1.032335	0.1834134	0.67132	1.393346	<.0001*
oldhwy95_1	White Bird	0.968861	0.1663146	0.64150	1.296217	<.0001*
peanut brittle	oldhwy95_2	0.635837	0.1662040	0.30870	0.962975	0.0002*
oldhwy95_2	Pine Bar	0.542758	0.1866559	0.17536	0.910152	0.0039*
oldhwy95_1	oldhwy95_2	0.489577	0.1822071	0.13094	0.848214	0.0076*
oldhwy95_2	White Bird	0.479284	0.1698839	0.14490	0.813665	0.0051*
peanut brittle	oldhwy95_1	0.146260	0.1625540	-0.17369	0.466214	0.3690
White Bird	Pine Bar	0.063474	0.1711770	-0.27345	0.400401	0.7111

Figure F 2 – Principal component two by LSRC geologic chert sources examined via PXRF (cont.).

Appendix G: Geologic Source Photographs

Below are photographs of samples of the geologic chert sources tested in this study.

Old Highway 95_1 Geologic Samples

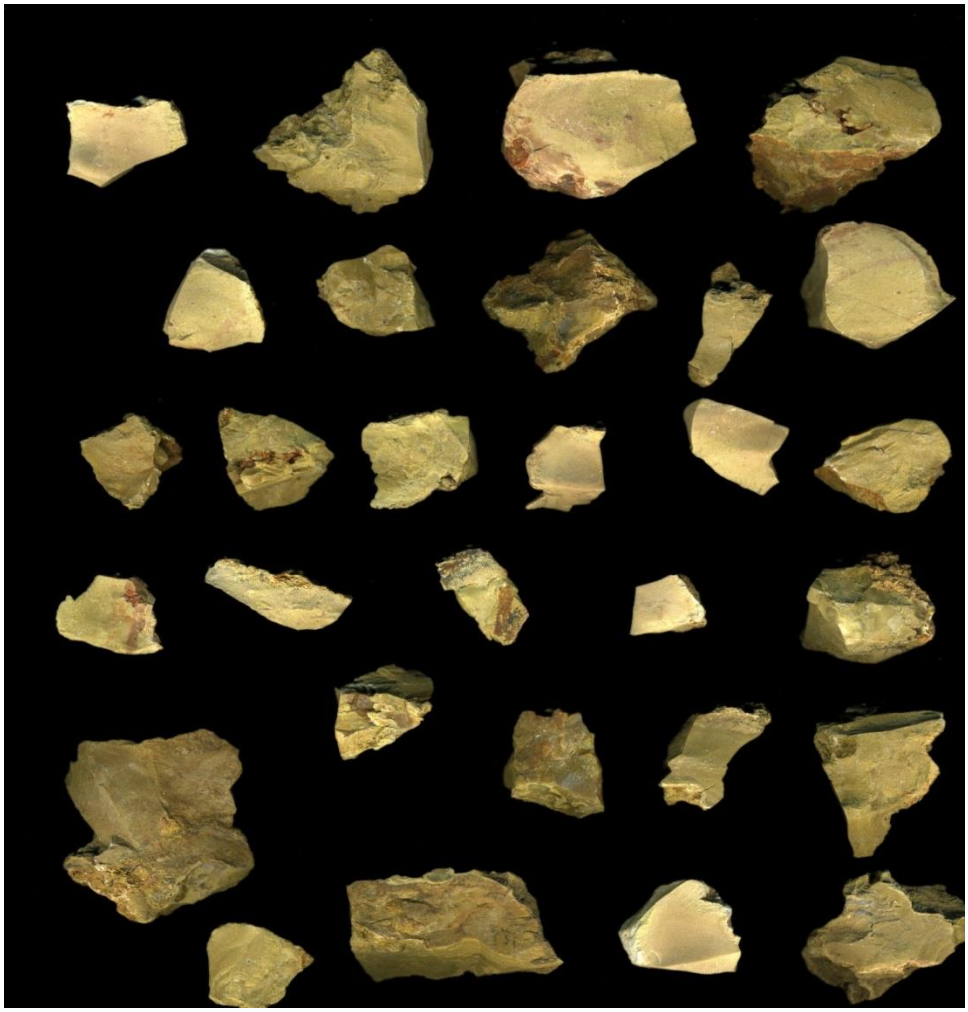

Figure G 1 - Old Highway95_1 geologic chert samples.

Old Highway 95_2 Geologic Samples

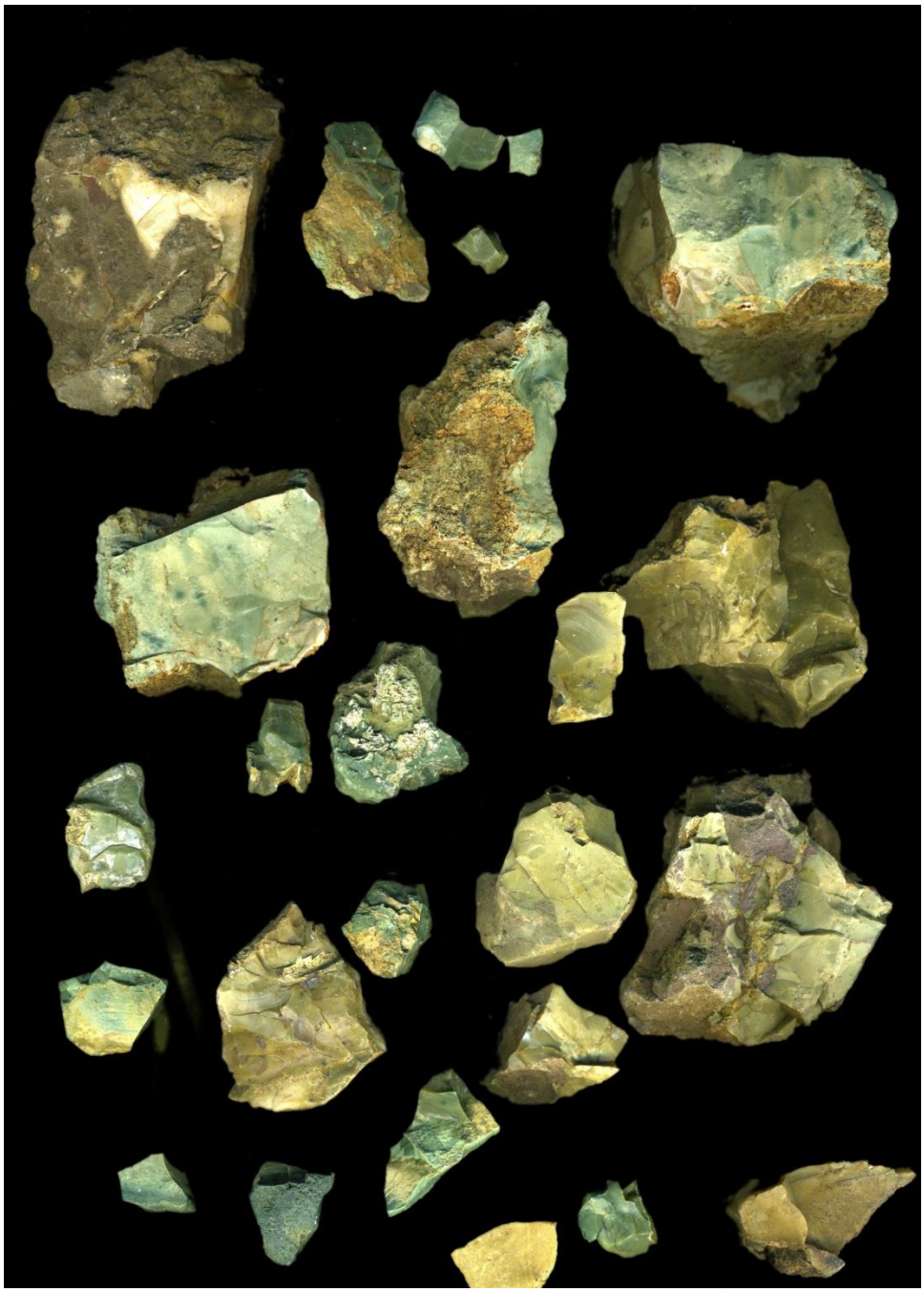

Figure G 2 - Old Highway 95_2 geologic chert samples.

Peanut Brittle Geologic Samples

Figure G 3 - Peanut Brittle geologic chert samples.

Pine Bar Geologic Samples

Figure G 4 - Pine Bar geologic chert samples.

Seven Devils Geologic Samples

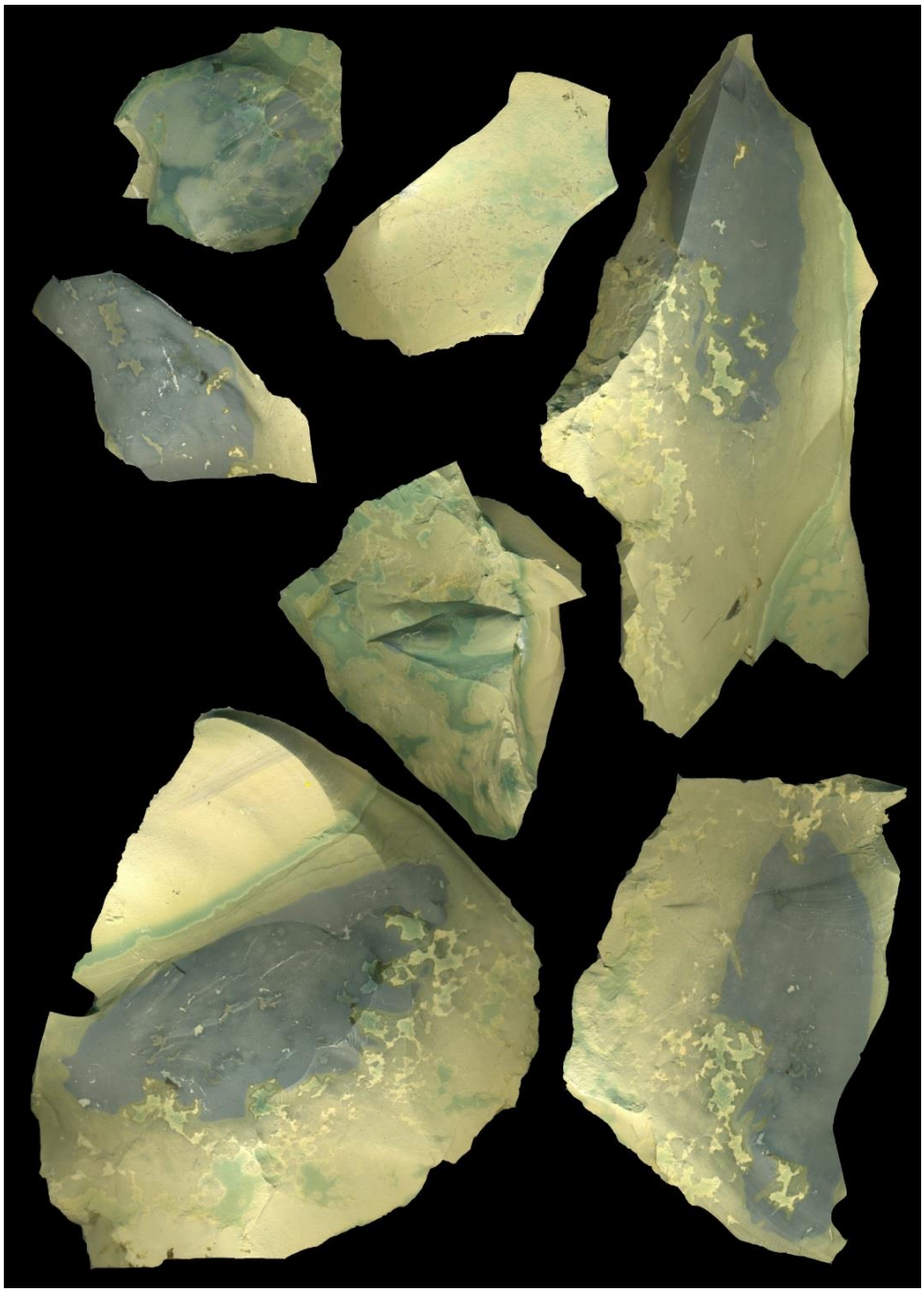

Figure G 5 - Seven Devils geologic chert samples.

White Bird Geologic Samples

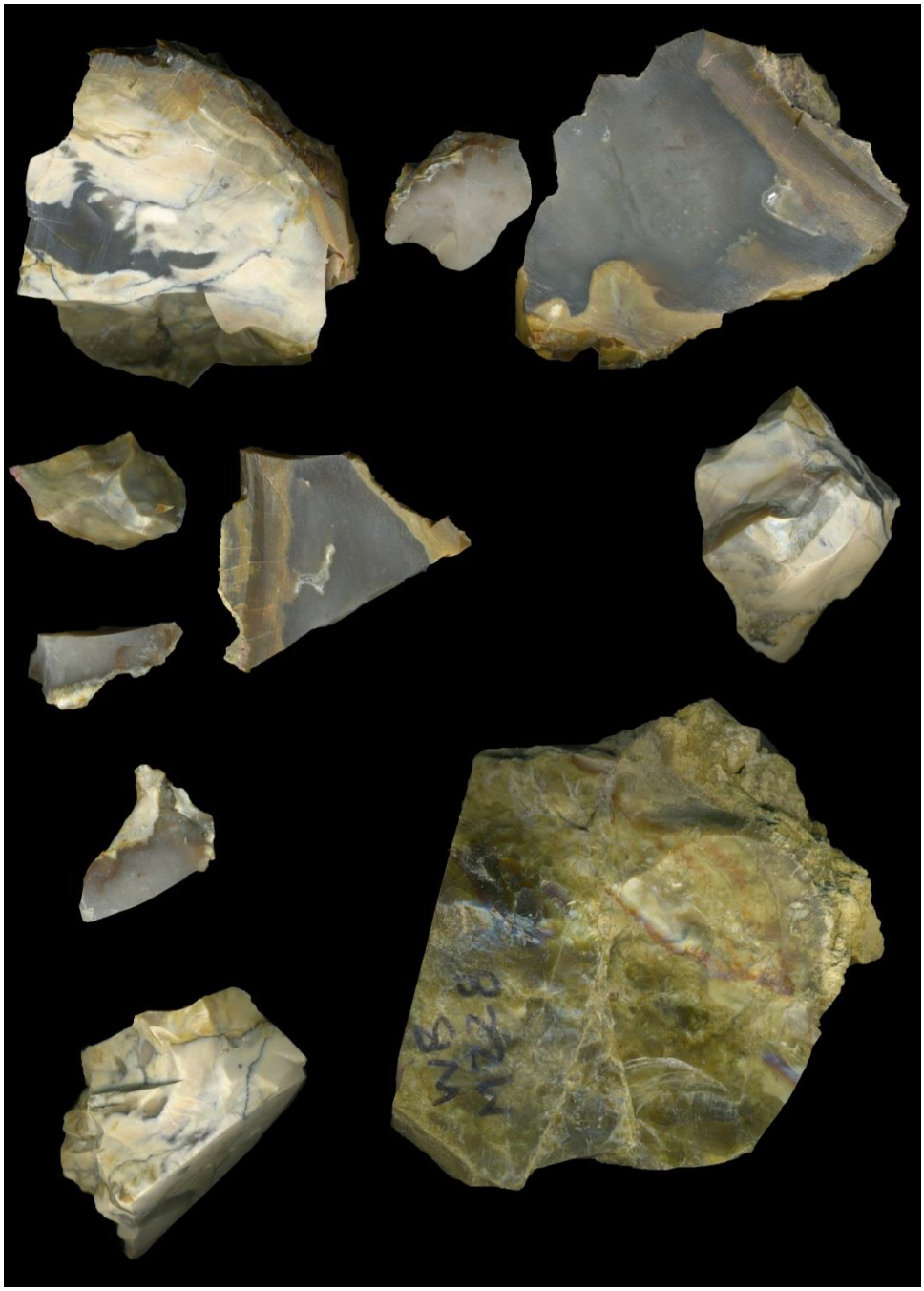

Figure G 6 - White Bird geologic chert samples.

Appendix H: Artifact Photographs

Old Highway 95_1 Artifacts

Below are listed photographs that were within one standard deviation of the Old Highway 95_1 chert source using discriminant analysis. Numbers below artifacts refer to assigned catalog number.

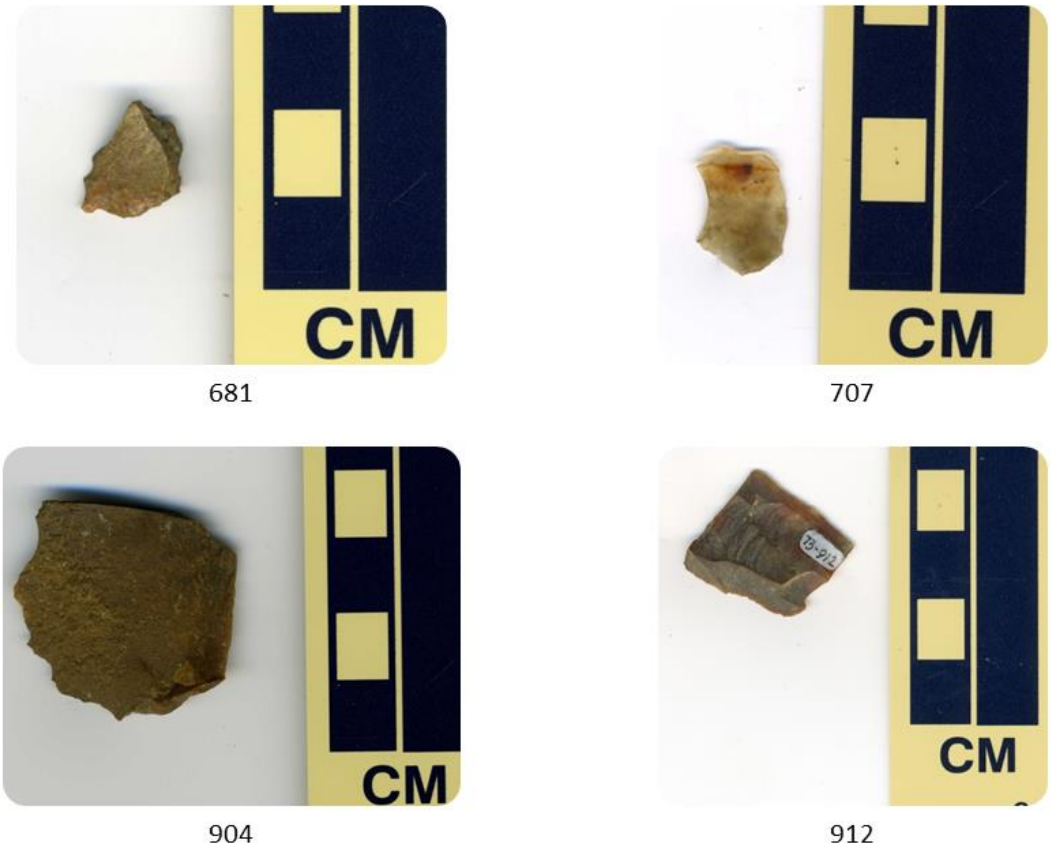

Figure H 1 - Artifacts within one standard deviation of the Old Highway 95_1 chert source.

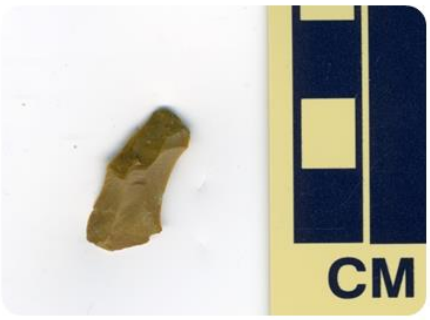

1230

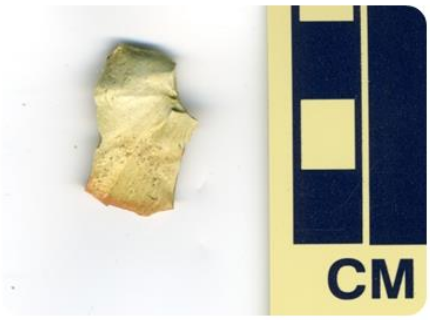

1253

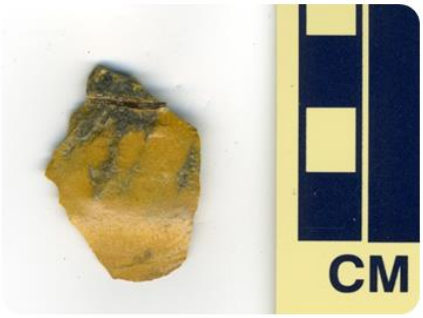

1831

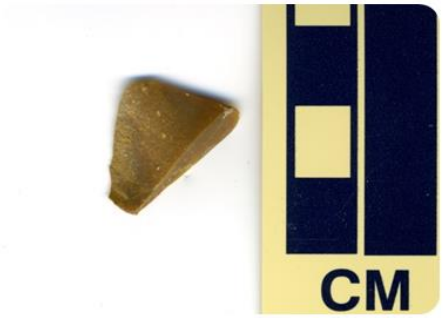

2028

Figure H 1 - Artifacts within one standard deviation of the Old Highway 95_1 chert source (cont.).

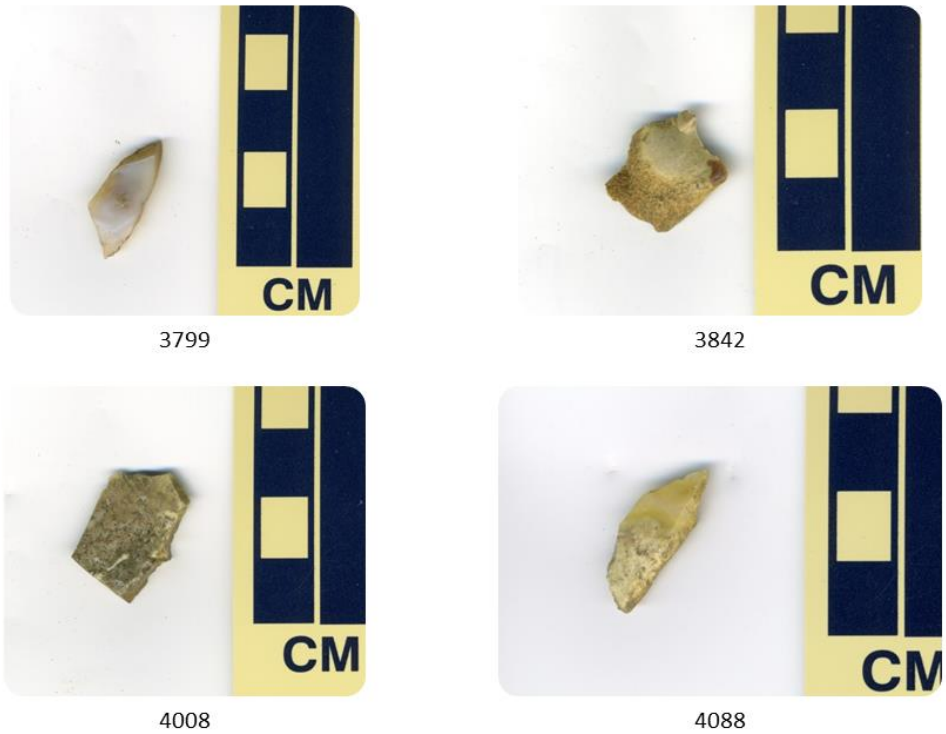

Figure H 1 - Artifacts within one standard deviation of the Old Highway 95_1 chert source (cont.).

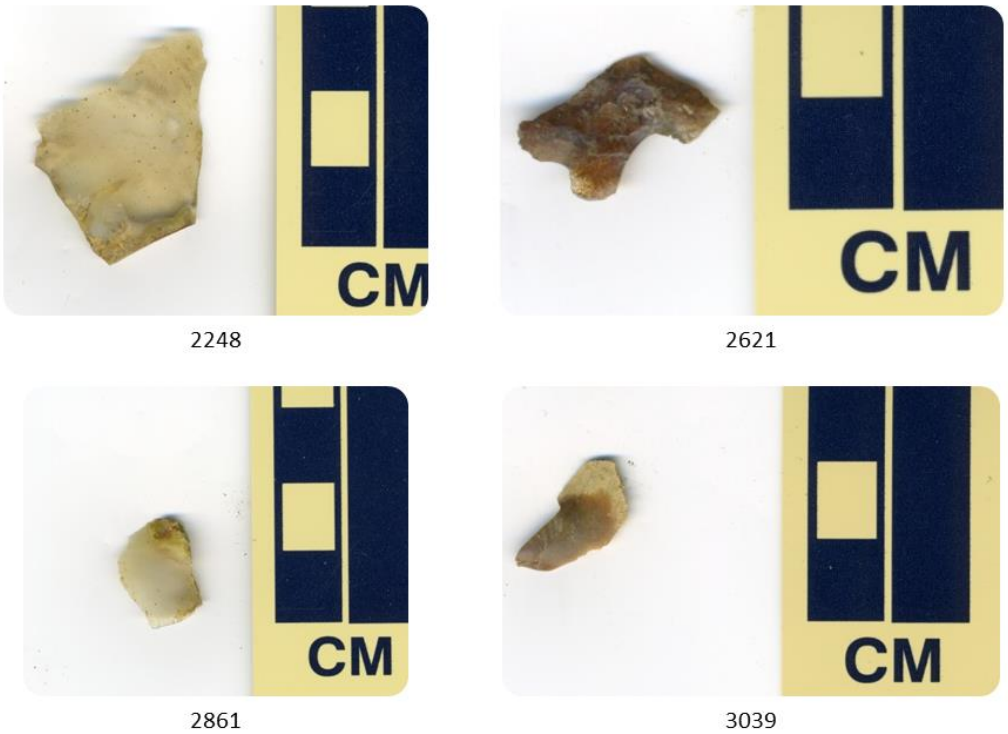

Figure H 1 - Artifacts within one standard deviation of the Old Highway 95_1 chert source (cont.).

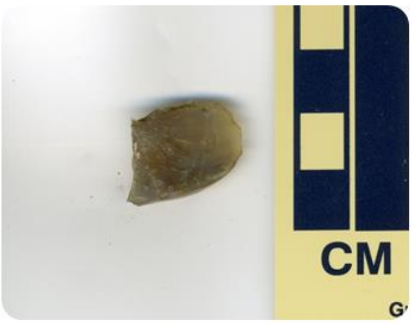

4621

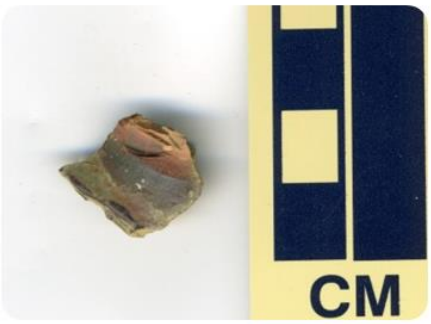

4776

Figure H 1 - Artifacts within one standard deviation of the Old Highway 95_1 chert source (cont.).

Peanut Brittle Artifacts

Below are listed photographs that were within one standard deviation of the Peanut Brittle chert source using discriminant analysis. Numbers below artifacts refer to their assigned catalog number.

368

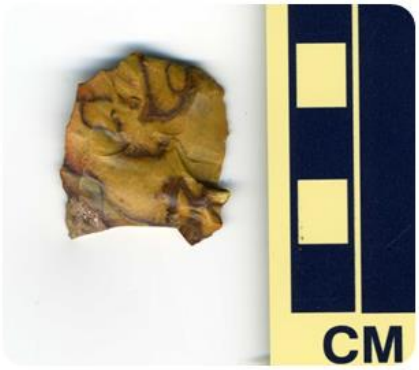

411

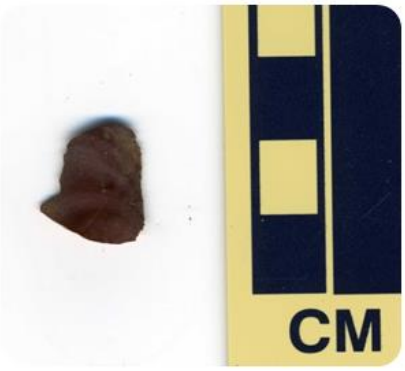

556

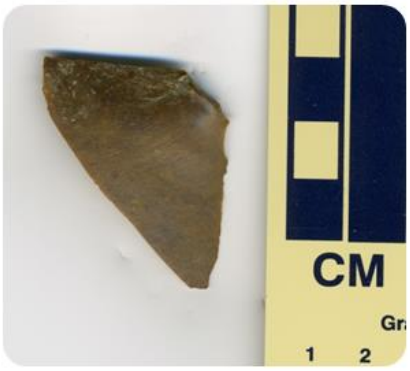

2778

Figure H 2 - Artifacts within one standard devation of Peanut Brittle chert source.

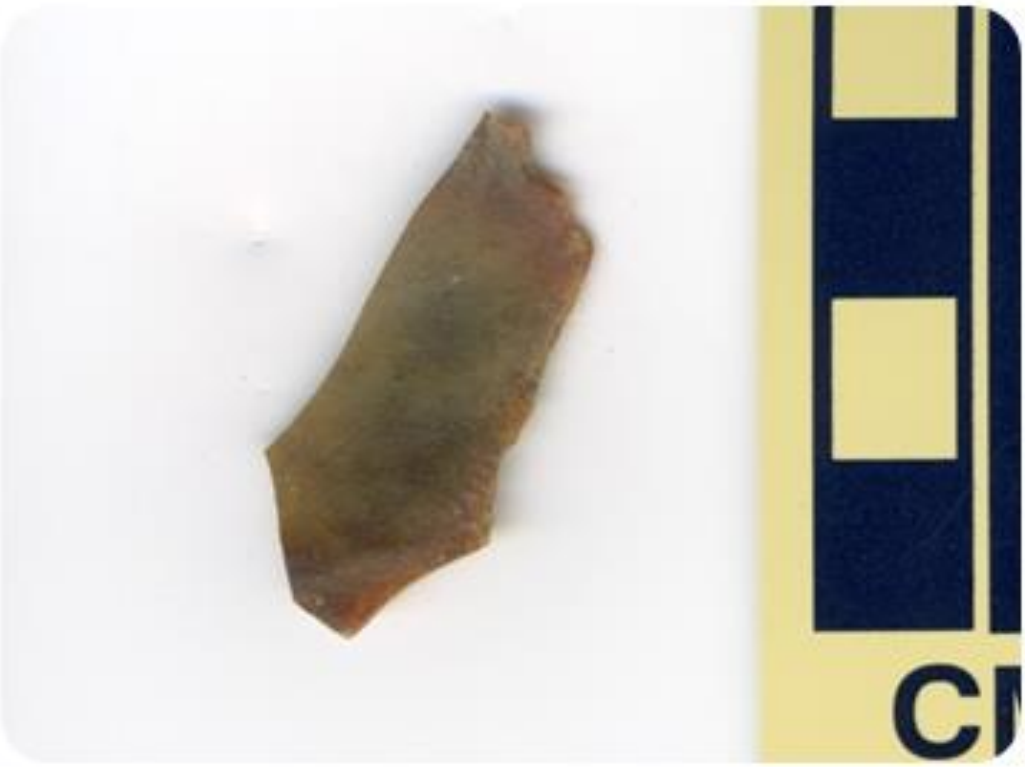

4052

Figure H 2 - Artifacts within one standard devation of Peanut Brittle chert source (cont.).

Pine Bar Artifact

Below is the artifact that was grouped with the Pine Bar chert source, catalog number 2302, using cluster analysis.

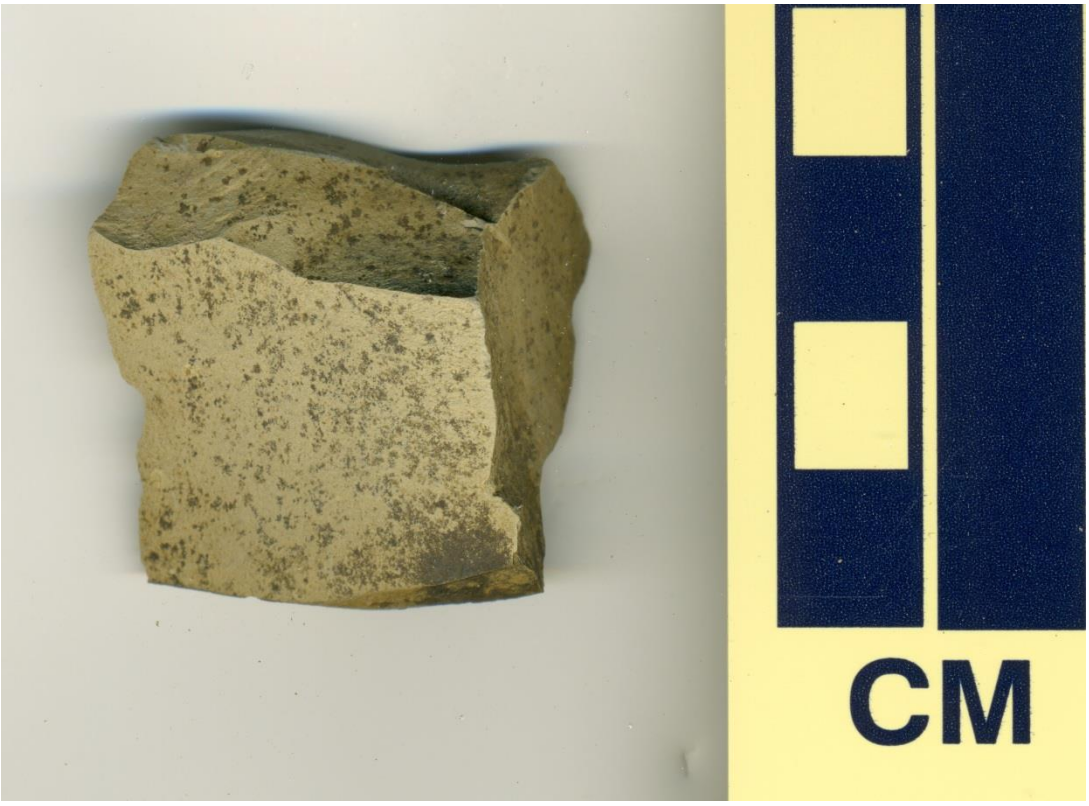

Figure H 3 - Artifact assigned to Pine Bar chert source using cluster analysis.

White Bird Artifacts

Below are listed photographs that were within one standard deviation of the White Bird chert source using discriminant analysis. Numbers below artifacts refer to their assigned catalog number.

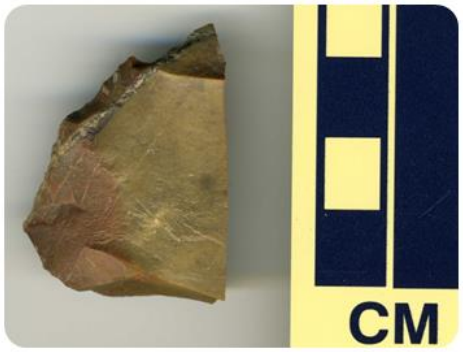

84

124

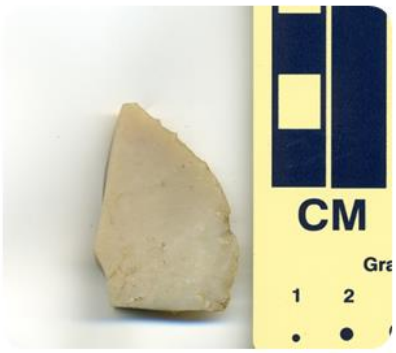

127

128

Figure H 3 - Artifacts within one standard deviation of the White Bird chert source using discriminant analysis (cont.).

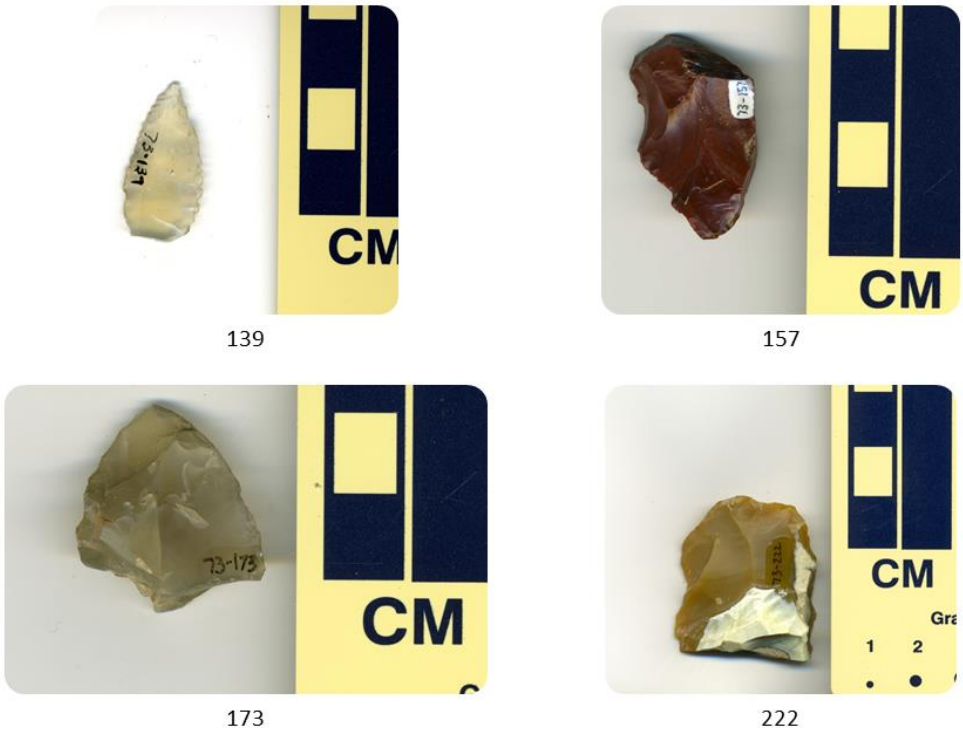

Figure H 3 - Artifacts within one standard deviation of the White Bird chert source using discriminant analysis (cont.).

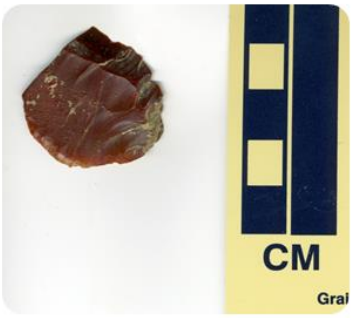

248

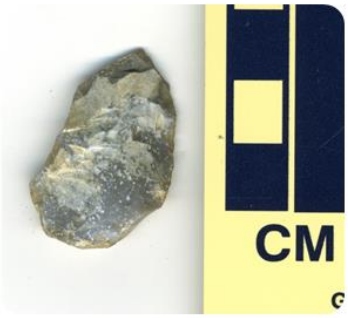

258

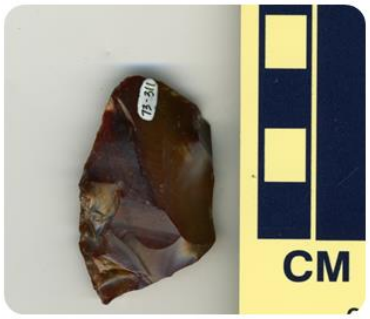

311

322

Figure H 3 - Artifacts within one standard deviation of the White Bird chert source using discriminant analysis (cont.).

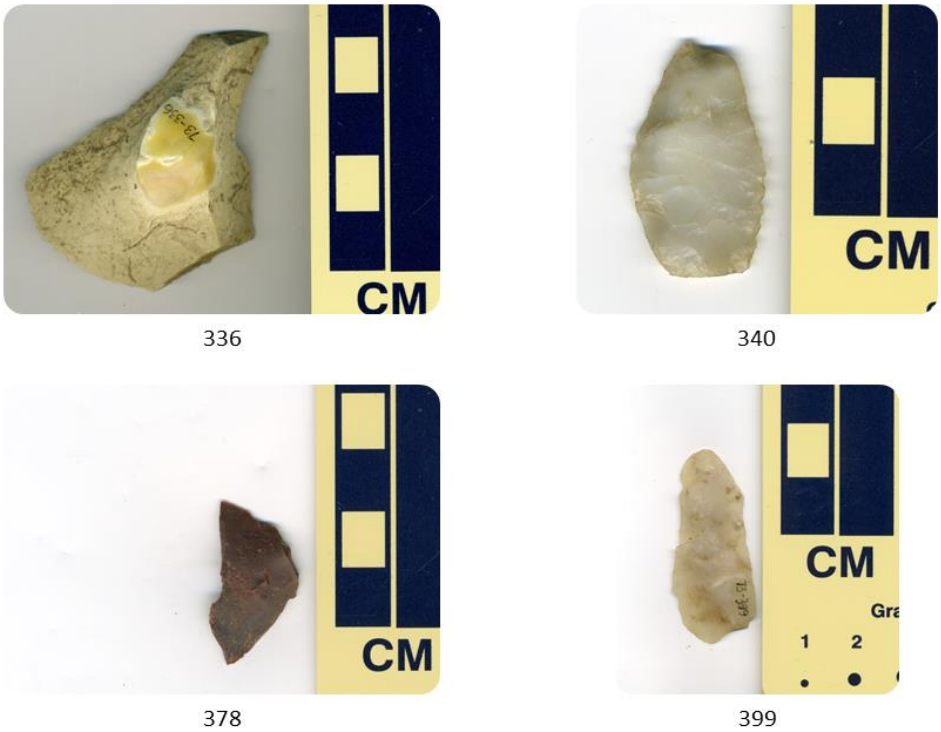

Figure H 3 - Artifacts within one standard deviation of the White Bird chert source using discriminant analysis (cont.).

471

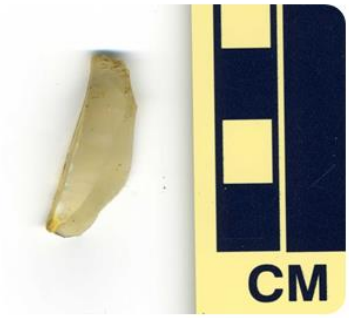

504

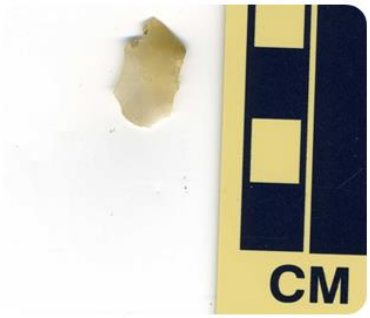

545

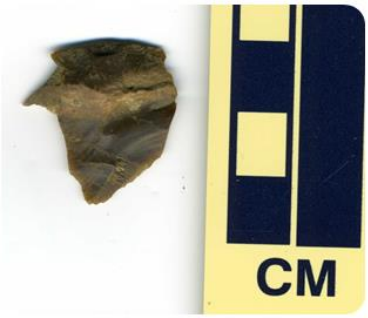

561

Figure H 3 - Artifacts within one standard deviation of the White Bird chert source using discriminant analysis (cont.).

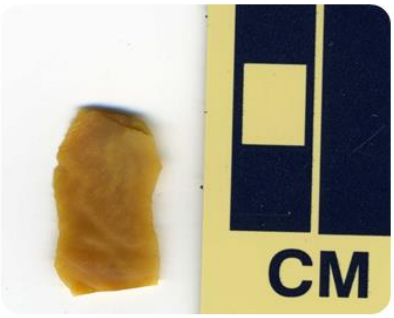

564

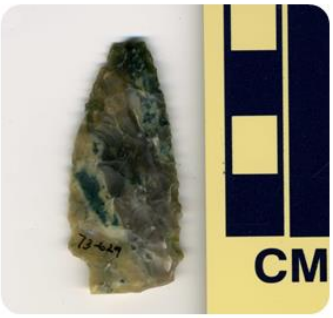

629

631

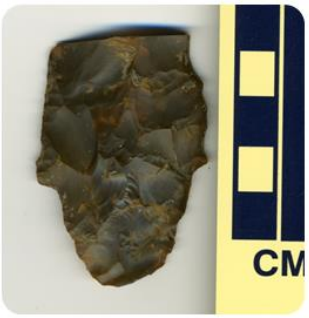

642

Figure H 3 - Artifacts within one standard deviation of the White Bird chert source using discriminant analysis (cont.).

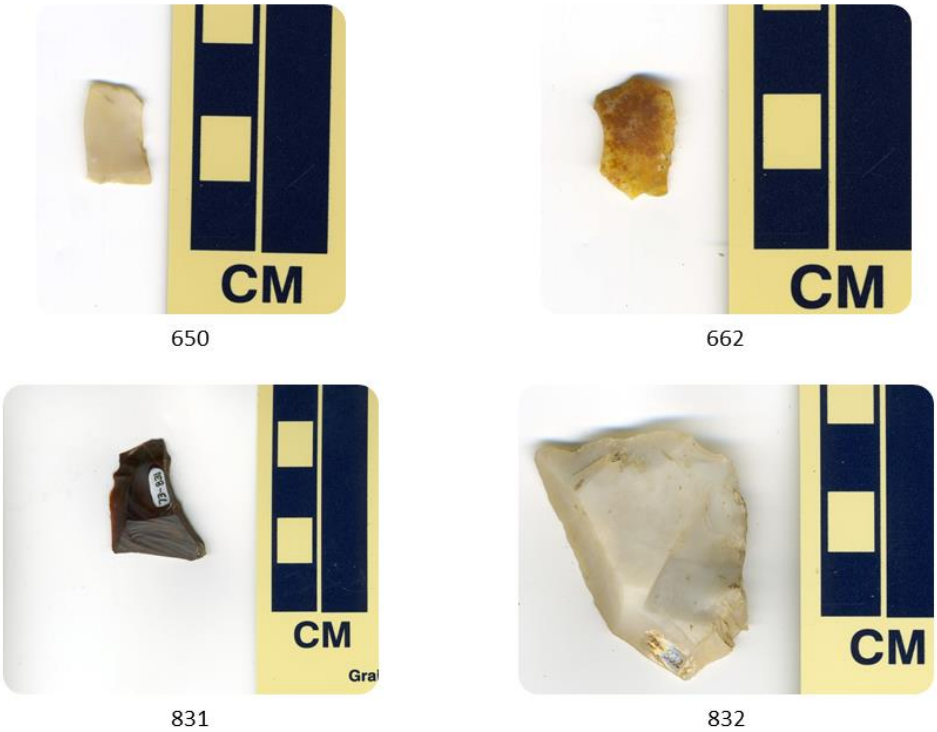

Figure H 3 - Artifacts within one standard deviation of the White Bird chert source using discriminant analysis (cont.).

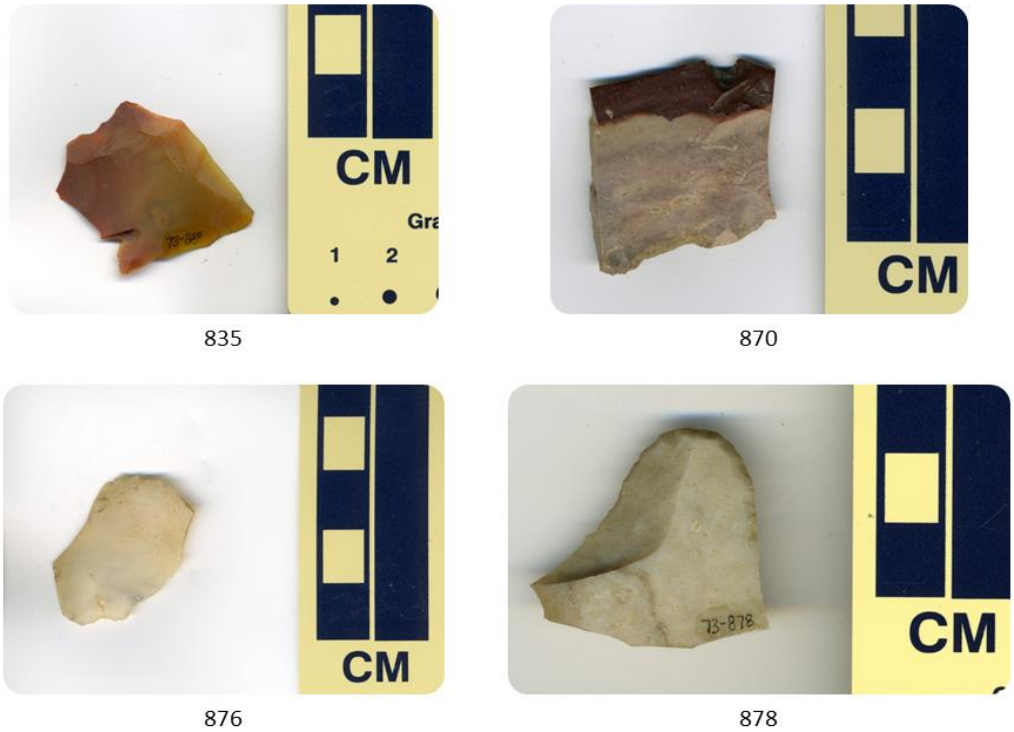

Figure H 3 - Artifacts within one standard deviation of the White Bird chert source using discriminant analysis (cont.).

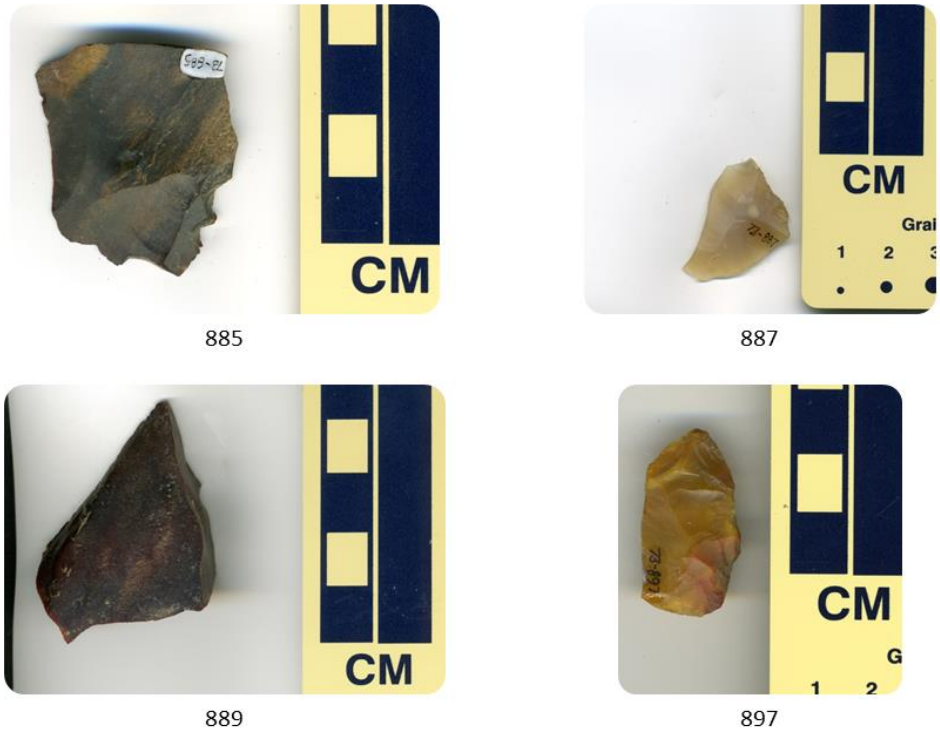

Figure H 3 - Artifacts within one standard deviation of the White Bird chert source using discriminant analysis (cont.).

899

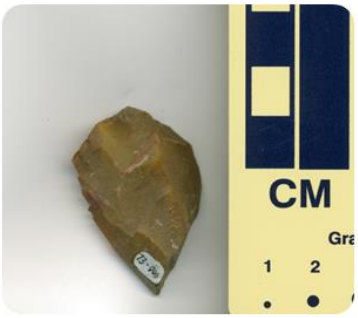

906

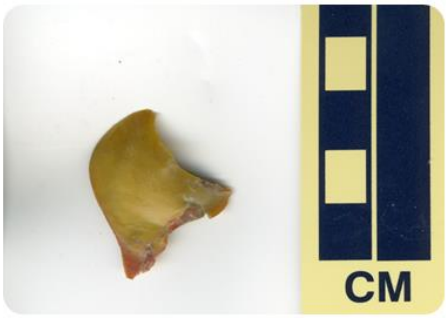

907

920

Figure H 3 - Artifacts within one standard deviation of the White Bird chert source using discriminant analysis (cont.).

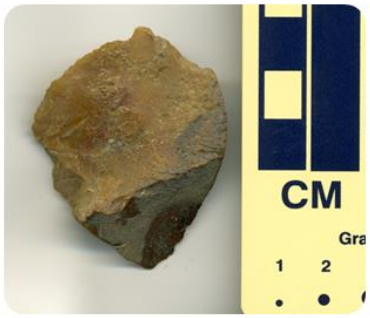

934

944

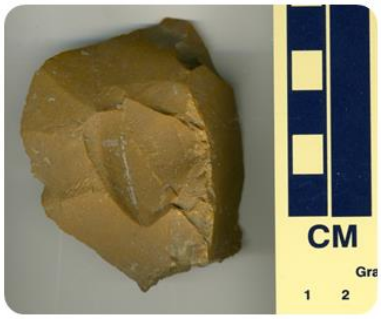

945

952

Figure H 3 - Artifacts within one standard deviation of the White Bird chert source using discriminant analysis (cont.).

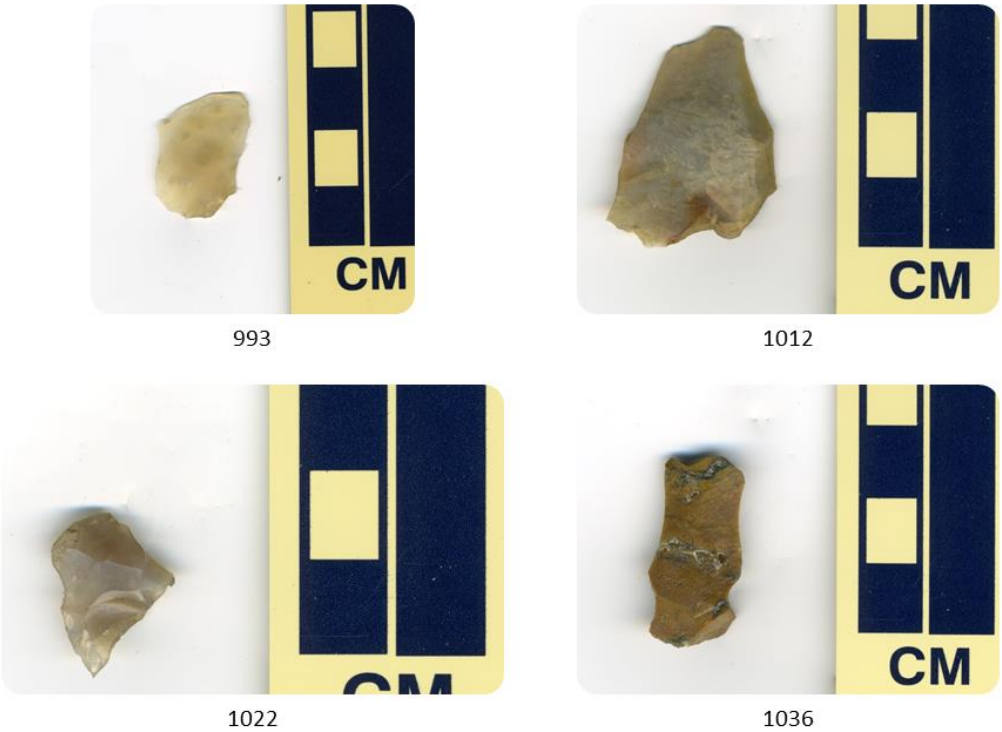

Figure H 3 - Artifacts within one standard deviation of the White Bird chert source using discriminant analysis (cont.).

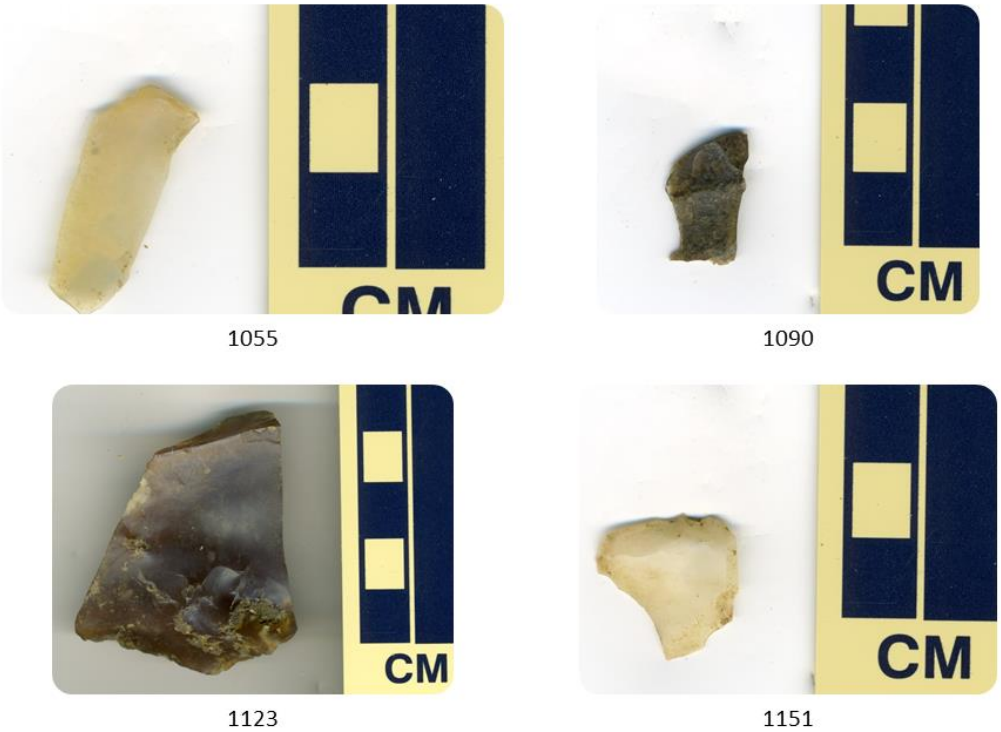

Figure H 3 - Artifacts within one standard deviation of the White Bird chert source using discriminant analysis (cont.).

1155

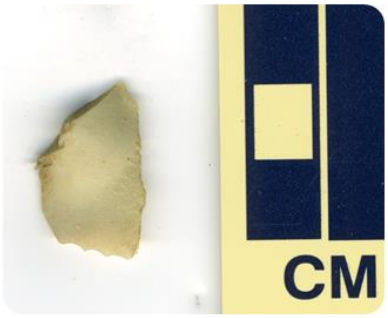

1178

1214

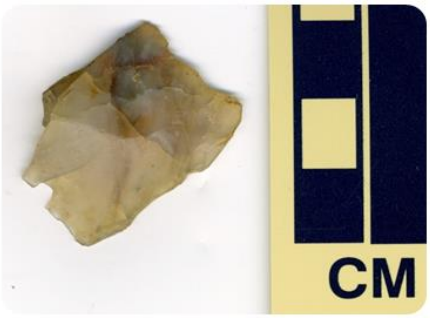

1240

Figure H 3 - Artifacts within one standard deviation of the White Bird chert source using discriminant analysis (cont.).

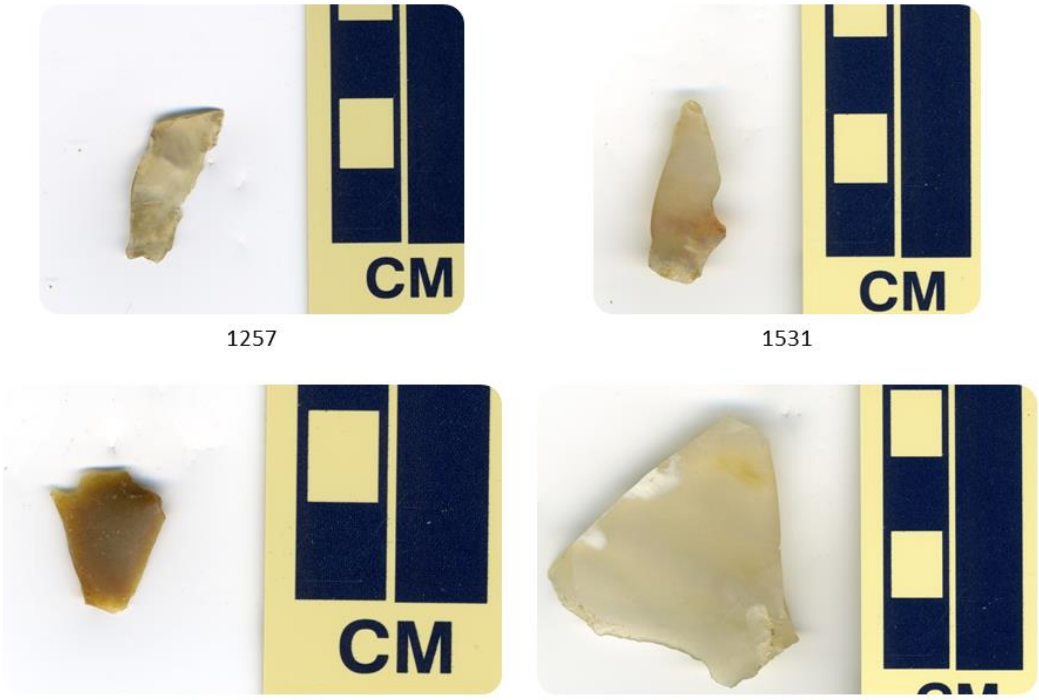

Figure H 3 - Artifacts within one standard deviation of the White Bird chert source using discriminant analysis (cont.).

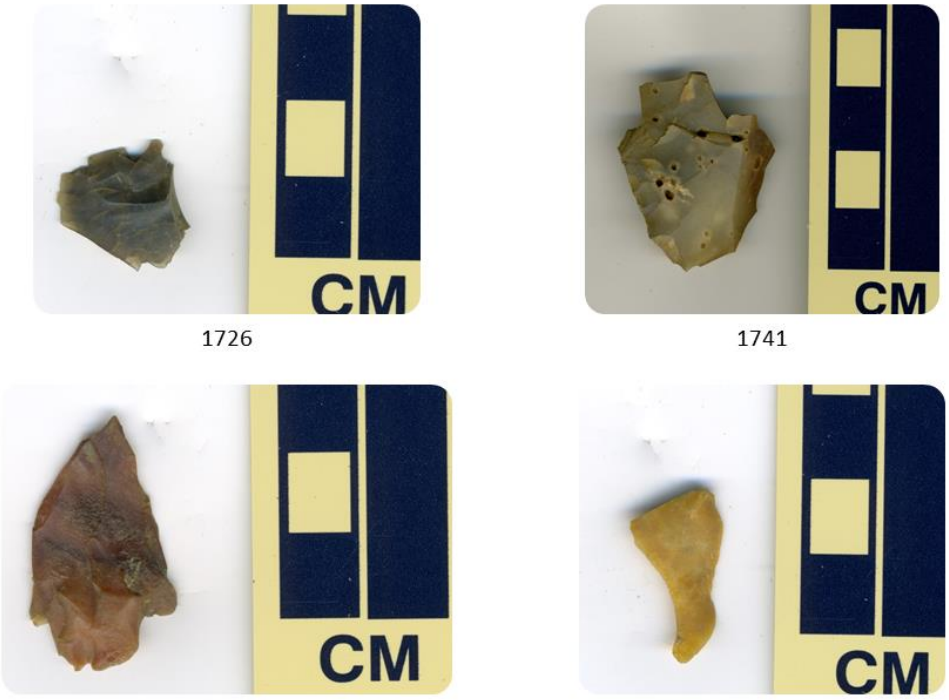

Figure H 3 - Artifacts within one standard deviation of the White Bird chert source using discriminant analysis (cont.).

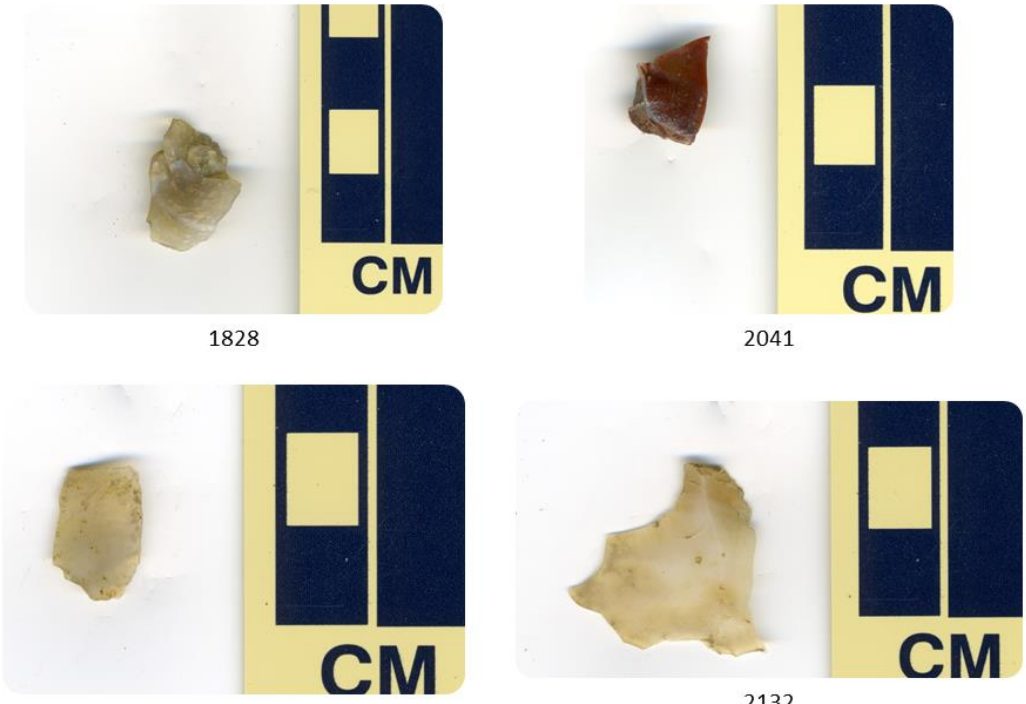

Figure H 3 - Artifacts within one standard deviation of the White Bird chert source using discriminant analysis (cont.).

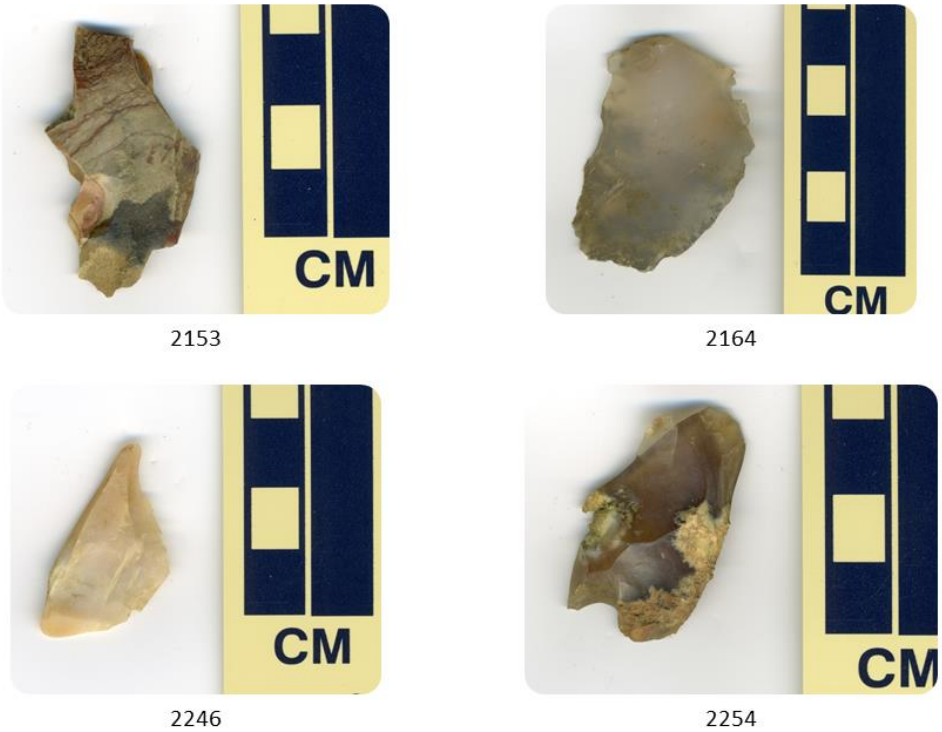

Figure H 3 - Artifacts within one standard deviation of the White Bird chert source using discriminant analysis (cont.).

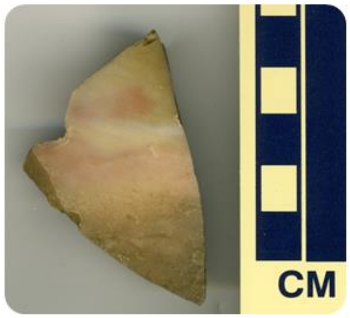

2306

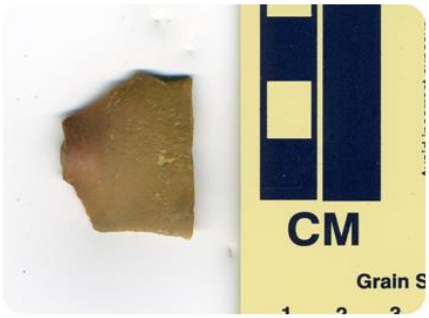

2309

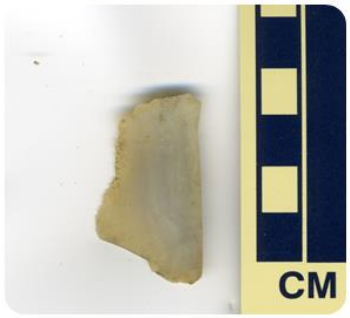

2370

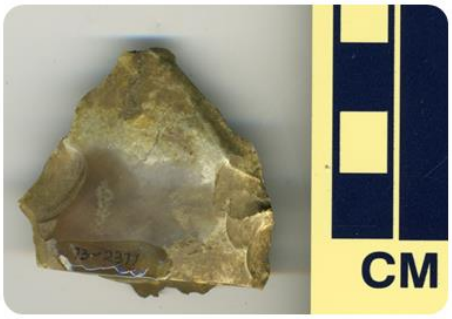

2377

Figure H 3 - Artifacts within one standard deviation of the White Bird chert source using discriminant analysis (cont.).

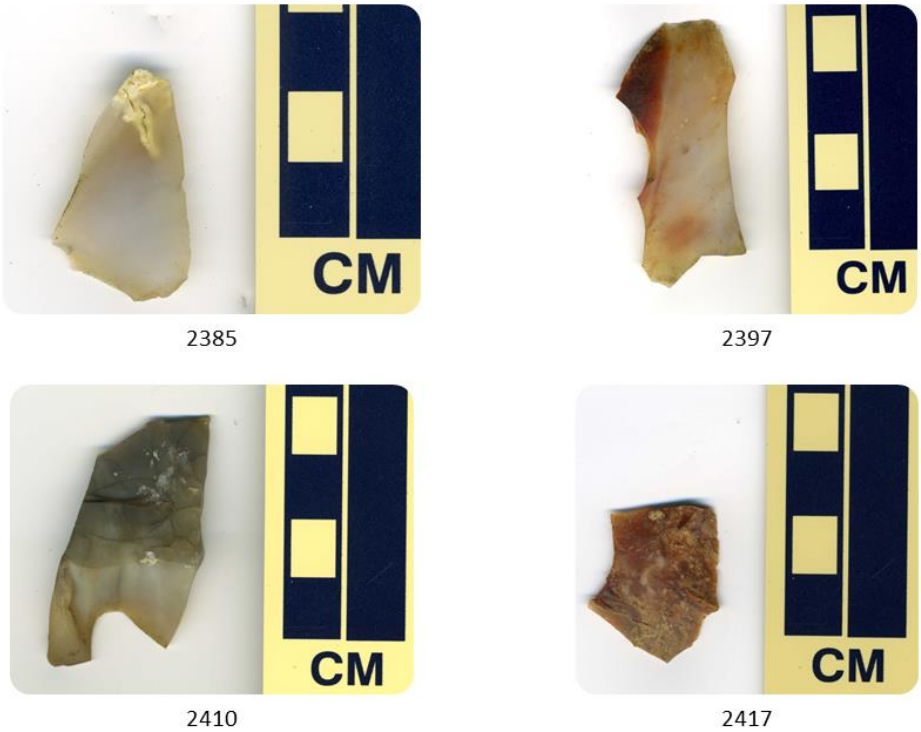

Figure H 3 - Artifacts within one standard deviation of the White Bird chert source using discriminant analysis (cont.).

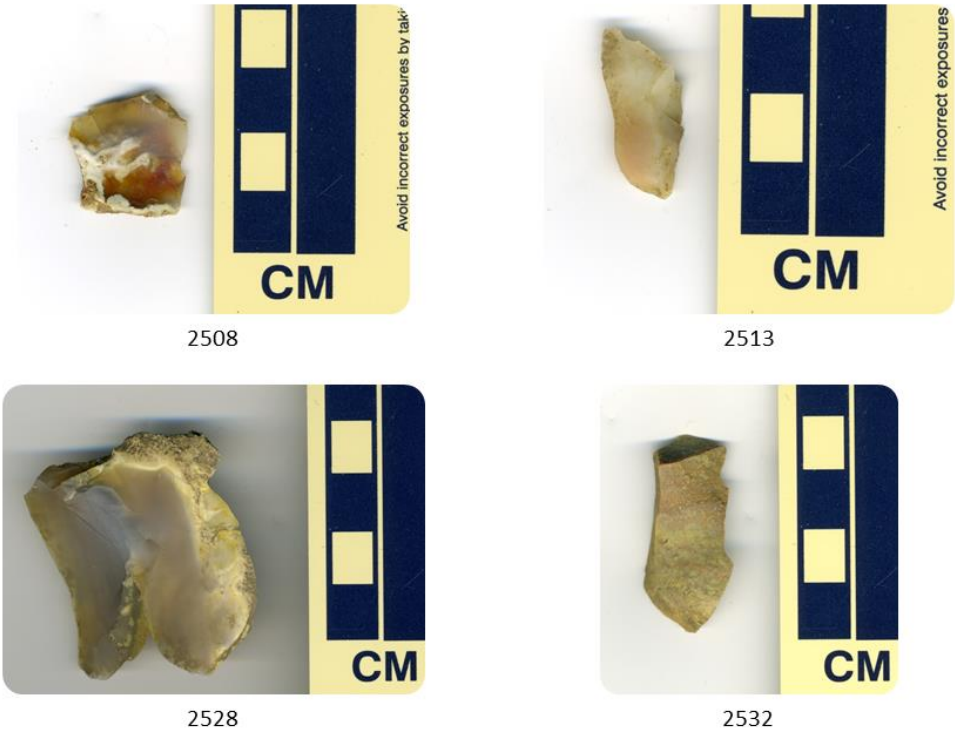

Figure H 3 - Artifacts within one standard deviation of the White Bird chert source using discriminant analysis (cont.).

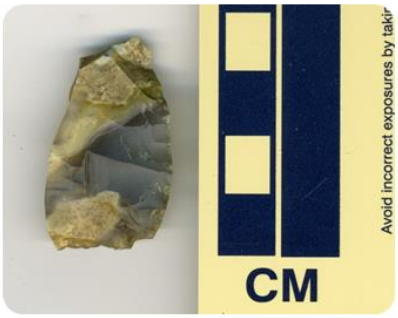

2555

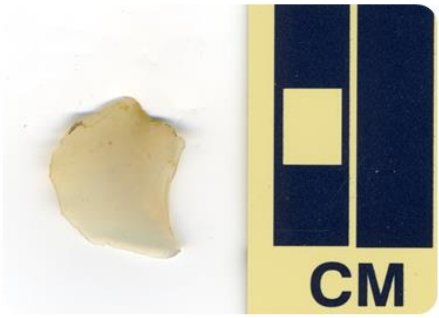

2701

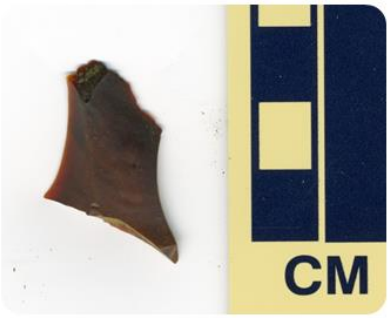

2821

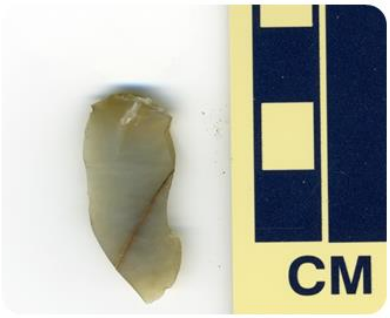

2877

Figure H 3 - Artifacts within one standard deviation of the White Bird chert source using discriminant analysis (cont.).

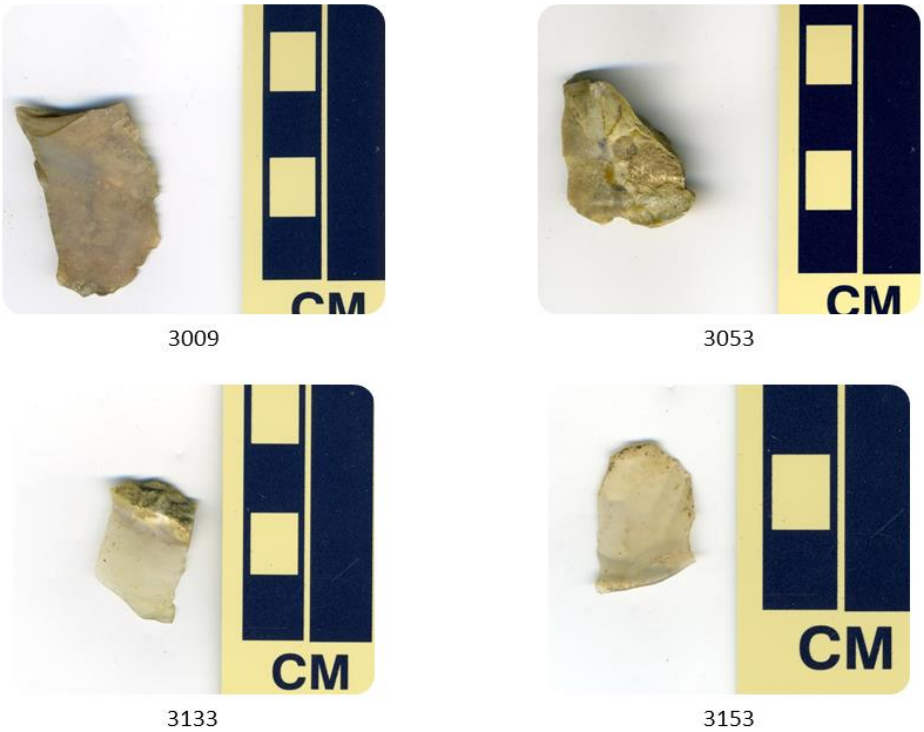

3009 3053

3133 3153

Figure H 3 - Artifacts within one standard deviation of the White Bird chert source using discriminant analysis (cont.).

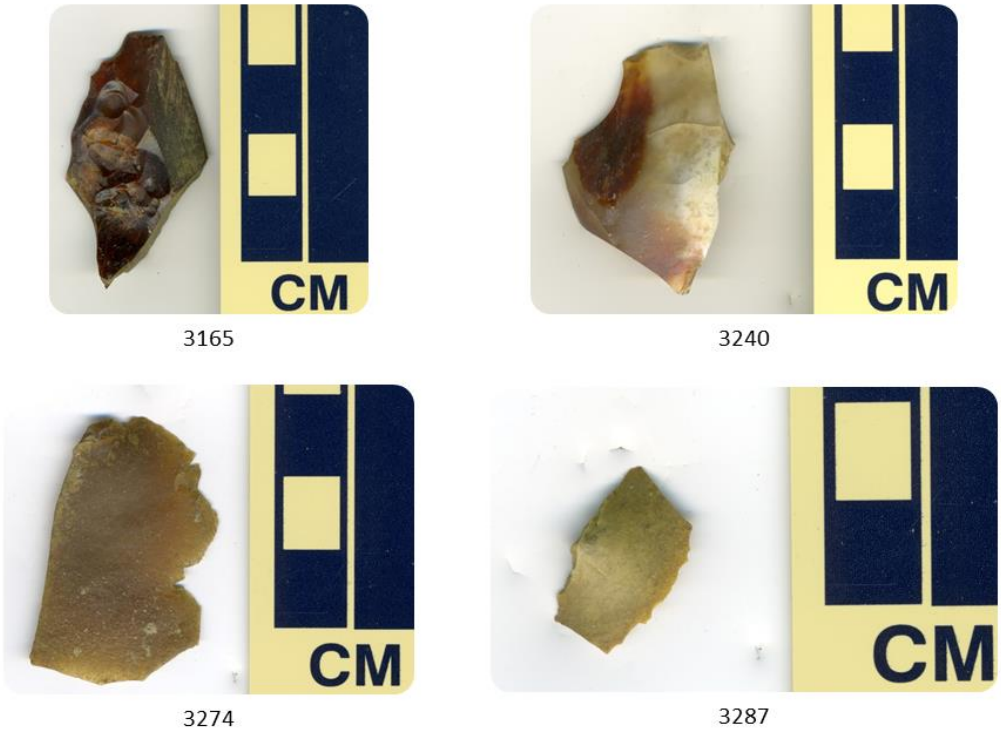

Figure H 3 - Artifacts within one standard deviation of the White Bird chert source using discriminant analysis (cont.).

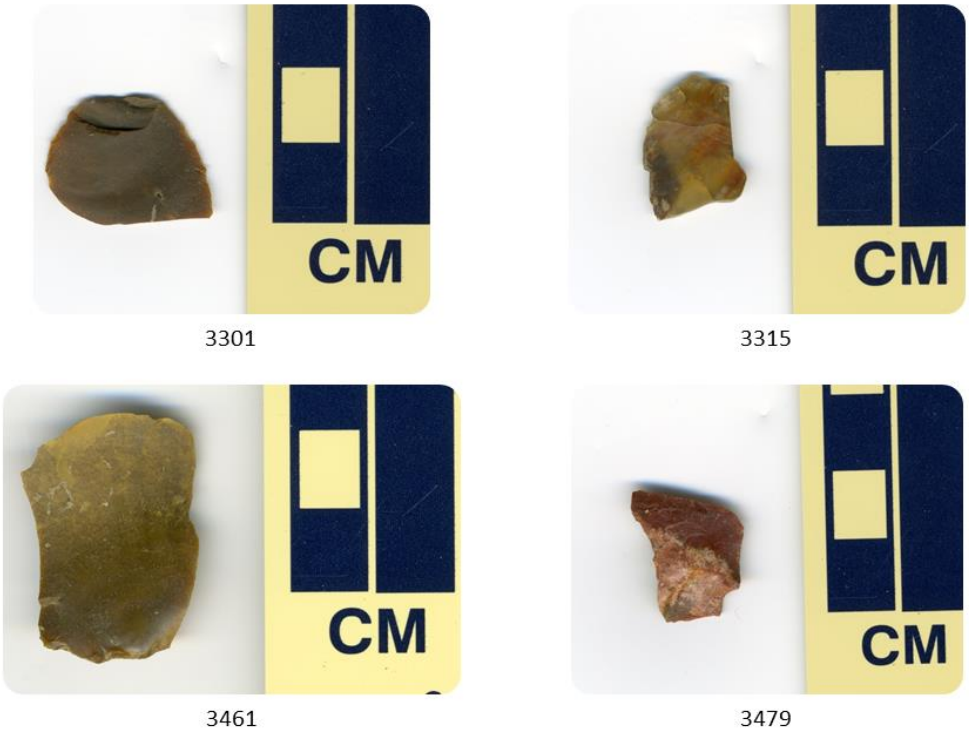

Figure H 3 - Artifacts within one standard deviation of the White Bird chert source using discriminant analysis (cont.).

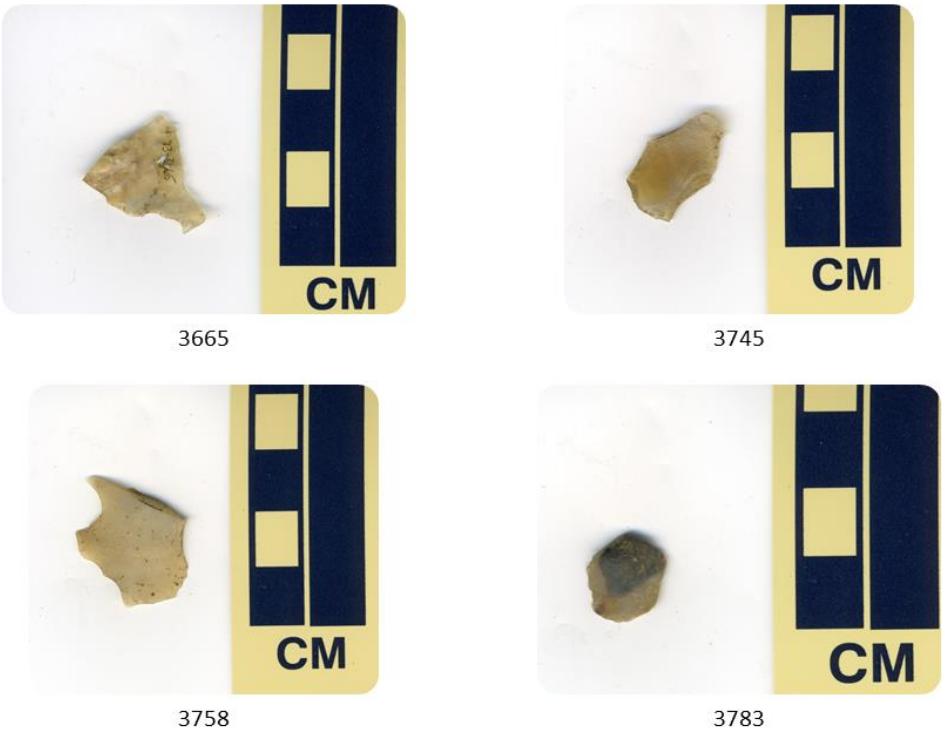

Figure H 3 - Artifacts within one standard deviation of the White Bird chert source using discriminant analysis (cont.).

3968

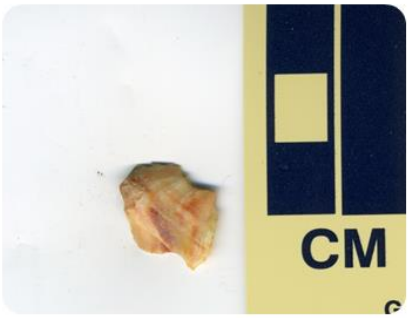

3971

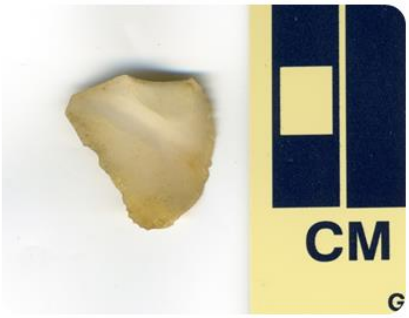

3991

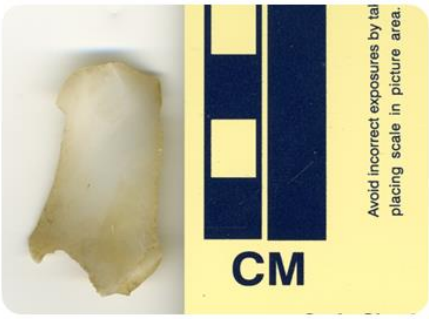

4109

Figure H 3 - Artifacts within one standard deviation of the White Bird chert source using discriminant analysis (cont.).

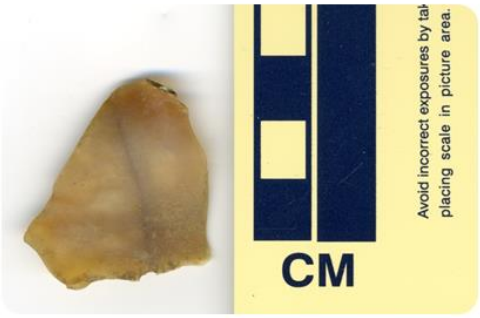

4161

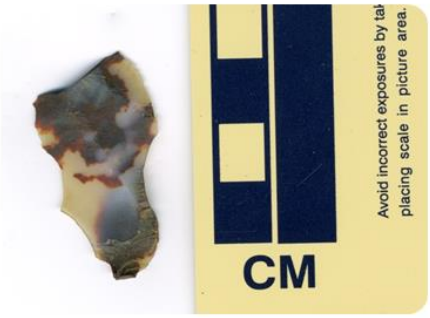

4164

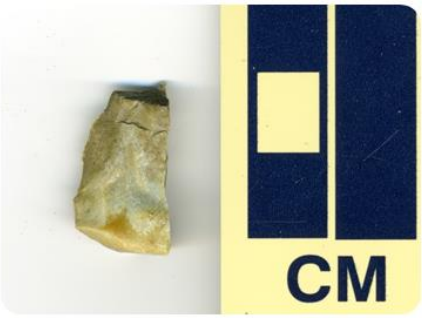

4183

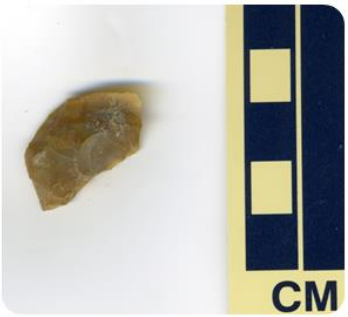

4259

Figure H 3 - Artifacts within one standard deviation of the White Bird chert source using discriminant analysis (cont.).

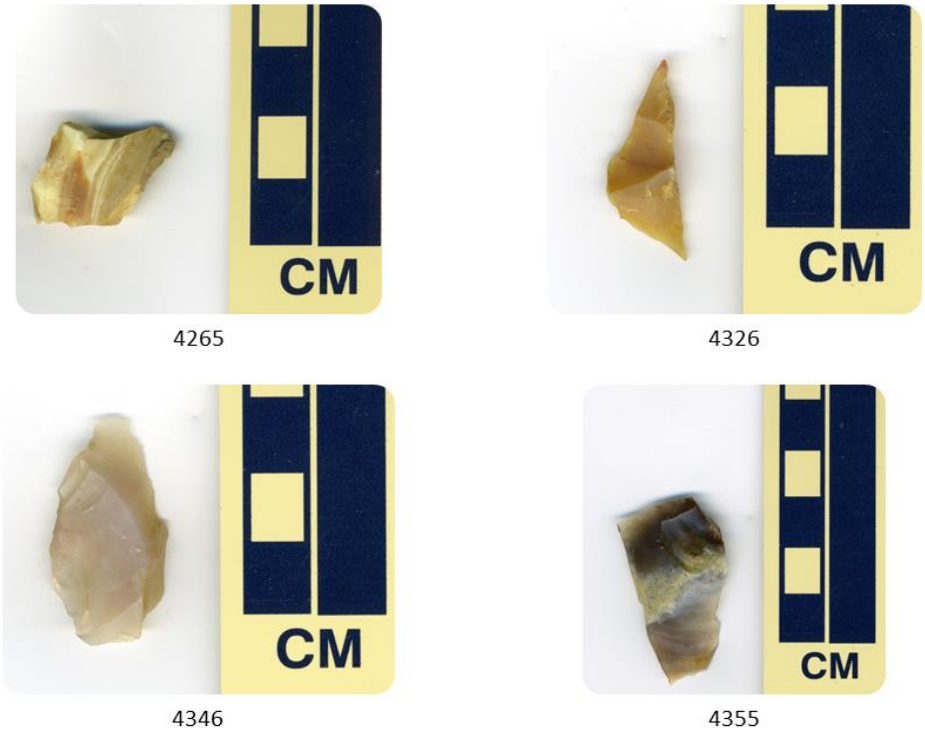

Figure H 3 - Artifacts within one standard deviation of the White Bird chert source using discriminant analysis (cont.).

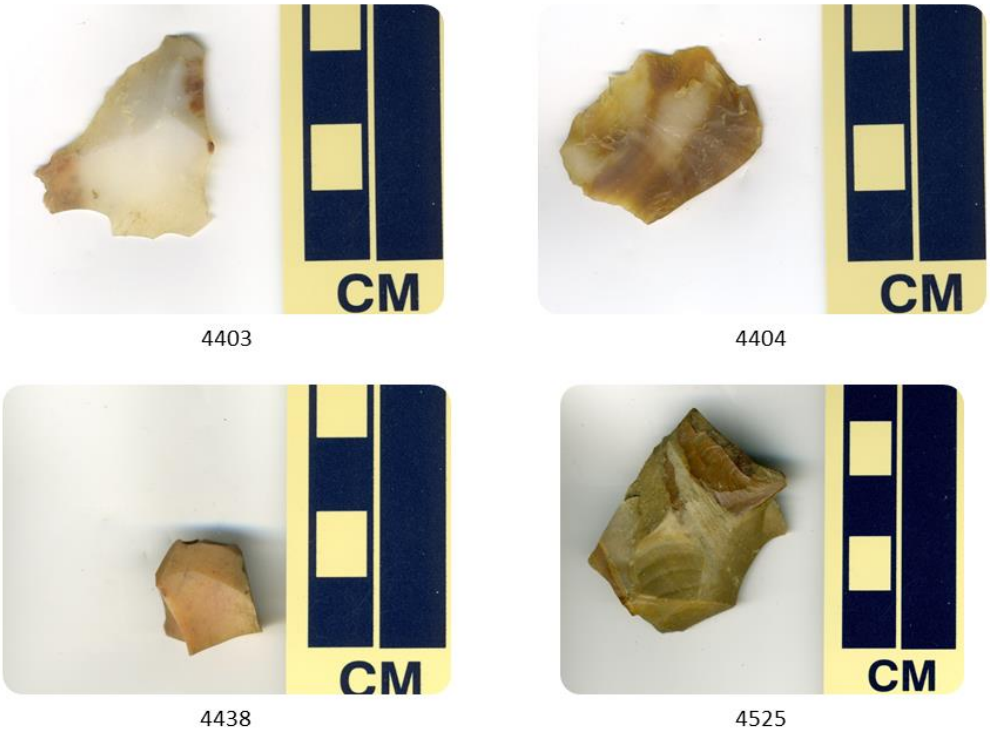

Figure H 3 - Artifacts within one standard deviation of the White Bird chert source using discriminant analysis (cont.).

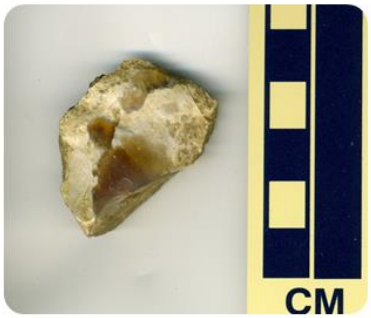

4536

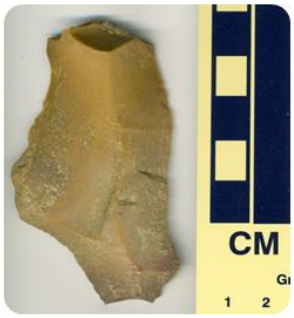

4634

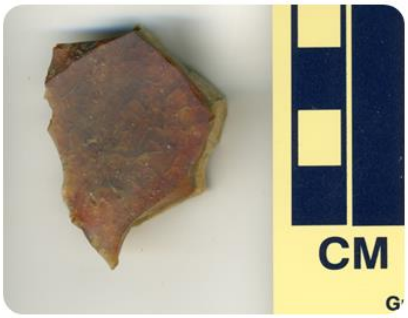

4646

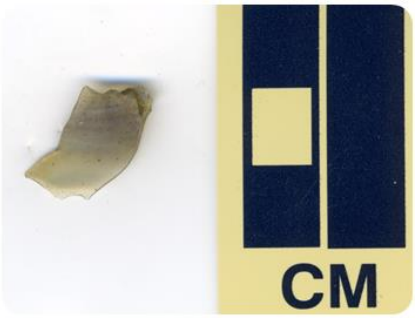

4762

Figure H 3 - Artifacts within one standard deviation of the White Bird chert source using discriminant analysis (cont.).

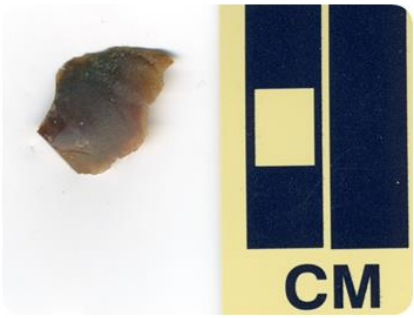

4767

5047

Figure H 3 - Artifacts within one standard deviation of the White Bird chert source using discriminant analysis (cont.).

Appendix I: Elemental Concentrations of Samples

Cat#	Ba	Ca / Fe	Ca / K	Fe / K	Cd	Cr	Cu	Mn	Pb	Rb	Sr	Ti	V	Zr
71	27.0096	0.699159	0.960861	0.261702	1.473455	6.390822	0.667891	32.51537	1.599137	0.28591	6.266659	90.42095	24.95735	1.524415
84	39.35229	-1.01347	-0.67927	0.3342	1.843833	6.036823	1.537702	19.90679	2.77049	0.806352	7.545368	81.60853	37.2467	4.827277
85	42.40715	-0.46355	0.455785	0.919338	1.711954	5.45215	0.792047	25.79982	3.154054	1.453882	5.564842	65.70899	29.87437	3.046842
86	7.234422	-0.03608	0.24562	0.2817	3.653111	3.249663	1.316242	51.61314	1.953933	0.830921	5.301237	78.80376	7.81937	2.416786
98	18.9551	-0.71638	-0.23626	0.480124	0.52485	1.670081	0.792605	44.763	3.233267	1.639214	5.987927	43.63674	42.30352	3.506071
108	38.36553	-0.19246	-0.02578	0.166675	1.473761	2.274004	0.629764	36.18528	3.723098	0.734972	0.089029	234.2405	37.14527	1.394273
113	34.31521	0.272108	0.482347	0.210238	3.151812	0.555621	0.339547	1.677471	1.156974	1.299265	5.31038	68.20875	27.77466	0.919929
121	35.77692	-0.20856	0.036024	0.244587	3.711603	1.605748	1.510382	47.91964	3.658273	1.701711	3.498583	17.36668	37.8411	2.138248
123	18.52154	0.347291	0.335457	-0.01183	2.776197	0.374522	1.510858	28.02945	1.255494	0.927167	6.745958	426.8506	12.98803	0.963652
124	1.148896	-2.2417	-1.81622	0.425474	1.740281	1.95173	0.586535	51.52549	0.387339	0.899906	2.718607	11.6565	27.24285	0.373188
125	1.942715	-0.96466	-0.7687	0.195961	2.984007	2.748654	1.008951	50.36097	0.995707	1.254529	4.178394	20.14611	23.86442	2.637923
127	9.751119	-1.29759	-1.09012	0.207467	0.168256	2.546518	1.040143	50.83481	1.605666	0.710057	7.196353	103.1589	38.17039	0.268391
128	38.79285	-1.7646	-0.97792	0.786686	2.606045	6.168057	0.740064	0.925905	1.66822	0.475683	6.104866	5.248323	6.156237	2.81702
129	14.82272	-0.19019	-0.11472	0.075467	10.34881	1.410389	1.302537	3.608379	0.070117	1.088153	1.165058	149.2323	27.63478	0.402455
131	5.21628	-0.13509	-0.03923	0.095858	15.00288	6.20703	0.585209	17.74366	2.79417	0.727467	2.389456	106.531	29.42521	2.347795
132	9.763118	-0.71503	-0.31428	0.400745	14.4751	3.655642	0.810502	8.152178	3.848906	1.115753	12.39138	68.20875	20.04101	2.21729
139	15.11238	-0.84744	-0.35886	0.488588	8.82305	7.70094	1.035002	32.47789	0.818834	0.798613	7.214115	8.565076	7.371242	1.13107
145	14.07815	-1.44697	-0.44723	0.999743	3.34481	1.372027	1.270031	15.8297	3.441443	1.17365	12.25883	153.6775	38.25902	1.724306
147	40.20102	-0.80462	-0.61002	0.194592	2.208207	1.400846	1.136143	22.10223	1.614717	1.329136	1.391877	32.63695	35.98147	4.414627
148	27.43307	-0.52669	0.107059	0.633747	8.487189	0.447186	1.176689	31.72132	0.572316	1.583629	11.3015	198.6459	11.42499	1.696059
149	1.496774	1.120539	1.459181	0.338643	1.670102	1.255173	0.745694	24.28945	3.43265	1.477414	9.99723	84.47863	35.89897	1.025264
150	990.174	-1.52839	-0.28678	1.241609	11.65387	0.752351	1.792179	285.5269	3.339681	0.890861	6.853571	496.2546	14.9582	3.417104
151	34.7393	-0.0652	0.11348	0.178676	0.472564	2.451006	0.711502	23.62687	3.59514	0.319022	2.24472	99.86363	16.3596	4.476109
152	436.0132	-1.64029	0.105357	1.74565	20.44382	7.936499	0.81265	21.40361	2.342869	1.373719	9.695532	68.20875	22.87766	4.987623
153	324.8707	-3.17436	-2.21241	0.961952	9.859418	4.780095	0.609792	38.14367	0.561702	0.636589	6.219716	43.63674	27.20374	2.220169
157	36.57675	-1.41596	-0.13667	1.279294	0.483974	6.284454	0.436426	32.80836	0.786772	1.212612	6.0403	5.292164	2.382583	1.4768
172	39.48102	-0.32449	-0.13834	0.186157	0.760092	4.942955	0.470904	39.28164	0.786145	0.478233	7.095221	140.643	33.29423	3.814611
173	34.2006	-0.99005	-0.77584	0.214212	1.741342	4.178392	1.068658	25.34936	0.458583	1.140862	6.858476	20.14611	42.05393	1.801021
179	40.90268	-0.63956	-0.05207	0.587489	2.615603	0.431143	1.238443	25.22013	3.285972	1.110457	5.360148	11.06873	40.35401	3.06718
186	16.14937	-0.18359	0.1994	0.382985	0.673446	4.20823	0.936736	32.6973	3.945844	0.215691	17.92228	385.6313	57.17053	1.064957
187	19.27598	-0.71454	-0.05259	0.661944	2.184911	1.798258	1.044822	38.53787	0.673867	0.35257	0.149003	43.63674	16.42402	3.503533
194	3.303558	-0.60136	-0.18279	0.418575	0.487179	1.57111	1.152676	41.30144	3.124766	1.740696	6.051472	162.8811	35.50038	4.221964
203	1.601702	-1.02113	-0.46695	0.554181	1.824545	7.911056	0.807843	27.19249	1.868575	0.36169	14.06984	51.86108	6.16526	3.507435
211	19.32503	-0.92739	0.097785	1.025173	14.27358	4.419366	1.46458	7.858395	0.678111	0.616933	12.52701	508.783	25.14587	1.494328
213	1.030904	-1.45117	-0.25543	1.195743	2.13806	6.752496	0.210024	2.404811	2.910578	1.132043	6.722418	0.360697	37.59218	0.146659
214	11.3141	-0.43852	-0.2745	0.164026	17.3539	0.064772	0.018984	49.05757	0.903488	0.913585	7.068747	65.70899	3.527442	5.701154
220	7.731449	-0.96174	-0.23987	0.721864	11.26044	2.423521	0.524599	10.53473	2.685041	0.575835	3.208141	73.38429	48.91167	1.89964

Figure I 1 - Trace element concentration data from PXRF analysis of geologic sources as well as archaeological artifacts.

221	35.66956	-0.46762	0.114453	0.58207	2.737084	6.672539	1.65846	11.39165	2.135482	1.200433	14.24457	198.6459	62.52314	3.507435
222	502.0686	-0.46969	0.214585	0.684279	19.98321	6.326298	0.878973	23.31013	3.16323	1.221595	8.587453	87.41558	39.01514	3.968667
223	31.61706	0.029314	0.182005	0.152691	10.55033	6.184687	0.811513	10.14968	1.23501	1.258457	5.716598	187.8327	41.25147	3.076133
224	17.87076	-0.65724	-0.205	0.452236	12.22004	0.708577	0.182942	39.13938	0.362413	0.71516	7.147511	158.2264	24.18954	0.490687
225	789.7508	-0.23661	0.092499	0.32911	16.21198	3.473543	0.73286	31.10231	1.882069	2.563097	3.451021	322.0315	34.18705	1.233407
228	7.052186	-0.04416	0.063469	0.107627	10.40639	6.009766	0.7003	17.76476	2.173676	0.896502	6.763547	187.8327	34.43304	1.211257
237	11.66038	0.183352	0.296844	0.113492	3.481552	4.244659	0.908694	41.91094	2.60572	1.455271	6.440011	227.9614	2.450367	0.066374
241	6.975238	-1.17529	-0.05585	1.119441	7.690721	1.069358	0.549171	44.10752	1.033015	0.837375	5.156944	8.587463	4.812098	3.497596
243	6.783577	0.138367	0.246225	0.107858	3.49213	5.322296	1.387889	6.51063	1.573883	0.972232	3.541072	106.531	38.38075	3.604333
248	22.38495	-1.72546	-0.9057	0.819762	3.35944	3.532179	1.509914	38.09823	1.740772	0.492525	8.731853	106.531	32.84448	2.339901
249	9.909114	-0.52578	1.282322	1.8081	1.147428	3.554371	24.04689	42.96945	0.76218	0.609612	11.41174	68.20875	3.721628	0.316231
250	11.04111	-0.13333	0.54609	0.679421	1.131161	1.951106	0.650108	37.37512	2.785313	1.229403	11.52456	84.47863	5.598359	3.350533
253	5.343818	-1.11788	0.523543	1.64142	1.78485	5.046232	0.79882	172.0569	3.726388	0.597905	15.1812	60.87889	109.8679	1.524442
256	11.12254	0.679733	0.722677	0.042944	0.961972	1.027726	0.828828	1.29589	2.951921	1.404204	2.158348	247.2409	5.150406	0.53445
258	17.16911	-1.23595	-1.01823	0.217719	2.80411	1.558141	0.2895	33.71387	2.627369	1.40433	5.8243	3.734673	38.4544	2.737471
259	26.45589	-1.63924	-1.88741	-0.24817	6.529604	7.727275	1.342022	22.5606	2.563758	1.070989	0.399681	78.80376	14.99714	0.852165
269	18.0307	-0.30589	-0.10591	0.199977	12.5559	7.56318	1.246186	23.571	2.287756	1.221189	3.345999	17.36668	28.2979	4.747467
278	2.96848	-1.03979	-0.25799	0.781803	13.44833	2.447333	0.865649	36.44956	1.953078	1.008087	3.042499	395.583	51.13713	0.149626
294	3.130688	-0.39923	-0.33404	0.065195	6.750312	5.393769	1.452298	15.36428	3.450058	0.208093	3.697115	113.5126	14.28036	0.07032
295	2.280251	-0.25741	-0.26484	-0.00744	4.696766	3.179084	0.433722	36.73569	0.326174	1.093403	7.113894	70.76673	22.56318	0.075355
302	16.13311	-0.18834	-0.09922	0.089115	15.6746	6.910108	1.401165	25.564	3.095611	1.000672	2.168136	37.94696	43.33198	1.965123
303	6.881715	-0.08414	0.005321	0.089457	1.341379	2.333901	1.46746	19.49407	2.27696	0.866294	8.940577	106.531	16.91428	4.988165
304	29.22446	0.297198	0.321897	0.024699	6.385664	1.594948	0.898668	2.665281	2.863932	1.594087	8.782246	158.2264	41.63013	3.044831
311	35.4283	-1.9875	-1.19515	0.792346	1.356076	5.658085	1.237866	6.567277	1.15891	0.835192	4.652677	34.36636	3.253782	2.198115
312	38.0927	-0.12202	-0.0059	0.116118	3.899457	6.64552	1.720357	43.81121	1.691996	0.976709	6.267047	18.7404	0.843284	0.54374
322	17.64409	-1.44905	-1.43289	0.016157	7.172536	7.233431	1.671348	48.5182	2.93373	1.147169	4.116352	68.20875	14.79492	2.572614
325	17.39564	0.286927	0.33576	0.048833	3.646794	7.397951	0.79449	0.271149	3.998895	0.584353	16.01215	215.8288	37.36979	19.43912
326	11.56639	0.24614	0.474899	0.228758	12.94933	7.398977	1.731332	8.015582	2.838315	0.957636	4.010097	267.8992	29.20094	2.528142
328	508.8858	-0.2031	0.094275	0.297372	9.120526	3.39804	61.78445	10.23432	3.146877	6.298221	20.86208	87.41558	22.43989	2.757836
329	2.707833	-0.90749	-0.46256	0.444927	2.850746	1.440027	0.79964	7.368765	1.14673	1.595424	9.695532	234.2405	12.7435	2.597033
336	35.22523	-1.07908	-0.55765	0.521427	3.559117	4.702311	1.821111	13.39532	0.387187	1.38552	6.477615	30.94691	23.90677	2.481341
338	149.2243	-0.41754	0.06504	0.482578	3.700566	0.56618	0.668794	48.87708	1.929406	1.49944	4.089769	76.06283	33.70736	2.398696
340	26.92076	-0.91361	-0.87376	0.039842	7.479608	7.473416	0.47258	6.238834	0.18334	0.722912	7.970821	39.80005	27.97042	2.914439
341	12.34089	-1.9705	-1.71845	0.252052	0.873393	5.825119	3.971776	5.466181	2.458991	0.658674	17.16446	29.29534	47.83679	6.577816
368	8.320643	-2.67188	-1.71112	0.960757	16.3943	7.164029	1.911691	24.67378	1.674674	0.732686	7.429595	10.95314	4.772952	1.38325
372	37.80972	-0.11265	0.090608	0.203254	0.384608	4.655225	0.874975	8.162343	2.534958	0.741681	6.827609	10.95314	40.85947	1.365908
375	13.12521	-3.52958	-3.3596	0.169976	15.12763	5.187542	0.267583	14.36822	1.430241	1.445356	7.404473	65.70899	33.97373	4.528646
378	7.987004	-1.73551	-0.86782	0.867683	10.10891	2.866146	0.828938	12.19319	1.779663	0.695933	1.681606	90.42095	42.77193	3.22926
385	18.32849	-0.92091	-0.84776	0.073154	8.218501	3.297435	1.509926	48.8528	1.631084	0.968164	7.340018	99.86363	34.74538	4.457587
388	1.596033	-1.1189	-0.56166	0.557232	8.189713	7.366643	1.121863	13.29991	3.840348	0.754512	5.268279	0.158085	39.30999	1.697308
399	17.4478	-0.85083	-0.6411	0.20973	0.75375	7.831979	1.145891	31.06185	2.49444	0.711246	4.040516	106.531	29.86676	1.38325
411	18.26581	-2.35009	-0.74094	1.609151	11.89377	6.174645	1.275683	17.0386	3.247685	1.108724	14.24457	96.64332	53.46748	1.064957
412	12.32774	-1.42518	-1.27157	0.153614	10.93417	4.238784	0.218526	32.03695	0.500629	1.667052	1.971373	65.70899	32.03962	0.376704
418	15.54769	-0.72218	-0.58045	0.141728	0.512801	2.237115	1.335867	10.65623	1.181748	1.132269	5.416338	20.14611	6.465043	1.216999
421	14.80736	-0.48376	0.050434	0.534189	15.17561	4.68598	1.273872	4.781024	1.08229	0.628594	14.06984	78.80376	24.0462	7.793523
436	5.725785	-0.67417	-0.51814	0.15603	9.667498	3.675382	0.452184	43.01448	0.998218	1.294371	5.439482	8.587463	27.41014	2.825628
453	31.69509	-0.27096	-0.2958	-0.02484	11.12609	1.121611	1.035346	33.51137	1.090356	1.148215	2.060821	43.63674	38.81542	1.716421
454	13.73309	-0.8087	-0.53643	0.272274	3.442445	7.5823	0.982492	33.81061	2.185374	1.295242	6.347997	253.9691	0.465547	0.751247
465	3.590825	-1.22002	-0.54457	0.675442	7.143748	5.620032	1.03934	1.458728	1.395221	0.963875	3.305548	330.5017	11.49645	3.528006
471	9.198071	-1.66066	-0.74902	0.911636	8.813454	7.667028	1.125961	1.369835	2.865669	0.891873	14.42337	4.170729	24.60708	2.21729
481	1.620894	-0.6421	-0.29377	0.348335	12.37357	7.896518	1.169758	5.260006	1.398392	0.79939	5.955239	63.26614	38.39274	1.168621
497	4.495016	-1.27884	-1.12928	0.149563	11.92256	0.001356	1.204069	21.49948	3.929221	1.143651	4.277198	49.73345	24.07663	1.843329

Figure I 1 - Trace element concentration data from PXRF analysis of geologic sources as well as archaeological artifacts (cont.).

504	1.516599	-2.05733	-1.88833	0.169003	12.58468	3.929192	1.630733	29.35399	2.875256	1.467612	6.683042	3.128658	40.28753	2.092813
506	16.91565	-2.14705	-1.33671	0.810337	3.644015	5.256838	1.210325	49.80753	2.294466	1.405866	14.06984	167.6443	32.71548	3.170471
510	0.946787	-1.1061	-0.88106	0.225042	6.39526	1.248737	1.148771	3.282832	2.498938	0.874645	5.018701	20.14611	9.843499	4.182517
528	4.083884	-0.93303	-0.86291	0.070124	10.31043	4.869172	0.970989	7.075232	0.746262	1.343032	4.423904	84.47863	37.49843	4.624949
541	14.18707	-1.32122	-1.27909	0.042129	14.715	6.638313	0.910799	6.958156	2.597047	1.177913	4.386802	103.1589	32.11957	0.231969
545	9.598754	-1.18993	-0.7753	0.414628	17.92007	7.56744	1.812552	35.16646	1.860822	1.02314	12.00272	7.740589	34.12672	5.912809
552	1.784612	-0.66375	-0.56656	0.097187	8.372037	3.348693	1.050874	9.368301	2.399356	0.605383	7.938824	70.76673	10.86255	0.402455
556	6.758965	-2.76881	-1.68578	1.083029	13.13166	7.74196	0.645911	42.03582	3.614559	1.243602	12.00272	120.8233	51.13713	0.316231
560	723.7424	-2.13442	-1.99911	0.135314	2.641475	3.087495	0.693709	13.98639	2.625054	1.128821	17.41127	366.4023	81.88352	4.497329
561	18.30456	-1.69149	-0.92866	0.762824	11.08771	0.340093	1.493758	27.41291	2.256611	1.151656	2.427861	56.26619	81.88352	3.123728
564	16.03086	-1.36453	-1.00774	0.356793	14.44631	0.739289	1.464603	52.20379	1.796954	0.64848	4.295748	124.6068	29.27429	0.864654
568	38.8997	-0.07401	0.217686	0.291697	2.383833	1.485134	0.710449	21.41283	3.239685	0.86828	7.023195	149.2323	37.91828	4.575793
573	0.916516	-0.19864	0.883928	1.082565	8.199309	5.331635	0.378852	11.54083	3.189862	0.545891	3.677745	24.56279	5.290187	0.492589
580	5.017965	-0.93566	-0.85081	0.084849	15.28116	2.819448	0.816056	48.33987	2.762156	0.754588	6.195606	162.8811	5.102479	0.767909
592	13.29494	-2.2414	-1.24254	0.998863	16.81652	5.842923	0.817634	7.161206	2.811452	1.090411	13.10188	198.6459	17.81611	2.481341
598	205.5007	0.168928	0.463339	0.294411	14.31197	0.084136	0.551508	9.481897	2.082218	1.504899	9.99723	959.9398	11.24079	3.155643
626	4.252621	0.409577	0.845022	0.435444	3.381525	6.536396	1.735936	21.77139	3.653948	1.214314	7.088832	7.444855	36.88931	3.938388
627	11.49988	-1.18607	0.126811	1.312886	3.817925	1.349483	0.711354	624.6351	0.809166	0.528855	2.166011	2.931249	10.74508	1.869359
628	27.35815	-0.38322	-0.00234	0.380883	2.943445	0.421548	1.553984	26.50491	2.215971	0.331526	9.42038	2.630402	14.32513	3.832658
629	12.27155	-1.45552	-1.07646	0.379056	7.997793	1.003667	1.087846	13.43578	2.337798	19.81301	0.30339	106.531	16.61754	1.607993
631	7.316268	-1.27147	-0.45402	0.817449	7.901833	2.734027	1.308335	34.88639	2.593561	1.121004	6.544766	58.54599	19.79734	2.022853
632	36.88533	-0.61753	-0.50003	0.117496	1.672626	7.013176	1.244445	49.74669	1.058563	1.164361	4.402469	10.95314	33.0357	2.186711
633	39.27702	-1.7619	-0.59492	1.166972	0.65091	3.013151	1.096099	164.3141	2.667664	0.991653	5.608065	103.1589	37.40592	1.872782
634	38.44324	0.202793	0.078062	-0.12473	2.505774	46.56165	0.980307	65.42964	1.146729	1.769632	5.705684	357.1148	42.6155	0.947148
635	94.07616	-0.53792	-0.23029	0.307632	1.58203	2.950675	1.20668	4.046303	3.806457	0.376657	5.748614	247.2409	38.71113	3.002318
636	36.11452	-0.77988	-0.66484	0.115039	2.300116	0.85343	1.130934	32.07045	3.525971	0.880493	3.881684	9.756686	35.51382	4.80766
642	38.41845	-0.9208	0.080446	1.001248	0.244355	2.074578	0.596022	48.39255	2.146724	1.13112	4.097998	0.14262	48.91167	1.230983
643	36.09706	-2.32119	-1.92221	0.398986	0.961336	3.36535	1.457408	14.4411	2.350957	1.243923	12.52701	93.49632	48.91167	0.767909
650	5.340979	-2.70076	-2.61905	0.081712	17.55542	7.598473	0.310182	43.79984	3.853085	0.57367	12.25883	23.05654	15.59507	6.129394
660	2.816916	-1.34571	-1.12417	0.221538	16.51905	6.232863	0.082854	2.188297	2.440705	0.769523	1.480118	124.6068	39.25597	4.000412
662	13.62135	-1.54667	-0.75695	0.789718	17.1236	3.465029	0.584979	48.24055	1.22978	1.530737	11.75813	36.13605	24.77767	3.507435
666	0.841713	-0.99449	-0.94605	0.048444	15.71298	5.497507	1.175985	47.84198	2.167738	0.898846	5.274939	136.4945	26.22751	5.094659
670	8.927719	-0.39047	0.186227	0.576693	11.06852	5.196178	0.785784	20.44581	2.518734	0.890801	14.79356	791.443	37.12802	1.965123
681	3.619663	-1.0279	-0.33951	0.688392	4.840706	6.653905	0.62224	29.54364	3.814548	1.209282	29.22235	772.4804	4.787913	10.05464
699	15.89648	-0.57773	-0.1157	0.462023	11.49074	4.526331	0.915292	7.627909	0.421884	1.01232	3.942992	13.43032	31.01229	2.333021
700	6.884774	-0.81144	-0.21324	0.598194	7.901833	6.318349	0.521477	24.14189	2.4552	0.997025	3.566303	41.69631	0.615342	1.561441
707	3.879299	-2.09302	-2.01793	0.075096	13.36196	1.322805	0.925802	50.35373	0.897566	0.25128	14.06984	198.6459	9.249066	8.320374
763	12.62102	-0.66488	0.802844	1.467727	4.83111	5.073672	1.837152	21.26154	1.674405	0.70394	28.20276	2050.923	32.33957	98.5683
771	13.63626	-2.10114	-1.06294	1.038196	6.088187	7.899469	0.97485	4.863338	0.471042	1.535885	2.219246	21.58457	28.78067	0.252807
784	15.23859	0.270385	0.3644	0.094014	15.79935	0.815192	0.287291	23.3336	1.809593	1.20739	14.24457	113.5126	24.78348	15.5992
794	7.385553	-2.03046	-0.54334	1.487112	6.500816	20.8318	0.563642	17.06594	2.657	1.214807	14.60634	60.87889	89.62039	4.936447
796	5.845282	0.16741	0.468395	0.300985	15.30995	6.568907	1.054747	19.12156	1.553103	1.165328	6.783507	87.41558	20.06848	2.004527
808	21.08097	0.124404	0.029684	-0.09472	1.577551	0.786378	1.252761	37.96695	2.368076	1.16704	9.554789	437.7624	41.87957	1.904296
809	10.85471	-2.09209	-0.78741	1.304683	3.12585	2.103986	1.305769	28.32681	1.112428	0.792564	9.842908	113.5126	50.01159	0.490687
817	202.0686	-0.5703	0.408683	0.978979	1.80386	4.008909	0.589607	232.0896	0.476355	0.793241	128.2272	2474.168	66.87384	111.0085
818	84.29713	-2.39442	-1.08166	1.312765	1.41061	5.656046	2.890634	10.47322	3.726622	0.848064	12.80783	5.237073	120.3046	1.046236
819	0.84537	-0.12348	-0.31018	-0.1867	2.528784	1.035579	1.046406	30.34539	2.973265	0.257878	8.286895	437.7624	28.6961	3.998937
820	8.304515	-0.40362	0.065079	0.468701	2.406721	2.602136	1.404251	45.50541	3.925788	0.990059	5.123445	240.6659	43.7317	1.404615
821	1108.745	-0.4385	-0.24418	0.19432	14.9549	3.584338	1.092226	197.544	3.961558	0.918354	7.252362	448.9284	43.39997	2.691195
822	35.61479	-0.01762	0.305654	0.323271	0.231612	5.605875	0.247338	48.72955	2.282308	1.153771	5.512994	60.87889	37.35254	4.192663
826	94.96944	0.706175	0.744681	0.038507	3.12513	1.24892	1.252482	50.18271	1.629502	1.156439	6.287081	37.94696	42.25016	4.281578
827	12.51679	-1.06654	-0.91294	0.153605	2.681022	7.35576	1.030735	26.87377	3.80181	0.899961	0.934746	204.2422	27.9546	2.473638

Figure I 1 - Trace element concentration data from PXRF analysis of geologic sources as well as archaeological artifacts (cont.).

829	19.32503	-0.74685	-0.51713	0.229714	2.438548	7.618426	0.964648	12.45924	2.544545	1.245649	7.708179	27.68136	32.26085	4.696333
830	31.20561	1.444018	1.248734	-0.19528	14.29277	7.693673	1.217328	2.058649	2.760718	0.364032	10.88504	215.8288	3.691823	2.950277
831	11.44316	-1.28619	-0.60108	0.68511	3.019997	3.114806	0.863902	43.5682	2.763696	1.33236	11.08847	8.60136	59.78522	0.620312
832	24.17115	-1.27709	-1.2689	0.008197	0.902277	4.67579	1.320263	17.04831	0.06203	0.356356	0.89915	90.42095	29.38599	1.580956
833	39.12817	-2.4733	-2.41054	0.062765	1.887334	7.407122	0.655902	3.432563	2.423264	1.640535	2.030622	76.06283	23.21323	0.743752
834	7.037305	0.642366	0.606381	-0.03598	0.593678	7.460657	0.723328	16.55099	3.670883	0.332836	8.634482	172.5184	30.30883	1.645914
835	8.0263	-1.32944	-0.76224	0.567209	3.898726	2.931055	0.930361	0.86284	0.593462	0.685282	12.25883	2.039339	16.30986	1.435522
837	10.94825	-0.75489	-0.60515	0.149743	2.95806	0.938927	0.771275	0.170853	0.776569	0.043612	7.535705	14.71234	42.0261	2.655261
838	26.87818	-3.04972	-2.53679	0.512936	3.639021	6.14756	1.767297	42.57373	1.079147	1.150997	8.940577	305.6649	120.3046	0.866518
841	6.812365	-0.62955	-0.496	0.133551	0.324713	7.533886	0.711908	28.63584	1.00036	0.304076	8.634482	73.38429	25.60444	4.041218
843	9.091801	-1.47042	-1.05094	0.419487	3.187308	0.963772	0.683395	21.19847	2.035988	1.268891	9.42038	103.1589	24.7664	4.090047
851	60.74283	-1.01161	-0.83397	0.177641	10.30083	3.924387	1.621312	34.18072	2.741246	0.166372	3.448418	234.2405	3.771858	3.628272
852	889.7508	-0.36188	-0.20747	0.154412	2.918569	1.949374	1.324497	30.84653	3.126471	1.264202	37.83955	260.854	35.82108	0.673648
853	3.663088	-0.94251	-0.59638	0.346129	0.247608	1.515298	1.364236	37.52337	0.8391	0.049029	9.842908	47.65424	23.92655	1.287518
856	455.0071	-0.07401	-0.20042	-0.1264	14.91651	5.92097	0.956495	48.18744	0.614628	0.822445	6.636074	605.0452	32.32818	2.541475
857	80.15985	-0.9994	-0.76879	0.230614	3.558218	1.629724	0.534881	8.006787	0.72587	1.319335	2.148895	20.14611	19.49975	0.680441
859	27.73715	-0.61145	-0.5206	0.090842	11.56751	3.687157	1.291782	6.51124	3.349394	1.542405	0.385457	99.86363	41.03434	3.231741
863	25.96355	-2.47677	-2.48853	-0.01176	8.276077	4.21865	1.280002	13.3115	1.564108	0.694185	6.437948	140.643	28.65304	4.875618
864	22.49703	-1.14356	-1.00703	0.136535	3.979973	4.759989	0.912283	4.065538	3.259849	1.304177	9.42038	132.4403	12.89291	3.97185
870	33.39887	-1.37222	-1.17603	0.196187	0.493864	5.758099	1.021454	24.30715	3.033807	0.116155	9.169438	90.42095	8.089682	1.326886
876	14.87855	-1.00659	-0.94189	0.064694	1.23598	4.000855	1.505994	29.63875	0.248503	1.446667	2.088357	106.531	24.14548	4.40185
877	168.9234	-0.88565	-0.97314	-0.08748	15.79935	5.285843	0.99665	48.85426	3.561604	1.591262	3.354529	158.2264	23.5122	1.057754
878	16.46715	-1.62156	-1.66564	-0.04408	8.515977	7.202056	1.075886	27.153	3.653659	1.671043	2.482582	76.06283	30.23031	4.582199
880	16.49948	-0.18701	-0.23045	-0.04344	3.900261	6.307846	0.929522	26.50292	1.743087	1.830962	8.995831	735.8404	36.39787	3.690497
882	4.077514	-1.23202	-1.10775	0.124271	3.205949	7.892925	0.886032	1.429718	3.928977	0.626606	8.731853	109.9816	31.35091	0.490687
885	418.2417	-1.46336	-0.42393	1.039427	11.5771	3.96441	0.553727	272.6772	3.975618	1.234319	10.32804	106.531	81.88352	2.845957
887	8.278349	-1.34917	-1.41292	-0.06376	1.949668	6.731552	0.932342	50.18176	0.162503	1.61029	8.995831	177.5061	5.669741	0.069157
889	614.7626	-1.60879	-0.95616	0.652632	11.26044	4.32588	1.271657	23.78853	2.055046	1.00028	9.554789	247.2409	26.9582	4.602222
891	39.18135	-0.62018	-0.46246	0.157719	13.45792	1.087294	1.450306	9.348894	0.635476	1.386158	10.50522	187.8327	30.2544	2.645114
893	47.90785	-0.91944	-0.90295	0.016488	0.015036	4.196245	1.241123	56.99005	2.529769	1.320643	7.656596	99.86363	6.92095	2.111993
895	7.756208	-0.95815	-0.88506	0.073089	0.113996	3.816087	0.537846	28.75708	1.410514	1.098701	6.794165	124.6068	8.306861	2.387784
897	3.634357	-1.02709	-0.57037	0.456726	1.033718	4.809112	1.326055	5.093906	0.175031	1.902477	1.844037	140.643	13.36043	1.965063
898	16.48361	-1.20788	-0.47003	0.737847	0.550879	6.090174	0.826562	26.1555	3.202263	0.399985	2.298655	132.4403	41.19895	3.039192
899	12.76808	-0.84918	-0.79696	0.052221	1.405114	6.240102	0.993918	41.1743	0.476586	0.976823	9.842908	144.8882	23.4089	0.402455
900	37.49288	-0.9506	-0.9232	0.027393	3.386384	5.181599	0.462032	27.99201	3.750599	1.314353	4.849849	56.26619	6.385321	2.489826
901	35.11989	-2.38288	-1.57563	0.807248	2.82233	5.251409	0.605556	47.13421	0.708483	0.465463	5.02198	70.76673	25.37163	3.203779
903	26.33015	0.080952	-0.10208	-0.18303	9.974571	0.512952	0.465762	33.96701	2.866641	1.21494	8.634482	348.0388	25.81347	0.989418
904	17.6874	-1.5315	-0.63864	0.892867	2.05849	0.228886	1.650295	80.49031	1.386809	0.781551	12.39138	330.5017	32.7561	1.29538
906	521.5797	-0.97806	-0.76223	0.215827	17.42107	7.784758	0.638651	3.009998	2.410627	1.20711	8.634482	460.3545	8.563861	0.812804
907	8.605727	-1.32832	-0.90161	0.426716	3.951473	4.526842	0.70768	12.38694	3.412139	0.500995	8.833812	23.05654	21.24966	0.212427
908	18.91942	-0.82367	-0.7586	0.065066	2.28267	7.143255	1.338126	48.24298	1.80791	1.188295	8.88658	76.06283	41.48866	4.837683
912	15.23223	-1.5042	-0.56155	0.942656	3.385116	1.727461	0.720699	206.8528	2.470259	1.030478	10.59692	140.643	36.10743	4.275368
913	7.823478	-2.48484	-1.49196	0.992874	2.543971	0.398565	1.168118	15.87172	3.77443	1.188769	10.59692	221.8253	3.584705	4.970876
915	15.95469	-1.34457	-0.69066	0.653915	3.4604	2.151295	1.029939	14.05919	3.26381	0.334977	2.446844	76.06283	16.0641	0.778617
918	1.343326	-0.91038	-0.74144	0.16894	9.955379	2.529127	1.09433	25.32653	3.21258	1.283544	7.439748	14.71234	8.816627	0.448825
919	9.181737	-0.66277	-0.58686	0.075909	0.295158	4.253867	1.076034	1.57981	0.823884	0.59588	2.389381	39.80005	1.735128	2.827922
920	25.18945	-0.99325	-0.96544	0.027808	8.506381	7.069916	1.045227	29.81444	2.994157	1.095647	2.191484	521.6033	36.08974	3.253765
926	9.121588	-1.36192	-0.96675	0.395165	1.606166	7.405159	30.35166	17.76612	3.795657	0.992301	12.00272	36.13605	12.66216	3.667991
927	34.33952	-0.15691	-0.12485	0.032058	1.363009	4.684676	1.401549	29.58242	2.768201	0.431816	0.968438	63.26614	26.95322	0.245304
928	288.1523	-0.24132	-0.12527	0.116047	9.49477	0.408253	0.785005	66.95312	3.203437	1.51304	8.88658	667.4333	11.84523	1.60895
931	8.224677	-0.56154	-0.57585	-0.01431	8.554361	7.544922	1.254778	50.5287	0.822329	0.765536	5.784225	153.6775	24.13896	1.821619
932	39.80454	-0.52825	-0.31819	0.210068	2.617268	4.061558	1.097265	121.8142	0.788994	0.646644	9.169438	267.8992	37.96326	2.12113

Figure I 1 - Trace element concentration data from PXRF analysis of geologic sources as well as archaeological artifacts (cont.).

934	301.1754	-1.4098	-0.79269	0.617117	11.25084	2.953345	0.106331	43.1505	3.339993	1.381464	8.587453	187.8327	6.22887	2.313113
936	37.2608	-0.83652	-0.79367	0.042852	0.33363	3.152434	1.454841	50.73539	2.329162	0.948263	5.25413	113.5126	29.90732	3.564353
939	32.48751	-0.56477	-0.46306	0.101718	11.98014	1.401739	0.938556	10.63141	3.355827	0.369391	4.201309	158.2264	41.17744	1.690621
944	332.8632	-1.08812	0.079621	1.167746	2.024084	2.659694	1.221521	902.8614	2.357817	1.230078	14.42337	204.2422	37.56593	0.316231
945	913.9633	-1.32389	-0.57617	0.747716	13.82257	0.804708	0.895791	76.86877	0.695026	0.914462	10.50522	193.177	2.080484	2.033059
948	40.33141	-0.23131	-0.38255	-0.15124	1.699838	1.308344	1.460774	26.48043	2.614394	0.968971	7.867917	172.5184	43.54736	1.213585
949	35.25113	-0.44572	-0.35851	0.087208	0.952005	0.402465	0.935501	20.21293	0.550431	0.924257	0.488033	3.128658	21.99447	1.247915
950	8.315066	-0.54495	-0.10908	0.435869	3.981117	4.584043	1.905883	40.20446	0.678399	1.059535	8.541494	124.6068	34.4225	1.912834
951	8.157556	-1.6254	-1.30205	0.323347	0.015958	5.312254	1.447972	44.92915	2.610751	6.745964	9.110232	39.80005	30.37034	1.912266
952	77.95016	-1.12492	-1.04188	0.083044	2.347397	4.367291	0.666002	7.586908	2.578214	0.765431	5.972588	45.62236	42.74371	3.26715
959	9.555532	-1.02329	-0.63644	0.386845	10.73266	0.71715	0.397141	36.37341	1.687263	1.199263	2.303277	30.94691	16.61832	4.528646
960	9.554517	0.256824	0.644381	0.387557	2.29574	4.468611	1.031563	36.58947	2.424475	0.538644	18.18675	605.0452	38.94203	0.767909
967	0.040194	-0.57945	0.325312	0.904765	11.50993	3.058102	0.809716	5.957386	1.252461	0.681147	1.978553	117.1259	53.46748	4.503954
970	1.7958	-1.07262	0.135726	1.208347	13.89934	3.858827	1.259588	41.94359	3.420689	0.948242	29.22235	2252.807	51.13713	147.4152
977	16.54077	-0.87904	-0.69425	0.184794	3.449465	1.677075	1.624252	34.33326	1.270224	1.107871	1.646272	144.8882	23.21817	3.402521
985	9.299358	-0.92949	-0.7172	0.212287	11.40438	5.557696	0.59659	12.70859	0.131701	1.047541	0.902356	36.13605	1.36855	1.52591
993	2.042871	-1.12102	-0.85015	0.270876	11.5867	4.758166	1.149353	44.47365	0.490225	1.36092	7.304915	34.36636	38.12342	2.347795
1012	23.88454	-0.92228	-0.68073	0.241558	3.442646	4.695199	0.598184	30.99304	0.569291	1.088059	4.257943	120.8233	36.65257	2.371464
1021	23.18625	0.323515	1.162848	0.839333	3.43007	1.598459	0.911219	25.89557	3.110568	0.91823	11.52456	90.42095	15.95504	0.88327
1022	11.07048	-2.12674	-1.73223	0.394513	2.501395	1.140719	1.119679	37.82416	3.886117	0.59651	8.496581	7.008987	21.1852	2.458164
1036	76.06958	-1.68678	-0.3647	1.322075	6.97102	1.597663	0.987812	8.824392	0.261685	0.538267	6.645216	0.330147	6.706317	2.351644
1055	10.14312	-1.37555	-0.88099	0.494558	0.255671	7.168354	1.233761	41.33709	0.246855	1.304009	3.489178	47.65424	33.16343	1.954658
1074	0.069402	-0.40891	0.045575	0.454487	3.880449	0.618385	1.83802	2.798832	0.492782	0.816059	10.98558	68.20875	20.20511	5.292187
1090	14.02185	-1.08651	-0.98621	0.100298	1.611106	4.637613	1.043589	1.83849	3.53473	0.703635	9.42038	124.6068	27.50004	0.767909
1098	5.598487	-1.94123	-0.92353	1.017703	3.699951	3.791385	0.725062	412.7008	0.426269	1.211735	10.78678	221.8253	114.9661	4.362974
1101	37.86003	0.786794	1.095221	0.308427	2.190521	6.624039	0.902226	29.23284	3.173638	1.275824	12.80783	140.643	7.633921	0.164552
1107	10.48398	-0.7817	-0.76185	0.019852	1.978759	6.879036	0.328232	8.858093	3.206388	1.341489	3.414814	153.6775	25.01588	0.170601
1108	4.467453	0.205676	0.714699	0.509023	3.20175	4.139874	1.264845	31.94824	1.279276	0.436958	9.052373	90.42095	42.90235	2.476601
1122	63.65773	-0.22147	0.439822	0.661296	3.301398	5.107419	1.687809	46.0786	3.924388	0.91394	13.89909	227.9614	50.01159	0.156733
1123	1090.879	-0.72753	-0.35466	0.372876	21.51857	3.685599	1.317443	38.73355	3.035988	0.930776	5.297179	113.5126	23.22165	3.822575
1127	10.60196	-0.22037	0.07191	0.292283	9.974571	1.388918	1.171685	9.373915	1.541593	0.992392	2.372918	16.02423	13.14068	1.840454
1133	4.353574	0.0862	0.084072	-0.00213	1.449547	3.121521	1.121374	37.04044	3.123064	0.98774	3.322955	339.1693	13.89466	4.8175
1148	34.48363	0.038812	0.174189	0.135377	0.128935	3.936613	6.623421	39.31685	2.132376	0.3417	7.748316	153.6775	32.8213	0.920013
1151	14.22116	-1.53035	-1.35601	0.174345	2.923908	4.05427	1.702572	20.9979	0.018914	1.417226	8.782246	58.54599	18.52259	3.979593
1155	15.1862	-1.03685	-0.70329	0.333557	6.059399	4.730308	1.024086	13.18915	3.566679	1.247542	4.474505	84.47863	5.378143	0.963652
1157	182.2285	-3.09033	-2.28003	0.810299	12.41196	1.219125	0.657823	10.17721	1.198258	0.833761	9.42038	158.2264	2.58861	4.201078
1170	35.2157	-0.89035	0.087508	0.977854	9.11093	2.379181	1.098183	176.064	2.663355	1.442549	30.84254	2592.732	22.9687	98.5683
1178	10.9778	-1.22719	-1.05023	0.176959	0.957565	3.279757	1.231925	8.796332	0.642527	1.201307	1.726928	348.0388	41.62066	3.367187
1181	1.253691	-1.20622	-0.92648	0.279736	2.408753	0.374141	0.827795	10.65934	0.300838	0.418133	4.847146	153.6775	14.20224	0.413476
1182	7.276245	-0.8326	0.362114	1.194712	2.021108	5.436434	1.272043	44.18422	0.715096	0.766028	0.553621	49.73345	11.53565	2.21729
1189	13.09994	-0.80307	-0.70214	0.100924	7.882641	6.075201	0.824171	35.521	2.699005	0.885835	2.240964	96.64332	8.041312	0.5156
1196	1.592588	0.202695	0.57676	0.374066	0.574181	6.5661	0.35935	15.44018	1.467451	2.292094	0.582554	330.5017	39.57308	3.779877
1212	543.5825	-1.77532	-1.67693	0.098389	18.95643	3.257889	0.950872	51.78234	3.397623	0.809813	9.486811	177.5061	8.04469	3.562994
1214	25.82016	-1.43351	-0.93099	0.502524	2.394716	7.776538	11.81291	9.175768	3.993181	1.243568	9.919181	149.2323	27.67312	0.826833
1221	13.62097	-0.48023	-0.38556	0.094666	1.990774	3.048974	0.929871	19.78121	2.557194	1.095257	6.086304	93.49632	2.85513	2.340544
1230	12.9977	-1.48979	-0.22703	1.262754	2.912439	7.59399	0.192425	49.36154	3.171758	1.548745	10.69076	76.06283	11.07065	6.351024
1237	16.73052	-2.28824	-2.3552	-0.06696	0.702233	0.320722	0.861722	12.80082	1.992127	0.661452	8.995831	366.4023	2.823787	2.481341
1240	14.99678	-1.41856	-1.46328	-0.04472	2.320629	5.140169	0.886259	51.50426	0.416736	1.477703	6.611198	167.6443	39.29987	1.797771
1253	1.579313	-1.0715	-0.16299	0.908506	3.332654	7.058506	1.907785	41.28387	2.043373	1.300094	15.1812	275.1086	13.0806	0.963652
1257	14.93473	-1.18992	-0.8234	0.366526	1.258975	3.656296	1.414917	38.72095	3.202708	1.071274	8.782246	76.06283	36.96119	0.673366
1274	40.49883	-0.32399	-0.15809	0.165899	3.864392	0.027519	1.093552	4.58207	0.865026	1.11661	12.25883	718.1435	38.68372	2.499135
1281	5.852635	-0.40034	-0.49385	-0.09351	3.204732	7.5737	0.318483	17.24515	1.079371	1.089039	3.489241	395.583	20.50469	0.648421

Figure I 1 - Trace element concentration data from PXRF analysis of geologic sources as well as archaeological artifacts (cont.).

1288	3.98168	-0.57441	-0.08734	0.487071	2.067221	5.102713	0.879469	23.29378	1.669843	0.498742	8.587453	177.5061	9.424058	3.455597
1342	12.75829	-0.58589	-0.47485	0.111048	0.129694	3.34533	1.155011	25.97309	2.800566	0.614491	4.597429	45.62236	36.23186	4.031423
1344	1.989726	-0.25346	-0.24659	0.006874	10.65589	4.96494	1.814457	27.76082	2.691045	0.711456	6.506249	215.8288	41.15023	2.964583
1373	11.24704	0.157823	0.137399	-0.02042	11.1165	6.222563	0.965058	24.64783	1.155192	0.911005	1.036528	240.6659	37.48284	1.597899
1399	35.25796	0.252916	0.510156	0.25724	10.98215	7.210375	1.359791	12.7474	2.903759	1.784536	16.45722	209.9688	16.08426	2.883084
1419	5.189972	-2.16721	-1.29135	0.875856	3.410538	5.470472	0.327998	292.1771	1.518096	1.046762	9.052373	215.8288	40.40611	0.151284
1531	22.13693	-1.08258	-0.70895	0.373629	3.094864	3.646975	1.183572	22.44377	3.622561	1.405156	5.048964	60.87889	15.75522	3.304855
1554	13.76211	-1.56922	-0.70964	0.859584	2.517957	2.166191	0.987329	38.1487	3.516773	0.375246	3.471097	0.624222	18.12668	1.453593
1590	20.11422	-0.96805	-0.8504	0.117647	7.959409	6.391002	1.693497	19.69979	1.271024	0.474953	5.037787	106.531	14.97759	1.72774
1597	7.96809	-0.92863	-0.69225	0.236383	1.947568	5.403078	1.395151	14.90965	0.57543	0.356072	1.473247	9.589528	37.538	0.326117
1675	27.59756	-0.66447	-0.40684	0.257624	3.858894	7.034653	1.575024	23.50284	3.199741	0.633725	0.064437	305.6649	19.42987	3.529187
1684	34.47329	-0.96916	0.419655	1.388819	2.479859	3.399646	0.290646	232.0896	1.76478	1.298805	36.43212	2716.885	18.87888	105.86
1688	11.40302	-0.88196	-0.86017	0.021796	1.495019	1.753123	0.962903	12.43088	2.423421	0.598844	2.818304	16.02423	23.26635	4.980707
1695	213.4462	0.735953	0.827081	0.091128	11.12609	2.926553	0.92975	10.69404	0.230837	1.504455	9.554789	153.6775	29.96958	1.108182
1726	5.274417	-1.16798	-1.04358	0.124404	2.450225	7.525118	0.455631	34.99807	1.686735	1.083512	5.987276	124.6068	1.935731	0.768837
1741	32.69821	-1.24356	-1.26107	-0.01751	12.22963	6.23805	0.955911	21.07637	1.684938	1.103239	9.486811	339.1693	42.66728	0.384752
1742	17.17197	0.252916	0.292962	0.040046	2.945841	0.894969	1.140938	20.76408	3.277617	0.698018	12.80783	484.0113	18.60888	6.577816
1756	7.452519	-0.7885	-0.02747	0.761032	3.805625	2.159114	0.894832	35.58782	0.79935	1.302272	8.88658	0.719051	11.69301	3.802127
1758	22.95305	-1.06375	-0.99655	0.067201	2.726588	6.233589	0.527492	13.40731	3.187301	1.914531	1.790708	297.76	24.36686	4.078992
1767	14.65762	-2.56269	-1.84896	0.713737	2.762795	7.375734	0.862145	5.294644	3.183826	2.527748	15.38182	153.6775	34.50135	7.539058
1774	8.669364	-1.43606	-1.40364	0.032418	2.390909	6.156048	0.479937	1.39518	2.27095	1.220324	10.15883	534.7222	41.7218	0.532902
1779	6.363609	0.043112	0.58643	0.543317	3.476036	3.389651	1.488059	47.99437	0.135221	2.563097	20.53672	247.2409	30.21038	5.292187
1800	15.31132	-2.61945	-2.54896	0.070489	1.477689	5.27956	1.082475	41.90433	0.730067	1.059524	3.228875	521.6033	5.878896	4.080784
1802	18.64328	-0.88673	-0.81868	0.068045	0.933987	1.703563	0.873135	21.83586	2.415159	1.083812	8.88658	167.6443	2.374332	0.279151
1803	1.515439	-0.22071	-0.04105	0.179662	7.431628	1.467087	1.435582	39.47215	3.62055	0.959346	1.903025	322.0315	38.77828	0.44498
1805	37.78798	-0.82674	-0.65452	0.172216	11.75943	2.192894	0.894088	48.9407	3.076143	0.384167	8.587453	81.60853	30.14288	4.566035
1807	507.3813	-0.16596	0.884713	1.050672	19.82967	0.647282	1.086554	28.58488	2.777458	1.263711	9.110232	70.76673	23.10742	4.29049
1828	0.895905	-1.31798	-0.99122	0.326766	1.21761	6.835476	0.858359	0.653311	0.907416	1.033566	5.265653	43.63674	18.61744	1.129854
1831	22.09698	-1.79247	-0.08135	1.711117	0.153414	0.613569	1.673268	164.3141	1.901162	0.717268	9.99723	221.8253	38.25096	4.714742
1844	20.67755	-0.96849	-0.51381	0.454676	6.472028	6.930986	0.317354	15.15199	2.477631	1.161852	8.833812	113.5126	11.05914	3.915188
1847	12.63081	0.247011	0.554424	0.307413	1.596772	5.609576	0.96004	18.97421	0.808897	1.510193	9.052373	113.5126	39.71247	0.057629
1850	461.9652	-0.82362	-0.7467	0.07692	7.028596	1.293452	1.030929	20.94163	0.614819	0.854916	6.983768	128.4785	41.20908	1.671571
1854	13.62691	-1.7929	-1.72182	0.071075	2.210772	3.37308	0.464579	27.05842	2.450633	0.62844	5.803167	305.6649	17.78261	4.617199
1860	139.7743	1.273717	1.38772	0.114003	11.0973	3.973642	1.115446	23.73937	2.000723	0.447136	15.58711	267.8992	42.38575	2.576197
1866	30.7652	0.600537	0.353797	-0.24674	2.834447	1.833568	0.527482	168.1409	0.310696	0.455259	16.01215	1406.069	15.06373	2.500059
1912	17.24356	-0.81278	-0.64008	0.172707	3.018003	4.271841	1.043721	8.731419	0.327005	0.534351	10.59692	120.8233	18.08991	3.946464
1921	16.71898	0.076083	0.121242	0.045159	3.333178	5.547035	1.658074	28.54754	3.454928	1.124873	8.587453	267.8992	21.37529	3.229221
1939	27.22896	-0.58557	0.177538	0.763109	6.951828	4.82834	1.075237	10.86702	1.46806	1.728186	10.41561	140.643	10.67259	4.867642
1954	9.133873	-1.42781	-1.09127	0.336537	1.664879	4.705663	0.543558	21.10344	2.226788	0.68522	10.0771	221.8253	4.059087	1.064957
1956	611.8007	-2.77516	-1.63179	1.143369	17.05642	4.935442	1.656474	41.38426	3.285595	1.166624	7.415036	7.817626	31.97855	0.141367
2015	6.999005	0.787549	1.057707	0.270158	3.654208	1.778405	1.26644	42.89586	2.589941	0.404307	10.88504	65.70899	6.022982	0.375318
2019	0.944537	-1.01632	-0.79508	0.221247	1.02419	7.099004	1.050494	7.30918	1.839609	0.480648	9.169438	136.4945	7.373809	0.864654
2028	1.991132	-1.3906	-0.44516	0.945445	0.602186	3.911993	1.047022	39.9428	1.824134	1.634376	9.62435	177.5061	14.47682	2.878915
2035	32.45227	-1.87068	-1.08571	0.784971	12.88216	5.811469	0.654409	38.51449	2.053496	1.713405	10.78678	153.6775	41.20713	4.525094
2036	29.36862	-1.03583	-0.94362	0.092214	1.948333	0.325911	1.02128	50.03649	2.747811	0.993093	8.587453	132.4403	27.27975	2.898534
2039	18.66794	-0.77654	-0.45186	0.324685	3.954143	2.276309	1.016664	16.60514	2.357547	0.482873	0.539182	0.174295	38.80163	1.191914
2041	28.1347	-2.27713	-1.16607	1.111064	12.80539	0.597545	1.358422	12.77867	2.288338	0.740761	9.842908	0.458224	28.99844	1.31111
2068	10.43162	-0.28777	1.043911	1.33168	1.705354	3.576359	0.99803	75.11959	1.886256	1.774141	12.25883	96.64332	16.45639	4.744396
2071	5.081237	0.133018	0.075143	-0.05788	0.147885	0.370823	1.495692	3.498325	2.137536	1.568706	12.00272	81.60853	30.09674	0.580975
2077	3.347457	-2.34071	-1.65754	0.683178	0.851187	2.42997	0.910245	6.173783	3.879756	0.807925	10.59692	182.6099	36.22657	4.172451
2113	6.75897	-1.58197	-1.44989	0.132087	3.613049	2.115583	0.2501	66.95312	0.875334	0.963513	8.940577	305.6649	31.31996	1.38325
2126	7.280784	-0.19423	0.026045	0.220272	1.460727	2.59247	1.082542	28.80348	0.958062	0.640269	11.41174	103.1589	10.53384	0.755111

Figure I 1 - Trace element concentration data from PXRF analysis of geologic sources as well as archaeological artifacts (cont.).

2132	18.98884	-1.71234	-1.44021	0.272134	1.091763	6.372368	1.414719	36.03342	2.100177	0.786505	8.541494	96.64332	17.47557	1.787814
2133	7.859959	-0.61885	-0.24253	0.376319	2.583802	5.30837	1.365178	11.55524	0.649056	1.592482	10.32804	1.83838	40.50999	2.757836
2153	26.75768	-1.59161	-1.11955	0.472056	6.625564	5.079105	0.395577	59.67474	1.052494	1.052661	11.64	260.854	12.70785	0.295784
2164	362.2943	-0.70806	-0.43931	0.268746	17.3539	4.556666	0.714617	18.3972	2.205651	0.795676	4.96119	78.80376	29.61887	3.847164
2169	3.400361	-0.99429	-0.50592	0.488366	0.825676	5.041088	1.406618	16.03313	3.572802	1.387529	8.833812	51.86108	40.16856	2.290771
2193	4.640737	0.238954	0.396893	0.157939	1.743865	1.897353	0.815708	38.80473	0.144095	1.319517	9.230024	167.6443	16.46843	0.04233
2203	21.13435	-0.67154	-0.75601	-0.08447	3.81135	3.906005	0.884534	31.94704	1.444687	1.333471	8.541494	357.1148	23.30076	2.597674
2225	9.629087	-1.15591	-0.94126	0.214653	2.356286	0.467899	1.399948	31.2939	0.61056	0.856627	8.634482	87.41558	42.94209	3.353915
2230	9.705229	-1.24961	-0.79143	0.458182	3.760166	1.782779	0.601056	40.07247	1.239203	0.941511	11.87902	103.1589	27.49442	2.809218
2241	8.320977	-1.01612	-0.85779	0.158327	2.97962	4.734647	0.120525	1.28966	1.713128	0.609932	8.88658	162.8811	36.09252	2.347795
2245	16.46502	-0.74213	-0.52235	0.219777	3.345318	0.909512	0.836686	29.16178	3.815534	0.948862	9.99723	117.1259	16.35787	4.528646
2246	10.84867	-2.0512	-1.87228	0.178926	0.290977	6.976052	0.694927	33.82408	2.926567	0.93407	5.56893	90.42095	7.531362	1.533235
2248	2.052951	-1.5809	-1.28243	0.298467	2.960936	4.73111	1.281831	42.87149	2.381337	1.120795	8.995831	109.9816	20.53111	4.405609
2250	13.40107	-1.13855	-0.80876	0.329789	2.287559	2.529232	1.49771	143.1149	2.909522	1.311949	11.41174	534.7222	38.63482	2.487839
2254	35.81385	-1.44801	-0.92706	0.520947	6.222531	4.581429	0.056727	26.01996	1.297381	1.537459	9.919181	51.86108	37.04909	2.258597
2262	472.6375	-0.5741	-0.32541	0.248693	16.79733	7.426046	0.570592	0.604002	0.2842	0.377018	5.005365	30.94691	37.90388	1.02432
2263	8.983653	-0.85287	-0.80586	0.04701	3.079925	5.306845	1.192031	36.62706	2.766845	1.404454	9.355461	73.38429	43.49477	4.253375
2266	3337.565	-0.73074	-0.57617	0.154571	13.96651	5.968066	0.687195	25.7859	0.526209	0.704609	35.08803	10.29297	15.77118	3.194058
2269	1051.199	-2.46945	-0.18202	2.28743	2.885558	1.776708	0.946161	1720.344	2.145805	1.258543	17.66383	385.6313	117.6047	1.74331
2278	14.33343	-1.21553	-0.30859	0.906938	2.178425	4.342362	1.69038	101.3248	3.654238	3.14045	20.53672	247.2409	39.50663	5.701154
2281	2.952458	-2.17563	-1.68831	0.487325	1.641899	7.37487	15.88711	3.616699	3.521319	1.450812	12.80783	198.6459	22.99099	5.701154
2285	8.634488	0.161749	0.029252	-0.1325	8.228097	2.588571	1.286001	10.0988	1.812393	0.948729	2.855729	700.8494	21.78088	3.025519
2298	6.259637	-1.1333	-0.85941	0.273887	1.145059	3.355582	1.071061	48.48754	1.430062	0.77033	1.639732	65.70899	30.16791	4.901628
2302	2981.241	-0.52116	-0.526	-0.00484	9.696286	4.773229	13.39479	1886.318	5.921047	22.40521	174.5043	2914.171	18.74308	68.79227
2306	73.10766	-1.58297	-1.69645	-0.11348	7.345264	7.493662	1.595335	13.99907	3.280755	0.899058	2.115116	172.5184	21.4763	4.018249
2309	27.62239	-1.47354	-1.02479	0.448745	6.414452	1.574283	0.588534	16.44161	2.74224	0.920931	6.384627	90.42095	17.74653	4.238837
2311	20.31785	-1.44919	-0.9916	0.457586	2.893328	2.529445	0.32538	39.41982	3.459531	1.620854	4.001708	0.162647	35.09054	0.252149
2327	17.06219	-1.68932	-1.65182	0.037497	3.998179	7.716176	1.718571	48.81351	3.552013	0.308758	10.41561	305.6649	5.670854	3.197202
2328	90.45604	-1.9129	-1.08733	0.825565	8.765474	1.685753	1.241131	88.25346	1.553424	3.423236	8.940577	267.8992	42.09226	3.659031
2348	31.67555	-2.41273	-1.2565	1.156223	10.69427	7.208992	13.54273	88.25346	3.235963	0.957707	9.99723	11.99557	5.449339	3.330283
2354	28.42164	-0.57904	-0.37347	0.205567	8.304865	4.195113	0.091757	9.543904	2.075636	1.571141	3.652379	56.26619	5.969384	2.776003
2370	7.47772	-1.56761	-1.24375	0.323855	1.309527	6.001274	0.937556	19.06773	0.270639	1.139903	8.782246	12.62369	41.84759	1.117823
2377	35.60359	-0.89623	-0.7404	0.155828	0.595746	3.226405	1.517258	7.781086	0.082764	0.305808	6.536038	34.36636	19.98116	4.566661
2385	22.38849	-1.01413	-0.70083	0.3133	3.909962	5.866146	0.685011	37.02786	1.960559	0.965403	3.365561	36.13605	7.512678	2.590691
2397	28.89146	-1.11357	-0.93289	0.180685	9.370022	3.135262	0.915184	17.86847	3.722305	1.47681	0.950957	65.70899	14.6346	3.420634
2410	15.87663	-1.5999	-1.50155	0.098348	1.698591	5.573754	0.315258	26.34219	3.173153	0.578617	7.801096	5.237073	22.65023	0.937925
2417	13.89604	-0.90302	-0.62747	0.275542	13.59227	6.695225	1.228054	44.71244	0.773015	1.755257	3.347793	65.70899	2.122672	0.767909
2433	5.386543	-1.17704	-0.85595	0.32109	6.711928	4.202039	0.524212	45.51526	1.013722	0.582895	7.855383	84.47863	37.60008	1.370736
2448	2.627022	-1.02698	-0.91867	0.108306	10.19528	4.200544	0.552073	19.04439	0.691246	1.12499	1.735601	103.1589	33.43241	3.805567
2494	11.79973	-0.82319	-0.59425	0.228939	0.78235	6.846131	0.578858	23.13042	2.768164	1.584908	7.821846	18.7404	35.44737	2.535547
2508	13.16003	-2.14296	-1.8551	0.287854	9.552346	6.509004	0.575039	15.49933	0.07857	0.974571	12.52701	177.5061	6.754329	2.21729
2513	2.791981	-1.20243	-1.0344	0.168031	7.719509	5.57358	0.996246	9.728778	2.425831	1.785496	1.227687	60.87889	15.68753	2.489812
2514	9.633017	-1.13061	-0.99928	0.131331	12.11448	4.99273	1.259753	38.5387	3.736199	1.498821	0.242907	93.49632	9.721044	0.231969
2528	37.03162	-1.55521	-1.3638	0.191412	3.265514	6.405869	0.894516	3.436527	1.013937	0.576048	1.212214	14.71234	36.59869	3.56759
2532	14.56693	-1.36755	-1.04932	0.318229	3.7647	6.766786	0.307223	12.63014	0.237457	0.857306	4.330133	153.6775	9.43451	4.614538
2555	38.70889	-0.8629	-0.67198	0.19092	2.376732	6.696166	1.290554	31.59964	2.850101	0.72005	6.366739	10.95314	38.58485	1.717442
2570	16.79071	0.210396	0.455931	0.245535	0.278766	0.594101	1.255929	0.300345	0.941477	0.821734	5.82357	405.7665	16.59722	1.930545
2576	5.782793	-0.81413	-0.56391	0.250219	3.961488	1.117945	1.584427	31.46395	1.099	0.925887	3.27793	47.65424	27.58383	1.407625
2605	2.831417	-0.95013	-0.38744	0.562692	1.506907	6.487674	0.444484	30.55845	2.099858	1.028468	10.41561	128.4785	8.972209	1.38325
2610	9.677707	-1.5019	-1.11283	0.389073	3.394172	4.291219	0.956944	59.67474	0.814066	3.859196	11.87902	162.8811	27.29956	4.029459
2616	18.12174	-0.50215	-0.3208	0.181351	2.394182	3.02005	23.56891	62.48595	2.494948	1.022297	13.4098	893.0907	25.19719	4.348498
2621	6.771285	-0.91696	-0.26003	0.656932	3.807665	1.61775	0.478162	31.39078	3.039632	0.844705	9.554789	204.2422	6.786619	4.137765

Figure I 1 - Trace element concentration data from PXRF analysis of geologic sources as well as archaeological artifacts (cont.).

2623	10.64006	0.205378	0.20488	-0.0005	3.827588	3.175745	1.702375	31.4575	3.575283	0.836746	7.768256	426.8506	23.3029	3.641586
2628	17.32728	-0.7231	-0.17343	0.54967	1.36925	4.562195	1.437991	149.8585	3.912217	1.19512	31.98655	2846.889	23.00595	93.97963
2651	13.01656	-1.063	-0.86545	0.197548	3.21111	3.330943	1.618469	14.18871	1.332511	1.133244	11.75813	267.8992	8.30309	7.047372
2701	15.15699	-1.01213	-0.89764	0.114491	3.0567	1.859822	1.933064	39.01545	2.486053	1.666754	8.452691	70.76673	0.16386	0.231969
2702	558.3451	-0.82274	-0.54913	0.273611	10.77104	1.92871	0.765535	50.87935	3.272795	2.728055	9.99723	128.4785	42.58936	4.278704
2717	8.228533	-0.15386	-0.33241	-0.17855	9.15891	1.383881	0.362756	12.62858	2.584792	0.762787	3.81926	590.3256	0.027645	7.290385
2725	18.63621	-0.72226	-0.75161	-0.02935	1.219399	1.093666	0.763517	46.45938	1.462562	1.205036	8.634482	136.4945	30.65228	0.767909
2727	17.69262	-2.00295	-1.57895	0.423997	3.429523	5.331739	29.72573	33.36642	1.906824	0.721617	9.486811	313.754	27.71334	4.705172
2737	8.737519	-0.99926	-0.69483	0.304424	0.982842	1.285543	0.786793	24.95244	1.557374	1.180114	0.554879	54.03828	25.527	3.832693
2741	2.334545	0.144101	0.053091	-0.09101	3.624827	7.549178	1.409469	7.222694	1.787992	1.267317	3.707945	198.6459	12.00237	4.123842
2743	3.424628	-1.3817	-0.45658	0.925121	1.242356	2.950413	1.136368	32.95756	1.387725	7.617886	11.41174	68.20875	14.39356	2.999541
2757	8.417016	-1.11739	-0.87085	0.246547	3.204906	2.240304	0.970924	25.59077	1.604441	0.929585	1.231318	78.80376	29.34966	1.474771
2775	28.36594	-1.5548	-0.97154	0.583262	15.07005	7.683514	1.262995	23.06244	0.271232	1.40187	2.374382	60.87889	13.32724	0.211694
2778	570.851	-3.0676	-2.16124	0.906356	17.8337	2.6317	0.569716	4.183039	3.673864	0.815979	2.016282	330.5017	12.9373	3.604565
2781	5.117549	-1.67904	-1.52899	0.150047	1.804452	0.055855	1.403819	29.64254	2.046744	0.984169	9.486811	103.1589	9.662216	0.490687
2805	15.68985	-1.53464	-0.81384	0.720803	0.213682	0.291809	1.257379	31.80895	2.922724	1.250235	12.95316	96.64332	7.693779	6.577816
2821	13.43791	-0.77784	-0.32015	0.457691	0.814733	3.87816	0.863099	40.80304	0.325997	1.005434	9.355461	96.64332	38.85525	0.113759
2837	17.07838	-0.68567	-0.21573	0.469933	0.123544	5.825012	1.648204	30.48933	2.316872	0.492837	9.169438	47.65424	19.90447	0.273514
2851	363.0465	-2.36928	-2.32778	0.041504	11.46195	4.953633	0.927645	42.83438	1.353354	1.127799	8.634482	132.4403	35.48205	0.140665
2856	414.5745	-2.42213	-1.87536	0.54677	12.90135	0.563761	0.398975	3.784421	1.097286	0.64446	1.830223	6.429365	36.65064	4.233094
2861	3.611198	-1.24499	-0.88084	0.364151	0.173877	5.009303	1.324873	47.69766	2.221647	0.762114	12.1293	149.2323	31.88499	2.089755
2862	304.5604	-1.96715	-0.66366	1.303485	13.64025	6.007051	0.618891	43.51837	3.890377	1.938131	9.919181	0.216973	24.74364	0.609392
2869	4.126272	-0.9055	-0.5162	0.389307	3.697894	2.0967	1.397549	21.56811	3.697486	0.702209	9.230024	51.86108	33.42575	0.836435
2877	13.22917	-1.40176	-0.69676	0.704997	1.040355	2.462222	0.413152	0.709131	2.098551	0.722914	8.587453	2.337992	3.067965	4.419633
2879	14.65225	-1.6107	-0.88281	0.727893	1.482285	4.271732	1.400589	17.69234	3.689992	1.558229	10.59692	140.643	14.14249	4.035518
2898	1.125752	-1.96355	-1.12361	0.839945	3.40265	2.70075	1.5924	2.309239	3.390544	0.738239	3.221989	117.1259	18.2738	1.575305
2909	10.57131	0.134869	0.128606	-0.00626	2.943859	3.95326	1.490212	47.75334	3.241552	1.186621	10.69076	297.76	13.97497	1.105274
2910	2.083341	-0.17133	-0.03341	0.137924	0.396389	7.525358	0.276302	38.36725	3.869747	1.763887	11.08847	1031.57	6.450497	3.038448
2918	5.166356	0.106125	0.013103	-0.09302	2.876078	6.092716	1.634991	33.55629	0.101364	0.549684	11.3015	416.1872	43.66887	2.089755
2920	9.641488	-0.21026	0.030078	0.240342	3.087896	2.730426	13.86139	237.4951	1.671477	1.052991	15.79718	1219.266	6.69194	7.290385
2921	24.05461	-0.73914	-0.45588	0.28326	0.432223	2.312263	1.332615	14.15354	0.925746	0.980072	1.262259	70.76673	1.862315	3.346863
2926	13.72217	-0.84926	-0.3755	0.473755	5.166971	7.493631	0.764179	39.44025	3.646263	0.868934	5.061856	260.854	19.03454	0.82471
2935	43.06535	-0.46011	-0.52363	-0.06352	0.988797	1.933623	0.766284	160.5745	2.364563	1.23313	5.185987	204.2422	41.03599	1.812569
2945	1.233947	-0.3645	-0.25666	0.107833	0.35899	4.036173	1.618271	143.1149	2.83668	0.948692	11.3015	1135.108	30.56621	5.094659
2949	7.467237	-2.04368	-1.27811	0.765564	2.80426	6.226251	0.619577	17.96563	1.70138	1.374846	10.50522	76.06283	41.11811	2.94974
2953	7.421577	-0.25247	-0.32232	-0.06985	3.890373	1.592203	10.60658	80.49031	2.97737	0.66096	10.24246	1056.567	41.20711	0.44458
2954	361.9182	-0.14991	-0.04776	0.102151	12.47913	2.302448	0.66833	143.1149	1.331651	1.677012	10.88504	635.5211	37.79676	3.038255
2959	3.720157	-0.33689	-0.2509	0.085991	1.75699	3.792004	1.592043	35.89709	1.338039	0.717382	5.461267	227.9614	22.72668	1.912143
2970	9.64645	-0.88701	-0.32927	0.557737	0.48495	3.350242	1.190563	48.25505	2.094362	1.354046	8.995831	140.643	16.23464	3.278455
2977	3.990846	0.174993	0.15299	-0.022	3.19065	7.071292	1.352765	88.25346	0.731972	0.873542	12.52701	2050.923	9.261901	3.899905
2991	5.623987	-2.1771	-1.98187	0.19523	1.303504	0.013708	0.842482	46.72564	3.785968	1.565134	9.842908	182.6099	41.64402	0.963652
3002	18.57428	0.004992	-0.06751	-0.0725	1.947763	2.230495	1.728747	106.099	3.011612	1.797551	8.782246	1340.913	32.59885	2.781635
3006	10.74247	-1.29333	-0.54742	0.745906	0.113408	2.560833	0.315938	14.91521	3.986077	1.663699	9.695532	167.6443	26.15498	1.168621
3009	20.47664	-1.30681	-1.38469	-0.07788	0.266739	1.014088	1.602979	28.53767	2.856644	0.607823	9.230024	124.6068	43.61926	0.514674
3039	1.948288	-1.21177	-0.70276	0.509009	3.33713	4.48174	0.194877	0.213319	2.979977	1.526391	14.60634	198.6459	23.17261	10.3677
3053	28.27041	-0.83813	-0.36743	0.4707	6.289703	5.369307	35.52976	113.6853	0.907145	2.244963	11.3015	282.4859	30.03627	0.316231
3055	239.4922	-0.58529	-0.67607	-0.09078	10.81902	1.20497	0.629493	5.953851	2.687423	0.30182	4.021009	348.0388	9.790133	3.553659
3056	40.66731	-0.16082	0.219973	0.380795	12.32559	0.867933	0.416242	86.24514	1.514108	1.45527	9.486811	290.0351	37.16271	1.153949
3078	30.3244	-0.99953	-0.00275	0.996774	3.172717	1.295319	1.206332	43.7568	1.091125	0.797354	13.4098	109.9816	4.890279	1.924439
3080	859.0033	-0.31848	-0.06926	0.249222	20.012	6.120796	0.96254	45.34508	0.528326	0.495402	9.230024	260.854	1.592489	1.749939
3108	10.68209	-0.80009	-0.59935	0.200744	14.42712	3.959143	1.17262	10.08932	0.467562	1.010651	1.279355	14.71234	13.40908	0.316231
3133	16.05007	-1.97328	-1.81204	0.161245	14.91651	3.080439	1.14522	36.50544	2.875795	0.417714	4.868882	36.13605	3.87155	0.864654

Figure I 1 - Trace element concentration data from PXRF analysis of geologic sources as well as archaeological artifacts (cont.).

3143	8.735241	-0.79469	-0.42297	0.371716	14.12964	2.230334	0.330216	8.172908	3.917509	1.430607	0.321652	10.95314	32.04667	3.478182
3153	14.99705	-1.57979	-1.51006	0.069733	15.81854	1.850578	0.853424	37.5761	2.332246	1.28324	3.618093	36.13605	5.560233	1.843329
3165	14.93329	-1.69237	-1.02306	0.669304	8.698301	2.646223	1.014264	6.016847	1.122797	0.852145	1.234165	198.6459	71.53571	1.256865
3167	4.4963	-0.72173	-0.56613	0.155605	8.96699	2.910737	0.655441	51.773	1.067787	1.135179	0.865257	16.02423	22.68435	1.143566
3190	14.3961	-1.77984	-1.46024	0.319602	16.94127	7.665935	1.909933	38.23361	2.918001	0.202777	12.52701	1.115138	16.62005	1.843329
3191	4.839085	-0.6651	-0.40282	0.262283	12.10488	2.06066	0.760146	46.2572	2.739746	1.098348	7.166375	43.63674	4.81178	1.54753
3207	0.266004	-0.50741	-0.29288	0.214537	3.266559	6.257733	1.093013	23.87329	1.862324	1.127773	8.634482	60.87889	15.262	3.864759
3212	8.238587	-0.92815	-0.36197	0.566175	2.722593	3.705364	11.32355	6.231354	3.069739	1.048079	9.052373	113.5126	23.01143	5.094659
3239	15.56716	-1.02188	-0.91304	0.108833	1.84636	0.266297	0.399853	32.27894	2.011147	0.446248	11.08847	247.2409	23.23257	4.000412
3240	419.8872	-1.04428	-0.44334	0.600938	9.101334	3.539972	1.236189	49.5457	0.926021	1.271619	9.110232	65.70899	15.38768	1.196564
3262	0.818023	-0.92805	-0.74478	0.183272	2.734615	1.909534	1.100831	3.070562	0.723515	1.382571	8.731853	132.4403	17.8782	1.155536
3272	18.99835	-1.01388	-0.60859	0.405288	3.800627	3.369148	0.638101	19.1199	0.890223	0.637019	9.486811	8.09693	23.17961	1.965123
3274	4.843074	-1.74029	-1.21175	0.528534	3.819932	6.240187	0.638269	17.85391	1.671427	0.776736	9.695532	73.38429	1.857284	0.918898
3276	892.6187	-1.98277	-1.25806	0.724711	18.66855	2.745566	1.30457	38.84479	3.241011	1.223686	3.466081	136.4945	12.44809	4.788807
3287	2.594773	-1.49066	-1.29655	0.194102	3.81091	7.793153	0.792078	16.11181	0.131738	0.518892	9.99723	290.0351	30.92161	0.281821
3291	24.6661	-0.22756	0.265044	0.4926	9.293254	1.719453	0.609996	168.1409	1.628913	1.385316	19.6044	405.7665	36.2338	1.168621
3301	6.394364	-1.62623	-0.19673	1.429498	12.48872	5.54187	0.427504	10.94933	3.485715	1.081673	3.305185	8.587463	22.15075	2.951653
3315	14.72678	-1.08039	-0.9361	0.144285	12.93014	5.464985	0.934256	20.55611	3.49394	0.731546	2.54753	140.643	39.44714	2.21729
3317	4.137583	0.449332	0.692318	0.242985	13.53469	5.881959	1.450803	5.096861	0.339081	1.023473	13.89909	204.2422	29.04204	3.350533
3381	1.277686	-1.72501	-0.6477	1.077306	8.794262	6.194955	0.497187	26.79156	2.264501	0.670201	5.385433	16.02423	18.98353	1.992381
3383	17.53785	-0.98726	-0.98167	0.005593	8.957394	1.818349	1.940795	31.12966	2.511365	0.726684	0.627911	267.8992	40.5653	1.354606
3385	3.203386	-0.29126	0.508044	0.799304	2.46224	2.981274	0.470461	1.933238	3.215864	0.884219	14.24457	132.4403	19.3893	2.364816
3399	8.397598	-0.69252	-0.25221	0.44031	13.25641	3.898411	0.624642	2.513942	2.163867	0.92036	14.06984	267.8992	31.06285	4.901628
3400	17.62142	0.22727	0.445303	0.218033	2.025743	2.451846	1.157305	24.75037	1.014237	0.729205	13.10188	472.0468	42.29324	2.35835
3402	36.0116	-1.08899	-1.00059	0.088406	2.977361	5.946044	8.535336	20.11483	2.308837	0.679054	12.6658	484.0113	41.71426	3.051669
3407	15.02963	-1.55863	-1.34807	0.210561	12.12408	7.28826	1.626682	26.46155	3.181289	0.766235	1.598572	14.71234	3.684912	0.423245
3413	14.00071	-0.72899	-0.61795	0.111038	3.928949	3.399983	1.309638	34.92898	1.784497	0.288538	1.86368	30.94691	19.028	2.922115
3422	4.788578	-0.82408	-0.5495	0.274578	16.69178	1.918945	1.027262	33.54005	1.337676	0.661522	20.53672	39.80005	0.758327	7.539058
3446	109.3559	-0.80613	-0.554	0.252127	3.796348	3.820868	1.95258	23.1142	0.391823	1.27912	13.10188	32.63695	7.062875	1.414747
3447	34.87151	-0.00416	0.64105	0.645213	9.418002	0.211709	1.263277	49.53389	0.048676	0.500188	29.75003	521.6033	53.46748	16.49392
3448	11.90539	0.16298	0.178375	0.015394	17.20996	6.030602	1.287128	22.61506	1.12598	1.516529	4.370501	149.2323	9.218409	2.617997
3456	4.480043	-0.93859	-0.76735	0.171244	8.276077	4.80417	0.968963	18.36167	1.593025	1.464199	2.05722	240.6659	27.74474	6.809892
3461	18.73271	-1.89427	-1.03424	0.860026	0.973512	4.479436	1.599438	39.02537	1.337372	1.853527	4.176131	58.54599	53.46748	2.617997
3464	1.09668	0.267433	0.228722	-0.03871	15.31955	5.820161	1.636124	12.49609	3.769086	1.490826	14.60634	215.8288	2.598578	5.701154
3466	10.38433	-0.18029	-0.04954	0.13075	1.641089	5.313999	1.023276	45.75023	3.761106	0.847944	4.048561	215.8288	27.14358	1.752654
3468	8.612555	-0.16542	-0.18775	-0.02233	1.714597	2.881773	0.999376	13.60619	2.408868	1.31497	9.99723	700.8494	6.113769	0.673366
3472	5.864516	-0.72764	-0.78257	-0.05493	15.04126	2.421111	0.968403	3.43478	2.534122	1.103275	4.724659	221.8253	19.81272	1.607993
3479	10.24745	-1.79519	-1.05404	0.741154	7.182132	2.694967	1.274859	5.083856	0.403203	1.299264	3.139551	32.63695	35.57933	4.961407
3518	17.73759	0.293985	0.274971	-0.01901	2.558874	1.959382	1.778679	35.03373	3.627357	0.828062	11.52456	267.8992	30.69495	7.047372
3541	349.3183	-0.05006	-0.04961	0.000451	10.65589	3.639318	1.240904	4.668194	0.421648	1.488198	8.833812	234.2405	10.82722	0.964124
3542	23.58114	-0.64355	-0.37581	0.267743	11.15488	7.038063	1.628613	7.972449	1.705054	0.941725	8.995831	221.8253	11.24402	0.022037
3550	12.2192	0.419284	0.545474	0.126191	3.685775	4.065083	1.091236	36.6935	1.721728	0.288285	9.99723	357.1148	42.67405	4.496485
3598	17.60704	-0.48627	-0.3806	0.105674	2.7764	1.958913	0.888127	11.22918	0.936094	0.872212	10.15883	158.2264	41.42222	1.471147
3602	24.42888	-3.31303	-2.82618	0.486847	0.02589	6.67392	0.725536	46.72157	0.931246	1.35391	9.169438	172.5184	65.39009	2.05217
3665	6.735289	-1.75768	-1.91501	-0.15734	0.272322	5.315685	0.659445	24.54412	0.634914	0.762943	10.41561	385.6313	15.84754	1.116964
3745	7.883762	-1.44321	-1.25579	0.187423	2.693728	0.309743	1.529402	45.75422	3.462531	1.176277	7.376118	117.1259	25.61063	0.178465
3758	9.484963	-1.60206	-1.61695	-0.01489	3.660806	3.963439	0.71861	61.06416	1.617808	1.474521	1.016702	260.854	31.24427	3.71955
3765	18.47808	-0.77672	-0.36277	0.413953	1.301293	2.513257	1.425707	19.73655	0.67109	1.327345	9.052373	149.2323	43.38151	2.766465
3775	5.647894	-0.48045	-0.64507	-0.16462	0.50818	4.558663	0.836571	27.93653	2.113359	0.02787	8.634482	496.2546	0.658136	1.925196
3779	5.371961	-3.45425	-2.82948	0.624762	0.386131	2.371645	16.66098	16.93368	1.054104	2.739837	14.24457	437.7624	5.631788	1.168621
3781	27.20822	-0.88367	-0.84228	0.04139	2.704322	2.338457	0.601169	15.30423	1.460961	1.382095	17.66383	132.4403	31.09238	1.141253
3782	6.785274	-0.65487	-0.64829	0.006581	2.633422	7.114271	0.089379	121.8142	0.245499	1.071757	0.025723	1082.147	34.3498	4.145123

Figure I 1 - Trace element concentration data from PXRF analysis of geologic sources as well as archaeological artifacts (cont.).

3783	2.767189	-1.67415	-0.7898	0.884354	2.220151	1.615687	1.017173	121.8142	0.140594	1.033872	13.89909	437.7624	222.5603	0.490687
3799	4.391003	-1.50534	-1.09068	0.414664	0.195208	2.894037	1.204372	24.26239	3.564691	1.502472	9.919181	158.2264	22.9807	3.913291
3812	36.60697	0.219173	0.069775	-0.1494	1.902474	2.052248	0.88566	88.25346	2.801498	1.364372	9.292021	1620.548	7.967885	0.645982
3818	1.451228	-0.78419	-0.40364	0.380557	3.679177	5.944393	0.892762	33.59343	1.706083	1.386569	0.483285	27.68136	10.81913	1.256101
3834	8.391815	-1.18088	-1.24097	-0.06008	2.657269	1.412915	0.878541	36.79317	1.321501	0.628817	9.919181	144.8882	39.69642	2.900932
3835	10.26832	-0.11722	-0.12952	-0.0123	2.671598	7.13451	1.230308	36.93753	1.538672	1.392393	1.745293	534.7222	2.906107	0.347467
3839	15.29984	-1.23445	-1.07916	0.155294	0.93219	4.15391	0.663391	12.19466	3.021318	0.584182	8.731853	149.2323	35.46068	3.553177
3842	1.650833	-1.07249	-0.73119	0.341305	0.636662	4.354061	0.869519	124.651	1.753742	2.351007	14.06984	651.2935	14.8473	3.507435
3855	1.391568	-0.84657	-0.85207	-0.0055	3.092414	1.53201	1.144332	70.10734	1.46437	1.532483	9.768372	496.2546	24.61648	0.864654
3857	11.44351	0.224791	0.085201	-0.13959	0.786336	6.897386	0.321844	61.06416	2.674293	0.939203	14.60634	1309.443	23.96649	5.292187
3874	16.19178	0.577181	0.482751	-0.09443	2.443054	3.63226	1.094422	18.83598	0.480243	1.151243	9.230024	260.854	18.81689	1.206876
3887	1.638365	-0.4804	-0.42933	0.051076	1.658053	3.12498	0.371016	65.42964	3.801443	1.034974	9.99723	718.1435	1.75258	3.667991
3894	32.09947	-0.73577	-0.60596	0.12981	13.7458	7.960109	0.840295	34.90464	1.942097	0.597586	8.541494	426.8506	25.6853	4.548054
3908	34.80129	-1.87419	-0.61868	1.255512	3.503489	2.951186	1.165481	82.36459	2.215037	0.686224	12.80783	140.643	30.62788	2.481341
3910	4.595529	-0.90132	-0.6053	0.296011	1.100174	6.009491	1.933932	35.44335	0.732017	1.10852	7.225605	58.54599	21.36587	1.135623
3927	16.63981	-0.64923	-0.30671	0.342523	1.157289	5.111773	1.330381	8.181515	3.889527	1.018414	5.517029	36.13605	41.6266	0.623752
3929	13.40948	-0.98942	-0.86071	0.128703	11.06852	2.938263	0.784336	22.44899	0.477832	1.166812	6.322559	60.87889	3.111113	3.759331
3943	2.560233	-2.71585	-0.96762	1.748227	2.987283	2.947622	0.171976	394.1273	1.317902	1.117888	15.1812	63.26614	73.16261	1.657625
3961	13.37624	-1.36253	-1.14643	0.216092	1.334378	0.126566	1.049219	48.94831	0.75751	0.479207	0.860707	124.6068	40.85989	1.193762
3965	14.52085	-0.4337	-0.41203	0.021675	2.679342	5.833086	1.796498	26.14319	2.771791	1.391862	5.047598	187.8327	11.30084	4.869856
3968	521.5327	-1.18572	-0.45104	0.734679	11.75943	0.276685	0.908164	4.81876	3.62404	1.514116	8.833812	41.69631	21.88945	2.640877
3971	17.60316	-1.10391	-0.74771	0.356206	2.180431	4.520062	0.782282	35.217	2.775458	1.633362	9.355461	32.63695	4.949747	1.843329
3977	0.774038	0.312535	0.1748	-0.13773	2.949368	2.189227	1.2659	24.09718	2.8969	0.501858	7.377551	416.1872	10.99141	4.682344
3990	17.2529	-0.1028	0.480065	0.582862	0.080779	0.562536	0.138842	43.57974	2.29822	0.193015	10.0771	43.63674	31.04816	2.480318
3991	8.089229	-1.49266	-1.23626	0.2564	1.204596	1.993279	1.290895	49.02308	2.41922	0.991029	0.744366	128.4785	38.10822	2.822305
3998	152.6093	0.144652	0.215625	0.070973	13.67863	7.008271	0.637736	101.3248	2.010253	1.154212	10.78678	635.5211	31.39359	0.673366
4006	13.22026	-1.75483	-0.81791	0.936923	1.739797	5.093677	0.917133	38.33764	3.200984	1.169137	8.782246	106.531	58.46282	4.936919
4008	16.27251	-0.69651	0.010203	0.70671	0.897219	6.324199	17.13896	654.0721	0.989036	1.039979	24.15347	753.9495	21.66626	4.901628
4033	4.212459	0.018768	-0.13715	-0.15592	2.229675	0.517485	0.85246	3.502994	0.998159	0.760763	1.758822	282.4859	22.40817	2.424091
4037	806.1119	-0.89105	-0.82542	0.065631	14.54227	6.101726	1.137174	28.255	1.031868	1.647657	9.768372	63.26614	24.36997	2.303004
4038	726.2811	-1.43309	-1.17629	0.256799	8.237693	6.061444	1.531147	37.62517	3.580885	1.264262	3.29196	56.26619	22.60254	1.744119
4041	48.42501	-0.35553	-0.49056	-0.13503	1.046316	3.237275	0.586134	6.313521	3.612126	1.730539	6.247982	247.2409	1.79343	0.986253
4045	40.61152	-0.60875	-0.51437	0.094376	2.420314	0.232256	0.316327	38.59419	3.132576	1.516309	2.549998	221.8253	27.02453	1.27092
4049	14.24404	-0.79859	-0.25669	0.541906	3.146829	2.793834	1.137725	48.52574	1.090271	1.575103	10.50522	182.6099	2.269771	2.900932
4052	9.87568	-2.93667	-2.1279	0.808775	0.069213	2.752261	1.13309	31.51363	1.271298	0.844315	10.15883	260.854	37.54086	0.482913
4074	9.979132	-0.71914	-0.98035	-0.26121	1.749947	5.394365	1.028751	16.43999	2.113768	0.757505	5.751856	172.5184	23.62395	3.200644
4078	3.32932	-0.27266	-0.50578	-0.23312	2.796375	2.00858	1.166306	7.477184	3.903794	1.049473	2.368601	322.0315	16.72012	0.291849
4085	19.32503	0.631226	0.432949	-0.19828	2.304368	7.011799	0.783934	1.691239	2.02506	0.86588	7.689858	521.6033	32.6841	0.231969
4088	0.524122	-0.93951	-0.59474	0.344768	1.880249	4.732344	1.265083	65.42964	2.596989	0.973239	11.19376	234.2405	6.682039	3.197202
4091	27.89082	-0.51264	-0.35316	0.159476	6.260915	3.07083	1.538524	8.294284	0.089014	0.774814	8.940577	128.4785	27.25528	1.047613
4109	18.37886	-2.30607	-2.19597	0.110098	6.5392	7.410328	1.084703	51.30249	1.481779	0.423633	1.130205	26.10412	14.07661	3.76215
4129	16.73929	-1.68753	-1.18536	0.502176	14.36954	1.136543	1.4198	41.21916	0.461252	1.292698	3.332269	63.26614	11.40408	0.069157
4137	6.268753	-0.96992	-0.84473	0.125187	6.644756	6.284605	0.820604	44.92804	0.498979	0.950777	1.253759	49.73345	19.9132	0.402455
4138	0.467314	-1.39645	-1.23832	0.15813	17.48824	3.110659	0.659765	42.81807	1.027719	0.713038	12.6658	70.76673	23.60439	6.351024
4155	36.39549	-0.94871	-0.14287	0.805834	3.095093	4.509955	1.05145	48.25964	3.930989	1.375569	14.06984	32.63695	20.14545	2.627459
4161	15.81553	-1.73557	-1.64028	0.095285	3.94865	0.750674	0.898158	13.25645	3.504326	1.509602	1.010722	240.6659	23.54614	3.126333
4164	3.68945	-1.5757	-1.46672	0.10898	7.556377	2.533387	1.296692	4.622844	2.610963	1.153763	0.468042	93.49632	39.47517	3.662856
4183	34.94208	-1.51354	-0.46679	1.046744	3.26649	5.928095	0.130872	0.474676	2.781085	0.714385	16.23212	9.895487	42.58219	2.70172
4187	3.729092	-1.11204	-1.09413	0.017917	2.309714	1.973786	0.961005	17.84537	0.728614	0.89556	1.771347	81.60853	21.04465	1.862767
4190	34.45779	-0.20365	-0.16827	0.03538	0.639739	2.270097	1.600654	11.90997	0.816525	0.098173	12.39138	305.6649	4.590822	2.129324
4191	114.8096	0.116756	0.524552	0.407796	3.987654	2.928148	1.36258	44.5866	1.383569	1.4472	12.95316	322.0315	25.02982	3.359469
4192	7.127848	-0.72586	-0.40047	0.325389	7.517993	3.205006	0.973984	26.37644	3.848828	0.817422	3.522891	3.715243	31.29549	1.857919

Figure I 1 - Trace element concentration data from PXRF analysis of geologic sources as well as archaeological artifacts (cont.).

4208	1.188515	-0.77461	-0.38206	0.392543	2.845261	6.643237	11.61944	51.12278	3.755988	0.749056	8.995831	54.03828	120.3046	0.621097
4211	3.087625	0.060705	0.097174	0.036469	3.977055	1.684419	0.401634	22.61107	0.450816	0.990902	3.551438	81.60853	24.59738	3.479759
4212	24.57263	0.650003	0.888426	0.238423	11.29882	6.197063	1.199061	10.06066	3.766592	1.582829	10.50522	90.42095	34.28545	4.170026
4221	4.844765	-0.32216	-0.47874	-0.15658	0.50743	1.405209	1.3356	47.15617	1.265331	1.451776	3.636699	282.4859	28.13284	2.054802
4227	14.62986	-1.66291	-1.18833	0.474585	0.804149	3.521805	0.984573	27.7276	3.962668	0.508825	9.919181	34.36636	31.51877	4.86846
4234	28.00255	-1.82179	-0.64209	1.179705	3.645231	2.435065	1.601162	116.3328	3.107124	1.20644	10.41561	109.9816	32.13565	1.928125
4237	5.933638	-1.43623	-1.41328	0.022955	0.228571	4.291434	0.45787	37.85026	3.649732	0.304485	3.102556	117.1259	15.99305	2.09084
4244	17.15969	-0.85127	-0.71805	0.133219	3.588212	0.452268	1.558492	38.38089	3.579016	0.50306	12.6658	87.41558	41.22167	1.501848
4248	8.243256	-1.41956	-0.87795	0.54161	1.142209	2.919716	1.033164	44.99495	1.090261	0.778634	10.15883	43.63674	33.41675	4.204701
4250	6.087865	-1.88221	-0.94229	0.939921	3.527823	4.450787	1.56444	35.81452	2.277659	0.647438	12.1293	162.8811	25.94548	1.286838
4256	17.27763	-0.41444	-0.43715	-0.02271	0.962368	4.118707	1.47124	15.81145	2.608042	1.755356	3.016056	204.2422	15.08185	0.231969
4259	80.9591	-1.26739	-1.04444	0.222956	9.629114	2.75748	0.720467	88.25346	0.519102	1.034592	9.42038	290.0351	33.25064	3.837889
4260	0.398214	-1.74283	-1.15265	0.590178	0.27631	7.499583	0.965764	1.127219	0.590041	0.445776	9.842908	144.8882	8.900768	0.489056
4265	24.74361	-1.05781	-0.26045	0.797356	10.43518	1.611968	1.313231	13.79936	2.092395	0.649925	8.940577	39.80005	32.44489	2.638521
4277	17.75757	-0.79361	-0.58884	0.204766	2.485017	0.520959	1.047268	18.32018	1.172047	0.878559	3.271754	290.0351	19.12659	2.900932
4306	6.747927	-1.46489	-0.72945	0.735449	0.893901	5.557399	1.111315	21.74585	3.229871	1.826778	13.89909	47.65424	18.92617	1.731684
4314	791.3963	-0.83245	-0.55921	0.273241	13.92813	4.503414	1.023479	18.08095	3.762417	0.801197	0.832551	54.03828	37.6578	2.769412
4319	7.132606	-0.93965	-0.62311	0.316538	1.356908	0.145419	1.661928	1.701216	3.627726	1.596657	9.42038	43.63674	95.90907	2.456956
4325	12.68127	-1.65228	-1.27194	0.380337	2.419688	0.499646	0.280011	1.237261	3.729975	1.351054	3.155916	76.06283	24.83623	3.021927
4326	6.694544	-1.28491	-1.23323	0.05168	2.346837	7.865193	0.499777	19.51646	0.815229	1.49993	2.874386	187.8327	2.388703	2.442503
4328	14.94447	-1.23566	-0.65762	0.578045	0.002077	4.711391	0.683645	11.92626	1.146058	2.504183	11.08847	124.6068	10.75729	3.350533
4329	33.71382	-0.77292	-0.75059	0.022335	6.481624	6.183914	1.850775	31.64005	3.097065	2.445269	8.682607	2.73018	16.29793	2.5022
4331	7.813759	-1.00245	-0.73347	0.268984	0.743506	0.558412	0.969439	35.28579	1.027167	1.014131	9.486811	10.17956	47.83679	3.944043
4346	232.7692	-0.90308	-0.46024	0.44284	14.27358	5.004727	1.235584	12.22923	3.062326	0.85694	10.24246	8.875397	35.85167	4.572664
4355	20.18804	-1.98077	-1.51143	0.46934	1.037331	1.510286	0.190922	11.2403	2.160708	2.598445	10.32804	7.851355	80.0581	2.706027
4365	8.876291	-0.70037	-0.44928	0.251095	0.495911	7.215528	0.194157	17.99851	0.69356	1.410146	8.4098	90.42095	5.447437	2.793506
4403	2.887052	-1.5042	-1.31533	0.188877	2.501753	2.388448	1.420469	10.75802	3.386875	1.475509	9.169438	11.51906	20.06126	2.931439
4404	9.824258	-0.91194	-0.53756	0.374372	2.517298	6.81363	1.673016	31.84181	3.913779	1.192767	5.856843	3.990142	7.315648	4.666639
4418	5.982513	-0.53286	-0.19896	0.333905	3.577728	1.03672	0.293618	14.7978	3.52591	0.485398	8.682607	4.749854	10.26183	3.110175
4424	361.9182	-1.0175	-0.0334	0.984095	8.333653	6.822351	15.07909	82.36459	3.332789	0.953015	18.45737	49.73345	38.86947	4.696419
4438	492.1016	-1.12008	-0.99547	0.124612	13.06449	5.631109	0.750344	43.54932	3.832499	0.428377	2.317088	204.2422	11.73466	1.512505
4441	0.835176	-0.71455	-0.52842	0.18613	1.082856	5.485166	1.162736	7.595544	3.52395	1.834902	3.167818	90.42095	35.2147	3.135683
4464	16.2592	-1.84999	-0.08779	1.762202	1.233718	7.588603	0.11738	38.98026	1.455896	0.408327	8.940577	47.65424	7.487984	1.089034
4481	10.87785	-1.61402	-1.05285	0.561163	2.622015	7.596866	1.043938	343.2738	2.931906	1.598408	9.695532	78.80376	19.32498	2.177602
4486	15.21612	-0.84871	-0.3736	0.475115	1.877944	4.822281	1.021501	3.671057	1.284054	1.016488	11.52456	253.9691	0.957671	2.347795
4488	1.113876	-2.15799	-0.39521	1.762774	3.377796	2.958047	1.481812	226.8072	2.357221	0.795604	15.58711	81.60853	279.7491	3.599813
4490	386.7889	-1.72552	-0.06121	1.664312	12.62307	2.312884	0.370237	44.11248	2.537928	3.27006	9.230024	2.902209	1.925174	3.341269
4503	28.1347	-1.05681	-0.98389	0.072927	7.738701	3.254278	1.525666	45.14659	3.075153	1.456287	3.381945	182.6099	3.242287	3.697855
4525	649.6474	-1.77812	-1.74135	0.036768	15.09884	4.420579	1.305346	59.67474	3.009151	0.529467	9.230024	496.2546	28.38739	3.053853
4535	525.5289	0.204847	-0.18864	-0.39349	13.83217	6.718339	0.403787	36.09441	3.933353	0.18083	1.184453	416.1872	18.54782	2.777016
4536	400.094	-1.35564	-1.28569	0.069947	16.57662	1.38715	1.294631	33.49059	0.10303	0.580681	9.62435	124.6068	41.96664	4.901628
4563	38.52152	-0.03845	0.279131	0.317582	0.64267	1.801392	1.430826	48.38378	3.292279	1.23355	13.25407	78.80376	3.279449	2.903009
4601	37.94269	0.477119	0.410044	-0.06707	14.49429	0.833445	0.840146	33.0011	0.30927	0.452791	9.169438	149.2323	16.67081	4.951379
4603	3.90221	-0.1061	-0.25433	-0.14823	0.754407	4.304603	0.817135	29.52659	3.971785	1.669882	1.325088	683.949	41.59216	3.094243
4615	9.583662	-0.8029	-0.60403	0.198877	3.530074	3.473873	10.83419	3.563395	2.743916	0.549028	12.95316	187.8327	28.30916	9.449734
4617	5.371535	-0.61345	-0.5021	0.111346	8.295269	2.6033	1.129324	16.1667	2.572056	1.001242	5.633489	34.36636	30.67847	2.847074
4621	2.381564	-1.83247	-1.46031	0.37216	2.165501	3.757485	0.715972	33.12094	3.744175	1.170109	8.541494	140.643	37.1503	3.537914
4632	39.27125	0.187747	0.189186	0.00144	13.11247	1.748429	0.899585	24.78611	1.760535	1.061455	8.782246	416.1872	0.545115	3.034051
4634	584.3912	-1.10238	-0.60325	0.499125	10.30083	4.083622	0.620671	168.1409	1.812633	1.027812	6.407335	113.5126	41.40269	0.259321
4644	32.5868	-0.57504	-0.17651	0.398523	7.805873	6.735801	0.928725	30.1903	0.797872	1.135313	0.050632	96.64332	36.89768	1.123152
4646	511.9417	-0.81713	-0.4499	0.367232	10.65589	5.688172	1.154134	51.50174	3.474556	0.900798	8.833812	68.20875	41.28238	3.325969
4760	4.520491	0.124204	0.659911	0.535707	0.491904	0.602538	1.186645	20.95951	1.040373	1.152715	7.709537	96.64332	11.7835	1.482414

Figure I 1 - Trace element concentration data from PXRF analysis of geologic sources as well as archaeological artifacts (cont.).

4762	12.44377	-0.88592	-0.82989	0.056032	1.171009	4.31792	16.39923	17.17448	1.082384	1.496109	4.778694	144.8882	26.38889	0.358632
4767	10.49668	-1.44003	-0.89867	0.541364	0.160603	5.217579	0.504925	32.20099	1.375354	0.90485	10.24246	149.2323	58.46282	0.149626
4776	464.41	-1.02126	0.282778	1.304035	1.94173	3.950559	1.481123	8046.563	1.843668	0.444164	22.60617	395.583	114.9661	3.558261
4777	365.0682	0.326646	1.926576	1.599931	20.4726	3.171312	0.571019	68.51207	2.755354	1.464284	8.634482	6.633284	5.789542	0.447791
4780	35.931	-0.65613	-0.80047	-0.14434	1.473627	1.964026	1.177371	22.78407	3.635406	0.41926	9.110232	54.03828	19.62541	2.46448
4786	6.03484	-0.85461	0.620247	1.474855	2.924664	1.434123	1.178805	4.147665	2.343474	0.299936	7.358144	0.7833	33.68966	1.443637
5026	0.444013	-0.4193	-0.43291	-0.01362	0.205353	3.173946	1.618987	44.31378	3.143124	1.086083	1.636016	144.8882	28.4464	4.726482
5027	16.85272	-0.50083	-0.08905	0.411781	0.96192	2.706993	1.327142	46.37595	0.47275	1.178012	0.846516	437.7624	4.651839	1.873825
5047	167.5129	-0.39386	0.528814	0.92267	3.611919	5.985539	1.42166	90.30857	1.580949	1.390199	16.01215	37.94696	51.13713	1.101848
5062	4.065212	0.346158	0.414188	0.06803	9.523558	5.869147	0.177087	22.87365	1.517464	1.14598	7.212663	198.6459	2.1724	4.412238
5063	18.87487	0.323378	0.318392	-0.00499	2.912235	4.750796	0.480363	51.65111	2.783934	1.127255	6.661968	198.6459	36.86993	1.625835
5072	14.61731	-0.1375	-0.21802	-0.08052	7.422032	4.937487	0.653499	35.59747	2.19886	0.600885	6.419858	561.8839	35.87113	0.490687
5074	629.3371	-0.15761	0.866085	1.023692	16.83572	3.432299	0.702856	211.6704	3.938132	1.175075	14.98515	683.949	151.0168	4.387144
5076	8.743847	-0.53104	-0.54977	-0.01873	1.81056	2.774642	0.656571	13.38765	1.477889	0.980923	6.97254	90.42095	19.76137	2.934579
5084	9.921593	-1.27481	-1.03729	0.237517	15.33874	7.09915	0.490204	37.51623	0.630826	0.771273	0.669448	56.26619	12.75296	1.965123
5089	35.67378	0.218219	0.293373	0.075155	3.886751	6.260256	1.833968	10.2648	3.569856	0.261083	1.32623	117.1259	27.74868	1.996741
5091	6.112016	-1.05442	-0.81159	0.242827	6.001823	1.236033	1.161047	34.16388	2.814458	0.372762	0.232989	149.2323	30.49579	4.104902
5092	37.29596	-0.29313	-0.0478	0.245325	1.136491	4.177782	1.39676	136.6748	0.468426	0.220166	13.25407	172.5184	13.0401	3.790902
5093	0.064842	-0.4385	-0.16259	0.275909	13.88974	6.498419	1.354589	18.13911	2.930689	1.766007	1.293332	267.8992	37.56098	2.466436
5094	9.277439	0.876584	0.895945	0.019361	9.63871	5.520383	1.159838	32.1456	2.809522	0.808072	12.1293	187.8327	19.72539	1.031791
5095	4.903099	-0.29487	-0.17225	0.122617	5.819499	4.714636	1.059747	9.245738	3.616925	0.459449	2.139193	791.443	40.58858	4.380809
5098	34.328	-0.2623	-0.14408	0.118222	2.014741	6.364988	0.830455	37.08806	1.454801	1.3259	2.76598	39.80005	28.20878	2.59312
5113	14.79273	-0.12796	0.566044	0.694006	8.679109	4.125058	1.410297	49.69456	2.054941	0.836909	6.457681	253.9691	0.655584	1.022098
5114	16.68485	6.88E-05	-0.06306	-0.06313	9.456386	2.117652	0.698084	15.3207	1.907046	1.229116	6.617538	167.6443	41.67246	2.545021
5115	5.454155	-0.13162	0.044159	0.175776	0.684473	5.761191	1.437209	34.02601	3.557709	1.264011	6.184435	103.1589	34.44615	2.544042
5153	15.64696	0.113965	0.163464	0.049499	2.100858	2.618886	0.261945	40.81219	1.594037	0.913915	2.568581	149.2323	38.17701	3.128027
5174	0.971571	-0.23151	-0.38619	-0.15468	7.230112	2.456112	1.073531	48.78753	2.812007	0.989071	2.146894	620.1078	1.427678	2.451672
5175	1.273916	-0.22876	-0.33194	-0.10318	2.968813	0.721574	1.377034	30.78054	2.365793	0.902357	6.849831	1219.266	26.42546	1.263789
5229	17.52403	-0.36144	-0.41391	-0.05247	0.920996	3.314691	1.862087	7.057412	3.820531	0.863104	4.318663	290.0351	8.234741	2.894018
5272	9.765001	-0.3269	-0.26895	0.05795	3.011628	2.477658	1.040232	6.352882	3.71438	0.40621	3.956081	508.783	36.51019	1.017293
5285	35.30446	0.167577	0.174116	0.006539	2.661154	3.443204	1.193319	21.86273	3.072956	0.800438	2.262491	339.1693	26.75175	4.110418
5288	4.332096	-0.02844	0.045591	0.074029	2.683806	4.240985	1.470802	38.22661	3.135249	1.289318	5.39944	113.5126	43.92246	3.676859
5289	37.89375	0.751506	0.66972	-0.08179	0.847065	4.728206	0.398675	40.80954	2.653846	0.303656	12.25883	405.7665	8.088155	2.062745
5291	1.420571	0.544344	0.368628	-0.17572	7.21092	7.883796	1.319392	42.03142	1.980996	1.002296	7.448186	437.7624	26.65411	4.062804
5292	10.08152	0.4824	0.361894	-0.12051	2.339322	1.250257	0.984909	31.07813	0.024611	1.023626	5.931305	322.0315	15.03545	3.075409
5293	16.78189	-0.08195	-0.16051	-0.07856	5.349295	6.407187	1.114406	41.92587	1.186589	1.484105	6.58169	103.1589	20.9916	1.126485
5294	18.85647	0.484159	0.378486	-0.10567	1.848248	1.74192	1.364199	22.75834	0.323337	0.591667	2.497706	385.6313	2.205946	2.586309
5295	1.924374	-0.13759	0.321983	0.459577	7.719509	7.541442	0.790721	13.06251	3.524982	1.474382	2.921435	140.643	33.98418	0.572575
5305	16.30054	-0.10116	0.488643	0.589808	7.604357	7.61275	0.23153	3.049693	3.610922	0.64123	5.13635	405.7665	26.54636	1.645049
5346	9.087274	-0.72797	-0.22166	0.506306	2.233348	4.052938	1.340226	38.65183	2.05913	1.308191	0.9426	240.6659	30.4025	2.417302
5347	1.635012	-0.72899	0.284177	1.013165	5.099798	3.162556	1.489263	22.7273	3.22738	1.213092	12.52701	177.5061	63.94011	0.519447
5596	19.32503	-1.19873	-0.38959	0.809141	4.485654	4.263755	0.698152	11.56318	0.65812	0.740434	0.936774	20.14611	27.34902	2.481341
5701	1.100545	0.06492	-0.04038	-0.1053	10.11851	7.814653	0.892284	15.73118	1.716421	0.174131	1.197399	260.854	20.25624	0.730362
oldhwy95_1.1	36.6221	-1.04693	0.257201	1.304128	0.171052	3.380096	1.215492	35.4434	3.957378	1.536922	14.24457	260.854	50.01159	5.701154
oldhwy95_1.10	32.9102	-0.96463	0.499384	1.464012	1.512502	4.645936	0.917599	101.3248	0.447709	1.199546	15.1812	437.7624	50.01159	5.912809
oldhwy95_1.11	35.73161	-1.07495	0.941753	2.016698	2.223968	19.07611	0.072707	254.4788	2.163679	0.921906	19.01768	426.8506	89.62039	11.69458
oldhwy95_1.12	34.47587	-0.38256	0.682136	1.064696	0.072142	7.127289	1.214508	4.84213	2.719384	0.331764	16.23212	339.1693	38.93632	26.01831
oldhwy95_1.13	3.175758	-0.67018	0.674335	1.344514	1.096136	1.901057	1.072874	14.55267	1.331228	1.417866	16.23212	267.8992	48.91167	12.04584
oldhwy95_1.14	16.64541	-1.01467	0.615643	1.630311	1.817618	1.025007	0.751361	106.099	2.026732	1.295688	15.79718	366.4023	55.90765	8.593038
oldhwy95_1.15	13.87811	-0.97607	0.935116	1.911187	0.643953	17.39943	0.952122	193.0479	0.408691	1.060007	18.18675	405.7665	104.9991	14.33205
oldhwy95_1.16	38.35146	-0.66646	0.681467	1.347923	1.129088	6.581044	1.026662	48.53355	3.159084	1.077257	16.23212	227.9614	63.94011	11.35132
oldhwy95_1.17	35.72313	-1.03871	0.703474	1.742188	3.526902	6.694852	0.480578	168.1409	0.230884	1.381678	16.68756	215.8288	83.75145	7.290385

Figure I 1 - Trace element concentration data from PXRF analysis of geologic sources as well as archaeological artifacts (cont.).

oldhwy95_1.18	35.02643	-1.07578	0.405145	1.480923	3.519125	0.480081	1.407284	46.58728	2.769312	1.131059	14.06984	234.2405	54.67352	4.528646
oldhwy95_1.19	363.9868	-0.26372	1.184641	1.448363	3.349289	2.897331	0.829576	30.14357	0.962961	0.915437	16.23212	339.1693	59.78522	8.872054
oldhwy95_1.2	35.63302	-1.04595	0.669395	1.715346	3.352649	3.81208	0.137205	28.74047	1.437449	0.945292	17.16446	297.76	87.61886	7.539058
oldhwy95_1.20	35.05331	-0.90178	0.688592	1.590372	3.451102	7.672598	0.189347	412.7008	1.92637	1.572687	16.23212	635.5211	57.17053	11.69458
oldhwy95_1.21	33.47438	-0.84035	1.087225	1.927578	1.595279	6.244889	0.332479	160.5745	1.953409	0.544319	17.92228	700.8494	107.4055	9.748705
oldhwy95_1.22	36.15678	-0.99695	0.50583	1.502783	3.602084	19.94385	0.848801	108.5697	0.692001	1.406809	14.79356	496.2546	59.78522	12.7731
oldhwy95_1.23	37.78798	-0.24612	0.749853	0.995974	0.747272	7.048461	0.614967	35.66609	0.463148	1.380509	16.23212	339.1693	40.37616	26.70321
oldhwy95_1.24	39.14523	-1.01746	0.63482	1.652283	3.079997	2.751746	1.152358	1.591586	3.133073	0.896047	16.23212	290.0351	66.87384	7.539058
oldhwy95_1.25	332.6751	-0.15154	1.248742	1.400281	3.543359	2.599074	1.255608	4.468534	0.518507	0.123382	16.23212	339.1693	71.53571	26.70321
oldhwy95_1.26	9.353485	-1.01581	0.409854	1.425665	2.899147	7.905024	0.431429	10.79395	0.370905	0.222217	14.06984	339.1693	1.771992	8.872054
oldhwy95_1.27	38.31637	-1.00769	0.757153	1.764844	2.411583	3.920989	0.955808	86.24514	1.540313	1.690501	17.41127	322.0315	65.39009	6.351024
oldhwy95_1.28	27.22144	-0.97006	0.552813	1.522869	0.882737	15.79822	0.569844	88.25346	2.455391	0.502679	17.66383	357.1148	18.88174	5.494316
oldhwy95_1.29	36.10288	-0.95191	0.591908	1.543817	3.387803	11.41415	0.559018	50.96345	3.866209	1.247303	14.98515	282.4859	37.11421	4.000412
oldhwy95_1.3	5.022086	-0.99839	0.875543	1.873937	1.113543	13.5305	1.643635	47.63919	2.899761	0.906078	19.30766	339.1693	71.53571	4.000412
oldhwy95_1.30	8.789368	-1.09481	0.626322	1.721136	0.147616	3.673274	0.334011	43.8795	2.771005	0.725054	16.92326	297.76	41.20665	6.809892
oldhwy95_1.31	8.858739	-1.14618	0.441827	1.588007	1.187729	5.370735	1.019885	0.429252	2.150803	1.12358	16.23212	234.2405	33.12769	4.172451
oldhwy95_1.32	36.19626	-0.66166	0.69182	1.35348	0.612897	3.344794	1.578444	23.51494	1.343266	1.140709	16.23212	260.854	11.30056	12.7731
oldhwy95_1.33	36.19626	-0.6421	1.01018	1.652283	1.658144	4.564255	1.231335	5.766577	1.955823	1.142117	16.23212	590.3256	73.16261	8.872054
oldhwy95_1.34	10.22431	-0.47206	0.708989	1.181047	2.763914	6.874005	0.900506	18.45202	2.827774	4.118416	16.23212	753.9495	48.91167	25.34899
oldhwy95_1.35	39.04141	-1.04704	0.460059	1.507095	2.122925	7.624787	1.173064	62.48595	2.491691	0.19326	13.73222	305.6649	13.1698	3.667991
oldhwy95_1.36	35.02509	-0.47171	0.835939	1.307653	1.4611	0.242221	1.559933	17.42001	0.119495	0.708191	16.23212	227.9614	8.119831	4.528646
oldhwy95_1.37	34.43328	-1.12915	0.538695	1.667846	1.696582	19.94385	1.082069	33.42601	3.746948	1.349162	15.1812	339.1693	61.13842	9.157569
oldhwy95_1.38	39.47906	-0.86178	0.563274	1.425052	2.768489	3.908573	1.05293	19.72591	2.356181	0.521704	16.68756	460.3545	15.04151	4.528646
oldhwy95_1.39	39.4184	-0.8412	0.909051	1.750253	3.787681	23.6217	0.612789	43.8842	2.052205	1.950789	16.23212	448.9284	57.17053	10.05464
oldhwy95_1.4	557.7339	-0.1918	1.141549	1.333346	1.790695	2.762564	1.043035	27.91542	2.401036	1.247391	16.23212	339.1693	54.67352	23.43109
oldhwy95_1.40	26.89234	-1.08513	0.444539	1.529667	1.865806	3.173986	1.485657	3.305268	2.296672	1.382077	15.1812	172.5184	1.035011	2.617997
oldhwy95_1.41	37.16543	-1.08523	0.758462	1.843689	2.820508	1.251714	1.203663	41.91438	1.227561	0.803268	16.68756	182.6099	104.9991	6.809892
oldhwy95_1.42	16.27938	-1.08151	0.922073	2.003578	2.008614	1.3421	1.022556	78.65869	3.298837	0.821579	16.01215	209.9688	69.94584	6.809892
oldhwy95_1.43	36.90081	-0.79712	0.874722	1.671839	3.405483	6.804907	1.469624	37.02309	3.506487	0.961586	16.45722	651.2935	58.46282	6.809892
oldhwy95_1.5	40.13759	-0.67565	1.163133	1.838779	2.262399	18.22812	1.322584	164.3141	1.637089	1.449449	16.23212	366.4023	22.67209	13.53463
oldhwy95_1.6	4.459937	-0.90175	0.648504	1.550256	0.977255	20.8318	0.484902	9.69345	0.094107	1.330632	15.1812	521.6033	98.1037	9.449734
oldhwy95_1.7	1.502014	-1.15766	0.522559	1.680218	1.243083	7.839182	0.88744	22.27557	0.975649	1.811673	14.98515	330.5017	58.46282	8.320374
oldhwy95_1.8	430.3244	-1.16019	0.757509	1.9177	1.611477	0.988165	0.741568	176.064	1.70763	1.71993	16.23212	534.7222	85.6629	19.97078
oldhwy95_1.9	51.43394	-1.10755	0.531072	1.63862	2.828181	4.020764	0.492664	285.5269	1.810602	1.303903	19.6044	508.783	83.75145	12.7731
oldhwy95_2.1	1.862801	-0.51239	0.234797	0.747184	2.598339	4.747092	1.139806	22.35791	1.1642	13.53281	32.57861	548.1467	22.36256	24.05573
oldhwy95_2.10	1768.97	0.280022	0.582049	0.302027	1.395934	4.524392	0.384254	41.6999	0.270937	7.205491	272.7289	484.0113	104.9991	21.07152
oldhwy95_2.11	139.2102	-0.36291	0.332955	0.695863	3.549005	6.116102	0.535405	40.20686	0.836498	6.463179	588.8641	667.4333	185.402	24.69492
oldhwy95_2.12	34.80525	-0.41477	0.262906	0.67768	0.046761	3.979801	1.201203	28.84591	3.262159	12.94368	29.75003	651.2935	12.57682	25.34899
oldhwy95_2.13	139.2102	0.3345	0.543479	0.208979	0.898918	5.482851	0.935255	49.86087	3.394748	1.561393	238.3845	683.949	125.8948	24.69492
oldhwy95_2.14	621.8148	-0.48089	0.185576	0.666463	3.730694	0.680795	0.308819	47.50702	0.342392	13.83917	28.70668	496.2546	14.81861	21.6412
oldhwy95_2.15	419.0409	0.055164	0.475054	0.41989	3.296942	0.13819	1.326499	43.85305	1.405981	2.786968	73.42491	667.4333	54.67352	24.69492
oldhwy95_2.16	1754.067	-0.35049	0.421154	0.771648	1.891008	5.491636	0.982136	44.32086	0.570435	0.509928	45.93644	667.4333	24.84528	24.69492
oldhwy95_2.17	454.2078	-0.35386	0.593257	0.94712	1.971801	1.27862	1.427403	36.52244	2.231707	4.118416	90.73575	667.4333	73.16261	24.69492
oldhwy95_2.18	32.81617	-0.35242	0.308816	0.66124	0.834937	4.149614	0.579312	49.00481	0.588958	11.41192	36.43212	561.8839	42.42608	28.85513
oldhwy95_2.19	60.13164	-0.35409	0.17061	0.524701	2.923624	1.548971	0.293997	5.748574	0.539975	8.619418	34.43884	700.8494	35.93846	21.6412
oldhwy95_2.2	643.2064	-0.21903	0.410182	0.62921	1.672964	1.676944	1.030206	20.45499	2.67598	0.666562	66.15433	893.0907	73.16261	24.69492
oldhwy95_2.20	145.087	-0.51414	0.283071	0.797212	3.96884	0.664713	0.290785	23.09184	0.403082	2.739837	38.56795	871.8143	80.0581	31.96565
oldhwy95_2.21	107.5693	-0.38687	0.217703	0.604573	3.700357	0.492617	0.430711	4.10833	3.038861	15.02922	59.67442	590.3256	42.14978	25.34899
oldhwy95_2.22	49.64739	-0.46198	0.171275	0.633251	1.302065	0.314578	0.997085	43.1162	2.288886	6.463179	31.98655	810.8473	14.04421	23.43109
oldhwy95_2.23	10.44418	-0.43313	0.252503	0.685629	1.190587	6.292193	1.064523	24.8994	1.288377	15.21774	40.85653	718.1435	8.426614	26.70321
oldhwy95_2.24	35.55607	-0.39641	0.198539	0.594946	2.15766	0.258333	0.883954	20.65539	1.38388	13.10864	29.22235	575.941	40.02277	27.40407
oldhwy95_2.25	37.60738	-0.73468	0.23354	0.968218	3.424785	0.721186	0.987835	44.1052	3.530761	12.40167	32.57861	496.2546	3.451674	24.05573

Figure I 1 - Trace element concentration data from PXRF analysis of geologic sources as well as archaeological artifacts (cont.).

oldhwy95_2.26	1862.2	0.336722	0.476542	0.139819	0.18047	0.34244	0.4246	17.91252	2.728383	1.35822	334.0174	810.8473	158.0544	32.78908
oldhwy95_2.27	139.2102	0.293929	1.000789	0.70686	0.720153	3.673064	0.950706	42.9521	1.158683	1.302814	502.1824	667.4333	222.5603	22.82067
oldhwy95_2.28	139.2102	0.120654	0.571988	0.451334	2.825398	0.323512	1.439581	23.69241	2.536003	0.630181	365.609	959.9398	154.4951	28.85513
oldhwy95_2.29	22.61401	-0.58145	0.222427	0.803878	2.463369	7.127699	0.748455	16.57479	1.017682	10.28078	27.7103	810.8473	16.69438	26.70321
oldhwy95_2.3	1944.006	-0.02322	0.730156	0.753376	3.461796	7.459625	0.766272	28.11489	0.929135	5.049252	285.2727	667.4333	125.8948	21.07152
oldhwy95_2.30	133.3333	-0.38862	0.335205	0.72382	0.446552	7.337917	1.390515	1.137122	1.389854	0.855979	36.43212	810.8473	47.83679	31.96565
oldhwy95_2.31	139.2102	0.048115	0.782284	0.734169	3.384138	0.519801	1.598905	18.50861	1.213535	2.421704	391.2874	667.4333	207.8182	24.69492
oldhwy95_2.32	35.41034	-0.38627	0.292674	0.678945	0.033238	0.810412	1.172503	24.1518	3.861263	10.31613	30.29	683.949	33.21353	28.12125
oldhwy95_2.33	1034.603	0.234834	0.588398	0.353564	2.670492	2.112133	1.14541	2.391056	3.441707	4.118416	298.4076	700.8494	95.90907	28.85513
oldhwy95_2.34	1450.259	0.297235	0.595502	0.298268	2.275989	5.333277	1.810893	49.86908	3.983751	8.06563	428.4044	851.0223	134.7778	28.12125
oldhwy95_2.35	35.92526	-0.43383	0.295572	0.7294	2.376628	4.106702	0.232951	18.3463	1.017532	10.44574	34.43884	635.5211	34.24597	28.85513
oldhwy95_2.36	73.62482	-0.4491	0.238444	0.687546	0.524671	0.825587	0.691915	24.6252	1.361954	12.14245	34.43884	575.941	41.2332	23.43109
oldhwy95_2.37	38.63463	-0.46683	0.235433	0.702261	3.098127	0.561623	1.213687	35.81336	1.805861	14.4283	31.98655	718.1435	36.61683	24.69492
oldhwy95_2.38	1437.706	-0.30086	0.346177	0.647036	0.217053	13.5305	1.34266	36.94236	0.803939	0.089655	70.41587	893.0907	89.62039	24.69492
oldhwy95_2.39	3.714151	-0.61416	0.332955	0.94712	3.543182	1.878043	1.62143	37.71814	3.349856	1.046184	16.92326	667.4333	62.52314	24.69492
oldhwy95_2.4	1688.105	-0.00755	0.593257	0.60081	1.495407	3.822904	1.329949	35.61261	3.96766	5.744433	260.7497	667.4333	104.9991	24.69492
oldhwy95_2.40	37.2019	-0.34843	0.256202	0.604629	1.783242	4.566528	1.553331	50.91399	2.081267	9.644515	28.20276	620.1078	14.47749	23.43109
oldhwy95_2.5	34.86487	-0.25247	0.269712	0.52218	1.595225	6.056712	1.225038	50.98901	1.720907	1.254452	39.31331	667.4333	65.39009	23.43109
oldhwy95_2.6	139.2102	0.168077	0.613174	0.445097	3.839824	12.10342	0.510938	32.36321	0.214534	1.337818	194.9956	472.0468	98.1037	24.69492
oldhwy95_2.7	139.2102	-0.22076	0.23612	0.456883	3.640409	1.210489	0.999598	13.11825	1.350879	3.965241	659.9149	667.4333	63.94011	22.82067
oldhwy95_2.8	235.1669	-0.22963	0.688259	0.91789	0.689403	1.423985	0.701492	26.54426	0.571399	7.794627	243.7842	667.4333	109.8679	24.69492
oldhwy95_2.9	1682.934	0.002888	0.698751	0.695863	0.623915	2.477875	1.409659	0.631097	0.746649	6.757747	341.6446	667.4333	123.0675	21.6412
peanut.brittle.1	110.9544	-2.16773	-0.00054	2.167191	3.715597	5.438633	1.012988	84.28252	1.577729	0.479807	12.52701	2.573974	25.00435	0.473201
peanut.brittle.10	64.26892	-1.68714	0.203758	1.890894	3.206675	49.6127	1.415419	78.65869	0.071548	0.654422	5.926814	267.8992	63.94011	2.159612
peanut.brittle.11	127.1744	-3.21805	-0.86581	2.352245	0.147931	75.39892	0.938989	66.95312	1.874152	0.978964	11.41174	1698.883	112.3877	3.633146
peanut.brittle.12	12.55289	-2.39389	-0.15409	2.239803	1.897328	7.372654	0.85102	13.47977	2.011246	0.493535	6.965044	11.11987	35.84224	2.793891
peanut.brittle.13	37.28316	-1.57948	0.164629	1.744111	3.058896	19.07611	0.044269	39.67258	2.855465	0.778537	3.674206	167.6443	50.01159	1.087347
peanut.brittle.14	168.6883	-2.74689	0.971853	3.718739	1.866292	59.65602	0.351259	111.0981	3.064111	0.366045	12.25883	10.44317	43.9192	2.486228
peanut.brittle.15	56.65256	-1.45225	0.542511	1.994762	3.151138	33.24669	0.870471	9.519935	0.206923	1.507553	9.768372	405.7665	22.56507	2.230669
peanut.brittle.16	340.7146	-2.31254	-0.26585	2.046691	1.50703	14.26907	1.01981	27.83375	1.691553	1.487752	0.033696	81.60853	20.4088	1.379117
peanut.brittle.17	93.98213	-2.03356	-0.04574	1.98782	2.061717	48.06961	1.069358	139.8577	3.158437	0.325325	12.39138	99.86363	50.01159	1.140645
peanut.brittle.18	340.7146	-2.38635	-0.5049	1.881451	7.796277	4.725317	0.779329	34.80714	3.911017	0.918481	9.768372	36.13605	3.657977	0.681248
peanut.brittle.19	134.6497	-2.78154	-0.3602	2.421343	2.229797	21.74044	0.6571	92.41155	0.664925	0.79186	9.768372	2.733945	18.39366	4.067288
peanut.brittle.2	340.7146	-2.44522	-0.3464	2.098825	2.735144	1.386644	0.269868	42.7177	0.343372	1.129564	1.838622	7.444855	30.39466	4.740335
peanut.brittle.20	36.07238	-1.7243	0.419161	2.143459	0.887169	1.848625	0.962828	127.554	3.172192	0.683975	12.80783	313.754	47.83679	0.952771
peanut.brittle.21	270.851	-2.56603	0.823615	3.389645	3.416457	45.08801	1.098962	168.1409	3.867054	1.546002	10.88504	4.250195	43.96224	3.615582
peanut.brittle.22	106.1589	-2.7459	-0.16418	2.581728	3.825512	28.72194	0.973652	52.74637	1.496134	1.42479	12.52701	6.460883	13.16366	0.595501
peanut.brittle.23	40.38758	-1.49851	0.555672	2.054187	0.396485	48.06961	0.703113	66.95312	0.636466	1.06278	6.590509	405.7665	57.17053	2.180434
peanut.brittle.24	36.18016	-2.35559	0.232692	2.588284	0.834791	5.787517	0.434073	36.17496	2.966765	1.348527	5.49634	12.48251	33.28471	3.663696
peanut.brittle.25	340.7146	-2.36623	0.055724	2.421954	16.22157	6.089905	1.621561	127.554	1.398134	1.456557	8.940577	437.7624	16.68184	2.285138
peanut.brittle.26	1213.399	-2.96322	-0.89985	2.063375	17.65138	3.276597	1.201272	23.37871	3.39581	1.18313	10.50522	60.87889	37.8641	0.606121
peanut.brittle.27	634.5557	-2.26087	0.225249	2.486114	11.73064	5.081703	1.131468	28.33351	3.855425	0.829329	9.768372	3.929617	42.08101	1.565243
peanut.brittle.28	29.95117	-2.49268	-0.32028	2.172405	8.420017	2.367231	1.30624	11.31815	3.827022	0.838566	9.169438	260.854	18.00187	0.183463
peanut.brittle.29	362.8115	-2.41745	0.984668	3.402118	10.6367	6.297611	1.399342	32.87786	0.39914	0.524159	8.541494	13.61544	38.03222	4.401713
peanut.brittle.3	39.98922	-1.75563	0.960297	2.71593	3.03844	108.0535	1.237218	29.06586	3.899083	0.478417	12.52701	5.363637	83.75145	2.183955
peanut.brittle.30	34.76301	-2.56533	0.078279	2.643607	1.607507	4.265003	0.908097	19.02136	1.035819	0.97325	8.782246	81.60853	22.7332	0.041864
peanut.brittle.31	939.7743	-3.49409	-1.19502	2.299075	2.709187	4.416764	0.511048	44.491	3.775531	1.322557	2.007606	68.20875	35.76088	1.43254
peanut.brittle.32	575.5054	-1.80846	0.235816	2.044277	13.9857	3.462529	0.95173	41.97258	1.313282	1.645944	8.940577	590.3256	2.920689	2.04331
peanut.brittle.33	1111.754	-2.39509	0.264873	2.659967	19.35947	2.510799	1.638993	3.410545	0.543166	0.49766	9.62435	2.434524	29.2792	4.465261
peanut.brittle.34	340.7146	-2.21897	-0.17424	2.044726	19.95442	2.492608	1.085952	38.95202	2.780891	1.14469	10.0771	260.854	128.7878	1.294508
peanut.brittle.35	539.3982	-2.38344	-0.28058	2.102854	13.0357	3.940675	1.164243	39.65583	2.960537	0.649833	9.768372	11.20209	23.12852	3.981581
peanut.brittle.36	1003.244	-2.28435	-0.07486	2.209495	11.95135	4.388206	0.744519	216.6003	3.871199	0.306136	10.41561	11.30496	2.235771	3.116224

Figure I 1 - Trace element concentration data from PXRF analysis of geologic sources as well as archaeological artifacts (cont.).

peanut.brittle.37	1004.984	-2.84667	-0.53166	2.315004	12.97812	40.86533	1.255727	143.1149	1.594451	0.83508	9.42038	1.567468	2.451699	1.274252
peanut.brittle.38	225.4819	-1.98386	0.059755	2.043619	9.427598	0.783341	0.418414	73.41023	1.342057	1.136291	9.768372	357.1148	17.9899	1.331885
peanut.brittle.39	546.7795	-2.4719	-0.54238	1.929523	16.12561	36.92449	0.942434	4.911406	2.577728	1.321685	9.919181	305.6649	10.48109	1.289556
peanut.brittle.4	40.96126	-2.36639	0.704139	3.070524	2.843772	61.46899	1.13043	108.5697	1.416779	1.123313	10.50522	1.347022	17.73973	1.998926
peanut.brittle.40	772.1674	-2.5865	-0.61448	1.972014	17.92966	4.712682	0.383123	46.30775	0.724519	0.727542	12.00272	4.21376	26.97839	3.228963
peanut.brittle.41	1130.042	-1.97842	0.284273	2.262695	12.7958	24.59532	1.15329	10.69987	3.666706	1.168959	9.768372	395.583	87.61886	2.695196
peanut.brittle.42	35.03583	-2.27596	-0.27644	1.999521	7.422032	2.106854	1.19197	44.77412	3.458915	1.765295	9.169438	162.8811	8.441294	0.918029
peanut.brittle.43	443.6295	-2.60013	-0.57211	2.02802	11.14528	4.619546	0.74441	88.25346	3.837569	0.406467	0.436699	140.643	5.077186	3.310929
peanut.brittle.44	461.0719	-2.17242	1.839707	4.012129	11.06852	4.151549	1.235258	121.8142	0.440179	0.863882	9.486811	120.8233	58.46282	0.044836
peanut.brittle.45	36.27264	-2.55499	-0.84081	1.714175	6.865464	6.563802	0.812436	47.36558	3.243912	1.224948	9.230024	193.177	69.94584	1.458021
peanut.brittle.46	323.5543	-1.84182	-0.09086	1.750967	12.72862	7.678461	1.626463	82.36459	0.648039	0.646158	8.88658	339.1693	80.0581	0.732816
peanut.brittle.47	340.7146	-3.19853	-0.84629	2.352245	5.051818	3.976303	0.978908	25.99093	0.715236	1.40724	11.52456	1739.424	137.8778	0.529326
peanut.brittle.48	340.7146	-2.26361	0.352213	2.61582	1.166959	2.429485	0.177778	3.540966	1.132029	1.369087	9.919181	6.750445	1.278102	0.664657
peanut.brittle.49	1073.249	-2.70103	-0.35358	2.347453	17.28673	0.730052	0.680639	25.54298	1.941702	0.526504	10.50522	0.085983	17.66684	4.926353
peanut.brittle.5	36.58883	-3.73944	-1.32142	2.418012	1.489193	7.76382	0.535852	4.908866	0.222325	1.247902	2.897679	13.2557	3.536567	4.214321
peanut.brittle.50	340.7146	-3.89573	-1.83631	2.059422	5.051818	6.092996	0.597103	44.95706	2.682447	1.940897	11.08847	4.372301	33.9704	0.410497
peanut.brittle.51	340.7146	-2.1376	-0.30469	1.832914	5.051818	4.245628	0.523968	7.554587	0.343805	0.651325	9.919181	385.6313	16.10935	4.661229
peanut.brittle.52	909.2619	-2.01792	0.185129	2.203051	3.131022	5.125522	1.708845	2.60351	0.353897	0.856877	12.95316	215.8288	38.92884	4.591331
peanut.brittle.53	293.0418	-2.64352	0.879728	3.523246	2.118171	0.356097	1.383572	32.3571	3.212762	1.069733	10.0771	11.27524	37.54797	4.592412
peanut.brittle.54	340.7146	-2.40978	-0.44545	1.964332	0.797389	6.27389	1.683773	36.3055	2.931164	0.866539	9.486811	136.4945	31.71541	0.655178
peanut.brittle.55	731.7819	-2.80749	-0.40871	2.398786	9.609922	7.971879	1.527203	82.36459	2.627279	1.431342	8.995831	5.366302	3.329672	1.542312
peanut.brittle.56	540.7616	-3.15375	-0.87116	2.282587	14.19681	3.330664	0.585724	47.03471	2.073427	0.094789	9.486811	209.9688	23.86008	4.938767
peanut.brittle.57	928.2558	-2.66256	-0.39354	2.269018	14.75338	23.6217	1.140519	136.6748	1.659187	0.512233	10.69076	8.129596	13.45302	1.113005
peanut.brittle.58	574.048	-2.75534	-0.05383	2.701511	0.74004	6.651763	0.97144	4.544837	3.974727	0.623663	9.842908	6.247348	36.00809	0.535297
peanut.brittle.59	506.2059	-2.64755	-0.35502	2.292535	12.64226	3.214259	1.470922	5.522978	2.866557	1.194964	9.292021	153.6775	22.28935	3.946374
peanut.brittle.6	214.7626	-2.83606	-0.52207	2.313988	1.747279	52.80754	1.251368	111.0981	3.889447	1.301324	9.768372	0.14262	29.74138	0.745937
peanut.brittle.60	837.7997	-2.74189	-0.43451	2.307384	14.36954	5.610244	1.1068	164.3141	2.845731	1.116927	8.88658	13.51422	23.84943	3.765965
peanut.brittle.61	357.8749	-2.43474	0.557977	2.992713	8.525573	7.04814	0.572116	17.07882	0.02908	0.844517	10.0771	162.8811	17.77529	0.572417
peanut.brittle.62	740.1504	-2.61383	0.40313	3.016957	11.80741	0.138794	1.787021	0.503513	3.757164	0.792948	0.053483	120.8233	7.782023	2.156129
peanut.brittle.63	1176.023	-2.20904	-0.33483	1.874213	11.89377	2.332767	0.902958	43.16622	0.919252	1.276002	13.25407	11.46898	12.27862	3.493017
peanut.brittle.64	771.7913	-2.9435	-1.2432	1.700298	13.17964	3.295438	0.132695	92.41155	1.355028	1.143662	9.355461	322.0315	18.87342	2.131093
peanut.brittle.65	651.528	-2.72908	-0.7196	2.009479	10.44477	6.186384	1.214988	30.72046	2.390072	1.179517	10.78678	144.8882	6.529897	0.475912
peanut.brittle.66	986.5538	-3.23614	-0.87671	2.359429	13.64025	3.612096	1.179567	143.1149	2.435272	0.55381	11.19376	1.783866	32.94943	0.410006
peanut.brittle.7	26.42219	-2.25213	0.668088	2.920216	1.398257	77.57859	1.083815	101.3248	1.28357	1.161477	10.98558	20.14611	4.569216	4.136714
peanut.brittle.8	144.3818	-2.12197	0.217477	2.339445	2.033693	52.80754	1.282772	50.18696	0.25258	1.443001	11.3015	45.62236	78.27424	0.819084
peanut.brittle.9	101.3164	-2.21048	0.156514	2.366994	1.117194	57.88432	1.337859	41.73638	3.313321	1.793047	13.10188	81.60853	89.62039	2.677482
Pine Bar.1	4036.342	0.031352	-0.66535	-0.6967	8.381633	0.143677	1.347302	496.1705	5.607663	68.28715	133.9608	348.0388	28.25155	34.49394
Pine Bar.10	4218.054	-0.11324	-0.70508	-0.59184	18.03522	6.884735	0.320936	556.7094	0.600697	66.64935	139.9647	282.4859	38.43337	34.49394
Pine Bar.11	3383.592	0.016991	-0.72287	-0.73986	8.611937	4.462545	1.079879	684.8964	0.886953	66.64935	136.9282	267.8992	33.59367	33.6317
Pine Bar.12	4425.059	-0.06473	-0.6986	-0.63387	12.70943	7.505778	0.37451	496.1705	6.669127	69.26511	122.7517	322.0315	24.99764	34.49394
Pine Bar.13	3230.654	-0.11324	-0.71177	-0.59853	13.46752	1.82517	0.542179	569.6762	8.22594	65.81277	131.061	187.8327	39.46025	34.49394
Pine Bar.14	4601.928	-0.09057	-0.7141	-0.62353	18.47663	4.780894	0.870753	556.7094	6.143449	67.4977	128.2272	375.9061	15.28439	31.16096
Pine Bar.15	4139.68	-0.03004	-0.639	-0.60896	10.05134	7.927529	1.075296	582.9451	1.215439	67.02639	146.2514	290.0351	37.19488	35.37626
Pine Bar.16	4184.579	-0.04593	-0.73531	-0.68937	18.51502	4.56863	1.042086	519.5531	7.235241	68.95876	136.9282	297.76	12.08424	33.6317
Pine Bar.17	4299.389	-0.16547	-0.76049	-0.59502	19.24431	5.343235	0.963022	556.7094	5.132531	65.71851	125.4579	234.2405	3.744334	37.20305
Pine Bar.18	4078.984	-0.03255	-0.62686	-0.5943	15.65541	7.807225	0.282398	684.8964	6.284978	61.24107	143.0719	313.754	39.0638	33.6317
Pine Bar.19	2718.665	0.068896	-0.57243	-0.64132	13.93772	4.665683	0.981782	733.8779	5.445916	61.33534	149.5051	221.8253	38.91986	31.96565
Pine Bar.2	3959.285	0.031352	-0.68024	-0.71159	15.9241	4.818817	1.368026	639.1842	10.96553	67.33274	136.9282	385.6313	24.66517	31.16096
Pine Bar.20	3924.024	-0.1079	-0.80355	-0.69565	10.34881	1.013973	1.323317	496.1705	6.568035	72.70567	131.061	234.2405	3.417461	37.20305
Pine Bar.21	3645.557	-0.08628	-0.78245	-0.69617	15.74177	0.627395	0.227777	519.5531	5.334715	72.42288	136.9282	167.6443	27.29564	33.6317
Pine Bar.22	3629.666	-0.10513	-0.73118	-0.62605	13.0357	6.931369	0.777924	610.4173	6.588253	69.83068	136.9282	348.0388	12.52815	35.37626
Pine Bar.23	4076.164	-0.12537	-0.76708	-0.64171	13.46752	0.686088	1.324987	507.7272	4.738273	66.64935	146.2514	209.9688	1.956709	38.14848

Figure I 1 - Trace element concentration data from PXRF analysis of geologic sources as well as archaeological artifacts (cont.).

Pine Bar.24	4960.367	-0.06609	-0.70508	-0.639	13.46752	2.902626	0.599528	463.0549	4.798928	67.55662	136.9282	405.7665	24.20709	33.6317
Pine Bar.25	4076.164	-0.07284	-0.69575	-0.62292	13.46752	6.618106	0.737945	700.8491	2.19929	67.78049	133.9608	395.583	6.170861	37.20305
Pine Bar.26	3106.488	-0.04326	-0.71031	-0.66705	11.12609	1.622087	0.597251	654.0721	8.923474	64.35171	131.061	215.8288	11.69256	31.16096
Pine Bar.27	3221.204	-0.00306	-0.59553	-0.59246	7.959409	1.50598	0.249961	442.2151	5.76941	62.40756	136.9282	385.6313	20.9583	35.37626
Pine Bar.28	4180.16	-0.09708	-0.7073	-0.61022	14.34075	5.200792	1.049349	733.8779	3.134344	65.95417	131.061	330.5017	5.955142	33.6317
Pine Bar.29	4199.295	-0.12816	-0.71518	-0.58701	9.648306	5.597203	1.674261	496.1705	0.997118	64.2928	136.9282	313.754	31.92946	31.96565
Pine Bar.3	4410.249	-0.12961	-0.74721	-0.61761	13.46752	4.762337	0.752105	569.6762	4.758492	66.49617	122.7517	193.177	39.83509	33.6317
Pine Bar.30	4076.164	-0.1514	-0.73861	-0.58721	13.46752	1.562662	1.497318	452.515	6.780328	69.39472	128.2272	193.177	29.08162	32.78908
Pine Bar.31	4011.331	-0.00053	-0.58333	-0.5828	10.52154	1.898445	0.831121	804.6788	6.295087	63.89219	146.2514	330.5017	6.79561	36.27914
Pine Bar.32	4076.164	-0.12961	-0.78034	-0.65073	13.46752	4.846558	1.407312	544.0377	5.607663	66.64935	146.2514	322.0315	19.86596	31.96565
Pine Bar.33	4076.164	-0.09057	-0.73403	-0.64346	13.46752	1.353011	0.739647	442.2151	8.984129	72.36397	133.9608	297.76	14.75523	32.78908
Pine Bar.34	3911.754	-0.07549	-0.66472	-0.58923	16.35592	5.906661	1.362137	556.7094	5.607663	65.87169	149.5051	297.76	12.55105	33.6317
Pine Bar.35	3255.994	-0.05399	-0.61505	-0.56107	10.91498	7.038656	1.136015	463.0549	5.02133	60.18063	136.9282	260.854	32.7496	33.6317
Pine Bar.36	3802.821	0.02074	-0.61242	-0.63316	13.95691	0.265449	1.087073	823.4215	8.852709	71.29174	152.8345	297.76	27.49296	32.78908
Pine Bar.37	4076.164	-0.19063	-0.77589	-0.58526	9.235678	4.306973	0.886257	610.4173	6.143449	62.00695	131.061	234.2405	15.50046	35.37626
Pine Bar.38	4076.164	-0.1202	-0.75568	-0.63548	13.46752	0.606681	0.769578	556.7094	5.607663	71.13856	128.2272	247.2409	19.07496	31.16096
Pine Bar.39	3662.106	0.015683	-0.62997	-0.64566	13.92813	4.958958	0.771793	700.8491	1.036691	62.86709	143.0719	234.2405	13.80962	37.20305
Pine Bar.4	4076.164	0.031352	-0.59824	-0.62959	19.79129	0.826056	1.066483	700.8491	6.042357	66.64935	146.2514	305.6649	30.23429	35.37626
Pine Bar.40	4374.33	-0.0567	-0.64602	-0.58933	13.46752	4.954625	1.29017	569.6762	6.113122	66.79074	139.9647	215.8288	2.039509	31.16096
Pine Bar.5	4201.598	-0.06609	-0.76796	-0.70187	14.63823	6.919637	1.380179	422.3133	0.700333	65.64781	149.5051	448.9284	33.26681	33.6317
Pine Bar.6	4899.483	-0.05533	-0.7685	-0.71317	14.4751	7.866743	0.426574	596.523	1.179039	69.90138	139.9647	322.0315	25.28681	38.14848
Pine Bar.8	4437.753	-0.16233	-0.79193	-0.6296	12.86297	1.006736	0.692124	484.8768	1.814101	66.64935	120.107	193.177	9.64777	33.6317
Pine Bar.9	4076.164	-0.0567	-0.72213	-0.66544	6.913444	5.535954	0.619641	768.4634	8.519106	59.30871	149.5051	395.583	9.998287	34.49394
seven.devils.1	0.486439	-0.56897	-1.05466	-0.48569	1.553091	3.6477	74.13224	43.55464	0.162623	61.92447	19.6044	1278.689	14.21587	37.20305
seven.devils.10	1414.245	-0.5903	-1.14708	-0.55678	14.01449	6.849304	67.08774	11.48639	1.272648	60.6755	21.53572	1509.606	0.947203	46.54932
seven.devils.11	1117.113	-0.66329	-1.21107	-0.54778	14.90692	0.814681	56.77706	42.4166	0.569271	60.6755	18.7343	1474.296	0.824337	42.1556
seven.devils.12	396.615	-0.83113	-1.3787	-0.54756	12.02812	2.20162	67.08774	10.10385	1.200135	60.6755	17.92228	1620.548	42.65031	50.12062
seven.devils.13	1318.853	-0.63579	-1.21992	-0.58413	16.73016	7.663219	67.08774	26.12184	2.266233	60.6755	23.36201	1509.606	7.213841	45.41266
seven.devils.14	1313.211	-0.68703	-1.24381	-0.55678	21.22109	0.495228	88.13019	32.01856	0.913672	60.6755	19.6044	1474.296	25.09742	40.10591
seven.devils.15	1273.39	-0.71211	-1.29082	-0.57871	16.8837	6.025091	76.79527	45.05057	2.293517	58.27183	19.01768	1082.147	28.55563	33.6317
seven.devils.16	401.6925	-0.66329	-1.20162	-0.53833	14.65742	4.415069	50.07397	14.31076	0.391498	60.6755	22.60617	1309.443	30.17185	40.10591
seven.devils.17	5.046253	-0.761	-1.17843	-0.41743	0.466956	1.961045	64.09469	42.0997	3.314967	66.13091	22.97974	1135.108	20.45879	40.10591
seven.devils.18	685.3785	-0.63579	-1.1059	-0.47011	13.86095	1.242051	61.59099	33.61448	1.445631	60.6755	22.97974	1439.79	39.13542	46.54932
seven.devils.19	1438.505	-0.7612	-1.23318	-0.47198	21.22109	0.050055	53.27188	45.56175	0.189415	66.08378	22.97974	1007.141	22.95292	32.78908
seven.devils.2	91.86648	-0.41748	-0.92893	-0.51145	7.422032	4.018091	43.93991	44.8602	2.452643	67.68623	20.53672	1309.443	31.67869	33.6317
seven.devils.20	860.2257	-0.63579	-1.06015	-0.42436	13.14125	2.965197	83.16832	30.38609	3.974114	59.13197	21.19503	1509.606	26.82167	40.10591
seven.devils.21	1252.045	-0.64958	-1.21555	-0.56597	14.74379	0.630436	67.62262	17.92771	1.273199	56.05667	19.6044	1373.116	21.22732	43.21639
seven.devils.22	1.334158	-0.74893	-1.34691	-0.59798	0.821559	4.065816	89.99659	36.80754	1.222434	60.6755	24.56308	1474.296	5.897062	40.10591
seven.devils.23	1168.97	-0.60815	-1.18428	-0.57613	11.93216	4.376083	62.5128	17.34778	0.68218	57.52952	20.86208	1582.713	29.89687	40.10591
seven.devils.24	1280.301	-0.73768	-1.16006	-0.42238	10.55033	5.840252	67.08774	6.766964	0.094221	57.51773	20.53672	1082.147	21.47574	40.10591
seven.devils.25	675.2233	-0.47929	-1.01762	-0.53833	3.41225	7.167631	60.86264	33.82191	2.461938	60.6755	25.41114	1406.069	30.50156	39.11593
seven.devils.26	798.1664	-0.47929	-0.91268	-0.43339	16.54784	5.406589	67.08774	34.88135	0.559227	54.73701	22.97974	1162.517	35.37513	40.10591
seven.devils.27	17.59675	-0.80359	-1.25814	-0.45456	3.575425	2.796098	79.41277	48.81038	1.76559	60.10993	21.19503	1278.689	36.9989	43.21639
seven.devils.28	1408.181	-0.63579	-1.26271	-0.62692	17.8433	7.601601	77.94469	25.1864	0.155901	65.84812	21.19503	1509.606	4.669847	44.30188
seven.devils.29	998.9657	-0.54292	-1.05548	-0.51256	17.65138	6.274432	61.55685	30.84898	3.896443	56.65759	21.53572	1248.636	1.242199	40.10591
seven.devils.3	15.00157	-0.69151	-1.12203	-0.43052	3.857276	1.448074	87.17423	37.79823	1.447287	62.69035	22.24111	1135.108	0.254544	39.11593
seven.devils.30	1017.489	-0.56626	-0.99357	-0.42731	15.49228	1.353596	47.7296	37.19421	2.442061	55.11406	23.36201	1439.79	1.628889	40.10591
seven.devils.31	1202.304	-0.6139	-1.13372	-0.51982	12.90135	6.091885	79.66314	19.39361	3.075997	60.6755	20.53672	1278.689	14.46596	42.1556
seven.devils.32	1369.488	-0.60875	-1.07696	-0.46821	24.64687	5.93435	76.22624	43.1624	3.177124	60.05102	22.24111	937.1417	33.9873	38.14848
seven.devils.33	1477.668	-0.60815	-1.17668	-0.56853	18.42865	0.891022	78.78684	34.31594	0.920092	67.78049	23.36201	959.9398	15.81482	40.10591
seven.devils.35	1547.297	-0.5898	-1.16209	-0.57229	19.25391	4.985454	57.83544	6.043732	3.036303	57.62378	18.7343	1082.147	17.73563	37.20305
seven.devils.36	1368.5	-0.442	-1.0433	-0.6013	16.20238	6.126218	67.24707	19.04305	4.910129	64.58737	18.18675	1248.636	6.545398	39.11593

Figure I 1 - Trace element concentration data from PXRF analysis of geologic sources as well as archaeological artifacts (cont.).

seven.devils.37	1105.454	-0.70979	-1.25862	-0.54882	16.18319	3.694731	67.08774	23.47701	0.058774	61.84199	22.97974	1248.636	12.38553	37.20305
seven.devils.38	1278.514	-0.82465	-1.44359	-0.61893	13.04529	2.523898	66.22283	47.32113	1.526265	65.69495	20.21876	1278.689	3.643407	41.11896
seven.devils.39	1287.306	-0.8339	-1.43492	-0.60102	15.96248	5.361482	51.67862	45.69736	3.18316	62.83174	21.19503	1248.636	10.57124	36.27914
seven.devils.4	29.05774	-0.62095	-1.08997	-0.46902	6.164955	4.390486	45.30557	29.00488	2.597772	56.69294	18.45737	1439.79	0.512848	35.37626
seven.devils.40	1100.047	-0.63579	-1.16806	-0.53226	11.52912	5.342563	53.74986	24.14285	1.894801	59.28514	22.24111	1190.565	40.26179	40.10591
seven.devils.41	18.00241	-0.66358	-1.1887	-0.52512	3.595689	5.046228	83.1797	50.00211	0.777139	63.99823	22.24111	1219.266	7.719177	50.12062
seven.devils.42	3.786874	-0.63579	-1.24655	-0.61076	1.867625	3.206017	73.60874	14.70869	0.687947	60.6755	21.88436	1309.443	20.13136	40.10591
seven.devils.43	1012.13	-0.79991	-1.36775	-0.56784	14.18722	6.146961	90.41766	0.790825	2.923358	59.28514	20.53672	1278.689	3.358213	40.10591
seven.devils.44	24.75138	-0.59897	-1.20028	-0.60131	3.422911	6.409807	81.07431	34.5967	0.727632	61.28821	20.21876	1190.565	6.153668	42.1556
seven.devils.45	658.204	-0.63579	-1.08507	-0.44928	12.73822	7.870032	78.61614	43.12035	0.777543	56.59868	18.45737	1278.689	12.85252	40.10591
seven.devils.46	1244.147	-0.75104	-1.37199	-0.62095	17.13319	6.052816	63.57118	16.70235	1.621323	60.6755	20.53672	1190.565	9.919769	43.21639
seven.devils.5	12.13335	-0.71956	-1.18173	-0.46216	3.533798	1.480824	74.72402	3.779238	2.824149	60.82868	19.01768	1373.116	2.780998	36.27914
seven.devils.6	4.991148	-0.60875	-1.05389	-0.44514	0.38678	2.15028	53.73848	46.14842	0.981687	66.17804	20.86208	1373.116	12.86201	39.11593
seven.devils.7	903.8082	-0.41127	-0.96804	-0.55678	10.36801	2.969858	80.3232	49.62664	0.597656	60.6755	23.36201	1278.689	30.75594	50.12062
seven.devils.8	1366.808	-0.57071	-1.08125	-0.51054	13.59227	7.651	62.49004	3.621719	2.910972	60.6755	19.6044	1406.069	9.386545	48.90267
seven.devils.9	1391.255	-0.5045	-1.04283	-0.53833	15.53066	6.444047	67.08774	10.99524	0.574224	60.6755	22.24111	1373.116	11.64053	43.21639
White Bird.1	359.6145	-0.91687	-0.37729	0.539579	9.888207	0.733815	1.153773	41.76267	0.554066	0.998855	4.570502	56.26619	76.53098	3.533091
White Bird.10	419.229	-0.71412	0.31012	1.024241	9.427598	2.570452	0.89682	3.176346	2.45883	0.455252	4.206398	3.758859	23.38218	0.478669
White Bird.11	826.1401	-1.04185	-0.2451	0.796756	18.09279	5.773645	0.143694	6.984188	3.805367	1.033952	1.186652	10.80638	29.07489	4.789458
White Bird.12	919.6521	-1.59092	-0.71429	0.876631	13.37156	0.905928	0.66324	47.58004	3.033396	1.363266	2.633861	124.6068	30.97656	0.571251
White Bird.13	472.7315	-1.52858	-0.16407	1.364502	11.74983	3.632103	0.976436	34.55866	0.863215	1.411466	9.62435	90.42095	16.0625	2.971431
White Bird.14	656.8406	-1.25583	0.785492	2.04132	13.07408	7.387383	0.789149	31.33055	2.335502	1.003718	9.99723	149.2323	76.53098	1.832725
White Bird.15	780.0188	-0.86557	0.098418	0.963985	15.99127	4.213598	0.961074	9.84938	1.108581	1.636097	4.868119	32.63695	30.88069	2.660885
White Bird.16	468.8293	-0.63858	0.304772	0.943354	13.64025	4.481456	0.740818	42.24832	0.113415	1.489537	8.452691	4.532402	10.99499	4.637505
White Bird.17	504.0433	-1.14207	0.154987	1.297057	14.44631	0.452855	1.201969	51.14396	1.71587	1.243679	3.39015	84.47863	68.39216	1.855778
White Bird.18	455.3832	-0.81961	0.985367	1.804981	0.61386	6.278851	1.282534	11.73229	2.988111	0.413312	8.496581	6.623781	31.25662	2.593376
White Bird.19	1045.463	-0.62562	0.483735	1.109357	20.75089	0.598825	0.939425	6.234425	0.949959	0.577791	1.641678	8.308722	14.93939	3.179211
White Bird.2	348.9422	-0.9308	0.255026	1.185822	6.654352	7.310186	0.647738	35.38776	3.665057	1.411496	10.78678	49.73345	100.3495	0.244639
White Bird.20	842.031	-1.63521	-0.70427	0.930941	15.21399	3.211931	0.233395	9.96104	1.880155	0.859132	11.41174	182.6099	12.02644	4.225277
White Bird.21	806.2529	-0.62415	0.326737	0.950891	13.08368	3.179744	0.980331	36.48454	3.413376	4.04772	16.01215	198.6459	5.773136	1.621458
White Bird.22	481.1942	-0.50263	0.301601	0.804236	14.74379	5.105383	1.230596	52.90412	2.391794	4.024155	16.45722	247.2409	18.34514	4.690736
White Bird.23	699.953	-0.46607	0.724315	1.190381	15.89531	1.970634	1.860761	24.33661	0.265193	1.036503	8.782246	5.537604	21.18069	0.540905
White Bird.24	455.3832	-1.02502	-0.19259	0.832428	3.055041	0.130716	1.13758	41.88549	3.664831	0.603786	1.57537	13.3638	23.04374	3.770081
White Bird.25	747.2026	-0.43581	0.59566	1.031472	10.35841	7.067209	1.191174	9.183502	0.485249	0.344514	5.836298	3.30136	26.86262	2.09596
White Bird.26	38.98897	-1.82406	-1.18753	0.636523	0.713932	6.6987	1.53381	43.69087	2.102543	0.467738	3.871504	9.005558	16.65275	2.238068
White Bird.27	455.3832	-1.45269	-0.45836	0.994327	2.479084	2.843698	0.544057	4.199939	0.112242	1.055905	4.979806	63.26614	47.83679	3.182865
White Bird.28	38.30936	-1.11998	0.080511	1.200494	0.030502	0.820867	0.816226	0.187863	3.747829	1.138028	7.458912	32.63695	78.27424	0.963652
White Bird.29	34.54972	-0.82842	-0.11613	0.712296	0.341027	6.719154	1.052856	50.96886	3.059894	0.370456	0.502829	8.335208	47.83679	3.938022
White Bird.3	748.0959	-0.88596	0.0165	0.902458	16.61501	3.472376	1.247849	45.22969	2.460958	1.56699	2.371056	60.87889	55.90765	2.756995
White Bird.30	37.17494	-1.16775	-0.26154	0.906214	2.596811	7.244966	1.015025	23.48785	1.504558	0.855934	4.28959	6.682765	41.36424	2.164191
White Bird.31	455.3832	-2.24113	-0.6331	1.608032	3.717223	6.566106	1.855211	52.43422	2.135508	0.503234	6.29272	144.8882	69.94584	1.494328
White Bird.32	152.3272	-1.42315	-0.64672	0.776437	0.835676	6.337643	1.027891	12.1001	2.020298	0.351629	0.771672	11.78206	26.69289	4.835177
White Bird.33	36.25203	-1.39474	-0.09441	1.300325	1.790107	6.450581	1.096455	42.73501	3.711618	1.313368	5.029966	10.97813	40.33438	3.03525
White Bird.34	38.04817	-0.8327	-0.0256	0.807097	0.850936	4.376473	1.195098	18.45508	3.133734	1.068044	2.668843	1.945617	35.15082	2.777876
White Bird.35	29.00799	-1.37745	-0.6576	0.719852	0.781243	5.42458	1.093992	52.65401	0.04502	1.139128	3.492439	12.53345	29.75751	1.993504
White Bird.36	28.0677	-0.97576	-0.1778	0.797957	2.74439	2.194782	1.018936	47.98514	2.943778	1.180192	3.540852	12.94514	39.10276	1.176198
White Bird.37	455.3832	-0.70166	0.017449	0.719112	10.52154	2.675654	0.805438	9.546724	0.464409	1.320237	4.617537	10.06985	15.83921	4.414714
White Bird.38	36.84826	-1.64248	-0.70147	0.941009	0.026766	2.746816	0.996997	43.26315	3.313335	1.052194	7.45504	18.7404	114.9661	3.128913
White Bird.39	976.3047	-0.83732	0.115293	0.952609	14.60944	7.431593	0.963421	35.56904	0.08303	1.067135	4.627134	43.63674	0.288022	3.657694
White Bird.4	705.5007	-1.69965	-0.49725	1.202401	9.63871	4.331026	0.409292	3.286284	2.229734	0.375488	9.169438	167.6443	38.57087	0.402455
White Bird.40	140.8087	-0.50352	1.172966	1.67649	14.92611	5.442305	0.92522	15.8082	0.209103	1.718894	15.38182	117.1259	151.0168	4.885743
White Bird.41	897.0851	-0.4107	0.813623	1.224323	14.10085	1.99997	1.83966	49.79415	0.313935	0.095339	0.966298	3.302593	22.16092	4.816668

Figure I 1 - Trace element concentration data from PXRF analysis of geologic sources as well as archaeological artifacts (cont.).

White Bird.42	1092.243	-0.78661	-0.2013	0.585305	13.15085	2.995432	1.398107	36.7169	2.565057	0.654788	3.272499	124.6068	17.01041	0.210101
White Bird.43	33.95526	-1.02995	0.349655	1.379605	11.1165	4.242563	1.033317	12.74498	0.609495	0.865173	10.15883	153.6775	54.67352	0.673366
White Bird.44	34.328	-1.9633	-0.66037	1.302924	11.93216	3.819002	1.270252	51.99744	2.217878	1.264615	10.69076	136.4945	91.66854	3.700486
White Bird.45	392.3836	-1.78228	0.722919	2.505203	8.343249	0.937605	0.951494	23.32127	2.008159	1.029357	8.496581	7.762852	30.9214	4.944108
White Bird.46	474.283	-0.82446	0.812694	1.637156	11.64428	0.745857	1.368498	51.32122	2.727185	1.154326	9.768372	76.06283	63.94011	4.186193
White Bird.47	585.7546	-1.35763	0.73418	2.09181	15.23318	6.72328	1.416602	2.415167	2.671798	1.516051	8.833812	103.1589	104.9991	0.993008
White Bird.48	455.3832	-1.32706	-0.58248	0.744582	2.783373	0.674083	1.403496	1.920748	1.398551	1.515575	1.888215	5.33363	14.13406	1.389612
White Bird.49	455.3832	-1.84957	-0.55643	1.293134	3.355244	1.985463	0.944519	8.442358	1.503932	0.626734	10.59692	187.8327	1.746365	0.316231
White Bird.5	672.6375	-1.58114	0.660532	2.241677	16.33672	4.575096	0.610652	6.492561	3.8559	1.053599	9.110232	113.5126	38.87769	3.492983
White Bird.50	813.6342	-0.50405	0.795447	1.2995	18.72613	6.49108	1.056473	13.36024	1.476796	1.56663	6.767182	4.058731	22.26878	3.305315
White Bird.51	247.3437	-1.51993	-0.09148	1.428451	1.807584	1.469967	1.431641	45.03033	0.529978	0.944564	17.41127	106.531	93.7644	0.069157
White Bird.52	37.96981	-0.78677	-0.03608	0.750689	0.986145	4.360346	1.518909	49.3269	3.37383	0.794586	7.106455	1.804602	42.01737	2.932856
White Bird.53	40.30991	-1.41406	-0.51789	0.896173	0.56929	1.878286	1.096105	36.29534	0.870166	1.030594	1.510956	3.974062	39.01073	2.918711
White Bird.54	36.68434	-1.71157	-0.41297	1.298602	3.057146	4.550039	0.867357	6.459374	0.467079	0.345554	3.00726	24.56279	0.67425	2.982598
White Bird.55	387.212	-0.80576	0.417187	1.222949	13.5155	0.758576	0.929942	23.00349	3.647667	1.670582	4.975386	45.62236	62.52314	3.290262
White Bird.56	924.6356	-1.29825	-0.39858	0.899666	15.50187	2.877539	0.248423	30.14489	2.864789	1.392905	4.004152	70.76673	17.97364	1.76858
White Bird.57	903.291	-1.50019	0.665313	2.165507	10.08013	1.216425	1.483213	21.0996	3.933978	0.703423	13.56915	60.87889	25.73105	0.025417
White Bird.58	802.8209	-0.61803	0.281978	0.900004	15.96248	4.193943	1.292258	34.0169	2.528175	1.272236	0.734493	11.5422	21.36502	2.064266
White Bird.59	37.95455	-0.53004	1.074982	1.605021	11.28922	5.708123	0.794726	40.26588	3.459446	0.708793	4.67965	6.200332	36.53566	2.666911
White Bird.6	702.7739	-1.5042	0.663758	2.16796	13.76499	6.518329	0.427008	19.05749	0.661844	1.750544	9.554789	209.9688	8.477694	4.987665
White Bird.7	637.6587	-0.87122	0.272899	1.144118	13.05489	5.30239	0.654438	17.14818	2.202145	0.452284	7.503411	39.80005	48.91167	4.530605
White Bird.8	704.6074	-1.33767	-0.56292	0.774751	16.27915	1.031535	0.694696	8.708795	3.7529	1.795959	10.0771	177.5061	36.02191	2.900932
White Bird.9	424.5416	-1.21177	2.004903	3.216671	17.01804	3.703592	1.819518	13.64788	3.771164	1.046922	10.98558	68.20875	91.66854	2.560095

Figure I 1 - Trace element concentration data from PXRF analysis of geologic sources as well as archaeological artifacts (cont.).